The roles of the NOOT-BOP-COCH-LIKE genes in plant development and in the symbiotic organ identity

Shengbin Liu

Thèse de doctorat

NNT : 2020UPASB005

université PARIS-SACLAY

The roles of the *NOOT-BOP-COCH-LIKE* genes in plant development and in the symbiotic organ identity

Thèse de doctorat de l'université Paris-Saclay

École doctorale n° 567 Science du végétal : du gène à l'écosystème

Spécialité de doctorat: Biologie

Unité de recherche : Université Paris-Saclay, CNRS, INRAE, Univ Evry, Institute of Plant Sciences Paris-Saclay (IPS2), 91405, Orsay, France.

Référent : Faculté des sciences d'Orsay

Thèse présentée et soutenue à Gif-sur-Yvette, le 21 septembre 2020, par

Shengbin LIU

Composition du Jury

Catherine RAMEAU Directeur de recherche, INRA, (Institut Jean-Pierre Bourgin, IJPB)	Présidente
Francisco MADUENO Directeur de recherche, (Instituto de Biología Molecular y Celular de Plantas, IBMP)	Rapporteur & Examinateur
Gilles VACHON CRCN, HDR, CNRS/CEA/INRA, (Laboratoire Physiologie Cellulaire Végétale)	Rapporteur & Examinateur
Pascal RATET Directeur de recherche, CNRS, (Institut des Sciences des Plantes de Paris Saclay, IPS2)	Directeur de thèse
Mathias BRAULT Maitre de conférence, (Institut des Sciences des Plantes de Paris Saclay, IPS2)	Invité

TABLE OF CONTENTS

ACKNOWLEDGEMENTS

Over these past four years, it is a quite long, but also very short and important time! It's an honor to have the opportunity to complete a doctoral study in a foreign country! Undertaking this PhD has been a truly life-changing experience for me and it would not have been possible to do this without the support and guidance that I received from many people. Here, I cannot express my gratitude to you with thousands of words!

First and foremost, I am extremely grateful to my supervisor Dr. Pascal Ratet for all the support and encouragements he gave me. Without his guidance and constant feedback, this PhD would not have been achievable. I cannot thank him enough for the platform he provided me with, by accepting me as a graduate student in "SYMUNITY" research team and equipping me with techniques and knowledge. I vividly remember the day we first met since I arrived in France to study 4 years ago, you welcomed me in Orsay-ville station and then helped me to set up CROUS and go shopping with me, also later register in the doctoral school, allowing me to start life and research abroad. In my doctoral work, I thank him in particular for his availability and his brilliant ideas in my research. As a mentor, he has taught me more than I could ever give him credit for here. He has shown me, by his example, what a good scientist (and person) should be and nobody has been more important to me in this project. I would also like to thank Dr. Jacqui Shykoff who made me join the doctoral school and permitting me to attend her lectures and brush up on my knowledge. I am especially indebted to Dr. Marianne Delarue, director of the doctoral school, who worked actively to provide me with the protected academic time.

I gratefully acknowledge the funding received towards my PhD from the China Scholarship Council (CSC) for the fact that I was given the scholarship to support me to carry out my thesis at IPS2 in France, thank you for the expedition of the government of China. I greatly appreciate the support received through the ANR.

I am grateful to all of those with whom I have had the pleasure to work during this and other related projects. I would like to express my deepest appreciation to my committee, Nathalie Glab, Christine Lelandais, and Leila Tirichine Delacour for their pertinent advice, leading my project to be carried out correctly. Each of the members of my Dissertation Committee has provided me extensive personal and professional guidance and taught me a great deal about both scientific research and life in general.

My deep appreciation goes out to the local field research team members. My sincere and heartfelt gratitude to Kevin Magne who composing a huge part of my research work, including manipulations in the work of genetic phenotype identification, mutant construction, hybridization, thesis writing, and great participation in our review work. I thank him very much for his irreplaceable work and kindness. I would also like to extend my deepest gratitude to thank Sophie Massot who has worked with me throughout 4 years and helped me too much: she is gifted to always be positive and encouraged me in my work. I also thank her very much for her organization in manipulations on the bench, as well as she brought a good atmosphere in the laboratory, and when I was absent she took good care of my plants. I would like to extend my sincere thanks to Marie Garmier, who also guided me in the research of my project. Many thanks to Veronique Gruber, who guided me a lot in my

research even though we didn't know each other for a long time, I don't forget our interesting discussions for the thesis projects, I also thank her for her snacks. Thanks also to Hamima Morin who helped me for ISH and imaging. Thanks should also go to Gautier Bernal who helped me with the application of the microscope. I also had the great pleasure of working with Marie Dufresne, I thank her for her help and reagents in experiments. Thanks also to Catherine particularly helpful to me during the COVID-19 epidemic took care of my plants when I could not present in the building, Special thanks to Dahmane, who encouraged me by saying thousands “you are the best”, which made me firmly believe that I am quite scientific. I very much appreciate as PhD student work in the same team with Elhosseyn Ait Salem who convinced me during our many discussions. His excellent work and suggestions have made an invaluable contribution to my PhD. I also wish to thank Claire and Alexis, who takes me home during a strike and the master students Adrien, I am also grateful to them and their families – for their friendship and the warmth they extended to me.

I’d also like to extend my gratitude to the members of the jury, Dr. Francisco Madueno, Dr. Gilles Vachon, Dr. Catherine Rameau, for their availability to participate in my thesis work. and Dr. Mathias Brault

I take this opportunity to express gratitude to all the colleagues of IPS2 for their help and support. I must also thank the director of the institute, Martin Crespi who leads this institute and manages all the sectors to function well. I thank the work of the greenhouse staff, Holger Ornstrup, Pascal Audigier, Florie Vion, the services of the administrative members, Arnaud Charpentier, Mélanie Atlan, Émilie Husgen, Rose Musaniwabo, without them it would not be possible for me to validate my doctorate. I am delighted for the vitality of IPS2 thanks to all our colleagues, thank you.

I would like to solemnly thank the people who took care of me attentively at the time of my father's death last year, who supported me mentally, like real families, Sophie, Elhosseyn, Marie, Siqi, Ying Huang, Yujuan Du, Gautier, Pascal, Dahmane, Véronique..., I thank them again for their friendships with all my sincerity. I especially thank the Chinese PhD students Ying Huang, postdoc Siqi Zhang and Yujuan Du, like the authentic friends and compatriots, I thank them for their help in everyday life. I’m extremely grateful to Dongdong Xu, who gives me much help in daily life and also help me draw some figures.

I would also like to say a heartfelt thank you to my family. I must express my very profound gratitude to my parents for providing me with unfailing support and continuous encouragement throughout my years of study to follow my dreams. I thank very much to my elder brother and sisters, who took good care of our parents in my place, which is important in my life.

I also place on record, my sense of gratitude to one and all, who directly or indirectly, have lent their hand in this venture.

Thank you!

Sincerely

LIST OF ABBREVIATION

2, 4-D	2, 4-Dichlorophenoxyacetic acid
A. tumefaciens	*Agrobacterium tumefaciens*
ACR4	AtCRINKLY4
ACTIN	ACTINNE
AGL24	AGAMOUS-LIKE24
AIB	Indole-3-Butyric Acid
ALOG	Arabidopsis LSH1 and Oryza G1
AM	Arbuscular Mycorrhizal
Ams	Axillary Meristems
ANT	*AINTEGUMENTA*
AON	Autoregulation Of Nodulation
AP1	APETALA 1
AP2/ERF	*APETALA2/ETHYLENE RESPONSIVE FACTOR*
ARA	Acetylene Reduction Assays
AS1	ASYMMETRIC LEAVES1
ATAF1/2	*ACTIVATION FACTOR 1/2*
AtBOP1/2	*Arabidopsis thaliana BLADE-ON-PETIOLE1* and *AtBLADE-ON-PETIOLE2*
ATH1	*ARABIDOPSIS THALIANA HOMEOBOX GENE1*
AVG	2-AminoethoxyVinyl Glycine
AXM	Axillary Meristem
Azs	Abscission Zones
BA1	*BARREN STALK1*
BAP	6-benzylaminopurine
BCP	Bromocresol Purple
Bd	Brachypodium distachyon
bHLH	basic helix–loop–helix
BNF	Biological Nitrogen Fixation
BNM	Buffered Nodulation Medium
BP	BREVIPEDICELLUS
bp	base pair
BRC1	*BRANCHED1*
BTB/POZ	BROAD COMPLEX, TRAM TRACK, and BRICK A BRACK/POXVIRUSES and ZINC FINGER
bZIP	basic leucine zipper
BZR1	BRASSINOZOLE-RESISTANT1
CAD	Cinnamyl Alcohol Dehydrogenase
CAL	CAULIFLOWER
CCaMK	*CALCIUM CALMODULIN-DEPENDENT PROTEIN KINASE*
cDNA	complementary DNA
CESAs	*CELLULOSE SYNTHASE A*
CHA	Cyclohexylammonium
CIM	Callus Induction Medium
CK	Cytokinins
CLE	*CLAVATA3/EMBRYO-SURROUNDING REGION*
COCH	*COCHLEATA*
COMT	*Caffeic acid O-methyltransferase*
CRE1	*CYTOKININ RESPONSE 1*
Crispr-Cas9	Clustered Regularly Interspaced Short Palindromic Repeats and CRISPR-Associated protein9
Ct	Threshold Cycle
CUC1/2/3	*CUP-SHAPED COTYLEDON1/2/3*
CUL4	*UNICULME4*
CUP	*CUPULIFORMIS*
d	dwarf
dad	decreased apical dominance
DET	DETERMINATE
DMI2/3	*DOES NOT MAKE INFECTIONS 2/3*
DNA	Deoxyribonucleic Acid
dpi	days post-inoculation
DS	Determinate Spikelets
EF1a	elongation factor 1-alpha
EMS	ethyl methane sulfonate
ERN1	*ERFREQUIRED FOR NODULATION1*
FLC	*FLOWERING LOCUSC*
FMs	Floral Meristems
FNB	fast neutron bombardment
FRI	FRIGIDA
FT	FLOWERING-TIME LOCUS T
FUL	FRUITFULL
FZP	TFRIZZY PANICLE
G. max	Glycine max
GA/BR	Gibberellins/Brassinosteroids
GCAT	Guanine Cytosine Adenine Thymine
GEA	Gene Expression Atlas
Gob	Goblet
GUS	b-glucuronidase gene
HAE	HAESA
htd	high tillering dwarf
Hv	Hordeum vulgare

IAA	Indoleacetic Acid
IDA	INFLORESCENCE DEFICIENT IN ABSCISSION
IDS1	*Indeterminate Spikelets1*
IM	Inflorescence Meristem
IPD3	*INTERACTING PROTEIN OF DMI3*
IPT1/2	*ISOPENTENYL TRANSFERASE1/2*
IRLC	Inverted Repeat Lacking Clade
IT	Infection Thread
JAG	JAGGED
JLO	JAGGED LATERAL ORGANS
KCl	Potassium chlorate
KN1	*KNOTTED1*
KNAT2/6	*KNOTTED-like from Arabidopsis thaliana 2/6*
KNOX	*KNOTTED1-LIKE HOMEOBOX*
KO	Knock-Out
L. japonicus	*Lotus japonicus*
LA	Leaf Angle
LAS/Ls	*LATERAL SUPPRESSOR/ Lateral suppressor*
LAX1	*LAX PANICLE1*
LAXA	*LAXATUM-A*
LBD	LATERAL ORGAN BOUNDARY DOMAIN
LD	long day
LF	LATE FLOWERING
LFY	LEAFY
Lg	Liguleless
LjLHK1	*Lotus histidine kinase1*
LjNFR1/ LjNFR5	*LjNOD FACTOR RECEPTOR 1 and 5*
LOB	LATERAL ORGAN BOUNDARIES
LOF1	*LATERAL ORGANFUSION1*
LORE1	*LOTUS RETROELEMENT1*
LPWG	Legume Phylogeny Working Group
LRR-RLK	*LEUCINE RICH-REPEAT RECEPTOR-LIKE KINASE*
LYK3	*LYSIN MOTIF RECEPTOR-LIKE KINASE3*
LysA	Auxotrophy for Lycin
M	mole
M. loti	*Mesorhizobium loti*
MCC	*Mimosoideae-Caesalpinieae-Cassieae*
MES	2-(N-Morpholino) Ethane Sulfonic acid
MOC1	*MONOCULM1*
MOS1	*MORESPIKELETS1*
MP	*MONOPTEROS*
Ms	Medicago sativa
MS	Murashige and Skoog
Mt	Medicago truncatula
MTOB	Meristem-To-Organ Boundaries
MtPLT2	*MtPLETHORA2*
MtSHR	*MtSHORT-ROOT*
MYA	Million Years Ago
MYB	Myeloblastosis oncoprotein
N2	Atmospheric Dinitrogen
NAC	*NO APICAL MERISTEM (NAM), ARABIDOPSIS TRANSCRIPTION ACTIVATION FACTOR1/2 (ATAF1/2)* and *CUP-SHAPED COTYLEDON2 (CUC2)*
NBCL	*NOOT-BOP-COCH-LIKE*
NCM	Nodule Central Meristem
NF	Nod Factor
NFP	*NOD FACTOR PERCEPTION*
NF-Y	Nuclear Factor-Y
NFYA1	*NUCLEAR FACTOR-YA1*
NH3	Ammonia
NIN	*NODULE INCEPTION*
NM	Nodule Meristematic
NOOT	*NODULE-ROOT*
NPAAA	Non-protein Amino Acid Accumulation
NPR1	*NON-EXPRESSER OF PR GENES1*
NPR1-LIKE	*NON-EXPRESSOR OF PATHOGENESIS-RELATED PROTEIN1-LIKE*
NSP1/2	*NODULATION SIGNALING PATHWAY 1 and NODULATION SIGNALING PATHWAY 2*
NVB	Nodule Vascular Bundles
NVM	Nodule Vascular Meristem
OBO1/LSH3	*BOUNDARY1/LIGNT-DEPENDENT SHORTHYPOCOTYL3*
OD	Optical Density
Os	*Oryza sativa*
P. sativum	*Pisum sativum*
P. vulgaris	*Phaseolus vulgaris*
PCR	Polymerase Chain Reaction
phan	PHANTASTICA
PIM	PROLIFERATING INFLORESCENCE MERISTEM
PIN1	*PIN-FORMED1*
PLT1	*PLETHORA*
PNF	*POUND-FOOLISH*

PNY	*PENNYWISE*
PR	PATHOGENESIS RELATED
PTS	*PETROSELINUM*
qRT-PCR	quantitive Reverse Transcription Polymerase Chain Reaction
R. leguminosarum	*Rhizobium leguminosarum*
RAM	Root Apical Meristem
RAX1	*REGULATOR of AXILLARY MERISTEMS1*
RIND	Root INDucer
rms	*ramosus*
RNA	Ribonucleic Acid
RNase	Ribonuclease
RNAseq	RNA sequencing
ROX	*REGULATOR OF AXILLARY MERISTEM FORMATION*
S. medicae	*Sinorhizobium medicae*
S. meliloti	*Sinorhizobium meliloti*
SAM	Shoot Apical Meristem
sgRNA	sequence-specific guides RNA
SID1	*Sister of Indeterminate Spikelet 1*
SIFT	Sorting Intolerant From Tolerant
SIN1	*SCARECROW-LIKE13 INVOLVED IN NODULA-TION1*
SL	Somatolactin
SlBOPs	*Solanum lycopersicum BLADE-ON-PETIOLE*
SLs	Strigolactones
SM	Spikelet Meristem
SOC1	*SUPPRESSOR OF OVEREXPRESSION OF CONSTANS1*
STM	*SHOOT MERISTEMLESS*
SWAM1	*SECONDARY WALL ASSOCIATED MYB1*
TALE	*THREE AMINO-ACID LOOP EXTENTION*
TB1	Teosinte Branched1
TCP	TEOSINTE BRANCHED 1, CYCLOIDEA, PCF1
T-DNA	Transfer DNA
TF	Transcription Fator
TFL1	*TERMINAL FLOWER1*
TILLING	*Targeting Induced Local Lesions in Genomes-Next Generation Sequencing*
TILLING	*Targeted Induced Local Lesions IN Genomes*
TMF	*TERMINATING FLOWER*
trl1	*tassels replace upper ears1-like1*
TSF	TWIN SISTER OF FT
TUB3	*BETA-TUBULIN3*
UBC18	*UBIQUITIN-CONJUGATING ENZYME 18*
Ubi	Ubiquitin
UNI	*UNIFOLIATA*
WOX5	*WUSCHEL-RELATED HOMEOBOX 5*
wps	weeks post sowing
WUE	Water Use Efficiency
X-gluc	5-bromo-4-chloro-3-indolyl-beta-D-glucuronic acid
YEB	Yeast Extract Buffer medium
Zm	*Zea mays*
Zmbd1	*Zmbranched silkless1*
Zmlgn	*Zmliguleless narrow*
Zmsln	*Zmsister of liguleless narrow*

SUMMARY

Les gènes *NODULE-ROOT* de *Medicago truncatula*, *BLADE-ON-PETIOLE* d'*Arabidopsis thaliana* et *COCHLEATA* de *Pisum sativum* font partie d'un clade spécifique NOOT-BOP-COCH-LIKE1 (NBCL1) hautement conservé et qui appartient à la famille plus large des gènes *NON-EXPRESSOR OF PATHOGENESIS RELATED PROTEIN1 LIKE*. Les gènes appartenant aux clade NBCL codent des cofacteurs de transcription contenant un domaine Bric-a-Brac Tramtrack Broad/POx virus et un domaine doigt de zinc (BTB/POZ), ainsi qu'un domaine de répétitions d'ankyrine. Les gènes *NBCL* jouent un rôle pléiotropique dans le développement des dicotylédones et des graminées. Une de leurs principales fonctions est de réguler l'établissement des frontières entre les méristèmes et les organes, ainsi que de promouvoir la différenciation des organes latéraux et l'acquisition d'identité. Chez les légumineuses, les membres du clade *NBCL1* sont connus comme les principaux régulateurs de l'identité des organes symbiotiques (nodosités) nécessaires à la mise en place de la symbiose fixatrice d'azote avec les rhizobia. Les membres du clade *NBCL2* (*MtNOOT2*) jouent également un rôle clé dans l'établissement et le maintien de l'identité de l'organe symbiotique, en redondance avec les gènes *NBCL1*. Les gènes *NBCL* sont aussi impliqués dans l'abscission des organes aériens. Les gènes *NBCL* sont également conservés chez les plantes monocotylédones chez lesquelles ils contrôlent différents aspects du développement (architecture et fertilité).

Ce travail de thèse a eu pour but de mieux comprendre le rôle des gènes *NBCL1* et *NBCL2* dans le développement chez les plantes légumineuses et chez *Brachypodium* (monocotylédone) et à découvrir de nouveaux acteurs moléculaires impliqués dans la régulation de l'identité des nodosités dépendante de *NBCL1*. Pour cette étude nous avons utilisé de nouveaux mutants d'insertion TILLING et *Tnt1* chez deux espèces de légumineuses (*Medicago* et *Pisum*). De plus, nous avons mis au point et utilisé la technologie CRISPR chez *Brachypodium* pour mieux comprendre le rôle de ces gènes chez les plantes monocotylédones.

Ce travail de thèse a permis d'élucider les nouvelles fonctions des gènes *NBCL1* de légumineuses dans le développement des tiges et par conséquence dans l'architecture des plantes. Le rôle de ces gènes dans le contrôle de l'homéostasie des hormones de dévelopement a aussi été étudié et a permis de découvrir une nouvelle fonction pour ces gènes. Nous avons également montré que les membres du clade

NBCL2, spécifique des légumineuses, fonctionnent de manière redondante ou antagoniste avec le clade *NBCL1* et jouent des rôles importants dans le développement des feuilles, des stipules, des inflorescences et des fleurs. De plus, nous avons montré un rôle dans le développement, l'établissement et le maintien de l'identité des nodosités, et par conséquent dans le succès et l'efficacité de l'association symbiotique.

Dans cette thèse, nous avons également exploré les rôles des gènes *NBCL BdUNICULME4* et *BdLAXATUM*-A, dans le développement de *B. distachyon* à l'aide de doubles mutants en construisant des mutants KO par la technologie CRISPR-Cas9. Nous avons confirmé les résultats précédents du laboratoire et en utilisant les doubles mutants crés lors de ce travail, nous avons révélé de nouvelles fonctions pour ces deux gènes dans l'architecture des plantes, la formation des ligules et des inflorescences, ainsi que dans la teneur en lignine.

Ce travail de thèse a finalement permis l'identification et la caractérisation de nouveaux mutants pour les gènes *ALOG* (*Arabidopsis LSH1 et Oryza G1*) de *M. truncatula*. Les protéines ALOG sont des partenaires d'interaction potentiels pour les NBCLs. L'utilisation de ces mutants a permis de montrer que certains membres ALOG jouent un rôle important dans le développement des nodosités et des organes aériens.

Dans l'ensemble, ce travail de thèse a permis de mieux comprendre le rôle des gènes *NBCLs* chez les légumineuses et les plantes monocotylédones et suggère qu'au cours de l'évolution, le programme de développement des nodosités symbiotiques a été recruté à partir de programmes de régulation préexistants pour le développement et l'identité des nodosités.

INTRODUCTION

INTRODUCTION

1. Legume crops in sustainable agriculture and ecology

For efficient growth, plants require energy provided by photosynthesis, water, and mineral macro and micro-elements. Among the macro-elements, nitrogen is an essential macronutrient for plants and can be a limiting factor in crop growth (Clarke *et al.*, 2014). The earth atmosphere is mainly composed of nitrogen and dioxygen (N_2, 79 %; O_2, 21 %) but atmospheric nitrogen is highly stable and not directly usable by plants.

On earth, active nitrogen sources have four origins, lightings of thunderstorms, combustion process, industrial processes, and the biological symbiotic fixation. In 1909, Fritz Haber and Carl Bosh invented the industrial process allowing ammonia production from N2. The industrial production of ammonia is an energivorous process still used nowadays to produce nitrogen-rich fertilizers in agriculture to meet the needs of consumers in rapidly growing economies. This practice is not sustainable because intensive nitrogen fertilization has had a negative impact on the environment (Foyer *et al.*, 2019).

The Fabaceae or Leguminosae family, commonly referred to as “legumes,” is the third-largest family of flowering plants, second only to cereals in terms of agricultural importance (Larrainzar & Wienkoop, 2017) and belong to the first plant species that have been domesticated by the human in the Fertile Crescent. Legumes have traditionally played a significant role in agriculture, providing economic benefits that are particularly important in low N input subsistence agriculture. Legumes are still often used in crop rotation systems or in intercropping with other crops of interest as an intermediary culture to reduce the use of inorganic fertilizer (Foyer *et al.*, 2019). Legume-based cropping systems not only increase grain yields but also improve soil fertility through symbiotic biological nitrogen fixation (BNF) of legume plants. This rotation also can be an effective strategy for improving soil N and water use efficiency (WUE), minimizing plant diseases and other pest infestation, and improving the productivity of subsequent cereals (reviews in: Woodburn et al., 2018).

Symbiotic nitrogen fixation generally takes place in an organ called the nodule. Nodule formation is restricted to actinorhizal plants, Parasponia and legumes. There are numerous types of nodules in these plants. Because part of my initial PhD work aimed at studying nodule organ identity we wrote a review (Liu *et al.*, 2020)

describing the nodule diversity, evolution, organogenesis, and identity. The following chapters (2 to 6) are extracted from this review.

2. Symbiotic association engaging plants and nitrogen-fixing bacteria

The term symbiosis (*Symbiotismus*) was introduced to define all cases in which two different species live on or in one another, irrespective of the role of individuals. In the case of the plant-bacteria nitrogen-fixing symbiosis, the atmospheric dinitrogen (N_2) is reduced to ammonia (NH_3) generally by soil nitrogen-fixing *rhizobia* or *Frankia* (*Actinobacteria*) entering symbiosis with plants. Following a molecular dialog between the two symbiotic partners, the plant-bacteria association results in the formation of specific organs called nodules on the roots or, in a few cases, on the stems of the host plant (Eaglesham & Szalay, 1983; Ndoye *et al.*, 1994; Fernandez-Lopez *et al.*, 1998). The nodulation ability is confined to the Rosid I clade including actinorhizal plants, *Parasponia* and legumes (Soltis *et al.*, 1995). Currently, nitrogen-fixing root nodule symbiosis is believed to have evolved only once, around 100 million years ago (MYA), using components of the signaling pathway from the ancestral and widespread arbuscular *mycorrhiza* symbiosis which itself appeared 400 MYA (Doyle, 2011; Werner *et al.*, 2014; van Velzen *et al.*, 2019). Nodule organs are specialized in N_2 reduction into NH3, which benefits to the host plant and is assimilated into organic compounds such as amino acids and nucleotides (Frendo *et al.*, 2013). In return, symbiotic bacteria receive photosynthetic carbohydrates within the protected nodule environment (Sprent *et al.*, 2013; Gresshoff *et al.*, 2018).

Rhizobia are unicellular, Gram-negative bacteria and belong to the widespread *Proteobacteria* division, whereas *Frankia* strains are filamentous, branching, Gram-positive bacteria. The alpha-proteobacterial genera (*Agrobacterium, Allorhizobium, Azorhizobium, Bradyrhizobium, Mesorhizobium, Rhizobium, Sinorhizobium, Devosia, Methylobacterium, Ochrobactrum,* and *Phyllobacterium*) and the beta-proteobacterial genera (*Burkholderia* and *Cupriavidus*) contain nodule-forming bacteria (Lindstrom & Martinez-Romero, 2007; Andrews & Andrews, 2017, Table 1). However, the majority of soil rhizobia strains are not able to form nodules on plants, often because they lack Nod factor (NF) producing genes needed to induce nodulation (Sachs *et al.*, 2010). Most *Actinobacteria* cannot be cultivated, making them less characterized than *Rhizobia* (Pawlowski & Demchenko, 2012).

Table 1. Leguminosae subfamilies organization and phylogeny of Papilionaceae subgroups

Order	Family	Sub-family	Sub-clade	Example of nodulating tribes - genera	Symbionts	Symbiont	infection	Infected tissues	Origin of first	Vasculature	Nodule
FAGALES	Casuarinaceae			Casuarina, Allocasuarina, Ceuthostoma, Gymnostoma	mainly *Frankia* clade I few *Frankia* clade III	vesicles	root hair	infected + uninfected cells	cortex, pericycle	central	indeterminate
	Betulaceae			Alnus							
	Myricaceae			Comptonia, Myrica							
CUCURBITALES	Datiscaceae			Datisca	*Frankia* clade II	vesicles	intercellular	entirely filled of infected cell	pericycle	central	indeterminate
	Coriariaceae			Coriaria							
ROSALES	Rosaceae			Dryas, Rubus, Purshia, Cowania, Cercocarpus,	*Frankia* clade III or *Frankia* clade II	vesicles	intercellular	variable depending plant species	pericycle	central	indeterminate
	Elaeagnaceae			Elaeagnus, Hippophae, Shepherdia							
	Rhamnaceae			Adolphia, Colletia, Discaria, Kentrothamnus, Retanilla,							
	Cannabaceae			Parasponia	*Bradyrhizobia, Rhizobia*	fixation threads	crack entry + IT	infected + uninfected cells	cortex, pericycle		indeterminate
FABALES	Leguminosae	Duparquetioideae		Absent							
		Cercidoideae									
		Detarioideae		Uncertain							
		Dialioideae									
		Caesalpinioideae including mimosoid clade or Mimosoideae-Caesalpinieae-Cassieae (MCC) clade		**Caesalpinioideae**: Dimorphandra, Campsiandra, Sclerolobium, Tachigali, Vouacapoua, Chamaecrista, Peltophorum, Moldenhawera, Cassia, Erythrophleum, Melanoxylon	***Caesalpinioideae:*** *Bradyrhizobia*	**Caesalpinioideae:** fixation threads with exceptions	**Caesalpinioideae:** root hair + IT	infected + uninfected cells	**Caesalpinioideae:** outer cortex	peripheral	indeterminate
				Mimosoideae: Parkia, Pentaclethra, Acacia, Anadenanthera, Entada, Mimosa, Stryphnodendron, Abarema, Albizia, Calliandra, Cedrelinga, Enterolobium, Inga, Pithecetlobium, Zygia, Chidlowia, Desmanthus	**Mimosoideae:** *Bradyrhizobia , Burkholderia, Rhizobia, Ensifer, Cupriavidus, Mesorhizobium, Ochrobactrum*	**Mimosoideae:** symbiosomes	**Mimosoideae:** mainly root hair + IT or epidermal		**Mimosoideae:** inner cortex with exceptions		
		Papilionoideae	outside the 50 kb inversion clade	**Swartzieae** (Swartzia, Ateleia, Bobgunnia, Cyathostegia)	*Bradyrhizobia*	NA	NA	NA	NA	peripheral	indeterminate
			50 kb inversion clade	**Andiraeae (Andira)**	*Bradyrhizobia*	fixation threads	crack entry	infected + uninfected cells	NA	peripheral	indeterminate
				Brongniartieae (Poecilanthe, Cyclolobium, Hovea, Templetonia)	*Bradyrhizobia*	fixation threads	NA	infected + uninfected cells	NA		indeterminate
				Leptolobieae (Diplotropis)	NA	NA	NA	NA	NA		indeterminate
				Sophoreae (Sophora, Ctathrotropis, Ormosia)	*Ensifer, Mesorhizobium, Phyllobacterium, Rhizobium, Bradyrhizobium, Burkholderia*	symbiosomes with expeptions	root hair + IT	infected + uninfected cells	cortex		indeterminate
				Podalyrieae (Cyclopia, Podalyria, Virgilia)	*Burkholderia, Rhizobium*	symbiosomes	root hair + IT	infected + uninfected cells	NA		indeterminate
				Genistoid or **Lupinoid** (Genista, Lupinus, Cytisus, Lotononis)	*Bradyrhizobia, Phyllobacteria, Ensifer, Mesorhizobium, Ochrobactrum, Microvirga*	symbiosomes	crack entry / no IT	entirely filled of infected cells	outer cortex		indeterminate (many lateral meristems)
				Crotalarieae (Crotalaria, Listia, Aspalathus, Lebeckia)	*Methylobacteria, Mesorhizobia Rhizobium, Microvirga sometimes Burkholderia*	symbiosomes	epidermal / no IT	entirely filled of infected cells	NA		indeterminate
				Dalbergieae (Arachis, Andira, Dalbergia, Etaballia, Machaerium, Platymiscium, Stylosanthes, Centrolobium, Pterocarpus, Zornia) **Aeschynomenoid** (Aschynomene) **Adesmieae** (adesmia)	*Bradyrhizobia, Rhizobium*	symbiosomes	crack entry / no IT	entirely filled of infected cells	outer or inner cortex depending plant species		determinate (developing at lateral root axil)
			NPAAA clade	**Mirbelioid** (Aotus, Gompholobium)	wide range of α- and ß-*rhizobia*	symbiosomes	root hair * + IT	infected + uninfected cells	NA		indeterminate
				Indigofereae (Indigofera)	*Burkholderia, Bradyrhizobium, Ensifer, Microvirga*	symbiosomes	root hair + IT	infected + uninfected cells	outer cortex		indeterminate desmodioid
				Millettieae (Millettia, Derris, Tephrosia, Dahlstedtia, Lonchocarpus)	Bradyrhizobium, Rhizobium, Ensifer	symbiosomes with exceptions	epidermal + IT	infected + uninfected cells	outer cortex *		indeterminate and determinate
				Phaseoleae (Glycine, Phaseolus, Vigna, Cajanus, Clitoria, Dioclea, Erythrina, Amphicarpaea, Bolusafra, Canavalia, Centrosema, Dipogon, Lablab, Neonotonia, Pachyrhizus, Pachyrhizus, Pueraria, Rhynchosia)	*Mesorhizobia, Rhizobia, Bradyrhizobia, Burkholderia, Ensifer*	symbiosomes	root hair + IT	infected + uninfected cells	outer cortex		determinate with exception
				Psoraleeae (Psoralea, Bituminaria, Otholobium)	*Mesorhizobium, Burkholderia, Ensifer, Bradyrhizobium*	symbiosomes	root hair	infected + uninfected cells	outer cortex	peripheral	determinate
				Sesbanieae (Sesbania)	*Azorhizobia, Ensifer, Rhizobium, Mesorhizobium, Bradyrhizobium*	symbiosomes	root hair + IT and crack entry	infected + uninfected cells	middle / outer cortex or inner / middle cortex		Both indeterminate / determinate
				Loteae (Lotus, Tetragonolobus, Coronilla, Ornithopus)	*Mesorhizobia, Rhizobia, Bradyrhizobia, Ensifer*	symbiosomes	root hair + IT and crack entry	infected + uninfected cells	outer cortex		determinate with exceptions
				Robinieae (Gliricidia, Robinia)	*Rhizobium, Ensifer, Mesorhizobium*	symbiosomes	root hair + IT	infected + uninfected cells	middle cortex		indeterminate
			IRLC	**Astragaleae / Hedysareae** (Astragalus, Hedysarum) **Cicereae** (Cicer) **Trifolieae** (Trifolium, Medicago, Melilotus) **Fabeae** (Pisum, Vicia, Lathyrus, Lens)	*Ensifer, Mesorhizobia* and *Rhizobia* somtimes *Bradyrhizobia, Neorhizobium, Phyllobacterium*	Symbiosomes (terminal differentiation)	root hair + IT	infected + uninfected cells	inner cortex	peripheral	indeterminate

This table is based on the matK Bayesian analysis to show the nodule characteristics.

Phylogenetic groups are based on the Legume Phylogeny Working Group data (LPWG). IT, infection thread; Ma, million years ago; NPAAA, nonprotein amino acid accumulating, IRLC, Inverted Repeat Lacking Clade. Adapted from (Dart, 1977; Newcomb & Pankhurst, 1982; Lawrie, 1983; Hafeez *et al.*, 1984; Becking, 1984; de Faria *et al.*, 1986; Sprent *et al.*, 1987, 2013, 2017; Corby, 1988; Sprent, 1988, 2007, 2008a,c, 2009; Souza *et al.*, 1992; Hirsch, 1992; Ndoye *et al.*, 1994; Soltis *et al.*, 1995, 2011; Pawlowski & Bisseling, 1996; Fernandez-Lopez *et al.*, 1998; Valverde & Wall, 1999; Lalani Wijesundara *et al.*, 2000; Laplaze *et al.*, 2000; Sy *et al.*, 2001; González-Sama *et al.*, 2004; Hocher *et al.*, 2006; Sprent & James, 2007; Michael J. Dilworth *et al.*, 2008; Dawson, 2008; Tajima *et al.*, 2008; Guinel, 2009; Madsen *et al.*, 2010; Doyle, 2011; Renier *et al.*, 2011; Boatwright *et al.*, 2011; Op den Camp *et al.*, 2012; Pawlowski & Demchenko, 2012; Gehlot *et al.*, 2012; Ardley *et al.*, 2013; LPWG, 2013a,b, 2017; Chen *et al.*, 2013; Imanishi *et al.*, 2014; Svistoonoff *et al.*, 2014; Werner *et al.*, 2014; Liu *et al.*, 2014; Behm *et al.*, 2014; Jiao *et al.*, 2015; Froussart *et al.*, 2016; Andrews & Andrews, 2017; Kanu & Dakora, 2017; Ibáñez *et al.*, 2017; Ren, 2018; Coba de la Peña *et al.*, 2018; van Velzen *et al.*, 2019).

3. Nodule shapes and evolution in the Rosid I clade

Several types of nodule shapes have been reported (Doyle, 1998; Guinel, 2009; Sprent, 2008; Sprent & James, 2007; Sprent, Ardley, & James, 2017). In general, the morphology of nodules is based on the determinacy of their apical meristem (persistent/non-persistent), on the type of bacteroid compartmentation (vesicles/ fixation-threads/symbiosomes), on the infection type (epidermal/crack entry/ infection threads), on the presence or not of interstitial cells in the infected tissues, on the position of the vascular tissues (peripheral/central). The shape of nodules appears to be mainly dependent on the host plant species, however genetic bases underlying the broad diversity of nodule morphologies are still poorly understood.

Actinorhizal plants represent approximately 260 species distributed among 24 genera in eight angiosperm families of the Cucurbitales, Fagales, and Rosales orders. Actinorhizal plants are able to form nodules infected by filamentous $Gram^+$ *Actinobacteria* called *Frankia* (Soltis *et al.*, 1995; Hocher *et al.*, 2006). Actinobacteria can infect their hosts by two ways, intracellularly, via root hair or intercellularly between epidermal cells, to finally form nitrogen-fixing vesicles (Berry & Sunell, 1990). Actinorhizal nodules formation tends to mainly originate from root pericycle cell divisions as for lateral root formation (Pawlowski & Bisseling, 1996). In addition, actinorhizal nodules present a single central vascular bundle that makes them resembling modified lateral roots (Franche *et al.*, 1998; Froussart *et al.*, 2016). Usually, mature actinorhizal nodules are indeterminate and branched, with each nodule lobe resembling a coralloid root (i.e. cycads/ nostoc symbiotic modified lateral roots presenting a peripheral infected-root cortex, without a root cap; Costa & Lindblad, 2002). Indeed, mature actinorhizal nodules contain a single and central vascular bundle surrounded by infected-cortex cells, an apical meristem and a superficial periderm (Pawlowski & Bisseling, 1996; Franche *et al.*, 1998; Laplaze *et al.*, 2000; Pawlowski & Demchenko, 2012; Froussart *et al.*, 2016, Table 1). In *Fagales* and *Rosales* nodules, infected cells in the cortex are interspersed with uninfected cells, while in *Cucurbitales* nodules the infected cortical tissues present interstitial uninfected cells, and infected cortical tissues form a homogeneous and uninterrupted domain (Newcomb & Pankhurst, 1982; Hafeez *et al.*, 1984a; Berg *et al.*, 1999, Table 1)

In the Fabale order, the *Leguminosae* family consists in ca. 751 genera and ca. 19,500 species. Legumes represent one of the most successful lineages in flowering plants (The Legume Phylogeny Working Group, LPWG, 2013a). The LPWG recently proposed an updated Legumes classification based on both chloroplast and nuclear markers in which Leguminosae sub-families have been revised (LPWG, 2013a, 2017; Sprent *et al.*, 2017)(LPWG, 2013a, 2017; Sprent *et al.*, 2017). The *Leguminosae* family now consists of six subfamilies: the *Duparquetioideae*, the *Detarioideae*, the *Cercidoideae*, the *Dialioideae*, *Caesalpinioideae*, and *Papilionoideae* (Table 1). Among these six *Leguminosae* sub-families, only the *Caesalpinioideae* (formerly called *Mimosoideae-Caesalpinieae-Cassieae* Clade, *MCC*) and the *Papilionoideae* contain legume species forming nodules. In *Caesalpinioideae* and *Papilionoideae* sub-families nodules present central infected tissues and peripheral vascular tissues, surrounded by parenchyma, endodermis, and cortex tissue layers (from the inside toward the outside of the nodule). Central infected tissue often contains a mixture of enlarged infected plant cells together with interstitial uninfected cells (Guinel, 2009; Sprent & James, 2007, Table 1).

Caesalpinioideae legumes occur primarily in tropical and subtropical regions and are mainly trees, some extremely large, as well as lianas and shrubs (LPWG, 2013b). Among these woody species, some *Caesalpinioid* genera are known to enter a symbiosis with nitrogen-fixing bacteria and to form indeterminate branched nodules (Sprent *et al.*, 2017). In *Caesalpinioid* species, the nitrogen-fixing bacteria are, in general, permanently retained within cell wall-bound structures called fixation threads (Table 1). These structures resemble infection threads (ITs) however, by contrast to ITs, bacteria hosted in fixation threads will never be released into symbiosomes, a plant membrane-derived organelle-like structure dedicated to host nitrogen-fixing bacteria into the plant cell.

Species belonging to the *Mimosoid* clade (formerly the *Mimosoideae* sub-family) are also generally woody. *Mimosoid* infection mainly occurs via root hairs and involves ITs. *Mimosoid* nodules are all indeterminate, often branched, with bacteroids released into symbiosomes. While fixation threads are never observed, the central infected tissues display interstitial uninfected cells (Table 1).

In the *Papilionoideae* subfamily, a clade known as the Inverted Repeat Loss Clade (IRLC), was defined by Wojciechowski *et al.*, (2000) on the basis of the loss of

one copy of the inverted repeat in the plastid genome (Lavin *et al.*, 1990). The IRLC contains *Astragaleae*/*Hedysareae*, *Cicereae*, *Trifolieae*, *Fabeae* (formerly *Viceae*) tribes (Table 1). These tribes are largely widespread from warm temperate to arctic climate regions and form indeterminate nodules with a persistent nodule meristematic region (NM) composed by an apical nodule central meristem (NCM) and multiple nodules vascular meristem (NVM, Couzigou *et al.*, 2012; Roux *et al.*, 2014; Franssen *et al.*, 2015). In the IRLC, nodules are often branched, infected through root-hair and develop ITs. Bacteroids are released in symbiosomes and undergo terminal differentiation, an irreversible plant-driven process consisting of bacterial cell enlargement, genome amplification and membrane permeabilization (Alunni & Gourion, 2016). The infected tissues of IRLC nodules contain a mixture of infected and interstitial uninfected cells (Sprent *et al.*, 2017). Many economically important legumes such as lentils (*Lens culinaris*), clover (*Trifolium spp*.), vetches (*Vicia spp*.), garden pea (*Pisum sativum,* hereafter *P. sativum*), chickpea (*Cicer arietinum*), and alfalfa (*Medicago sativa,* hereafter *M. sativa*), as well as the model legume barrel medic (*Medicago truncatula,* hereafter *M. truncatula*), belong to the IRLC (Table 1).

Outside of the IRLC but still in the monophyletic Non-Protein Amino Acid Accumulating (NPAAA) clade, characterized by the accumulation of a non-proteinogenic amino-acid called canavanine in seeds, species belong to the *Phaseoloeae*, *Psoraleeae* and *Loteae* tribes form determinate nodules (also called desmodioid nodules) with determinate apical NCM and NVM meristems (Corby, 1988; Magne *et al.*, 2018b). In these tribes, nodule primordia tend to mostly originate from outer root cortical cell divisions (Hirsch, 1992). Due to the non-persistent NCM mitotic activity, these nodules have a determinate growth (Corby, 1988; Guinel, 2009; Sprent, 2008, Table 1). Consequently, determinate nodules are usually spherical, in contrast to indeterminate nodules that have an elongated shape. Regarding infection features, infections occur mainly via root hairs, ITs are formed, infected tissues contain a mixture of infected and interstitial uninfected cells, and bacteroids are released within symbiosomes (Sprent & James, 2007; Guinel, 2009). In addition, by contrast to indeterminate nodules, determinate nodules are unable to branch and often display lenticels, which are loosely packed clump of cells with large intercellular spaces that regulate the gas permeability of nodules. Lenticels usually draw a white star or stripes at the nodule surface and represent a typical feature of determinate

(Sprent, 2007). The NPAAA clade also integrates the *Mirbelioid*, *Indigoferoid*, *Millettioid*, *Sesbanieae* and *Robinieae* tribes. In these tribes nodules, characteristics are more variable. Nodules tend to be indeterminate even though many exceptions occur with species forming determinate nodules. Intermediate nodule structures, called indeterminate-desmodioid nodules, can also be found in the *Indigoferoid* tribe (Ren, 2018). Moreover, it also exists species able to form both indeterminate and determinate nodules, e.g. Sesbania (Ndoye *et al.*, 1994; Fernandez-Lopez *et al.*, 1998). In *Mirbelioid*, *Indigoferoid*, *Millettioid*, *Sesbanieae* and *Robinieae* tribes, the infection mechanism involves root hair and the formation of ITs seems to be a dominant feature. The nodule vasculature is peripheral, central infected tissues consist in a mixture of infected and interstitial uninfected cells, and most species are able to release bacteroids into symbiosomes (Table 1).

In the Papilionoideae subfamily, outside of the NPAAA clade but still in the 50-kb inversion clade (termed based on a 50-kb inversion in the chloroplast genome), the aeschynomenoid (or dalbergioid) nodule type is found in species belonging to the *Dalbergioid* tribe. In aeschynomenoid nodules, the NCM is determinate, resulting in small and oblate nodules which develop at the upper root/lower stem transition, always in associated with the axil of a lateral roots. Aeschynomenoid nodules are often numerous and look-like determinate nodules, however, they are generally smaller and without lenticels. Aeschynomenoid nodules infection occurs by crack entry, does not present ITs and the infected tissues do not present interstitial cells (Sprent & James, 2007; Table 1).

The genistoid (or lupinoid) nodule type is found in the genera *Genista, Lupinus, Cytisus* or *Lotononis* (Table 1). Genistoid nodules have lateral meristems, girdle the subtending root and displaying indeterminate growth. These nodules are roughly spherical, quite large and collar-shaped (Corby, 1988; Sprent, 2008). As for the aeschynomedoid nodules, Lupinoid nodules are initiated by a crack-entry infection mechanism, ITs are absent and the central nodule tissue is entirely filled with infected cells (Sprent & James, 2007; Table 1).

The *crotalarioid* tribe is phylogenetically close to the genistoid and contains both herbaceous and woody species. Crotalarioid nodules are indeterminate, laterally flattened, thin, and form fan-like structures (Corby, 1988). Crotalarioid nodule infection seems to occur without root hair infection nor ITs formation, and infected

tissues do not contain interstitial uninfected cells, similarly to the aeschynomenoid and genistoid nodules (Renier *et al.*, 2011, Table 1).

In the 50-kb inversion clade, besides the *aeschynomenoid*, *genistoid* and *crotalaroid* tribes, species from the *Andiraeae*, *Brongniartieae*, *Leptolobieae*, *Sophoreae* and *Podalyrieae* families are also able to form indeterminate nodules with peripheral vasculatures. In these tribes, nodulating species are less studied but it seems that the less sophisticated fixation threads bacterial compartmentation system is more frequent (Table 1).

Still in the Papilionoideae family, outside the 50-kb inversion clade, the basal Swartzieae group also contains few genera that have been described to form nodules, such as *Swartzia*, *Ateleia*, *Bobgunnia* or *Cyathostegia*. The nodulation traits in these groups are not well described but it seems that Swartzieae mostly associate with *Bradyrhizobia* and form indeterminate nodules with peripheral vascular bundles (Table 1).

Outside of the *Leguminosae* family, in the Rosales, *Parasponia* sp. belongs to the *Cannabaceae* family and represent the only known non-legume lineage to have evolved a symbiosis with *rhizobia* (Op den Camp *et al.*, 2011, 2012; Behm *et al.*, 2014)(Camp *et al.*, 2011; Op den Camp *et al.*, 2011; Behm *et al.*, 2014). The *Parasponia* genus is represented by five species and is phylogenetically close to the non-nodulating *Trema* genus (van Velzen *et al.*, 2019). In *Parasponia*, nodules are indeterminate and root infection occurs via crack-entry, a less-sophisticated infection mode than root hair infection (Behm *et al.*, 2014). In addition, *Parasponia* hosts its rhizobial partners in permanent fixation threads. Importantly, *Parasponia* nodules have a central vasculature surrounded by peripheral cortex-infected-cells comparable to Actinorhizal nodules. Infected tissues in Parasponia nodules consist of a mixture of infected and interstitial uninfected cells (Behm *et al.*, 2014).

4. Indeterminate versus determinate legume nodules

In legumes, nodules can harbor indeterminate or determinate meristems (Hirsch, 1992; Guinel, 2009). Indeterminate nodules are elongated due to the presence of a persistent meristem, and the indeterminate nodule primordium arises from root inner cortex cell divisions. By contrast, the transient activity of the determinate nodule meristem results in globular shaped-nodules. Determinate nodule primordia tend to mostly originate from root outer cortex cell divisions (Hirsch, 1992; Guinel, 2009,

Table 1). *M. truncatula* and *P. sativum* nodules are among the best characterized indeterminate nodules, and typical determinate nodules are well described in *Lotus japonicus* (*L. japonicus*), *Glycine max* (*G. max*) and *Phaseolus vulgaris* (*P. vulgaris*). The development of these legume nodules is described below.

Xiao *et al.*, (2014) established a cellular fate map for *M. truncatula* indeterminate nodules. This fate map precisely describes the root cellular origins of the different nodule tissues. In this pioneer work, authors highlighted that the NCM originates from the third root cortex cell layer and that once this NCM starts functioning and producing NCM derived-cells, it marks the transition between a nodule primordium toward a functional nodule. The continuously active NCM adds cells to the nodule all along with its lifespan (Hadri *et al.*, 1998; Lotocka *et al.*, 2012). There are mainly two types of NCM-derived cells: bacteria infected and uninfected cells. The central zone of the nodule presents a developmental gradient from the youngest cells adjacent to the NCM to the oldest cells near the root attachment point. In their study, Xiao *et al.*, (2014) also showed that uninfected cell layers at the very base of nodules derived from root endodermis and pericycle cells divisions, and that the first infected cell layers at the base of the nodule derived from the inner fourth and fifth root cortical cell layers.

In indeterminate nodules, from the nodule apex to its base, six-well defined histological zones can be observed: the zone I correspond to the meristematic apical region producing cells of the central tissue of the nodule. The zone II corresponds to ITs penetration zone. The Interzone II-III corresponds to a region where the bacteria are released into plant cells and where they differentiate into bacteroids. The zone III corresponds to the nitrogen-fixing region. The zone IV corresponds to a region where the bacteroids start to senesce. Finally, the zone V corresponds to the oldest infected part of the nodule, where bacteria turn into a saprophytic behavior.

The zone V then contains non-differentiated free-living rhizobia that live at the expense of the host plant (Lotocka *et al.*, 2012). These central tissues are surrounded by multiple peripheral uninfected tissue layers, consisting from the inside toward the outside of the nodule in the nodule parenchyma, the nodule endodermis and the nodule cortex (Vasse *et al.*, 1990; Guinel, 2009; Lotocka *et al.*, 2012). The nodule vascular bundles (NVB) are located between the nodule parenchyma and the nodule endodermis, and are ontologically related to root pericycle and endodermis cell layers

(Couzigou *et al.*, 2012; Magne *et al.*, 2018a). NVBs develop through the activities of different apical NVMs (Roux *et al.*, 2014; Franssen *et al.*, 2015; Magne *et al.*, 2018a).

Determinate nodules can be also broadly subdivided into central and peripheral tissues. The determinate nodule primordium originates from subepidermal cell divisions taking place in the outer root cortex. Later, cell divisions also occur in the root pericycle and inner cortex, several cells layers away from the initial divisions (Hirsch, 1992; Gauthier-Coles *et al.*, 2019). Cells derived from the outer root cortex cell divisions will give rise to the rhizobia-infected central tissues. The determinate nodule expansion appears to be the consequence of bacteroids multiplication in infected cells (Guinel, 2009). Peripheral tissues of determinate nodules are similar to those of indeterminate nodules, even though the parenchyma, endodermis and cortex peripheral tissues completely surround the nodule central tissues in mature nodules. In addition, by contrast to the NVMs of indeterminate nodules, which are continuously active throughout the whole nodule lifespan, the NVMs of determinate nodules are also determinate (Corby, 1988; Magne *et al.*, 2018b).

5. Nod factors signaling-dependent activation of nodule organogenesis

The current knowledge regarding the molecular mechanisms underlying legume-rhizobia symbiotic interaction, from partners recognition until mature nodule development has been principally established using two model legumes, *M. truncatula* and *L. japonicus* (Udvardi *et al.*, 2005; Young *et al.*, 2011). Plant-bacteria early signaling and nodule organogenesis are less described for actinorhizal plants (Froussart *et al.*, 2016). Studies based on legumes have shown the importance of the bacterial NF perception for the symbiotic partners specific recognition and association (Dénarié Jean and Debellé Frédéric, 1996; Oldroyd *et al.*, 2011; Oldroyd, 2013; Wang *et al.*, 2018). As the NF signaling cascade controls the symbionts recognition, the rhizobial infection, and the nodule organogenesis, it is difficult to precisely define the specific roles of NF signaling genes in organogenesis. However, the identification of spontaneous nodulation mutants, forming nodule-like structures in the absence of rhizobia, and symbiotic gene overexpression studies, clearly showed a role for several actors of the NF signaling pathway (see below) in the initiation of the nodule organogenesis (Truchet *et al.*, 1989; Tirichine *et al.*, 2006a,b, 2007; Murray *et al.*, 2007; Suzaki & Kawaguchi, 2014).

NFs are perceived by plant specific NF receptors/perceptors recognition complexes (e.g., the *MtLYSIN MOTIF RECEPTOR-LIKE KINASE3*, *MtLYK3* and the *MtNOD FACTOR PERCEPTION, MtNFP* in *M. truncatula* or the *LjNOD FACTOR RECEPTOR* 1 and 5 *LjNFR1/ LjNFR5* in *L. japonicus*). These proteins are receptor kinases containing LysM-domain (Limpens *et al.*, 2003; Radutoiu *et al.*, 2003, 2007; Arrighi *et al.*, 2006; Smit *et al.*, 2007). These LysM receptor kinases are known to associate with the *LEUCINE RICH-REPEAT RECEPTOR-LIKE KINASE* (*LRR-RLK*) *MtDOES NOT MAKE INFECTIONS 2* (*MtDMI2, LjSYMRK* in *L. japonicus*) and to induce calcium oscillations in the nucleus. These calcium oscillations are perceived by *MtDOES NOT MAKE INFECTIONS3* (*MtDMI3*) a *CAL-CIUM CALMODULIN-DEPENDENT PROTEIN KINASE* (*CCaMK*; Levy *et al.*, 2004; Mitra *et al.*, 2004; Tirichine *et al.*, 2006). This *CCaMK* is able to phosphorylate *MtINTERACTING PROTEIN OF DMI3* (*MtIPD3, LjCYCLOPS* in *L. japonicus*) and to form a complex with this latter (Yano *et al.*, 2008; Horváth *et al.*, 2011; Singh *et al.*, 2014; Cerri *et al.*, 2017). *MtIPD3/LjCYCLOPS* represent key symbiotic actors for nodule organogenesis and can directly bind the promoter of the RWP-RK-type TF *NODULE INCEPTION* (*NIN*) essential for nodule organogenesis (Marsh *et al.*, 2007; Singh *et al.*, 2014) as well as the promoter of the *APETALA2/ETHYLENE RESPONSIVE FACTOR* (*AP2/ERF*) TF, *ERFREQUIRED FOR NODULATION1*, to activate their expressions (*ERN1*; Andriankaja *et al.*, 2007; Middleton *et al.*, 2007; Cerri *et al.*, 2017). *MtERN1* and *MtERN2* are essential for nodule organogenesis since primordia do not form in the *Mtern1ern2* double mutant (Cerri *et al.*, 2016). In addition, GRAS-type TFs, *NODULATION SIGNALING PATHWAY* 1 and 2 (*NSP1* and *NSP2*; Smit *et al.*, 2005; Kaló *et al.*, 2005; Heckmann *et al.*, 2006; Murakami *et al.*, 2006; Hirsch *et al.*, 2009), *PsSCARECROW-LIKE13 INVOLVED IN NODULATION1* (*PsSIN1*; Battaglia *et al.*, 2014) and the gibberellin signaling. DELLA proteins (Fonouni-Farde *et al.*, 2016, 2017; Jin *et al.*, 2016), also act downstream the calcium spiking signaling and might potentially associate with *MtIPD3/LjCYCLOPS* to form a heteromeric regulatory complex required for organogenesis. *NIN* activates the *MtNUCLEAR FACTOR-YA1* (*MtNFYA1*) subunit gene encoding a CCAAT box-binding TF that interacts with DELLA proteins (Fonouni-Farde *et al.*, 2016). Both *NIN* and NF-Y play important roles in the reactivation of cortical cell divisions (Combier et al., 2006; Soyano et al., 2013; Laporte et al., 2014). *NIN* also activates the cytokinin receptor *MtCYTOKININ*

RESPONSE 1 (*MtCRE1*) gene expression (*LjLHK1* in *L. japonicus*). The perception of cytokinins via *MtCRE1* activates cytokinin responses notably in the root cortex to promote nodule organogenesis (Tirichine *et al.*, 2007; Vernié *et al.*, 2015).

The de novo nodule organogenesis is promoted in the root cortex by the NF-induced cytokinin signaling pathway which involves the cytokinin receptor *MtCRE1/LjLHK1* and regulates and/or requires the expression of the TFs *NIN*, *NSP1*, *NSP2*, *DELLA*, NF-Y subunits, *SIN1*, *ERN1* and *ERN2* (Stougaard *et al.*, 1999; Smit *et al.*, 2005; Kaló *et al.*, 2005; Heckmann *et al.*, 2006; Andriankaja *et al.*, 2007; Marsh *et al.*, 2007; Battaglia *et al.*, 2014; Soyano & Hayashi, 2014; Vernié *et al.*, 2015; Cerri *et al.*, 2017; Diédhiou & Diouf, 2018). Some of these transcription factors are post-transcriptionally regulated by microRNAs, which therefore also participate in modulating nodule organogenesis (Lelandais-Brière *et al.*, 2016; Hossain *et al.*, 2019). The reactivation of cell divisions following NF signaling pathway also involves the reactivation of the cell cycle machinery (Kuppusamy *et al.*, 2009; Breakspear *et al.*, 2014).

Plant hormones also play a major role in nodule organogenesis (see above for cytokinin perception and the role of the gibberellin signaling DELLA proteins) and their roles in nodule organogenesis were recently reviewed by Liu *et al.*, (2018) and in the dedicated chapter dealing on hormonal regulations of nodulation. Briefly, cytokinins play a pivotal and positive role in the initiation of legume nodule organogenesis (Tirichine *et al.*, 2007; Plet *et al.*, 2011; Gamas *et al.*, 2017). Strigolactones and local accumulation of auxins also participate in nodule organogenesis, the latter being regulated depending on the *CRE1*-dependent cytokinin signaling (Ng *et al.*, 2015; Kohlen *et al.*, 2018; Gauthier-Coles *et al.*, 2019). Gibberellins through DELLA proteins may function as a hub to integrate different hormonal signaling pathways, especially cytokinins, to modulate nodule organogenesis (Fonouni-Farde *et al.*, 2017; McAdam *et al.*, 2018). In contrast, auxins rather than cytokinins are necessary for the actinorhizal nodule organogenesis (Froussart *et al.*, 2016; Gauthier-Coles *et al.*, 2019) likely in relation to their root-like structure. Other hormones are likely involved in nodule organogenesis; even though specific knowledge to conclude specifically about this is mostly lacking.

6. Symbiotic organ identity regulation

Following nodule initiation stages, molecular mechanisms supporting nodule development and defining nodule identity remain poorly understood. The nodule identity directly influences nodule growth and shape, and might partly explain the diversity of nodule structures observed among nodulating species. Recent genetic studies using either bacterial or plant mutants pointed out the root origin of legume nodules. Assuming a common evolutionary origin for the nodulation capacity of the Rosid I plants, actinorhizal and Parasponia nodules, resembling more to modified lateral roots, might represent more ancients and less sophisticated nodule structures (Pawlowski & Bisseling, 1996; Santi *et al.*, 2013; Svistoonoff *et al.*, 2014; Behm *et al.*, 2014).

The limited information related to nodule identity regulation has been obtained using legume species belonging only to the NPAAA clade. The alteration of the nodule identity is often characterized by nodule-to-root conversions, or by the formation of calli structures. Such phenotypes have also been observed in *M. sativa* and *Trifolium* sp. indeterminate nodules by increasing the growing temperature conditions (Dart, 1977; Ferguson & Reid, 2005) or following hairy root transformation in Arachis (Sinharoy *et al.*, 2009). The molecular bases of these organ identity changes are unknown. Nodule-to-root conversions were also observed in G. max determinate nodules inoculated with *Bradyrhizobium japonicum* mutant strains altered for *PhyR* and *EcfG* locus which encode response regulators involved in various stresses tolerance (ΔphyR, ΔecfG ; Gourion *et al.*, 2009). Similarly, in *P. vulgaris*, inoculation with Rhizobium *elti* mutant strains presenting an auxotrophy for lysin (lysA) also resulted innodules forming ectopic roots (Ferraioli *et al.*, 2004). These bacterial mutants were thus classified as Root INDucer (RIND) bacterial mutants (Ferraioli *et al.*, 2004). An altered infection process caused by these bacterial mutants may alters phytohormonal levels in nodules, probably the cytokinin/auxin balance, and results in an asynchronous development of NCM and NVM, altering the proliferation rate of the different nodule tissues (Ferraioli *et al.*, 2004; Gourion *et al.*, 2009). *M. truncatula* infected by the *Sinorhizobium meliloti exoY* mutant also develops root-like structures with central vasculature suggesting that a successful bacterial infection is required for a proper nodule development (Guan *et al.*, 2013).

Similar phenotypes were also observed using the *M. truncatula Mtlin*-4 and *Mtvapyrin*-2 infection deficient mutants (Guan *et al.*, 2013).

Several genes participating in root development and identity are expressed during legume nodule development. This suggests that root- related genes have been recruited during evolution to regulate nodule organogenesis and identity. In *M. truncatula*, the *MtPLETHORA* genes (*MtPLT1*-4) are differentially expressed in both NCM and NVM, and probably function redundantly to coordinate the activities of the different nodule meristems and to allow nodule meristem maintenance (Franssen *et al.*, 2015). Similarly, the root-related *WUSCHEL-RELATED HOMEOBOX* 5 (*WOX5*) TF, probably together with the *CLAVATA1* receptor and the *CLAVATA3/EMBRYO-SURROUNDING REGION* (*CLE*) peptide encoding genes were recruited during nodule development (Osipova *et al.*, 2012). In addition, Di Giacomo *et al.*, (2016) and Azarakhsh *et al.*, (2015) showed that in *M. truncatula*, three class II *KNOTTED1-LIKE HOMEOBOX* (*KNOX*) genes (*MtKNOX3*, *MtKNOX5*, and *MtKNOX9*) belonging to the *MtKNAT3/4/5-LIKE* sub-clade were linked to nodule organogenesis. Class II *KNOX* likely participates to the definition of nodule boundaries, shape and size. These authors suggested that these class II *KNOX* control cytokinin-related regulatory modules required for nodule development.

Among the *NON-EXPRESSOR OF PATHOGENESIS-RELATED PROTEIN1-LIKE* (*NPR1-LIKE*) gene family, members of the *NOOT-BOP-COCH-LIKE* (*NBCL*) sub-clade are essential regulators of plant development and shape. This clade was called *NBCL* because it includes the *M. truncatula MtNODULE-ROOT* (*MtNOOT*), the Arabidopsis thaliana *AtBLADE-ON-PETIOLE1* and *AtBLADE-ON-PETIOLE2* (*AtBOP1/2*), and the *P. sativum PsCOCHLEATA* (*PsCOCH*) genes (Couzigou *et al.*, 2012). Besides, few exceptions, most legume species possess a second *NBCL* gene grouping in a legume-specific sub-clade called *NBCL2* (Magne *et al.*, 2018a). Among legumes, *L. japonicus* represents one of these exceptions because it possesses a single *NBCL* copy called *LjNBCL1* or *LjCOCH1* (Liu *et al.*, 2018a; Magne *et al.*, 2018b). Genes belonging to the NBCL clades encode transcriptional co-factors containing a Bric-a-Brac Tramtrack Broad complex/POx virus and Zinc finger (BTB/POZ) domain, as well as an ankyrin repeats domain. *NBCL* genes play pleiotropic roles in both dicots and grasses development because one of their major functions is to regulate the establishment of the meristem-to-organ boundaries (MTOB), as well as to

promote both lateral organs differentiation and identity acquisition (Khan *et al.*, 2014; Žádníková & Simon, 2014; Hepworth & Pautot, 2015; Wang *et al.*, 2016). In legume plants, NBCL functions have been recruited for nodule formation and appear particularly important for the establishment of a well-organized symbiotic organ as well as for the robust maintenance of the nodule identity (Ferguson & Reid, 2005; Couzigou *et al.*, 2012).

In *M. truncatula* and *P. sativum* indeterminate nodules, the loss-of-function of *NBCL1* genes does not significantly impact the early nodule infection process, however, the development of the nodule is drastically altered (Ferguson & Reid, 2005; Couzigou *et al.*, 2012; Magne *et al.*, 2018a). *nbcl1* mutant plants are characterized by the outgrowth of ectopic roots arising from NVMs. This suggests that the control of the root identity at the NVM is impaired in the absence of *NBCL1* genes (Ferguson & Reid, 2005; Couzigou *et al.*, 2012, 2013). This phenotype is in agreement with the *MtNOOT1* spatial gene expression pattern which specifically associates to the developing part of the NVB and to the distal NVM regions. In nbcl1 mutants, the nodule-to-root conversion is asynchronous and can occur randomly from the nodule primordium formation, to later developmental stages, and even until nodules are mature (Couzigou *et al.*, 2012). In *M. truncatula*, the paralog of *MtNOOT1*, *MtNOOT2*, is mostly expressed in the NCM and surrounds the NVMs. The *Mtnoot2* mutant does not present any symbiotic phenotype, however, the loss-of-function of both *MtNOOT1* and *MtNOOT2* genes leads to the complete loss of the nodule identity. This complete loss of nodule identity is characterized by the presence of only non-functional nodules converted into roots which are unable to host rhizobia. This revealed that the success of rhizobia accommodation is fully dependent on the nodule identity and that both *MtNOOT1* and *MtNOOT2* genes participate in the nodule identity establishment and maintenance (Magne *et al.*, 2018a). In addition, this complete loss of nodule identity is associated to drastic changes in gene expression. Indeed, symbiotic genes expression is drastically decreased while defense and root apical meristem (RAM) marker genes expression is increased (Magne *et al.*, 2018a). As an example, the expression of the RAM markers *MtCRINKLY4*, *MtSHORT-ROOT*, and *MtPLETHORA2* was significantly up-regulated in *Mtnoot1* and *Mtnoot1noot2* nodules in agreement with the nodule-to-root identity shift. In addition to these gene expression changes, the spatial expression pattern of the class II *MtKNOX9* identity

gene was modified in *Mtnoot1* and *Mtnoot1noot2* converted nodules. Such a drastic spatial gene expression modification highlights a major role of NBCL in the definition of nodule domains as well as in nodule identity acquisition (Magne *et al.*, 2018a).

More recently, using *L. japonicus* as a model to study the determinate nodule identity, it was shown that determinate nodule identity was also NBCL-dependent. Indeed, despite the absence of a persistent NCM indeterminate nodule, the loss-of-function of the unique *LjNBCL1* gene triggers the outgrowth of nodule ectopic roots arising from the NVMs. The loss of nodule identity in *L. japonicus* nodules is associated with the reorganization of the NVB vessels. This phenomenon consists in a switch from the xylem/phloem collateral organization typical of NVB toward an alternate xylem/phloem organization reminiscent of a root vascular bundle organization. *NBCL1* functions are thus not only conserved between *M. truncatula* and *P. sativum* indeterminate nodules, but also in *L. japonicus* determinate nodules, for the maintenance of NVB and NVM identities as well as for nodule identity (Couzigou *et al.*, 2012; Magne *et al.*, 2018b).

Until now, from the plant side, these unique nodule-to-root homeotic events have only been reported for *nbcl1* mutants, making *NBCL1* genes key regulators of nodule development and identity.

7. Gene networks controlling biogenesis of shoot apical meristem (SAM), axillary meristems (AMs), and floral meristems (FMs)

Plants produce new organs from a population of pluripotent cells in meristems whose function is related to stem cells in animals. Meristems are located at different positions of the plant body and give rise to different organs. During the post-embryonic development of flowering plants, the shoot apical meristem (SAM) and root apical meristem (RAM) generate aerial and underground parts, respectively. The SAM contains pluripotent stem cells and resides at the tip of each stem, divided into the central, peripheral, and rib zones, which gives rise to all above-ground organs under a dynamic balance of growth and differentiation. In monocots, such as rice and maize, the SAM is formed laterally, at the base of a single cotyledon (Barton, 2010). Primordia are initiated from the peripheral zone of the SAM in a predictable pattern, and develop into leaves during the vegetative stage subsequently into flowers and fruits during the reproductive phase. Whereas axillary meristems (AM) that give rise to lateral branches and flowers and allow recovery from injury arise from the

boundary as do specialized organs such as stipules (appendages at the base of leaves) and nectaries (Bowman & Eshed, 2000). SAM also transformed into the main inflorescence meristem (IM) during the floral transition, when environmental and developmental conditions are optimal for plant reproductive success. The main IM either produces flowers or remains indeterminate to produce branch meristems, which could iterate the pattern of the main IM. Flowers develop from floral meristems (FMs) that are formed on the flanks (floral primordium) of the SAM in response to environmental and endogenous cues (Pidkowich *et al.*, 1999).

The *NAC* (*NO APICAL MERISTEM* (*NAM*), *ARABIDOPSIS TRANSCRIPTION ACTIVATION FACTOR1/2* (ATAF1/2) and *CUP-SHAPED COTYLEDON2* (*CUC2*) transcription factors confer boundary identity in higher land plants (Maugarny *et al.*, 2015), which including the petunia gene *NAM* (Souer *et al.*, 1996), the snapdragon (*Antirrhinum majus*) gene *CUPULIFORMIS* (*CUP*) (Weir *et al.*, 2004), the *Arabidopsis* genes *CUC1*, *CUC2* and *CUC3* (Aida *et al.*, 1997; Takada *et al.*, 2001; Vroemen *et al.*, 2003) and their tomato ortholog *Goblet* (*Gob*) (Brand *et al.*, 2007; Berger *et al.*, 2009). These factors initiate the SAM (Fig. 1A) and establish boundaries in conjunction with *SHOOT MERISTEMLESS* (*STM*), a *three-amino acid loop extension* (*TALE*) class I *KNOTTED1*-like (*KNOX*) homeodomain protein (Hamant & Pautot, 2010; Hay & Tsiantis, 2010). *CUC-STM* forms a conserved module in development that was first identified in embryos (Aida *et al.*, 1999, 2002; Takada *et al.*, 2001). Activated *CUC1* and *CUC2* are redundantly required for *STM* expression and loss of CUC1 and CUC2 gene function causes a lack of embryonic SAM (Aida *et al.*, 1997). In turn, *STM* directly maintains the expression of *CUC1* and indirectly promotes *CUC2* and *CUC3* in establishing a feedback loop that ultimately restricts *CUC* expression to the axils of cotyledons. *STM* maintains indeterminate growth by interaction with BELL homeodomain proteins encoded by *PENNYWISE* (*PNY*), *POUND-FOOLISH* (*PNF*), and *ARABIDOPSIS THALIANA HOMEOBOX GENE1* (*ATH1*) and promoting cytokinins (CK) and repressing *BOP1/2*, gibberellins/ brassinosteroids (GA/BR) accumulation in the SAM. Conversely, *BOP1/2* restricts *KNOX* expression in the proximal region of leaves to control patterning.

CKs are known to promote cell division in the shoot and to positively regulate SAM size and activity (Barton, 2010). Formation of an AM (Fig. 1B) requires the depletion of auxin from the leaf axil followed by a burst of CK (Müller *et al.*, 2015).

Transcript accumulation of CUC1 and CUC2 is modulated by microRNA miR164, fine-tuning the number of secondary meristems per leaf axil (Laufs *et al.*, 2004; Raman *et al.*, 2008). The R2R3 MYB (myeloblastosis oncoprotein) transcription factors, *LATERAL ORGANFUSION1* (*LOF1*), which is a regulator of *REGULATOR OF AXILLARY MERISTEMS1* (*RAX1*) functions to promote AM and organ separation (Lee *et al.*, 2009). *CUC1-3* are redundantly required for AM initiation functioning downstream *RAX1*, to promote the GRAS-domain protein *LATERAL SUPPRESSOR* (*LAS*/Ls) (Schumacher *et al.*, 1999; Greb *et al.*, 2003) to maintain *STM* expression in AMs. *LAX PANICLE1* (*LAX1*) and *BARREN STALK1* (*BA1*) were characterized as key regulators of the shoot and inflorescence branching in the monocots rice and maize, respectively (Komatsu *et al.*, 2003b; Gallavotti *et al.*, 2004). *REGULATOR OF AXILLARY MERISTEM FORMATION* (*ROX*) is the ortholog of *LAX1* and *BA1* in Arabidopsis, which expressed in the adaxial boundary between leaf primordia and the SAM. LAS and *RAX1* promote AMs via the bHLH transcription factor *ROX* (Yang *et al.*, 2012). *BOPs* are required for the production of various determinate axillary shoots including stipules, nectaries, and flowers in dicots (Khan *et al.*, 2014). Barley *CUL4* is a *BOPs* homolog required for tiller formation (Tavakol *et al.*, 2015). Moreover, *BOP1/2* homologs *BdCUL4* and *BdLAXA* act antagonistically to control the tillering in *Brachypodium* (Magne *et al.*, 2020). *BOP* expression is downregulated at an early stage of indeterminate IM formation and moves to the boundary between the meristem and AM demonstrating a transient role similar to *ROX* (Xu *et al.*, 2010; Yang *et al.*, 2012). The contribution of *CUL4* or *BdLAXA* in AMs production suggests partial conservation of *BOP* function in monocots and dicots.

Floral inductive signals acting on the SAM result in an acquisition of IM fate and new patterns of aerial development and the *PNY* and *PNF* BELL members were required for completion of this process. In *pny pnf* mutants, apices support the production of leaves, but internode elongation and flower initiation are blocked due to misexpression of *BOP1/2* and its downstream effectors *KNAT6* and *ATH1* (Hake *et al.*, 2004; Kanrar *et al.*, 2008; Lal *et al.*, 2011), which prevent the accumulation of floral meristem identity genes including LFY, CAULIFLOWER (CAL), and APETALA1 (AP1) required for flower production (Khan *et al.*, 2015). The setting of lateral boundaries by PNY and PNF via the restriction of *BOP1/2-ATH1-KNAT6* expression

is critical for meristem integrity and specification of flowers (reviewed in: Hepworth & Pautot, 2015).

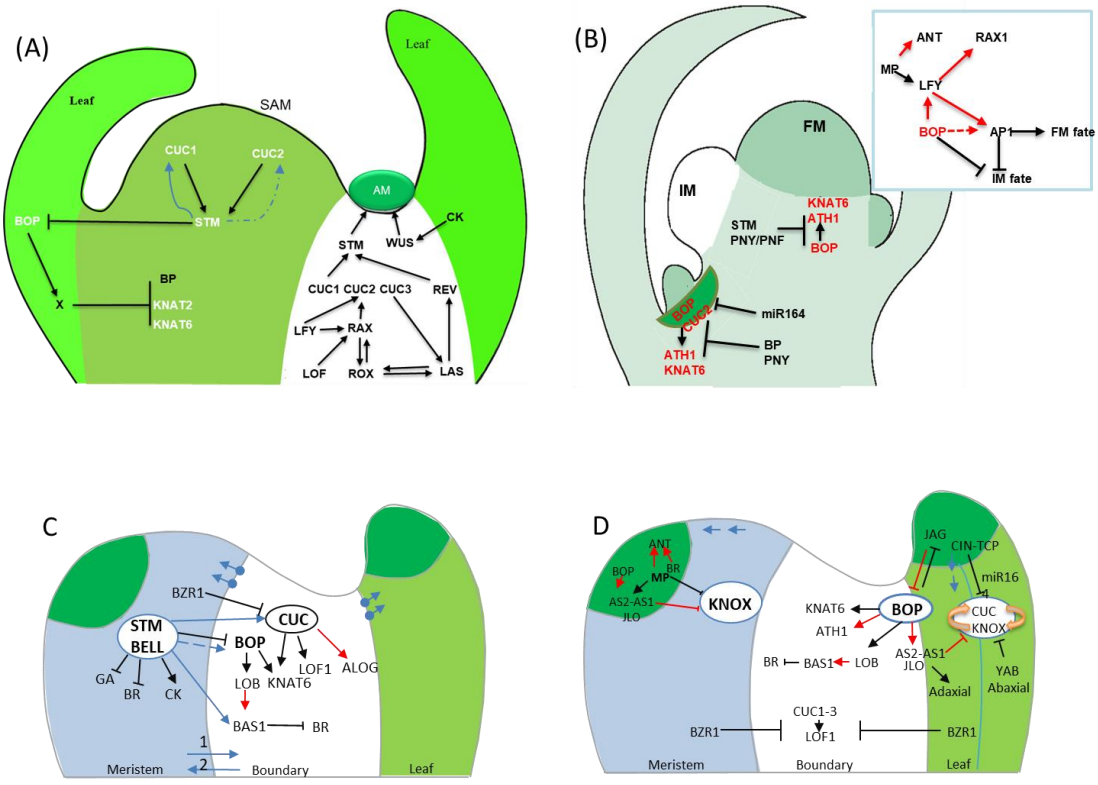

Figure 1. Homologous boundary gene networks controlling the biogenesis of SAM, AMs, FMs, and leaf-SAM boundary.

(**A**) A model shows the factors involved in the regulation of SAM initiation, maintenance, and AM formation (olive-green). *STM* represses *BOP1/2* to maintain indeterminacy in the SAM. Conversely, *BOP1/2* restricts KNOX expression in the proximal region of leaves to control patterning. Formation of an AM requires depletion of auxin from the leaf axil followed by a burst of CK. *CUC1-3* are redundantly required for AM initiation functioning downstream of LFY and RAX1 to promote *LAS*. *LOF1/2* contributes to *RAX1* promotion. *CUC1*, *LAS*, and *ROX* activities are required for sustained expression of *STM* and establishment of the AM. (**B**) IM activity. PNY and PNF restrict *BOP1/2-ATH1-KNAT6* expression to boundary domains flanking the IM essential for meristem maintenance and flowering (white). FMs (duck gray). MP directly activates ANT and LFY to initiate FM formation. LFY directly promotes the expression of RAX1 and AP1 whose products confer floral fate. *BOPs* facilitate the establishment of FMs via the promotion of LFY expression, activation of AP1, and repression of IM identity genes. Inflorescence architecture; BP and PNY are expressed in the stem cortex where they collectively promote internode elongation, stem differentiation, phyllotaxy, and pedicel angle by restricting boundary genes *BOP1/2* and downstream effectors ATH1 and KNAT6 to the pedicel axil (green). *CUC2* expression is restricted by miR164 to the pedicel axil to maintain internode patterning. (**C**) Summary of gene networks at the meristem-boundary interface. (**D**) Summary of interactions at the leaf-boundary interface. FM, floral meristem; IM, inflorescence

meristem. CK, cytokinin; BR, brassinosteroid; GA, gibberellin; and IAA. Red and white lettering, SAM-leaf boundary genes. Red arrows, direct regulation. Dashed line, putative interaction, inhibition symbols, repression, blue arrows indicate the direction of auxin flow, respectively. Adapted from (Hepworth & Pautot, 2015; Xue *et al.*, 2020).

The FMs are AMs with a determinate fate that formed in the axil of leaves whose rapid proliferation represses outgrowth of the subtending leaf (Long & Barton, 2000). The initiation of flowers (Fig. 1B) is an auxin-dependent process similar to that in leaves. LFY and APETALA1 (AP1) are the major regulators of FM identity in *Arabidopsis* (Blázquez *et al.*, 2006; Liu *et al.*, 2009). Auxin responsive transcription factor *MONOPTEROS* (*MP*) directly activates *AINTEGUMENTA* (*ANT*) and *LFY* to initiate FM formation but does not bind to the *LFY* promoter during the vegetative stage indicating (Yamaguchi *et al.*, 2013). *LFY* reinforces this loop via direct activation of *RAX1*, *AP1* and *CAL* genes whose products confer floral fate in the auxin pathway (Wagner *et al.*, 1999; William *et al.*, 2004; Winter *et al.*, 2011; Yamaguchi *et al.*, 2013). Genetic studies reveal that *BOPs* facilitate the establishment of FMs via the promotion of *LFY* expression (Karim *et al.*, 2009), the proliferation of the floral meristem, and determinacy in part through direct activation of *AP1* and repression of IM identity genes (Xu *et al.*, 2010). Loss-of-function of the *Arabidopsis NBCL* (*bop1bop2*) also causes subtle defects in floral-meristem identity signified by enlarged floral bracts, a delay in the node of the first flower, the occasional absence of cauline leaves at the base of lateral branches, and branched flowers (Ori *et al.*, 2000; Norberg *et al.*, 2005; Xu *et al.*, 2010). Inactivation of *BOP1/2* or *CAL* greatly enhances the floral branching defect in *ap1* mutants caused by derepression of CK biosynthesis in sepal axils leading to ectopic FM initiation and loss of shoot determinacy (Levin & Meyerowitz, 1995; Xu *et al.*, 2010; Han *et al.*, 2014). In lotus, combinations of inflorescence organizations highlight the crucial role of the *LjNBCL1* gene for the floral meristem fate acquisition. In *Ljnbcl1*, the secondary inflorescence meristem and floral primordia also were affected in a very early stage (Magne *et al.*, 2018b)

8. The *NBCL* genes in lateral organ boundary regulation

Boundaries are domains of restricted growth that maintain the balance, propagation of stem cells at the center of the meristem and the initiation of organs at the periphery, by separating the meristem from the growing primordia and by forming an interface between organs (Žádníková & Simon, 2014). Lateral organ boundaries

are specialized junctions in different regions of the plant body and have diverse functions in development. One role is to separate different cell groups from the meristem or plant body and the second important role of boundary zones is the formation of new meristems (Aida & Tasaka, 2006a; Rast & Simon, 2008). There are two types of boundaries in the developing shoot apices. M-O (meristem-organ) boundaries separate leaf and flower primordia from the SAM, whereas O-O (organ-organ) boundaries develop between individual floral organs and create space between them (Norberg *et al.*, 2005; Fu & Dong, 2013).

In general, boundaries are characterized by a low number of cell divisions (Hussey, 1971; Reddy *et al.*, 2004) and specific patterns of gene expression (Souer *et al.*, 1996; Aida *et al.*, 1997; Takada *et al.*, 2001; Vroemen *et al.*, 2003; Weir *et al.*, 2004; Berger *et al.*, 2009). The boundary separates the SAM from the primordia that rely on the depletion of auxin and BR from boundary cells thereby maintaining a low rate of growth relative to surrounding tissues (Fig. 1C). Spatial regulation of polar auxin transporters is accomplished in part by PIN-FORMED1 (PIN1) (Heisler *et al.*, 2010) and required CUC2, which is repressed by miR164 and auxin. JAGGED LATERAL ORGANS (JLO) has been identified as a modulator of boundary establishment in Arabidopsis (Borghi *et al.*, 2007), which encodes a transcription factor of the LBD family and expressed at the boundary between the SAM and organ primordia (Borghi *et al.*, 2007; Bureau *et al.*, 2010; Rast & Simon, 2012). The LBD transcription factor LOB maintains low levels of BR to inhibit growth at boundaries (Bell *et al.*, 2012; Gendron *et al.*, 2012), which was identified as an enhancer trap line showing expression in the boundaries between meristems and lateral organs (Shuai *et al.*, 2002). Auxin-induced BR in the leaf activates LOB1 (Chung *et al.*, 2011) which in turn directs activation of cytochrome P450 gene BAS1 to inhibit BR accumulation at the boundary (Bell *et al.*, 2012). BOP1 and BOP2 reinforce this pattern by promoting LOB1 expression in the boundary domain (Ha *et al.*, 2007). BR-activated transcription factor BRASSINOZOLE-RESISTANT1 (BZR1) fails to accumulate in the nuclei of boundary cells thereby allowing expression of CUC genes which in turn repress growth at the boundary (Gendron *et al.*, 2012). In addition, *CUC2* was found to bind to the *LAS* promoter, positively regulating its expression (Tian *et al.*, 2014). Two *ALOG* (*Arabidopsis LSH1* and *Oryza G1*) family members *ORGAN BOUNDARY1/LIGHT-DEPENDENT SHORTHYPOCOTYL* (*OBO1/LSH3*) and

OBO4/LSH4 genes were the only known direct targets of *CUC1* and thought to repress differentiation of boundary cells (Cho & Zambryski, 2011; Takeda *et al.*, 2011). They are specifically expressed in the boundary zones of shoot organs.

The expression patterns of *Arabidopsis BOP1/2* define them as markers of the lateral organ boundary (Ha *et al.*, 2004; Norberg *et al.*, 2005; Hepworth *et al.*, 2005; McKim *et al.*, 2008; Xu *et al.*, 2010; Khan *et al.*, 2012b). In the boundary, *BOP1/2* genes modulate differentiation and growth through the repression of class I *KNOTTED1*-like homeobox (*KNOX*) genes (Ha *et al.*, 2003, 2007). KNOX activity provides a positional cue in establishing the SAM-leaf boundary (Bolduc *et al.*, 2012; Johnston *et al.*, 2014; Tsuda *et al.*, 2014). Grasses have a blade-sheath boundary containing hinge-like auricles that control leaf angle and a fringe of epidermal tissue called the ligule whose formation is under the control of boundary genes. Transcriptomic studies in maize focusing on the blade-sheath boundary of leaves further reveal that *CUCs*, *TALEs*, and *BOPs* are downstream targets of *KNOTTED1* (*KN1*) under positive regulation (Bolduc *et al.*, 2012; Johnston *et al.*, 2014). The *UNICULME4* is a *BOP* homolog required for ligule outgrowth either in Barley or *Brachypodium* (Tavakol *et al.*, 2015; Magne *et al.*, 2020). Taken together, the common feature is that these genes contribute to the establishment of a critical zone, called the boundary zone, which is delimiting the development of different morphological structures, such as cotyledons, leaves, leaflets, floral organs, and ovules.

9. The role of *NBCLs* in leaf formation and patterning

The architecture of flowering plants observed in nature shows an enormous heterogeneity. This variation is, to a large extent, caused by differences in the form of their leaves and the branching patterns of their shoots. Leaves are the sites of photosynthesis and are the main carbon source for higher plants.

In angiosperms, lateral organs such as leaves initiate as small groups of homogeneous founder cells set aside on the flanks of the pluripotent SAM. These leaf primordia are separated from the main shoot through the establishment of a boundary between the organ-forming cells and the meristem cells that provides a permissive environment for differentiation. During the final stages of leaf development, cell and tissue specification occurs through coordinated processes of cell division, expansion, and differentiation along the proximal-distal, adaxial-abaxial and central-lateral axes

(Waites & Hudson, 1995; Engstrom *et al.*, 2004). Dependent on the species-specific genetic program and environmental conditions, leaf primordia develop either into simple leaves or into compound (complex) leaves. Simple leaves have an undivided leaf blade, whereas compound leaves of typical eudicots have a divided blade composed of several pairs of leaflets, which originate from a zone of transient organogenetic activity at the leaf margins, the marginal blastozone (Hagemann & Gleissberg, 1996). Individual leaflets of a complex leaf are separated from each other and their central stalk, called the rachis, by boundary zones. In both cases, a narrow petiole joins the blade to the stem (Champagne & Sinha, 2004; Hay & Tsiantis, 2010). The boundary zones between the meristem and leaf primordia show similar properties to the boundaries between leaflets (Busch *et al.*, 2011), supporting the view that these are homologous structures as a result of descent from an ancestral shoot system (Floyd & Bowman, 2010).

Threshold levels of auxin trigger activation of the auxin-responsive transcription factor MP, which down-regulates *STM* and activates *ANT* and ASYMMETRIC LEAVES1 (*AS1*) genes to initiate leaf development (Long & Barton, 1998; Besnard *et al.*, 2011; Yamaguchi *et al.*, 2013). Leaf differentiation requires the maintenance of *KNOX* repression, which is accomplished by an interacting network of leaf and boundary factors, and the restriction of *CUC2/3* expression along the leaf margin. In this network (Fig. 1D), *AS1* as a key player that acts in a trimeric complex with the *LBD* transcription factors AS2 and JLO (Guo *et al.*, 2008; Rast & Simon, 2012). BOP1/2 activity in organ initials partially overlaps with *JLO* and likewise resolves to the boundary of emerging leaves and petiole domains during outgrowth (Ha *et al.*, 2004; Norberg *et al.*, 2005; Hepworth *et al.*, 2005; Borghi *et al.*, 2007). *BOP1/2* has a dual function, which represses genes that confer meristem cell fate and induce genes that promote lateral organ fate and polarity (Ha *et al.*, 2007). BOP1/2 transcripts are first detected in the boundaries of the torpedo stage embryos consistent with a function downstream or in parallel with *CUCs* (Ha *et al.*, 2004). *STM* represses *BOP1/2* to maintain indeterminacy and conversely, *BOP1/2* restricts *KNOX* expression to pattern the leaf, and *BOP1* binds directly to the promoter of *AS2* likely recruited by a TGA factor (Jun *et al.*, 2010). A prolonged phase of morphogenetic competence in *bop1 bop2* petioles coupled with KNOX reactivation results in the initiation of ectopic leaflets reminiscent of development in a compound leaf (Ha *et al.*,

2003, 2007; Khan *et al.*, 2014). Synergistic enhancement of meristematic activity in *bop1 bop2 as1* and bop1 bop2 as2 petioles shows that *BOP1/2* repression of *KNOX* genes is not entirely via *AS1-AS2* and is likely indirect. Leaf patterning defects in *bop1 bop2* are also attributed to misexpression of abaxial/adaxial organ polarity determinants and the C2H2 zinc finger transcription factor JAGGED (JAG) which promotes cell proliferation (Norberg *et al.*, 2005; Ha *et al.*, 2007; Jun *et al.*, 2010) and was restricted to the distal blade where it represses *BOP2* to allow extension of the leaf margin (Schiessl *et al.*, 2014). The rachis of a compound leaf is likewise sensitive to alterations in *KNOX-PIN-CUC* expression. While simple leaves have a single undivided blade in which KNOX repression is continuous, compound leaves have a divided blade consisting of pairs of leaflets attached to a central rachis. Down-regulation of tomato *BOPa* (one of three homologs) further enhances leaf complexity by extending the window for rachis responsiveness to auxin (Ichihashi *et al.*, 2014). *BOPa* fulfills this function in part by forming a complex with *LSH3b* (an ALOG family member) that represses tomato *KNATM* encoded by *KD1/PETROSELINUM* to modulate *KNOX* activity (Ichihashi *et al.*, 2014).

In Pea , the *Pscoch* mutant is affected in stipule formation (Wellensiek, 1959; Blixt, 1967; Couzigou *et al.*, 2012). At the base of leaves and stipules, PsCOCH1 inhibits PsUNI to prevent blastozone fate in stipule primordia and generate simple foliaceous stipules (Gourlay *et al.*, 2000) and avoid stipule primordia to form the compound leaf-like structure in the leaf-blade program (Kumar *et al.*, 2009). In the *Medicago noot1* mutant, the stipules were simplified and in all *noot* alleles, the number of digitations remains low throughout the development of the plant (Couzigou *et al.*, 2012). In the *Ljnbcl1: LORE1* mutants, the nectary glands which were proposed to be modified stipules (Heyn, 1976), are completely absent and the leaves with additional leaflets (Magne *et al.*, 2018b).

10. The *NBCL* genes control flowering-time, inflorescence architecture and internode patterning

The switch to flowering is governed by internal signals, including age, sugar content, and gibberellin (GA), in conjunction with external cues based on photoperiod, vernalization, ambient temperature, and responsiveness to light or stress stimuli (Srikanth & Schmid, 2011; Wang, 2014). Inputs from flowering-time path-ways converge to regulate the expression of a small number of genes with floral integrator

activity including *LEAFY*(*LFY*), *FLOWERING-TIME LOCUS* T (*FT*) and *SUPPRESSOR OF OVEREXPRESSION OF CONSTANS1* (*SOC1*) whose upregulation in shoot apices promotes the production of an inflorescence (Parcy, 2005). LFY is the central floral meristem identity regulator in Arabidopsis and its loss-of-function generates a large increase in secondary inflorescences, floral bracts, and some branched flowers (Schultz and Haughn, 1991; Weigel et al.,1992).

FT is a central component of the photoperiod response (Srikanth & Schmid, 2011; Andrés & Coupland, 2012), and encodes a small globular protein that shares high homology with mammalian phosphatidylethanolamine-binding proteins/Raf-1 kinase inhibitory protein. It is synthesized in leaves and travels through the phloem to the SAM (Kardailsky *et al.*, 1999; Kobayashi *et al.*, 1999; Corbesier *et al.*, 2007; Jaeger *et al.*, 2007; Mathieu *et al.*, 2007; Tamaki *et al.*, 2007; Kanehara *et al.*, 2014; Romera-branchat *et al.*, 2014). At the meristem, FT is proposed interacts with the bZIP transcription factor FD to activate down-stream genes conferring inflorescence identities, such as the MADS-box transcription factors *FRUITFUL* (*FUL*), *AGAMOUS-LIKE24* (*AGL24*) and *SOC1* (Abe *et al.*, 2005; Teper-bamnolker & Samach, 2005; Wigge *et al.*, 2005). During the transition to flowering, *AGL24*, *SOC1*, and *FUL* are upregulated in shoot apices to drive the production of primary and secondary inflorescences (Mandel & Yanofsky, 1995; Hempel *et al.*, 1997; Ferrándiz *et al.*, 2000; Yu *et al.*, 2002). These factors in turn promote the expression of floral meristem identity genes *LFY*, *AP1*, and *CAL*, which confer floral fate (Bowman *et al.*, 1993; Xu *et al.*, 2010; Andrés *et al.*, 2015).

BOP1 and *BOP2* are involved in flowering-time regulation by repressing the expression of *FD* in the SAM, also have a role in controlling floral initiation with delayed flowering in *bop1 bop2* mutants. However, this delay is to a large extent caused by a slower leaf initiation rate in *bop1 bop2* (Andrés *et al.*, 2015).

Flowering plants display a remarkable variety of inflorescence architectures selected to optimally display flowers for pollination and seed dispersal. Spatial regulation of *BOP1/2* expression is an important determinant of inflorescence architecture. Genetic and expression studies show that by the localized misexpression of lateral organ boundary genes *KNAT6*, *ATH1*, *BOP1/2* and to a lesser extent *KNAT2* in stems results in *bp* (*BREVIPEDICELLUS*, *BP*) and *pny* inflorescence defects (Ragni *et al.*, 2008; Khan *et al.*, 2012b,a). *BOP1/2* requires the functions of these downstream genes to

exert changes in inflorescence architecture suggesting a linear pathway (Khan *et al.*, 2012b,a). *BOP1* directly activates *ATH1* whereas activation of *KNAT6* is indirect (Khan *et al.*, 2015). *BOP1* directly activates *AS2* whose product is a transcriptional repressor of *BP* (Jun *et al.*, 2010). *BP/STM* was recently shown to promote xylem differentiation in the cambium through the repression of *BOP1* and *BOP2* (Liebsch *et al.*, 2014). Thus, the restriction of the *BOP1/2-ATH1-KNAT6* boundary module by *BP-PNY* is critical for plant architecture. Arabidopsis *BOP1/2* expression in the primary stem is excluded from internodes and restricted to lateral organ boundaries in the axils of pedicels (Khan *et al.*, 2012b). Gain-of-function studies revealed that BOP misexpression in stem tissue alters the length and pattern of internode elongation (Norberg *et al.*, 2005; Ha *et al.*, 2007; Khan *et al.*, 2012b,a). Strong BOP-o/e lines have short irregular internodes similar to *bp pny* double mutants and broad leaves with a short petiole because of *BOP1/2* act downstream of *BP-PNY* in functional opposition (Norberg *et al.*, 2005; Khan *et al.*, 2012b). In the lotus *Ljnbcl1* mutant inflorescences, one additional adaxial bract, maximum three were displayed. In addition, fused trumpet-like lamina structure and cryptic bract were observed and more than 56 different combinations of inflorescence organization were observed in *Ljnbcl1* mutants (Magne *et al.*, 2018b). In monocot, the *BOP* homolog *laxatum-a* (*lax-a*) in barley (*Hordeum vulgare*) also required for controls internode length and homeotic changes of the inflorescence (Jost *et al.*, 2016). Recently, the *BdCUL4* and *BdLAXA*, *BOPs* homolog in *B. distachyon* were shown to be antagonistically required for the control of inflorescence architecture (Magne *et al.*, 2020).

11. The role of *NBCL* genes in floral patterning and symmetry

Typical eudicot flowers are composed of four concentric whorls of organ types: the protective sepals, the showy petals, the male stamens, and the female carpels (Alvarez-Buylla *et al.*, 2010). Floral-meristem identity factors *LFY* and *AP1* provide A-class activity by promoting sepal and petal identities and by antagonizing C-class function in the outer whorls. Similar A-class activity for *BOP1/2* was revealed by triple mutant analyses with *lfy* and *ap1* (Causier *et al.*, 2010). The arrangement of floral organs in most eudicot flowers is tetramerous or pentamerous. The option for dorsal-ventral (adaxial-abaxial) asymmetry is superimposed on this pattern (Smyth, 2005). Loss-of-function *bop* mutations in *Arabidopsis*, pea, and *M. truncatula* all increase the number of floral organs and perturb dorsal-ventral growth patterns,

altering flower symmetry (Yaxley *et al.*, 2001; Hepworth *et al.*, 2005; Couzigou *et al.*, 2012). Flower symmetry is also affected, with the formation of additional organs (Ha *et al.*, 2003; Norberg *et al.*, 2005; Xu *et al.*, 2010). During reproductive development, *BOP1* transcripts are detected in young floral buds, and at the base of the sepals and petals. *bop1 bop2* mutant flowers are frequently subtended by bract-like organs developing ectopically on the inflorescence. The mutant flowers have an open structure with two petaloid, in which the abaxial sepals are missing, irrespective of whether the flowers are subtended by bracts or not (Norberg *et al.*, 2005; Hepworth *et al.*, 2005; McKim *et al.*, 2008). Typical pea *coch* flowers are dorsalized with enlarged floral bracts and supernumerary organs in all whorls (Yaxley *et al.*, 2001; Kumar *et al.*, 2011; Couzigou *et al.*, 2012; Sharma *et al.*, 2012). The patterning changes in *bop1 bop2* and *coch* mutants seem to be concentrated on the abaxial (ventral) side of the floral meristem. Dorsalization of *coch* flowers suggests that *COCH* might inhibit ventral expression of *CYCLOIDIA-TCP* genes to maintain asymmetry. *BOP1* and *BOP2* act redundantly during reproductive development to control bract suppression, floral patterning, and floral organ number. In addition, the defect in gynoecium formation was observed, with half of the *bop1-4 bop2-11* gynoecia contained only a single, fertile carpel (Ha *et al.*, 2007).

PsCOCH1 was shown to be required for the *P. sativum* inflorescence development and flower organ identity acquisition (Yaxley *et al.*, 2001; Couzigou *et al.*, 2012; Sharma *et al.*, 2012). The *Pscoch1* mutant displays a range of phenotypes from normal flowers to open ones, which lead to quick drying of the pollen that largely reduced self-fertility, and show supernumerary organs at each whorl with abnormal organ fusion and aberrant organ mosaic (Yaxley *et al.*, 2001; Couzigou *et al.*, 2012). The number and the development of stamens are also affected and more or less ten abnormally fused anthers are present. In addition, up to 4 occasionally fused carpels may be present in *Pscoch1* mutant (Yaxley *et al.*, 2001) and more complex bracts are present in mutant flowers (Couzigou *et al.*, 2012). In *Medicago noot1* mutant, the flower modification is subtle and all the *noot* alleles possess additional organs (petals and stamens) in flowers (Couzigou *et al.*, 2012). In the lotus *Ljnbcl1:LORE1* mutants the first striking phenotype is their defective flower development leading to almost complete sterility (Magne *et al.*, 2018b).

In monocotyledon, mutation of *BOP* homologs *HvLAX-A* and *BdLAXA* results in additional stamenoid lodicule or stamen organs in barley and *Brachypodium*, respectively (Jost *et al.*, 2016; Magne *et al.*, 2020). The modified development of the flower in *Arabidopsis*, pea, *M. truncatula*, barley, and *Brachypodium* indicates that the *NBCL* genes have a conserved function in floral organs in eudicot and monocot plants.

12. The *NBCL* genes involved in shoots and inflorescence branching

The multitude of plant forms observed in nature is the result of the activities of different meristems during postembryonic development. In seed plants, the primary axis of growth, together with the primary shoot and root apical meristems, is laid down during embryonic development. A major aspect of post-embryonic plant development is the formation of secondary axes of growth: vegetative branches, inflorescence branches, or flowers. In vegetative development, axillary meristems initiate the formation of several leaf primordia, resulting in an axillary bud. The pattern of vegetative shoot branching depends not only on the initiation of axillary meristems in the leaf axils but also on the regulation of bud outgrowth (Shimizu-Sato & Mori, 2001).

Plants overexpressing *AtBOP1/2* show a branching phenotype, producing extra paraclades in leaf nodes (Ha *et al.*, 2007). Loss-of-function bop1 bop2 also causes branched flowers (Norberg *et al.*, 2005; Ha *et al.*, 2007; Xu *et al.*, 2010). *BOPs* promote floral meristem determinacy at two steps. At late stage 2, *BOP1/2*, *LFY*, and *AP1* activities converge in blocking the continued expression of inflorescence meristem identity genes (Liu *et al.*, 2009; Xu *et al.*, 2010). Prolonged expression of *AGL24* in *ap1-1* and *lfy* flowers is associated with “branching” caused by the ectopic initiation of second-order floral meristems in the axils of sepals (Liu *et al.*, 2009). Branching complexity and misexpression of inflorescence identity genes is dramatically enhanced in *bop1 bop2 ap1* and *bop1 bop2 lfy* triple mutants with phenotypes suppressed by loss-of-function *agl24*. These genetic interactions suggest a role for *BOP1/2* in maintaining determinacy through repression of *AGL24* (Xu *et al.*, 2010). Furthermore, enlarged floral bracts and branched flowers are also found in *coch* mutants, indicating a conserved function in pea (Yaxley *et al.*, 2001; Couzigou *et al.*, 2012). The pea ortholog of *AP1* is *PROLIFERATING INFLORESCENCE MERISTEM* (*PIM*) (Taylor *et al.*, 2002). Flowers in *pim coch* double mutants are

similarly replaced by highly branched leafy shoots. Recently, it was reported that *BOP* is directly activated by teosinte branched (*tb1*) to regulate axillary bud growth in maize (Dong *et al.*, 2017). The BOP-Like gene *UNICULME4* controls tillering in barley (Tavakol *et al.*, 2015), in *Brachypodium* the *BdUNICULME4* and *BdLAXATUM*-A act antagonistically to control the branching (Magne *et al.*, 2020).

13. The role of *BOP* in fruit architecture and lignin biosynthesis

The architecture of the inflorescence, which conditions how many flowers (and therefore, fruits and seeds) are produced, and their position in the plant, has a profound impact on key agronomical aspects such as crop management, yield, and yield stability. Preliminary evidence suggests that an antagonistic interaction between KNOX-BELL and BOP1/2 activities also governs the architecture of fruits. The *Arabidopsis* silique is a fruit pod composed of two fused carpels (termed valves after fertilization which representing modified leaves) joined at their margins to a meristematic replum that generates seeds attached to the interior (Ferrándiz *et al.*, 2010). Many interactions defining the SAM-leaf boundary are conserved in ovule and fruit development (Ferrándiz *et al.*, 2010; Reyes-Olalde *et al.*, 2013; Arnaud & Pautot, 2014). *BP* and *PNY* provide meristematic function in the replum and set the expression boundaries of genes that confer valve identity (Roeder *et al.*, 2003; Alonso-Cantabrana *et al.*, 2007). The valve margin expresses a pair of stage-specific MADS-box transcription factors encoded by boundary genes *KNAT2/6* and *BOP1/2* that are activated later during carpel development (Liljegren *et al.*, 2000; Ragni *et al.*, 2008; Khan *et al.*, 2012b). Inactivation of bop1 bop2 or knat2 knat6 rescues replum formation in *pny* fruits, consistent with their co-expression in the valve margins (Ragni *et al.*, 2008; Khan *et al.*, 2012a).

The collective downstream targets of KNOX and BELL TFs include genes that modulate the abundance of cytokinins and gibberellins and that encode enzymes for cell wall remodeling and lignin biosynthesis (Mele *et al.*, 2003; Hay & Tsiantis, 2010; Etchells *et al.*, 2012; Townsley *et al.*, 2013). *BP* and its orthologs repress secondary stem development (Mele et al., 2003; Townsley et al., 2013). *BOP1*/2 and *BP* have opposing roles in the maturing stem where they function as antagonistic regulators of lignin biosynthesis (Khan *et al.*, 2012b). BOP-o/e stems have an expanded pattern of lignification similar to *bp pny* double mutants, consistent with a promotive role for *BOPs* in lignin biosynthesis (Smith & Hake, 2003; Khan *et al.*, 2012b). Genetic and

biochemical data suggest that *BP* directly represses lignin biosynthesis genes in the stem (Mele *et al.*, 2003) and lignin biosynthesis genes whose transcripts are upregulated in bp stems (*PAL1*, *C4H1*, *4CL1*, *C3H1*, *CAD5*, and *PRXR9GE*) were restored to near wild-type levels by *bop1 bop2* mutation (Mele *et al.*, 2003; Khan *et al.*, 2012b). Four of these same genes are dramatically up-regulated in BOP-o/e stems and reinforced the role of *BOP* in the promotion of lignin biosynthesis. *BP* repression of *BOP1/2* in the stem delays the differentiation of lignified interfascicular fibers, thereby maintaining indeterminacy until internode elongation is complete (Khan *et al.*, 2012b). Interestingly, *BOP1/2* misexpression in the root and hypocotyl has a selective impact on xylem differentiation during the expansion phase where the production of lignified fibers and vessels is blocked (Liebsch *et al.*, 2014).

A role for *BOPs* in the regulation of lignin biosynthesis is strengthened given that boundaries specialized for floral organ abscission and pod shatter undergo lignification as a normal part of development (Hepworth & Pautot, 2015; Woerlen *et al.*, 2017).

14. *NBCLs* are essential for differentiation and separation of abscission in dicot

Plants alter their body plan in response to developmental and environmental cues by the addition of lateral organs, such as leaves and flowers. However, plant form is also shaped by the removal of these organs. Organs may be actively shed by the plant in a developmentally regulated process known as abscission (Patterson, 2001; Chuck *et al.*, 2002; Lewis *et al.*, 2006; Patterson *et al.*, 2016). Lateral organ boundaries at defined positions are specialized in detachment or release: abscission mediates the detachment of spent or diseased organs from the plant body whereas dehiscence mediates the release of seeds and pollen from fruit and anther compartments, respectively (Aida & Tasaka, 2006a; Rast & Simon, 2008). Primary abscission zones (AZs) at the site of the detachment of leaves, floral organs, and fruits differentiate simultaneously with lateral organs at the boundaries where they are connected to the plant body (Estornell et al., 2013). Prior to shedding, cells in the abscission zone become responsive to an integrated set of hormonal, developmental, and/or environmental signals leading to abscission. Responsiveness to these signals requires a pair of leucine-rich receptor-like kinases, HAESA, and HEASA-LIKE2, whose ligand is a secreted peptide called INFLORESCENCE DEFICIENT IN

ABSCISSION (*IDA*) (Liljegren, 2012). After the organ is shed, the cells exposed at the AZ on the plant body differentiate to form a protective surface (Patterson, 2001).

BOPs are essential in abscission, a process that merges potential functions in development and defense (Roberts *et al.*, 2002; McKim *et al.*, 2008; Wu *et al.*, 2012). A variety of plant species lacking BOP activity fail to form an AZ (McKim *et al.*, 2008; Couzigou *et al.*, 2012; Wu *et al.*, 2012). *BOP1/2* quite possibly perform this function via *ATH1* and *KNAT2/KNAT6*. Inactivation of *ATH1* has a mild abscission defect in which the formation of the stamen AZs is delayed. A functional AZ eventually develops and organs detach (Gómez-Mena & Sablowski, 2008). In Arabidopsis, only the floral organs abscise but vestigial abscission zones differentiate at the base of cauline leaves and pedicels (Norberg *et al.*, 2005; Hepworth *et al.*, 2005; McKim *et al.*, 2008). In tobacco, a NtBOP2: GUS fusion was expressed in the receptacle where overexpression of antisense *NtBOP2* blocks differentiation of the corolla abscission zone and delays petal senescence in transgenic flowers (Wu *et al.*, 2012).

In contrast, *NBCL* genes are regulating the abscission of multiple organs (fruits, floral pieces, leaflets, and leaves) in different legume species including *Lotus japonicus*, *M. truncatula*, and *P. sativum* (Couzigou *et al.*, 2015). The petals stay attached to the pod of mutant plants throughout their development and even after pod dehiscence (Couzigou *et al.*, 2015). The *Ljnbcl* mutant retains all of the senescing leaves even when completely dried and leaflets remained more attached to the rachis on *coch* mutants than the corresponding WT plants; in the *noot* background, leaves, leaflets, and pods remained attached to the plant body even after they reached complete maturity or senescence. Interestingly, fruit abscission is only observed in *noot* mutant. Instead, *L. japonicus* and *P. sativum* use pod dehiscence as a seed dispersal strategy (Couzigou *et al.*, 2015). However, the abscission phenotype was not observed in monocots, such as *Brachypodium*, where the mutations of *BOPs* homologs, either *BdCUL4* or *BdLAXA* were not required for AZ formation (Magne *et al.*, 2020).

15. *BOPs* interact with other factors to mainten development

NBCL genes encode plant-specific co-transcriptional factors containing BTB/POZ domains and without the DNA-binding domain. TGA bZIP proteins are a distinct subclade in the bZIP superfamily (Jakoby *et al.*, 2002). NPR1 exerts most or

all of its function via TGA factors based on genetic evidence: systemic acquired resistance is abolished in *tga2 tga5 tga6* triple mutants recapitulating the *npr1* mutant phenotype (Zhang *et al.*, 2003). BOP1/2 physically interacts with a subset of TGA factors (Fig. 2) including PERIANTHIA (PAN), a class V TGA, to regulate flower development, particularly sepal numbers (Hepworth *et al.*, 2005). Recently, Wang *et al.*, (2019) demonstrate that BOP1 and BOP2 and two clade I TGA proteins, TGA1 and TGA4, together regulate meristem maintenance and inflorescence architecture and they associate with the same promoter region of ATH1. In addition, TGA1 and TGA4 are required for BOP2 promotion of stem elongation. BOP2 also interacts with the CULLIN3 ubiquitin ligase and recruits PHYTOCHROME INTERACTING FACTOR4 (Zhang et al., 2017) or LEAFY TFs (Chahtane *et al.*, 2013) as ubiquitination substrates for degradation, to modulate photomorphogenesis/ thermomorphogenesis or flower identity, respectively. Previous studies in inflorescence development in tomato have shown that *TMF* (*LSH6*), which affect vegetative/reproductive transition (Chakrabarti *et al.*, 2013), interacts with three *Solanum lycopersicum BLADE-ON-PETIOLE* genes (*SlBOPs*) and *BOPa* (MacAlister *et al.*, 2012; Xu *et al.*, 2016), and that *LSH3b* interacts with *BOPa* and also binds to the PETROSELINUM (PTS) promoter (Kemmeren *et al.*, 2002; Ichihashi *et al.*, 2014), this suggests that *BOPa* can physically interact with *LSH* (Kimura *et al.*, 2008), and might affect KNOX targets via regulation of PTS expression (Ichihashi *et al.*, 2014).

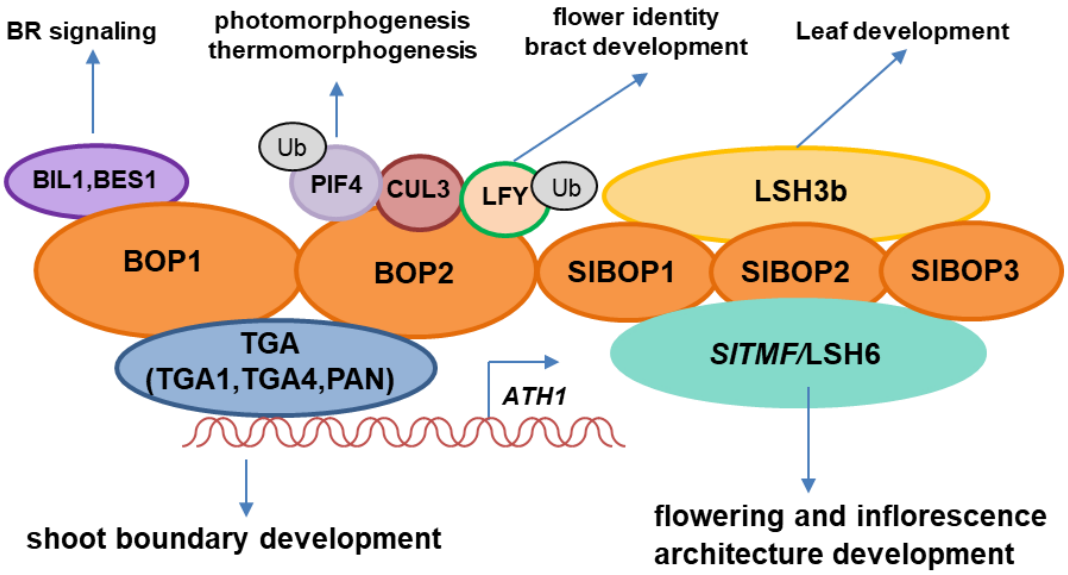

Figure 2. Schematic representation of interacting partners of BOPs in *Arabidopsis* and tomato.

In *Arabidopsis*, *BOP1* and *BOP2* interact with TGA TFs including TGA1, TGA4, and *PERIANTHIA* (*PAN*). TGA1 and TGA4 bind to the promoter of *ATH1*, which regulates the boundary development of shoot organs. *BOP1* interacts with *BRZ-INSENSITIVE-LONG HYPOCOTYL 1* (*BIL1*)/*BRASSINAZOLE-RESISTANT1* (*BZR1*) or *BRI1-EMS-SUPPRESSOR1* (*BES1*), which are master regulatory TFs in BR signaling. *BOP2* also interacts with *CULLIN3* (*CUL3*) ubiquitin (Ub) ligase and targets ubiquitination substrates including *PHYTOCHROME INTERACTING FACTOR4* (*PIF4*) in photomorphogenesis and thermomorphogesis, and *LEAFY* (*LFY*) in bract and flower development. In tomato, the *BOPs* interact with *ALOG* (*LSH3b* and *LSH6/slTMF*) to control the inflorescence architecture and flower development. Adapted from (Yu, 2019a).

16. The other roles of *BOPs*

BOP1/2 are expressed in roots according to *in silico* and the microarray data (Brady et al. 2007) and transcript analyses (Hepworth *et al.*, 2005), patterns of expression for *BOP1* and *BOP2* were nearly identical. Both genes were expressed in root vasculature, particularly in the upper region of the maturation zone. However, the analysis of mutants showed no significant changes in either the length of primary roots or the number of lateral roots in mutants compared to wild-type control plants, suggesting that *BOP1/2* activity is dispensable for normal development of primary and lateral roots. In addition, a role for *BOPs* genes was found in *Arabidopsis* root organ development in which *BP/STM* promote xylem differentiation through the repression of *BOP1* and *BOP2* (Liebsch *et al.*, 2014; Woerlen *et al.*, 2017)(Liebsch *et al*., 2014; Woerlen *et al*., 2017).

BOPs and NPR1 share homologous functional domains and the *NPR1* signaling mechanism serves as a paradigm for *BOPs*. *BOPs* are involved in the trade-off between development and defense. Indeed, *AtBOP* genes are overall associated to plant developmental processes but they were also shown to be involved in the regulation of plant defenses, especially in the methyl jasmonate induced resistance (Canet *et al.*, 2012). *BOP1* functions as a transcriptional co-activator in the nucleus but this activity is salicylic acid-independent (Canet *et al.*, 2010; Jun *et al.*, 2010). A more detailed role of BOPs was reviewed by (Khan *et al.*, 2014).

17. PhD objectives and structure of the manuscript

The objective of my thesis work was to better understand the role of the *NBCL* genes in legume and monocot plant development. This work on *NBCL* genes was initiated in the laboratory by the description of the *Medicago noot* and pea *coch1* mutant (Couzigou et al., 2012). K. Magne followed this work during his PhD and I

participated (co-author) in some of his PhD work and publications on the characterization of the *Medicago NOOT2* (Magne et al., 2018) and *Brachypodium NBCL* genes (Magne et al., 2020). These parts are not presented in my manuscript.

The work presented in my PhD manuscript corresponds to the following of these PhD works on legume and monocot plants. The 4 chapters of the manuscript are presented as papers. The figures and supplementary figures for future papers are included in the text to facilitate reading. Supplementary Tables are placed at the end of the chapters. To avoid redundancy, all the references are grouped at the end of the manuscript. To present complete stories, some unpublished parts of K. Magne PhD work are also included in these chapters. The implication of K. Magne in these papers is indicated at the beginning of the corresponding paragraphs.

In the introduction of my manuscript, I have inserted several chapters corresponding to a review on nodule diversity, evolution, organogenesis, and identity (Liu et al., 2020). For the result part, I have described the phenotypes of the *nbcl* mutants in the legume plants using genetic and molecular approaches. I have characterized new phenotypes of the mutant plants in the two legumes and, using double mutants, showed that the *NBCL2* genes are also important for plant development. This work is described in the two first chapters are entitled “Legume NBCLs genes are redundantly required for aerial organ development and root nodule identity” and “ The *COCHLEATA1* gene controls branching and flowering time in pea”, respectively.

I have also constructed CrisperCas9 KO mutants in *Brachypodium* to study the role of the *BdLAXA* gene in this plant using simple and double mutants with *BdCul4*. This work shows that the two genes are essential for the *Brachypodium* development and is described in the third chapter is entitled “The *Brachypodium distachyon* BLADE-ON-PETIOLE-Like proteins *UNICULME4* and *LAXATUM-A* are redundantly required for plant development”.

In the fourth chapter, I have initiated some work on putative partners and targets of the *NOOT1* and *NOOT2* proteins in the *Medicago*. This chapter presents preliminary results and is entitled “Characterization of potential *MtNODULEROOT1* and *MtNODULEROOT2* interacting partners participating in nodule and aerial organ development”.

In the discussion part, I discussed the common role of these genes in plants.

CHAPTER I.

Legume *NBCLs* genes are redundantly required for aerial organ development and root nodule identity

Legume *NBCLs* genes are redundantly required for aerial legume organ development and root nodule identity

Shengbin Liu[1,2] , Kevin Magne[1,2], Marion Dalmais[1,2], Jean-Malo Couzigou[1,2], Christine Le Signor[3], Abdelhafid Bendahmane[1,2], Richard Thompson[3] and Pascal Ratet[1,2, a]

[1] Institute of Plant Sciences Paris-Saclay IPS2, CNRS, INRA, Université Paris-Sud, Université Evry, Université Paris- Saclay, Bâtiment 630, 91405 Orsay, France

[2] Institute of Plant Sciences Paris-Saclay IPS2, Paris Diderot, Sorbonne Paris-Cité, Bâtiment 630, 91405, Orsay, France

[3]Agroécologie, AgroSup Dijon, Institut National de la Recherche Agronomique (INRA), Université Bourgogne Franche-Comté, 21000, Dijon, France.

* Present address: Laboratoire de Recherche en Sciences Végétales, UMR 5546 CNRS-Université Paul Sabatier, 24 chemin de Borde Rouge - Pôle de Biotechnologies Végétales
31320 Auzeville-Tolosane – France

[a] Denote corresponding authorship e-mail: pascal.ratet@cnrs.fr

ORCIDs:
(KM): 0000-0002-6779-5683; (SL): 0000-0001-7512-4225; (MD): 0000-0002-1673-3095;
(AB): 0000-0003-3246-868X; (PR): 0000-0002-8621-1495

Author contributions

SL, JMC, KM, PR, conceived the research plans. SL, JMC, KM designed the experiments, performed the research experiments and analyzed the data. CLS and RT produced the pea TILLING population and AB and MD developed the TILLING-NGS strategy. SL, KM and PR wrote the article.

Abstract

Medicago truncatula NODULE ROOT1 (*MtNOOT1*) and *Pisum sativum COCHLEATA1* orthologous genes of the *NOOT-BOP-COCH-LIKE* (*NBCL*) gene family, were identified as required for organ identity. In the *MtNOOT1* and *PsCOCH1* mutant plants, stipules present development defects and in addition flowers are modified. The *MtNOOT1* paralogous gene *MtNODULE ROOT2* (*MtNOOT2*) in *M. truncatula* and *COCH2* in *P. sativum* belongs to a NBCL subclade distinct from the one containing *MtNOOT1*. The *MtNOOT2* gene plays a key role in the establishment and maintenance of the symbiotic nodule identity. We have isolated the *PsCOCH2* mutant and shown that it is involved in nodule and aerial organs development. The *MtNOOT2* and *PsCOCH2* mutants show wild type nodules, stipules and flower development but smaller pods and seeds. In addition, the *Medicago noot1noot2* double mutant exhibits a complete loss of the stipule and flower organ identity with the formation of leaf-like stipule structures and pod-like structures from aborted floral primordia leading to sterility. Similarly, using the *Pscoch1coch2* double mutant we showed that the *PsCOCH2* gene is involved in the patterning of aerial organs such as stipules, leaves and flowers and participate to nodule formation and functioning.

In this study, we uncover a new molecular actor involved in legume plant development. Our findings support the fact that legume specific *NBCL2* genes play important roles in stipule, flower and the indeterminate nodule development, identity establishment and maintenance.

Key words:

Stipule, inflorescence, boundary, organ identity, development, *NBCL* genes, *Pisum sativum, Medicago truncatula*

INTRODUCTION

Among the *NON-EXPRESSOR OF PATHOGENESIS-RELATED PROTEIN1-LIKE* (*NPR1*-LIKE) genes family, the members of the *NOOT-BOP-COCH-LIKE* (*NBCL*) sub-clade are associated with the regulation of plant development. This clade was called *NBCL* because it groups the *M. truncatula MtNODULE-ROOT* (*MtNOOT*) genes, the *Arabidopsis thaliana AtBLADE-ON-PETIOLE1* and *AtBLADE-ON-PETIOLE 2* (*AtBOP1/2*) genes, and the *P. sativum PsCOCHLEATA1* and *PsCOCHLEATA2* (*PsCOCH*) genes (Couzigou *et al.*, 2015). The *M. truncatula* (*MtNOOT2*) and *P. sativum* (*PsCOCH2*) belong to a legume-specific NBCL subclade (*NBCL2*) (Magne *et al.*, 2018a). In lotus, only one gene exist and is called *LjNBCL1*(Magne *et al.*, 2018b). Genes belonging to the NBCL clade encode transcriptional co-factors containing Bric-a-Brac Tramtrack and Broad complex/POx virus and Zinc finger (BTB/POZ) and ankyrin repeat domains. These genes are generally expressed in lateral organ boundaries and control the architecture of leaves, fruits, flowers and nodules.

So far, the best-characterized *NBCL* genes are the *Arabidopsis AtBOP1/2* genes and the corresponding mutants have been extensively studied (Khan *et al.*, 2014; Hepworth & Pautot, 2015; Wang *et al.*, 2016). BOP1/2 have a dual function, repressing genes that confer meristem cell fate and inducing genes that promote lateral organ fate and polarity (Ha *et al.*, 2007). BOP1/2 are required for production of various determinate lateral organs including stipules, nectaries, and flowers in dicots (Khan *et al.*, 2014). *BOP* expression is down-regulated at an early stage of indeterminate inflorescence meristem (IM) formation and moves to the boundary between the meristem and axillary meristem (AM) demonstrating a transient role similar to *REGULATOR OF AXILLARY MERISTEM FORMATION* (*ROX*) (Xu *et al.*, 2010; Yang *et al.*, 2012). The *BOP1/2* genes also play important roles in regulating leaf morphogenesis and patterning (Ha *et al.*, 2003, 2007). The most dramatic developmental effect is on leaf development, with the *bop1-1* dominant-negative and *bop1bop2* null mutant leaves displaying extensive lobe formation and forming ectopic outgrowths of blade tissue along petioles of cotyledons and leaves. This phenotype suggests a role in proximal-distal organ pattern formation. Indeed, the *BOP* genes negatively regulate the expression of the class I *KNOX* genes *BREVIPEDICELLUS* (*BP*), *KNOTTED-like* from *Arabidopsis thaliana 2* (*KNAT2*), and *KNAT6* in

developing leaf primordia (Ha *et al.*, 2003, 2007; Norberg *et al.*, 2005; Hepworth *et al.*, 2005).

Tomato *SlBOP1/2* represses leaflet formation and are involved in the diversity of leaf complexity (Izhaki *et al.*, 2018). Similarly in rice *OsBOPs* determine the leaf sheath blade ratio through activation of proximal sheath differentiation and suppression of distal blade differentiation (Toriba *et al.*, 2019). Furthermore, the monocot *BOPs* are required for ligule and auricle development in barley, rice and *Brachypodium*, indicating that the *BOP* function is conserved in at least one aspect of proximal-distal patterning in grass species (Tavakol *et al.*, 2015; Toriba *et al.*, 2019; Magne *et al.*, 2020).

Gain-of-function studies revealed that BOP mis-expression in stem tissue alters the length and pattern of internode elongation, pedicel orientation, and accelerates lignin deposition via antagonism of KNOX-BELL transcription factors leading to dramatic changes in plant stature and inflorescence structure (Norberg *et al.*, 2005; Ha *et al.*, 2007; Khan *et al.*, 2012b,a). *BOP1* or *BOP2* overexpression in plants results in either short plants with floral pedicels pointing downward (Ha *et al.*, 2007) or short bushy plants with irregular internodes (Norberg *et al.*, 2005) similar to *bp-pny* (*PENNYWISE*) double mutants, and broad leaves with a short petiole (Norberg *et al.*, 2005; Khan *et al.*, 2012b).

BOP1 and *BOP2* are in addition involved in flowering-time regulation by repressing the expression of bZIP transcription factor *FD* in the shoot meristem and may also have a role in controlling floral initiation with delayed flowering in the *bop1bop2* mutants despite that this delay is to a large extent caused by a slower leaf initiation rate in *bop1bop2* (Andrés *et al.*, 2015). *BOP1* and *BOP2* act redundantly during reproductive development to control bract suppression, floral patterning, floral organ number and also gynoecium formation (Ha *et al.*, 2007). In addition, flower symmetry is also affected, with the formation of additional organs (Ha *et al.*, 2003; Norberg *et al.*, 2005; Xu *et al.*, 2010).

Preliminary evidences suggest that an antagonistic interaction between KNOX-BELL and BOP1/2 activities also governs the architecture of fruits. The Arabidopsis silique is a fruit pod composed of two valves joined at their margins to a meristematic replum that generates seeds attached on the interior. The valves are homologous structures to leaves. The valve margins that separate the valves from the replum are

lateral organ boundaries specialized in dehiscence, made of a separation layer adjacent to a layer of lignified cells required in pod shatter (Lewis *et al.*, 2006; Girin *et al.*, 2009). Last but not least, *BOP* activity in Arabidopsis and tobacco (Nicotiana tabacum) is essential for differentiation of abscission zones (McKim *et al.*, 2008; Wu *et al.*, 2012) and BOP1/2 were also shown to be required for floral organ abscission (Norberg *et al.*, 2005; Hepworth *et al.*, 2005; Xu *et al.*, 2016).

The studies on the roles of *NBCL* genes in legume originate from the discovery of the Pea *Pscochleata* (*Pscoch1*) mutant affected in stipule formation (Wellensiek, 1959; Blixt, 1967). *PsCOCH1* was later shown as required for the *P. sativum* inflorescence development and flower and nodule organ identity acquisition (Yaxley *et al.*, 2001; Couzigou *et al.*, 2012; Sharma *et al.*, 2012). The molecular characterization of the *PsCOCH1* gene lately revealed that *PsCOCH1* was orthologous to the *AtBOP* genes of *A. thaliana* (Zhukov *et al.*, 2007; Couzigou *et al.*, 2012). There is only one gene orthologous to the *AtBOP* genes in *Lotus japonicus* called *LjNBCL1*. In the *Ljnbcl1:LORE1* homozygous mutants, 13% of the leaves have additional leaflets relative to wild type, produced multiple axillaries at a single leaf axil and exhibited a significant increase in petiole length (Magne *et al.*, 2018b). Moreover, the nectary glands which were proposed to be modified stipules (Heyn, 1976), are completely absent in *Ljnbcl1*. In addition, the mutant shows striking defects in flower development leading to almost complete sterility, with the secondary inflorescence meristem and floral primordia affected in a very early stage (Magne *et al.*, 2018b). These results suggested that *LjNBCL1* is not only required for leaf patterning, nectary development, and the control of the axillary meristem numbers but also plays a crucial role in the floral meristem fate acquisition.

In the *Medicago noot1* mutant, we previously showed that stipules were simplified with the number of digitations remaining low throughout the development of the plant (Couzigou *et al.*, 2012). Furthermore, flower modification was subtle in the *MtNOOT1* mutant, suggesting a reduced penetrance of the mutation but all the *noot* alleles possessed additional organs (petals and stamens) in flowers (Couzigou *et al.*, 2012).

In this work, we isolated KO mutants for the *P. sativum COCH2* gene and constructed *coch1coch2* double mutants to study them in parallel to the *M. truncatula noot2* and *noot1noot2* mutants. We report that the *MtNOOT2* mutant displays wild

type stipules, while the *Mtnoot1noot2* double mutant exhibits an increased modification of the stipules as compared to the *MtNOOT1* mutant. Similarly the *MtNOOT2* mutant shows no modification of the flower development, in contrast to the *Mtnoot1noot2* double mutant with strongly modified flowers, often open with the pollen drying rapidly and reduced fertility. In consequence, no or a reduced number of seeds are produced in the double mutant. In *MtNOOT2* and *MtNOOT1MtNOOT2*, smaller pods and seed size were observed when compared to the R108 wild type suggesting that the *MtNOOT2* promote aerial vegetative mutant phenotypes and fruit development. Similarly, the *PsCOCH2* gene is involved in the patterning of aerial organs such as stipules, leaves, and flowers. As observed with the *noot2* mutant (Magne et al., 2020), the *PsCOCH2* single mutant develops WT nodules contrary to the *Pscoch1coch2* double mutant producing supernumerary and poorly developed nodules converted to root and with reduced nitrogen fixation performances. Together, our findings show that legume specific *NBCL2* genes play important roles in stipule, flower and indeterminate nodule development, identity establishment, and maintenance.

RESULTS

MtNOOT1 and *MtNOOT2* genes expression in *M. truncatula* aerial organs

The *MtNOOT1* and *MtNOOT2* genes are expressed in wild-type *M. truncatula* R108 aerial organs. *NOOT1* shows a high expression in internode, leaf, and apical meristem (supplemental Fig. 1a). *NOOT2* highest expression was detected in nodes (supplemental Fig. 1a). Due to the insertion (*Tnt1*) nature of the *noot1* and *noot2* mutations, the expression of the genes in their corresponding mutant backgrounds does not reflect the reality. The expression level of *NOOT1* was increased in node, leaf, and apical meristem of the *noot2* mutant, especially in the apical meristem (40% increases). The *NOOT2* expression significantly decreased in node and apical meristem of the *noot1* mutant, with 25% and 72% decrease in internode and leaf, respectively (Fig. 1a). Using the promoter NOOT2:: GUS fusion, we detected *NOOT2* expression in young seedling stem (sup. 2a, f), at the base of the stipules (sup. 2b, g), in the leaf petiole (sup. 2c, h), in flower primordia (sup. 2d, i) and also in young pods (sup. 2e, j) either in wild type *M. truncatula* R108 (a, e) or in the *noot1* mutant background (f, j) (sup. 2a-j). Together, the *NOOT1* and *NOOT2* genes were co-

expressed in all the tested tissues and their relative expression varied in these tissues indicating that they function redundantly.

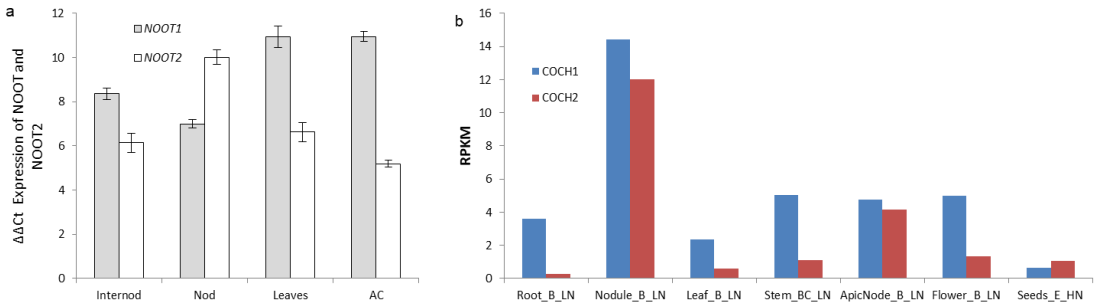

Supplemental Figure 1. *NBCLs* gene expression level.

a, *MtNOOT1* and *MtNOOT2* gene expression in wild type *M. truncula* R108 aerial part**; b**, *PsCOCH1* and *PsCOCH2* gene expression profiles from the *P. sativum* Gene Expression Atlas. *MtNOOT1* and *MtNOOT2* gene expression data from internode, node, leaf and shoot apical meristem when plant started to flower. *PsCOCH1* and *PsCOCH2* gene expression profiles were established using the probeset *Ps*Cam036654 and *Ps*Cam048389 respectively, using the dataset available from the *P. sativum* Gene Expression Atlas. Gene expression data from plant starting to flower (stage B) and grown under low nitrate condition (LN), similar to our growing conditions and stages of development have been retained and organized by organs. RPKM, Reads Per Kilobase Million; stage C, 20 days after the start of flowering; stage E, 12 days after pollination; N, grown under nitrate condition; dap, days after pollination.

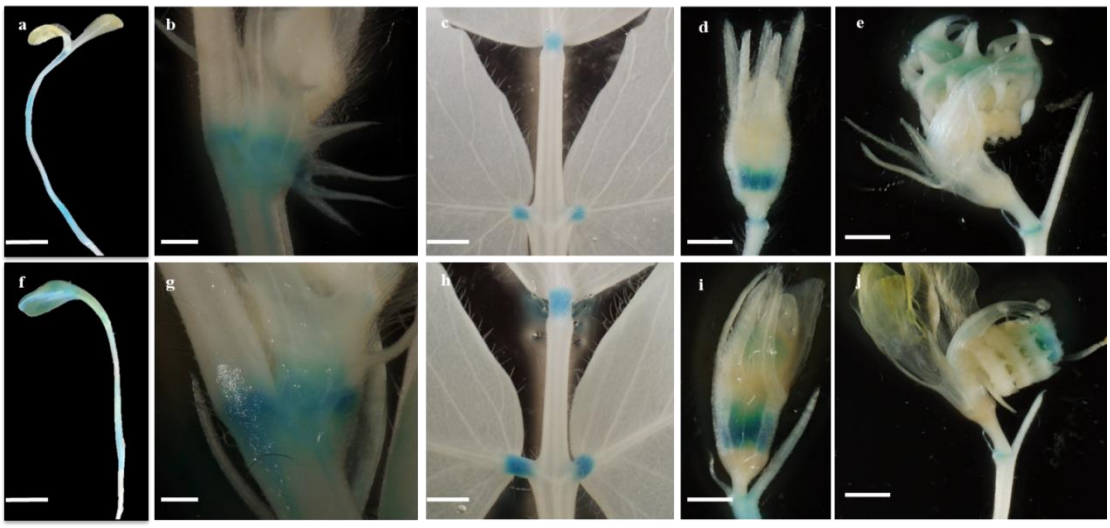

Supplemental Figure 2. Promotor *NOOT2* expression in aerial part in *M. truncula* R108 and in *Mtnoot1* mutant background.

a-e, promoter *NOOT2:GUS* expression in R108 (**a-e**) and *noot1* (**f-j**); the expression was observed in young seeding of the stem (**a**), at the base of the stipule position but not the stipule (**b**), the petiole (**c**), the flower primordia (**d**) and pod (**e**) of the mature plant. The same expression patterns were observed in *noot1* background (**f-j**). Scale bars **a-j**: 0,5 cm.

PsCOCH1* and *PsCOCH2* are co-expressed in aerial organ and are induced in indeterminate nodules of *P. sativum

The *P. sativum PsCOCH1* and *PsCOCH2* genes are orthologs to the *M. truncatula MtNOOT1* and *MtNOOT2*, respectively (Couzigou *et al.*, 2012; Magne *et al.*, 2018a). *PsCOCH2* but not *PsCOCH1* expression was detected in internodes (Fig. 1b). *PsCOCH1* and *PsCOCH2* low-level expression was detected in nodes according to the RNAseq data from *P. sativum* Gene Expression Atlas (PsGEA; http://bios.dijon.inra.fr/FATAL/cgi/pscam.cgi; Alves-Carvalho et al., 2015). According to this Gene Atlas *PsCOCH1* and *PsCOCH2* are also expressed in stem and apical nodes (Fig. 1b; sup. 1b). *PsCOCH1* and *PsCOCH2* transcripts accumulated in young leaves and were less abundant in developing leaves (Fig. 1c; sup. 1b). The expression was higher in young flowers than in developing flowers (Fig. 1c; sup. 1b). Transcript accumulation differences between young and more developed organs such as leaves and flowers suggest a preponderant role for these *NBCL* genes during early organ development. In nodes, in leaves and flower organs, *PsCOCH1* transcripts were always more abundant relative to *PsCOCH2* in agreement with the PsGEA data (Fig. 1b-c; sup. 1b). *PsCOCH1* and *PsCOCH2* transcripts were also detected in young seeds and their abundances increased during seed development (Fig. 1c; sup. 1b). Together RNAseq data and qRT-PCR gene expression analysis reveal that *PsCOCH1* and *PsCOCH2* are often co-expressed in the different organs analyzed with *PsCOCH1* expression often higher relative to *PsCOCH2*.

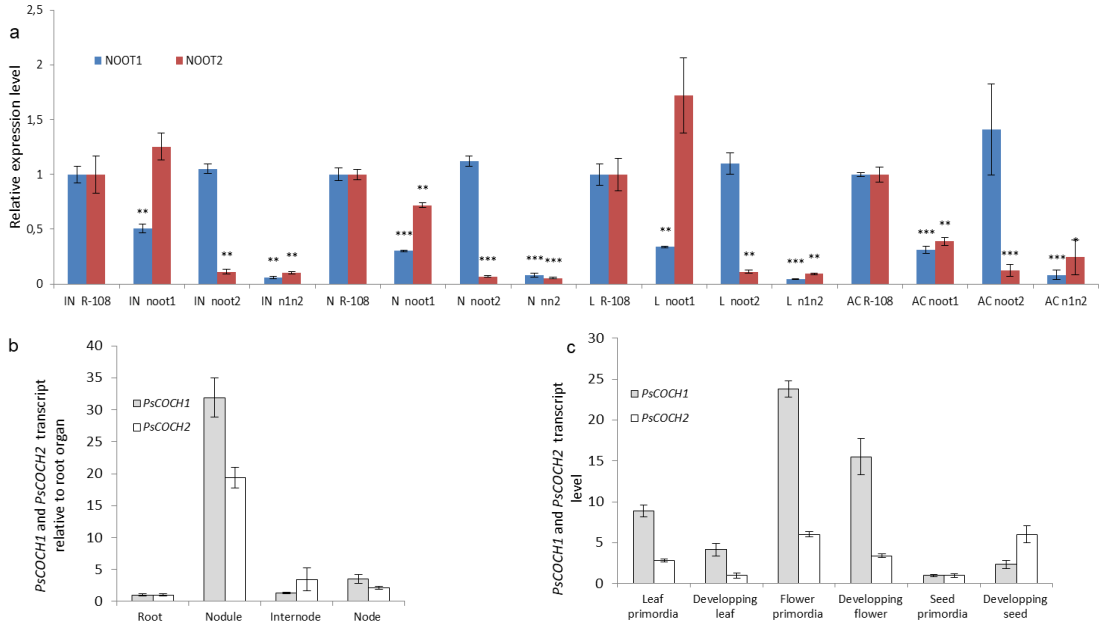

Figure 1. Expression level of *MtNOOT1* and *MtNOOT2* in *M. trunctula* and *PsCOCH1* and *PsCOCH2 in P. sativum*

a, *MtNOOT1* (blue bars), and *MtNOOT2* (red bars) qRT-PCR relative gene expression analysis in *M. trunctula R108* and *noot1*, *noot2*, *n1n2* mutants. Gene expression analysis in internode, in node, and in leaf and shoot apical meristem. Gene expressions were normalized against the constitutively expressed *MtACTIN* and *MtRRM* and against WT R108. **b-c**, *PsCOCH1* (grey bars), and *PsCOCH2* (white bars) qRT-PCR relative gene expression analysis in *P. sativum cv. Caméor*. **b**, qRT-PCR gene expression analysis in denodulated root, in nodule (27 days post-inoculation), in internode and in the node. **c**. qRT-PCR gene expression analysis in young leaves (2 first leaves from shoot apical meristem), in developing leaves, in young flowers (sepal and petal at the same level), in developing flowers (closed flower before aperture), in young seeds (under 2 mm wide) and in developing seeds (4-5 mm wide). All organs were collected on 35 days old plants inoculated with *R. leguminosarum* wild-type strain P221 (Laguerre *et al*., 1992), developing seeds were collected from 42 days old plants. Gene expressions were normalized against the constitutively expressed *PsACTIN* and *PsBETA-TUBULIN3* and against denodulated root organ (**b**) and on *PsACTIN* and against young seed organ (**c**). Results represent means ± SEM of three technical replicates and three biological replicates. IN, internode; N, node; L, leaf, and AC, shoot apical meristem. Star representative p-value, one *=p<0,05, two ** =p<0,01 and three *** =p<0,001.

In *M. truncatula*, *MtNOOT1* is constitutively expressed in root and induced during nodule development while *MtNOOT2* is not expressed in the root but early induced in the nodule. *PsCOCH1* and *PsCOCH2* gene expression analysis by qRT-PCR in wild-type Caméor show a strong expression of both genes in nodule at 27 dpi and a lower expression was observed for *PsCOCH2* compared to *PsCOCH1*, in agreement with the *PsCOCH1* and *PsCOCH2* gene expression data available from PsGEA and to the previous results obtained in *M. truncatula* indeterminate nodule (Fig. 1b; sup. 1b; Magne et al., 2018a). PsGEA and qRT-PCR experiments reveal that *PsCOCH2*, like *MtNOOT2*, is not expressed in root and thus appears nodule specific. In *M. truncatula* and *P. sativum* indeterminate nodules, *NBCL1* and *NBCL2* genes are well induced during the nodule symbiotic organ.

MtNOOT1 and *MtNOOT2* redundantly control stipule development

In wild-type, *M. truncatula* plant leaf, a pair of stipules is developing at the base of the petiole. These stipules have one to two digitations below the third stem node. The number of serrations of these stipules increased forming more complex organs after the third node of older plants (Fig. 2a; sup. 3a). Couzigou et al., (2012) showed that stipules were simplified in the *MtNOOT1* mutants (Fig 2b; sup. 3b). We have

identified a *Mtnoot2* insertion mutant from a reverse genetic screen of the *Tnt1* retrotransposon-tagged population (Magne *et al.*, 2018a). The *Mtnoot2* mutant shows a wild type leaf and stipules phenotype (Fig. 2c sup. 3c). To know if the *MtNOOT1* gene could complement *MtNOOT2* in the *Mtnoot2* mutant, we performed crosses between *Mtnoot1* (*NF2717*) and *Mtnoot2* (*NF5464*) and the resulting double mutant (*Mtnoot1noot2*) was analyzed for morphological phenotypes. In the *Mtnoot1noot2* double mutant, stipules were significantly reduced for the number of digitations as compared to wild-type plants (Fig. 2d; sup.3d). Moreover, the stipules in the double mutant have a range of variations as the plant grows older contrary to the *Mtnoot1* ones, which were stable in shape with two digitations for each stipule (Fig. 2b; sup.3b). Most of the stipules in the double mutant had just one digitation with a needle-like structure (Fig. 2d; sup.3d). Note that the position of these stipules was asymmetric on the stem. In some cases, a branch formed or one needle-like structure was present only on one side of the stem (Fig. 2e, f). Besides, one needle-like on one side and two or three on the other side could be observed at the base of the petiole (Fig. 2g, h; sup. 3e-f). Finally, abnormal leaflets or an abnormal leaflet with a needle-like structure (Fig. 2i-j) or misplaced needle-like structures in the middle of the petiole, instead of being formed at the base of the petiole (Fig. 2k) could also be observed. Interestingly, in the double mutant modified stipules were occasionally converted to leaf-like structures, with ectopic leaflets and asymmetric lateral leaflets displayed needle-like structure with modified serrations on the leaf margin (sup.3g-m). Both terminal and lateral leaflets of these trifoliate leaves were dramatically decreased in length, width, perimeter, and area compared with WT counterparts (Fig. 2l-o). Furthermore, the stipule lamina significantly increased in length in *noot1noot2* double mutant compared to WT or *noot1*, *noot2* single mutants, and was on average 2 fold longer (Fig. 2p; sup. 3n). Together, we propose that *MtNOOT2* shares a redundant function with *MtNOOT1* to control stipule development.

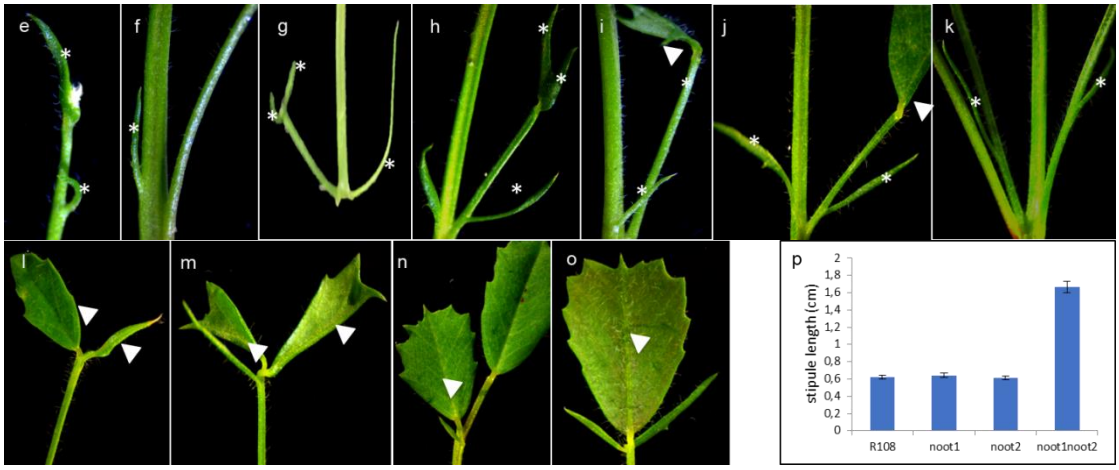

Figure 2. Stipule phenotype of the *noot* mutant.

a-d, comparison of a wild-type *M. trunctula* plant (**a**) with *noot1* (**b**), *noot2* (**c**) and *noot1noot2* (**d-o**) mutants. In wild-type *M. truncatula* plant leaf, a pair of stipules is developing at the base of the petiole and these stipules display several serrations above node 3 (**a**). *noot1* reduced the serrations (two at each side) of stipule (**b**) and *noot2* is without alteration (**c**), the *noot1noot2* presents a range of alteration, mostly with a needle-like structure and increased the defect observed in *noot1* (**d**). Some other leaflet-like stipules or branched stipules were observed (**e-o**). In addition, the length of the stipules also increased in the *noot1noot2* double mutant (**p**). The five-pointed star represents WT stipules, the star represents a modified stipule, the triangle represents a modified leaflet stipule.

In wild-type *Medicago* plants, the first leaf, or the so-called juvenile leaf, is always simple, and later developed leaves are trifoliate, consisting of a pair of lateral leaflets, a terminal leaflet, a petiole and a pair of stipules. In the *MtNOOT1* and *MtNOOT2* single mutant, the leaf phenotype is not modified. In contrast, most of the double mutants increased the size of the trifoliate leaves (sup. 3o). The phenotypes observed in the double mutant suggests that *MtNOOT1* and *MtNOOT2* work together to control leaf size and shape during trifoliate leaves development.

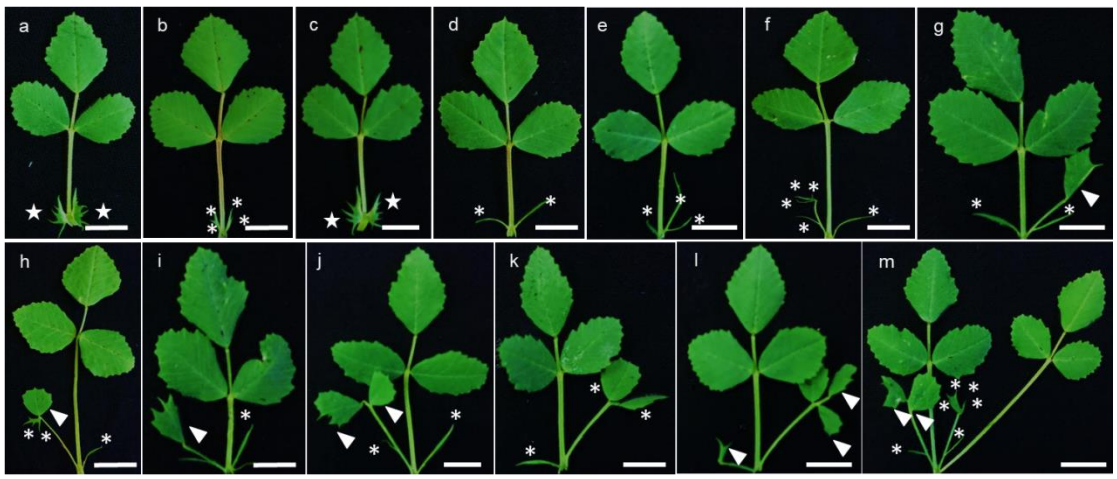

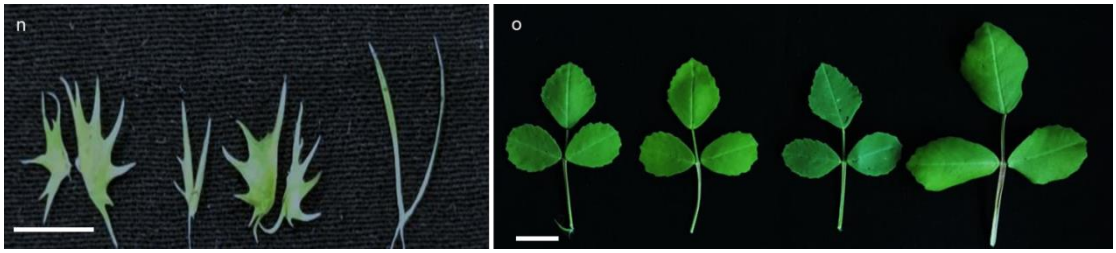

Supplemental Figure 3. Stipule and leaf phenotypes of the *noot* mutants.

a-m, comparison of a wild-type *M. trunctula* plant (**a**) with *noot1* (**b**), *noot2* (**c**) and *noot1noot2* (**d-m**) mutants. In wild-type *M. truncatula* plant leaf, a pair of stipules is developing at the base of the petiole and these stipules have several serrations above node 3 (**a**). *noot1* reduces the serrations (two at each side) of stipules (**b**) and *noot2* has no alteration (**c**), the *noot1noot2* presents a range of alterations, mostly displaying a needle-like structure and increasing the defect observation *noot1* (**d**). Branched stipule (**e-f**) or leaflet-like stipule (**g-m**). In addition, the length of the stipules also increased in *noot1noot2* double mutant (**n**). The stipule in wild type (left), *noot1* (middle left), and *noot2* (middle right) were shorter but the *noot1noot2* (right) shows an increased stipule length. In addition, the leaf size (**o**) in *noot1noot2* also increased (right) compared to wild type (left), *noot1* (middle left) and *noot2* (middle right). The five-pointed star represents normal stipules, star represent modified stipule, the triangle represents a modified leaflet stipule. Scale bars a-o: 1 cm.

PsCOCH2 mutation increased the *PsCOCH1* aerial vegetative mutant phenotypes

The *PsCOCH1* gene is known to confer stipule identity but a role in leaf development was not reported. Here studied the role of *PsCOCH2* in vegetative organs development such as stipules and leaves using the *Pscoch1*, *Pscoch2* single mutants, and the *Pscoch1coch2* double mutant.

Leaves from the first nodes of the *Pscoch* mutants were looking for most of them like the wild-type Caméor with two proximal leaflets and distal tendrils (Fig. 3a). In *Pscoch1*, we found few leaves that showed minor defects in leaf patterning, often limited to an additional proximal leaflet and also a small leaflet appearing with distal tendrils (Fig. 3b). *Pscoch2* presented no particular leaf phenotypes (Fig. 3c). In *Pscoch1coch2* most of the leaves did not present patterning defect, however, some leaves (about 16%) presented an increased leaf complexity. Modified *Pscoch1coch2* leaves presented more than two proximal leaflets and besides the distal parts of the leaf were often reiterating compound leaves or leaflets (Fig. 3d). On later nodes, once leaves become compound, all the leaves in the different *Pscoch* mutants showed a wild-type phenotype with at least two pairs of proximal leaflets and a terminal tendril (Fig. 6e, f, g). Occasionally, the *Pscoch1coch2* mutant showed leaf patterning defects

such as the fusion of more than five leaflets (Fig. 3h) or dichotomy in leaves along the proximal-distal axis (data not shown).

Analysis of the stipule morphology revealed that Caméor and *PsCOCH2* have wild-type peltate stipules (Fig. 3i, k). *PsCOCH1* stipules morphology is drastically affected as previously described in the literature and shows a range of stipule phenotypes, such as the absence of stipules, thread-like stipules, leaflet-like stipules or compound leaf-like stipules (Fig. 3j). Similar modifications were observed in the *Pscoch1coch2* double mutant (Fig. 3i). The stipule modifications and the penetrance of this phenotype are already particularly strong in *Pscoch1* and it was difficult to assess if this phenotype is increased in the *Pscoch1coch2* double mutant. To investigate if the *Pscoch2* mutation increased the stipule phenotype of *Pscoch1*, the stipules morphology was checked node by node form 1 to 13 in Caméor, *Pscoch1*, *Pscoch2*, and *Pscoch1coch2*. This analysis revealed that Caméor and *Pscoch2* present only a wild-type peltate stipule (Fig. 3i, k; supplemental Table S4). *Pscoch1* presented mainly an absence of a stipule from nodes 1 to 5, thread-like stipules from nodes 6 to 7, and leaflet-like stipules from nodes 8 to 13 (Fig. 3j; supplemental Table S4). *Pscoch1coch2* presented mainly an absence of a stipule from nodes 1 to 9, thread-like stipules at node 10, and leaflet-like stipules from nodes 11 to 13 (Fig. 3l; supplemental Table S4). These results show that the absence of stipules is prolonged along with the nodes of the double mutant and thus suggests that the stipules alteration is increased in *Pscoch1coch2* double mutant compared to *Pscoch1* (supplemental table S4) revealing the role of *Pscoch2* in stipule development.

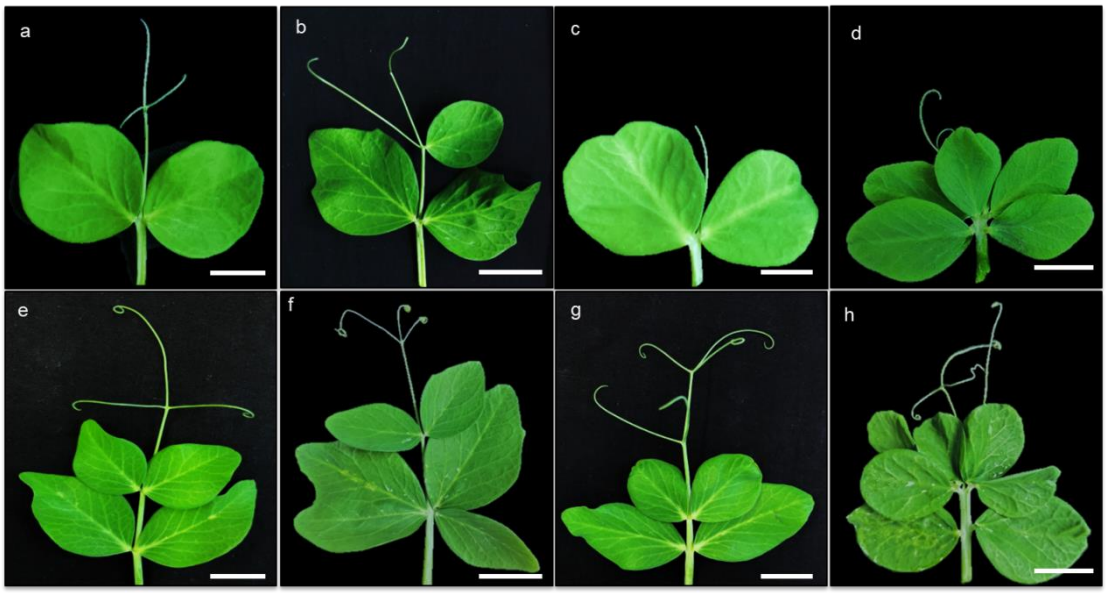

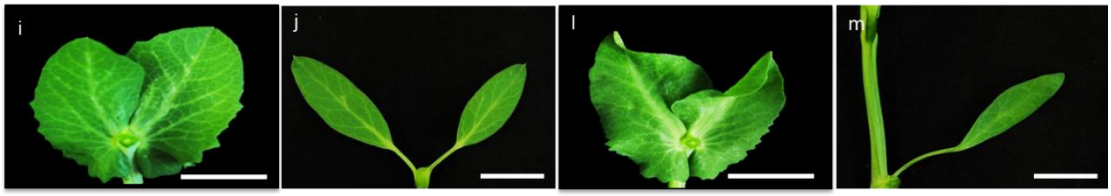

Figure 3. *Pscoch* single and double mutants aerial phenotype

a-d. Leaf phenotypes in *Pscoch* mutants relative to wild-type. **a**, *Ps*caméor shows wild-type leaves with two proximal leaflets and distal tendrils. **b**, *Pscoch1* mutant shows mainly wild-type leaf phenotype but displays occasionally an additional proximal and distal leaflet. **c**, *Pscoch2* mutant shows wild-type leaves: alteration of the leaf patterning was not observed. **d**, *Pscoch1coch2* double mutant shows mainly wild-type leaf phenotype but occasionally displays strong leaf phenotype consisting of an increase of the leaf complexity, with additional proximal leaflets when they are at a young stage. **e-h.** Compound leaf phenotypes in *Pscoch* mutants relative to wild-type. **e**, **f**, **g**. *Ps*caméor, *Pscoch1*, and *Pscoch2* showing wild-type compound leaf phenotypes with at least two pairs of proximal leaflets, a pair of distal tendrils, and a terminal distal tendril. **h**, *Pscoch1coch2* double mutant shows wild-type compound leaf phenotype but displays occasionally leaf morphology alteration. **i-l**. Stipule phenotypes in *Pscoch* mutants relative to wild-type. **i**, **k**. *Ps*caméor and *Pscoch2* show wild-type peltate stipules. **j**, **l**. *Pscoch1* and *Pscoch1coch2* show a range of stipule phenotypes. Scale bars **a-l**: 1 cm.

NBCL genes are important for plant architecture

A vegetative shoot consists of a series of reiterative modules known as phytomers to generate the aerial parts of the plant. Each phytomer comprises a node to which a leaf is attached, a subtending internode, and a bud at the base of the internode (Sussex, 1989). Internode patterning is a key determinant of inflorescence architecture, with variations in the length and pattern of internode elongation contributing to diversity in inflorescence height and organization of secondary branches and flowers on the primary stem (Sussex, 1989). In Arabidopsis, ectopic expression *BOP1* or *BOP2* results in either short plants with floral pedicels pointing downward (Ha *et al.*, 2007) or short bushy plants with irregular internodes (Norberg *et al.*, 2005).

In this study, we found that *M. truncatula NBCL* genes also play a role in internode elongation. The loss-of-function mutants *Mtnoot1* and *Mtnoot2* play no major roles in internode elongation. *Mtnoot2* displays a bit longer internodes compared with the wild type but *Mtnoot1* has wild type plant height or is a bit shorter (Fig. 4a, b). However, the *Mtnoot1mtnoot2* double mutant plants are taller, with longer internodes and continuous growth of the shoots because of infertility (Fig. 4a, b). The average length of internodes was increased 1.5 times compared to wild type

(Fig. 4b). In addition, we also found that the average length of the floral pedicels was doubled in the double mutant when compared to wild type and *Mtnoot1* and *Mtnoot2* single mutants (Fig. 4c-d). These results suggest that *MtNOOT1* and *MtNOOT2* work together to repress internodes and floral pedicels elongation to maintain the plant architecture.

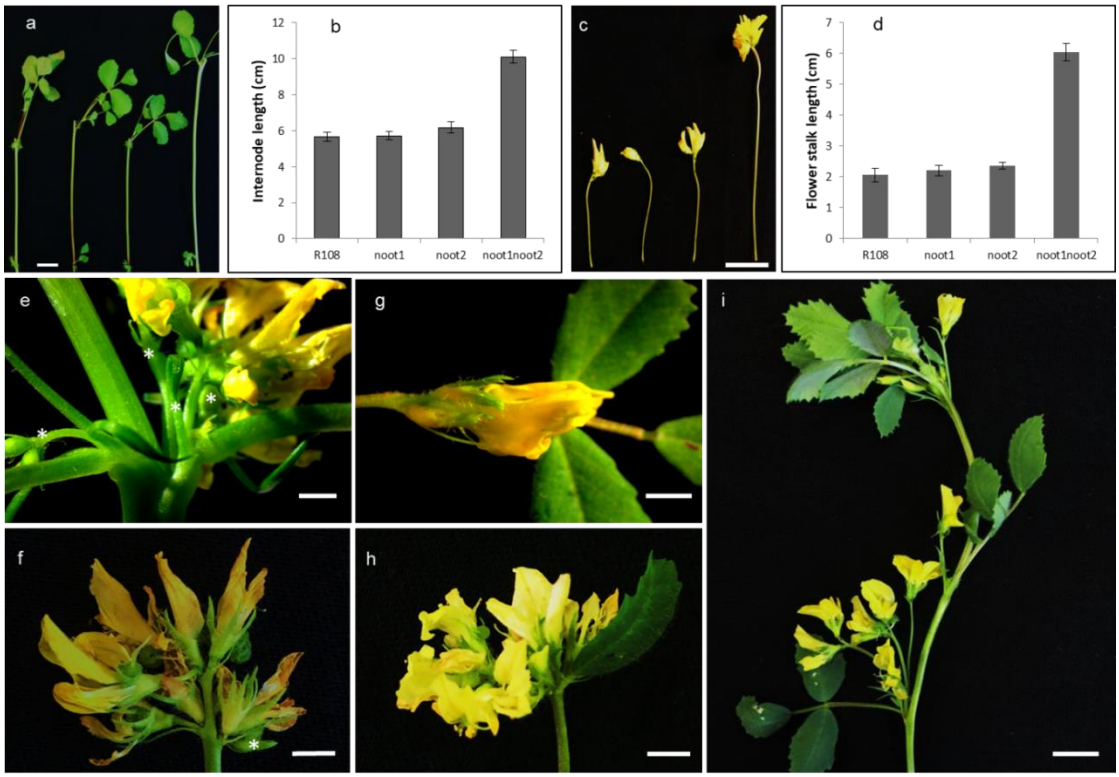

Figure 4. Inflorescence phenotype of *noot1noot2* double mutant.

a, **b**. internode length of *noot1* (middle left), *noot2* (middle right) and *noot1noot2* (right) double mutant compare to *M. trunctula* WT R108 (left); **c**, flower stalk phenotype of WT (left), *noot1* (middle left), *noot2* (middle right) and *noot1noot2* (right) double mutant and average length of flower stalk in different genotype (**d**). **e-i**, inflorescence of *noot1noot2* double mutant showing mostly more than 8 flowers in one inflorescence. The star indicates small flower buds that continue to grow even then the first opened flowers were nearly dry (**e**, **f**). Some flowers directly formed on the node without flower stalk (**g**) and occasionally a leaflet is present on the flower (**h**). Several inflorescences originating from the same node position (**i**).

In wild-type *Medicago* plants, one to three flowers developed on a single stalk. Flower number was reduced to just one in *Mtnoot1* mutants, however, most of the *Mtnoot2* inflorescences are made of 3 flowers and a few have 4 flowers on a single stalk, although this character was variable (Fig. 4c). In the *Mtnoot1mtnoot2* double mutant, however, up to 10 flowers were formed and clustered on a stalk (Fig. 4e, f).

Young flowers can still be formed even when the first formed flowers were already dried on these structures (Fig. 4f). Furthermore, some flowers formed directly from the vegetative shoots at node position without the pedicels (Fig. 4g) and we also observed inflorescences with an ectopic leaflet and shortened petiole in these structures (Fig. 4h). We also observed multiple inflorescences formed on a single node (Fig. 4i). These results suggest that *MtNOOT1* and *MtNOOT2* work together to control inflorescence formation at vegetative nodes.

In pea, *PsCOCH1* and *PsCOCH2* also function redundantly in plant architecture. The *coch1* mutant displayed a shorter plant height and more stems, however, the *coch1coch2* displayed a higher stature even if the *coch2* mutant was not different from the WT Caméor (data not shown here). In pea, the secondary inflorescence meristems (I2), produced from primary inflorescence meristems (I1), usually produce 1-2 floral meristems (FM) before it ceases growing, forming a residual organ or stub (sup. 4a). Simultaneous mutation of *PsCOCH1* and *PsCOCH2* also increased the inflorescence complexity with more flowers in a single flower stalk in *coch1coch2* mutants. Most of the *coch1* mutant flowers are similar to WT but some inflorescence meristems also produce more than 3 FMs which increased the flower numbers (sup. 4b). Interestingly, although the inflorescence phenotype of *Pscoch2* was similar to wild type Caméor (sup. 3c), the *Pscoch1coch2* double mutant displayed increased FM on I2 as compared to *Pscoch1* (sup. 4d) with at least three flowers in a single flower stalk (sup. 4d-f). Similar to *MtNOOT1* and *MtNOOT2* in *M. truncatula*, the *PsCOCH1* and *PsCOCH2* also function redundantly in flower stalk elongation. The lengths of flower stalks were significantly increased in the *coch1coch2* double mutant even if they appear a bit shorter than in the WT Caméor in the *coch1* and *coch2* single mutants (sup. 4g). This indicates that the two genes are complementary to repress FM number and flower stalk elongation.

Above all, the results suggest that *MtNOOT1* and *MtNOOT2*, as well as *PsCOCH1* and *PsCOCH2*, function redundantly to repress internodes and floral pedicels elongation to maintain the plant architecture. The modified development of the internode and the floral pedicels in *M. truncatula*, *P. sativum* and *Arabidopsis* indicates that the *NBCL* genes have a conserved function in aerial organ development in eudicot plants.

Supplemental Figure 4. Inflorescence phenotype of *coch1*, *coch2* and *coch1coch2* mutant.
a-d. inflorescence of wild type Caméor (**a**), *coch1* (**b**), and *coch2* (**c**) and *coch1coch2* double mutant (**d**) in Caméor background when the flower was completely opened. **e**, **f**, inclose view of *coch1coch2* double mutant inflorescence when the flower bud just appeared (**e**) and was already opened (**f**). **g**, separated inflorescence and flower stalk phenotype of WT (left), *coch1* (middle left), *coch2* (middle right) and *coch1coch2* (right) double. The Caméor wild type and *coch2* mutant generally have 1-2 flower in one inflorescence (**a**, **c**, **g**), the *coch1* mutant mostly shows a wild type inflorescence phenotype with 1-2 flowers in one inflorescence but occasionally with three or more. The coch1coch2 double mutant mostly has more than 3 flowers in one inflorescence. Scale bars a-g: 1 cm.

MtNOOT1 and *MtNOOT2* are required for flower development

In wild-type *M. truncatula*, the flowers have pentamerous organs in the outermost four whorls (sepals, petals, and outer and inner stamens) and a central carpel (Benlloch *et al.*, 2003; Wang *et al.*, 2008). At the early stage, the non-open flowers have a pea-like closed structure (Fig. 5a) and subsequently show a corolla with three smaller petals (Fig. 5b). In addition, the central carpel is enclosed by a stamen tube (Fig. 5d) made off 10 anthers (Fig. 5e). Sepals have five teeth at the base of the flower (Fig. 5f). The *M. truncatula noot1* mutant also has a pea-like closed structure (Fig. 5g) and flower modifications are subtle with additional organs, such as petals and stamens (Fig. 5h-i; Couzigou et al., 2012). Histological analysis of juvenile flowers also show the fused petal (sup. 5b) compare to wild type (sup. 5a), but the floral organs such as central carpels and sepals were not modified (Fig. 5j-l). The *noot2* mutants displayed the WT flower phenotype (Fig. 5m-r, sup. 5b). In *Mtnoot1* and *Mtnoot2*, however, all mutants flowers were precociously opened (Fig. 5s) and

resulted in premature anther senescence. The histological analysis of these juvenile flowers also highlighted the premature stamens senescence (sup. 5d). Furthermore, the petal number was increased in double mutants due to frequent floral organ fusion (Fig. 5t-u), although this increase was variable among flowers. In wild-type plants and single mutants, the central carpel is enclosed by a stamen tube, however, it was frequently separated and not able to enclose the carpel in the *Mtnoot1noot2* double mutant (Fig. 5v, sup. 5d). Moreover, the stamens were abnormal, the anthers were dried resulting in sterility and the central carpel developed to a pod-like structure (Fig. 5w, sup. 5e). Furthermore, circular sepal had an increased number of teeth (Fig. 5x). Taken together, these phenotypes indicated that the *Mtnoot1noot2* double mutant is defective in floral organ identity, showing that *MtNOOT1* and *MtNOOT2* are redundantly required for *Medicago* flower development.

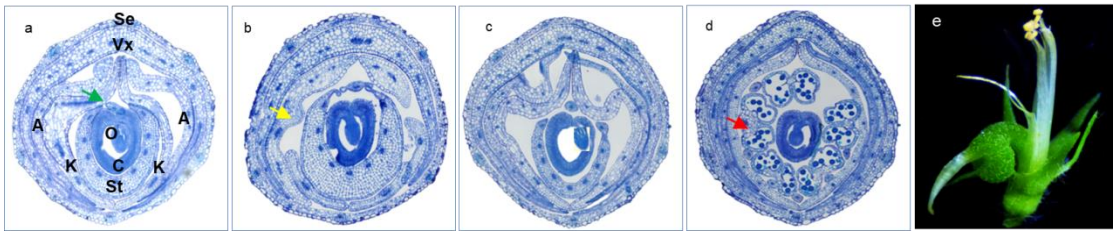

Supplemental Figure 5. The histological analysis of juvenile flowers in the wild-type and different Mtnoot mutants and the pod phenotype. (**a-d**) Cross-section and morphology of juvenile flower in the wild-type (**a**), *noot1* (**b**), *noot2* (**c**), and *noot1noot2* (**d**). The green arrow points to the stamen filament separated from the fused nine, yellow arrow points to the extra petal, and red arrow indicate exposed anther, respectively. Se, sepal; Vx, vexillum; A, alae; K, keel; St, staminal tube; C, carpel; O, ovule. Bar = 100 µm

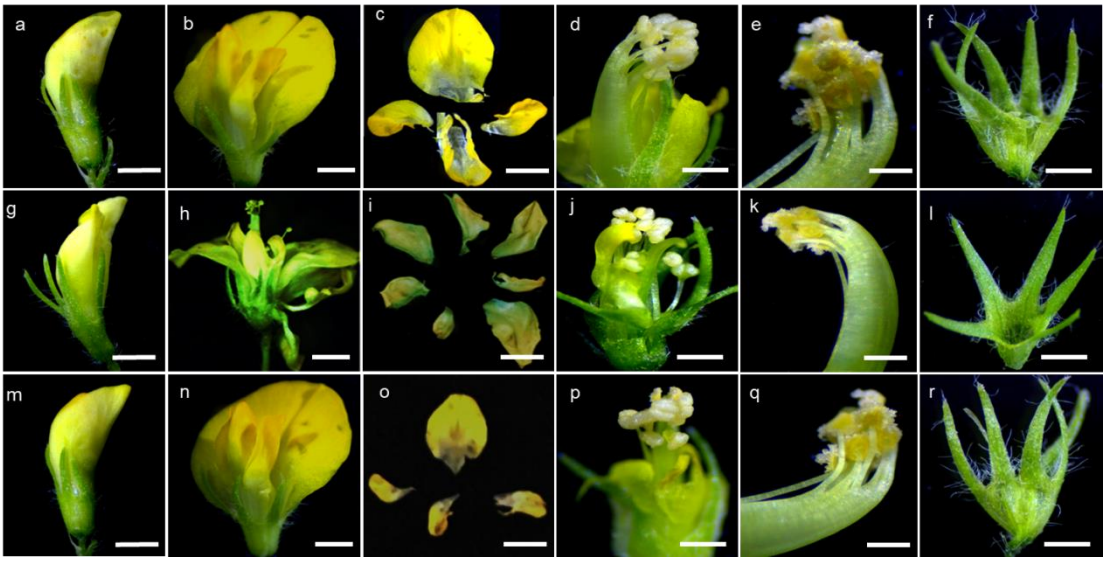

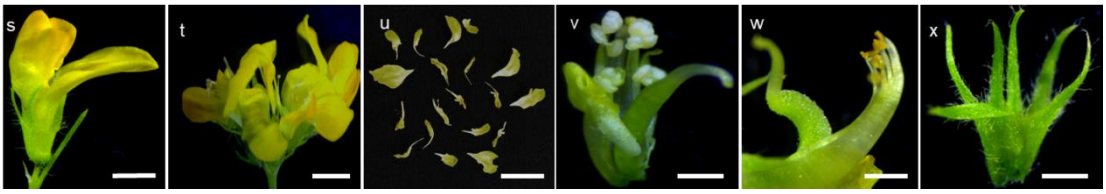

Figure 5. Floral defect of *M. trunctula noot1* and *noot1noot2* mutants.

a-b. Global views of wild-type *M. trunctula* R108, *noot11* single mutant (**g**, **h**), *noot2* single mutant (**m**, **n**), and *noot1noot2* double mutant (**s**, **t**) flowers. c-f. Dissected views of wild-type R108, *noot1* (**i-l**), *noot2* (**o-r**), and *noot1noot2* (**u-x**) floral organs. *M. trunctula* WT R108 shows a closed flower composed of five sepals at their bases, four petals and ten stamens (**a-f**). *Mtnoot1* shows occasionally open flowers with a range of floral patterning defects, increased petals number, petals identity defects (**h**, **i**), the central carpal, and stamen also the sepal were not altered. *noot2* shows a WT phenotype (**m-r**). *Mtnoot1noot2* double mutant showed stronger floral patterning defects than the *noot1* single mutant, with mostly open flowers (**s**, **t**). *noot1noot2* mutant tends to show increased floral defects relative to *noot1* and often fusion between adjacent flowers resulting in flowers with supernumerary petals (**u**) The central carpel was not well closed by stamen (**v**) and the anther were dried early (**w**) finally resulting in sterility. The sepal teeth number also increased (**x**). Scale bars a-h: 1 cm.

Pscoch1coch2 present accentuated floral patterning

Previous studies showed that the *coch1* mutation alters various aspects of flower development (Yaxley *et al.*, 2001; Couzigou *et al.*, 2012). *Pscoch1* displayed a large range of floral alterations and a mis-organization of floral organs that impact the symmetry and the whole structure of the flower (close to open) leading to self-fertility alteration (sup. 6a-d). *Pscoch1* display regularly an incorrect number of floral organs at each whorl, aberrant fusions between organs and mosaics of different floral organs reflecting organ identity alterations (sup. 6a-l). Here, using the double mutant *Pscoch1coch2*, we tested the role of the *PsCOCH2* gene in flower formation.

Global observations revealed that *Pscoch1* flowers share a similar open flower phenotype but a small wing appeared (Fig. 6a-b, sup. 6f, h) and the *Pscoch2* flowers show a WT phenotype. The *Pscoch1coch2* mutant also showed a plethora of strong floral organization defects (data not shown) difficult to discriminate from the *Pscoch1* single mutant. However, in the *Pscoch1coch2* double mutant originating from four independent crosses, we observed a striking additive phenotype which generally consists of the fusion between two flowers, or resulting in impressive complex floral phenotypes (Fig. 6d). Wild-type Caméor pea flowers are composed of two fused keel petals, two wing petals, and a standard petal (Fig. 6e), while the *coch1* has additional wing petals (Fig. 6f, sup. 6f, h). In contrast, the *coch2* mutant has WT flowers. In the

Pscoch1coch2 double mutants, the bases of two flowers are frequently fused resulting in a single calyx showing supernumerary sepals (Fig. 6h). In the third whorl, petals of the two flowers co-exist resulting in a complex corolla showing supernumerary petals. Roughly at the center of these kinds of flowers, two petals that look-like two wings were fused along their adaxial side indicating the site of fusion between the two flower corollas (Fig. 6d, h). In contrast to WT Caméor and the *coch2* mutant having ten anthers and a single central carpel (Fig. 6i and 6k), in *coch1* we observed an increase of the anther number and rarely two central carpels (Fig. 6j). In contrast, the *Pscoch1coch2* double mutant displayed striking alteration of the anther number and most of the flowers had two (occasionally three or four) central carpels (Fig. 6l). Furthermore, six or more sepals were found in *coch1* (Fig. 6n, sup. 6j, l) and *coch1coch2* mutants (Fig. 6p) when WT and *coch2* plants have five sepals (Fig. 6m, o). These phenotypes were to our knowledge not reported in the literature concerning *Pscoch1* single mutant. Such strong alterations of the floral patterning in the *Pscoch1coch2* double mutant suggests that the *Pscoch2* mutant increased the *Pscoch1* mutant phenotype and reveals that both genes are involved in the flower development in pea.

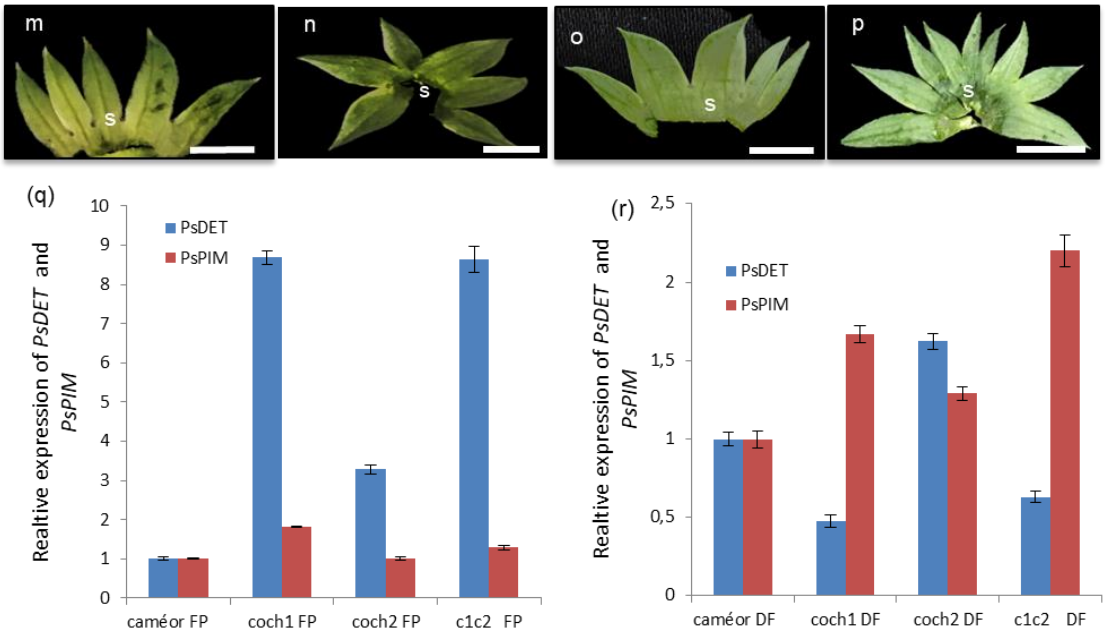

Figure 6. Floral defects and relative expression levels of flower marker genes.

a-d. Global views of Pscaméor wild-type pea (**a**), *Pscoch1* single mutant (**b**), *Pscoch2* single mutant (**c**), and *Pscoch1coch2* double mutant (**d**) flowers. e-p. Dissected views of Pscaméor wild-type pea (**e**, **i**, **m**), *Pscoch1* single mutant (**f**, **j**, **n**), *Pscoch2* single mutant (**g**, **k**, **o**), and *Pscoch1coch2* double mutant (**h**, **l**, **p**) floral organs. Pscaméor shows closed flower composed by five sepals at their bases, five petals (one adaxial large standard, two lateral wings and two short abaxial keels fused on their adjacent edges), and ten stamens (**a**, **e**, **i**, **m**). *Pscoch1* (**h-k**) shows mostly open flowers with a range of floral patterning defects, increased sepals, petals, and stamen number, petals identity defects, and a loss of the symmetry (**b**, **f**, **j**, **n**). *Pscoch2* shows a WT phenotype (**c**, **g**, **k**, **o**). *Pscoch1coch2* mutant tends to show increased floral defects relative to *Pscoch1* and often fusion between adjacent flowers resulting in flowers with supernumerary sepal and pepal organs with petals adaxially fused (**d**, **h**, **l**, **p**). St, standard; w, wing; k, keel; s, sepal; pe, peduncle. Dotted lines represent symmetry. Scale bars a-h, **m-p**: 1 cm; **i-l**: 500µm. **q-r**. Expression levels of *PsDET* and *PsPIM* in flower primordia (**q**) and developing flower (**r**). The transcript abundance is relative to *ACTIN* and *PsBETA-TUBULIN3* in various genotypes and Caméor is defined as "1". RNA was extracted from dissected flowers of 3 plants and quantified by real-time PCR. Data are means ± SE (n = 3).

In pea, FM identity is controlled by the *PIM/PEAM4*, homologs of the *APETALA1* (*AP1*) gene from *Arabidopsis* (Berbel *et al.*, 2001, 2012; Taylor *et al.*, 2002) and I1 identity is regulated by *DETERMINATE* (*DET/PsTFL1a*), a homolog of the *TFL1* gene from *Arabidopsis* (Foucher *et al.*, 2003; Berbel *et al.*, 2012). The *PsCOCH1*, *PsCOCH2*, *PsDET* and *PsPIM* expressions were investigated in *Pscoch1*, *Pscoch2* and *Pscoch1coch2* mutants and respective wild type. The *PsCOCH1* expression was not detectable in *Pscoch1*^{Cam}, *Pscoch1*^{JI,} and also *Pscoch1coch2* mutant due to the deletion nature of the *coch1* mutation (data not are shown) while a

decreased expression was detected in *SGEapm* flower compared to its wild type. *PsCOCH2* expression was slightly increased in developed flowers of *coch1* mutant lines (Sup. 6n). In flower primordia of all the *coch1* mutant lines, the *PsDET* expression was up-regulated (Fig. 6q; sup. 6m, o). In the *Pscoch1coch2* double mutant, this expression was 8 times higher than in WT (Fig. 6p). In contrast, the *PsDET* expression decreased in *Pscoch1*^{Cam}, *Pscoch1*^{Cam} *Pscoch2*^{Cam,} and *Pscoch1*^{JI}, *SGEapm* developed flowers (Fig. 6r; Sup. 6n, p). The *PsDET* expression increased in the *Pscoch2* flower primordia and developed flowers (Fig. 6q-r). These results suggested that the *Pscoch2* mutation may increase the *coch1* flower determinacy. Interestingly, the *PsPIM* transcripts were slightly increased in flower primordia and significantly increased in the developed flower of *coch1* and *coch1coch2* mutant lines (Fig. 6q-r; sup. 6n, p) and moderately increased in *coch2* (Fig. 6q-r). These results suggest that *coch1* and *coch1coch2* mutant flowers are indeterminate and that the *PsCOCH1* and *PsCOCH2* genes act antagonistically to control flower determinacy.

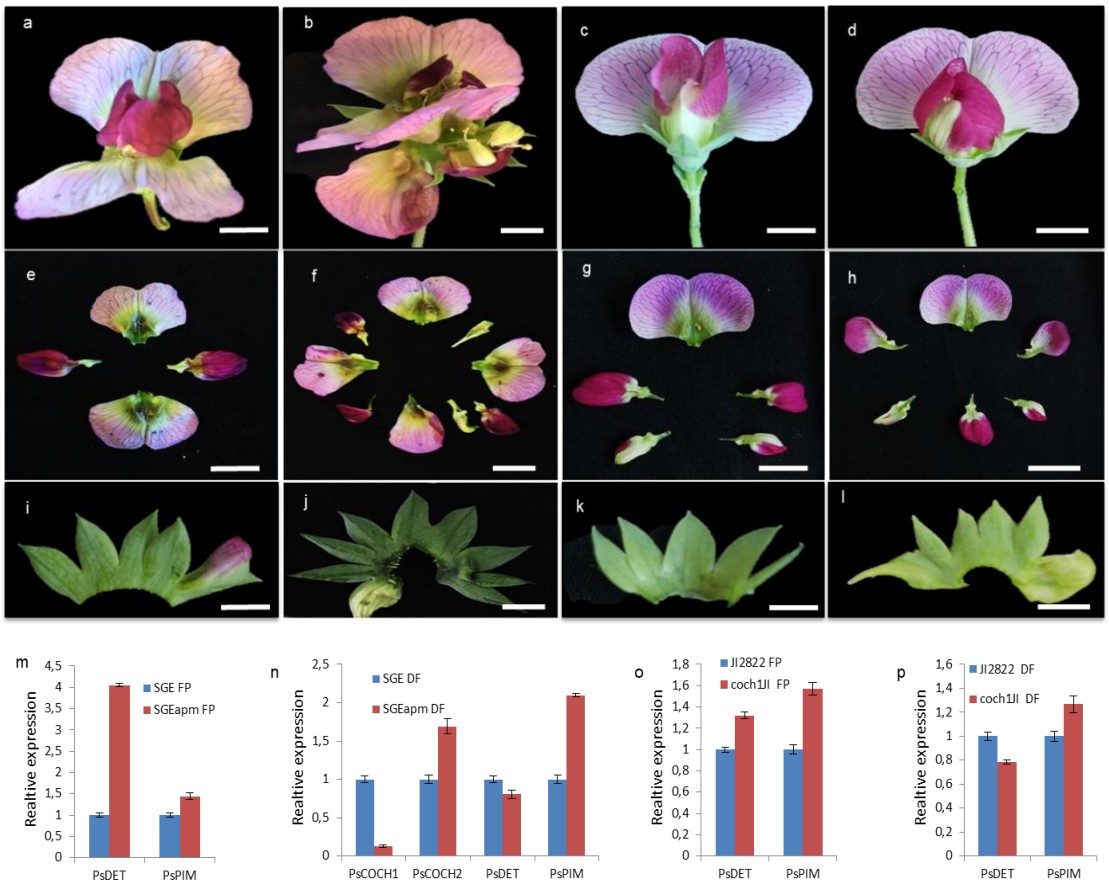

Supplemental Figure 6. Floral defects in *coch1* mutant and relative expression levels of flower marker genes.

a-d. Global views of Pscaméor wild-type pea SGE (**a**), *SGEapm* mutant (**b**), JI2822 wild type (**c**), and *coch1JI* mutant (**d**) flowers. **e-p**. Dissected views of SGE (**e**, **i**), *SGEapm* (**f**, **j**), JI2822 (**g**, **k**), and *coch1JI* mutant (**h**, **l**) floral organs. Wild type SGE and JI2822 show closed flower composed of five sepals at their bases, five petals. *Pscoch1* shows mostly open flowers with a range of floral patterning defects, increased sepals and petals number, petals identity defects, and a loss of the symmetry. Scale bars a-l: 1 cm. **m-p**. expression levels of *PsDET* and *PsPIM* in flower primordia (**m**, **o**) and developing flower (**n**, **p**). *COCH1* and *COCH2* expression in developed flowers of SGE and *SGEapm* mutant. The transcript abundance is relative to *ACTIN* and *PsBETA-TUBULIN3* in SGE lines and JI2822 lines and wild type is defined as "1". RNA was extracted from the dissected of flowers of 3 plants and quantified by real-time PCR. Data are means ± SE (n = 3).

Legume *NBCLs* control pod number and seed size

Organ size is an important parameter in the characterization of organ morphology and function and also a major agronomic trait that determines grain yield and biomass production in crops. To investigate the possible role of the *NBCL* genes in pod and seed development, we analyzed these characters in the single and double *nbcl* mutants.

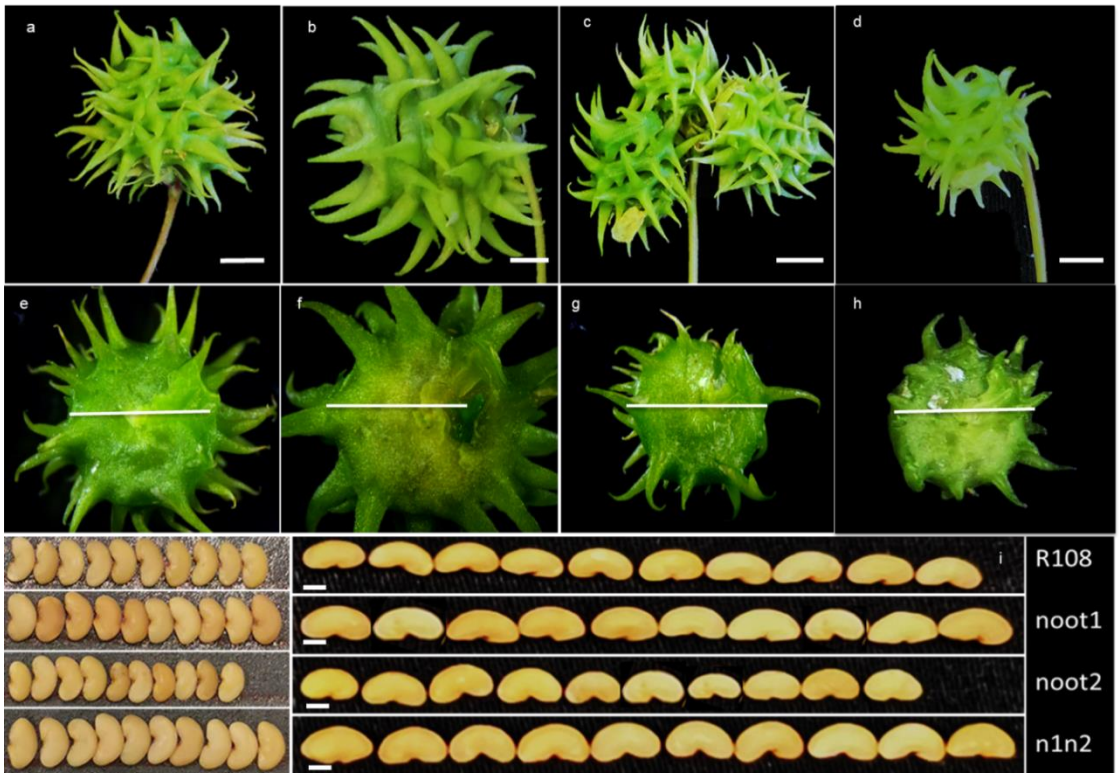

Figure 7. Pod and seed phenotype of *M. trunctula* noot1 noot2, and noot1noot2 mutants.
a-d. Global views of wild-type *M. trunctula* R108 (**a**), *noot1* single mutant (**b**), *noot2* single mutant (**c**), and *n1n2* double mutant (**d**) pod. The *noot1* show a bigger pod and noot2 show reduced pod size but with more pods in one inflorescence, the *n1n2* also displayed a reduced pod compares to wild type. **e-h**.

Dissected views of wild-type R108 (**e**), noot1 (**f**), noot2 (**g**), and noot1noot2 (**h**) pod diameter. **i**, the size of the seed (width and length) of *noot1*, *noot2*, and *noot1noot2* compared to wild type. Scale bars **a-h**: 1 cm, **i**: 1mm. n1n2: *noot1noot2*

Wild type Medicago plants produce generally one or two, occasionally three pods per inflorescence (Fig. 7a, e). In contrast, the *Mtnoot1* mutant only formed one pod on each inflorescence and the pods have an increased number of spikes on their surface even when they were totally dry (Fig. 7b, sup. 7a). Furthermore, the *MtNOOT2* mutants regularly produce three pods on an inflorescence and spikes were very short (Fig. 7c, sup. 7b). In contrast, the *Mtnoot1noot2* double mutant formed an abnormal pod-like structure (sup. 5e) and only a few succeeded to form pods with a reduced size. A global observation revealed that *MtNOOT1* loss of function leads to enlarged fruits, whereas, *Mtnoot2* produces smaller pods compared to wild type (Fig. 7a-c, sup. 5a). Interestingly, the *noot1noot2* double mutants also displayed a reduced pod size even if just a few pods formed on plants due to partial sterility (Fig. 7d). Pod cross-sections show that the *noot1* pods have an increased diameter while the *noot2* and *noot1noot2* pods had a reduced diameter compare to WT (Fig. 7e-h). The average seed size of the *Mtnoot1* plants also increased, either in width or length (Fig. 7i). The *Mtnoot1* seed weight (average 100 seeds) increased by nearly 30% relative to WT while *Mtnoot2* mature seeds were 10% lighter as a result of seeds size reduction (Fig. 7i, sup. 5g). Pods of the *noot1noot2* double mutant just contain few seeds, but the size of the seed was larger than the control. This increase can result from reduced production of seeds in the double mutant. These results suggest that the *MtNOOT1* and *MtNOOT2* genes control pod and seed number and size.

Supplemental Figure 5. The pod phenotype wild-type and different Mtnoot mutants.

a. Pods phenotype of wild-type and different Mtnoot mutants; **b.** Average seeds weight of wild-type and different Mtnoot mutants (100 seeds).

The number of flowers per I2 (multipod/multiflower) is an inflorescence trait related to the activity of the inflorescence meristem (IM) that might be amenable to improvement in grain legumes. The possibility of increasing the number of pods appears as an attractive option to increase yield in grain legumes. In pea, Caméor and *Pscoch2* pods mainly formed on the main stem were normal in appearance and set the most seeds (Fig. 8a, e). In *Pscoch1*^{Cam} more pods were produced but mainly on the lateral shoots, were abnormal in appearance, and set few seeds (Fig. 8a, e). This phenotype was observed in all *coch1* lines (coch1JI and SGEapm; Fig. 8e) except for SGEapm that produced mostly empty pods. In addition, two pods resulting from the fertilization of two pistils were occasionally observed on a single flower (data not shown). This is consistent with the previous report showing that *coch1* mutant flowers were largely self-sterile and that *coch1* plants normally produced no more than ten seeds per plant (Yaxley *et al.*, 2001). *Pscoch2* and *Pscoch1coch2* have a WT pod number and seed set (Fig. 8a, e). In addition, in the double mutant, two to four pods were observed on a single flower stalk or resulting from the fertilization of two to four pistils due to flower fusion (Fig. 8c, d). The seed size was reduced by 18% in *coch2* (Fig. 8b, e) but increased in *coch1*^{Cam} and *coch1coch2* (Fig. 8b). Consequently, the single seed weight was increased 1.4 and 1.2 fold in *coch1*^{Cam} and *coch1coch2* respectively when compared to WT Caméor, (Fig. 8b, e) and the weight of the total seeds was reduced in *coch1* but increased in *coch1coch2*.

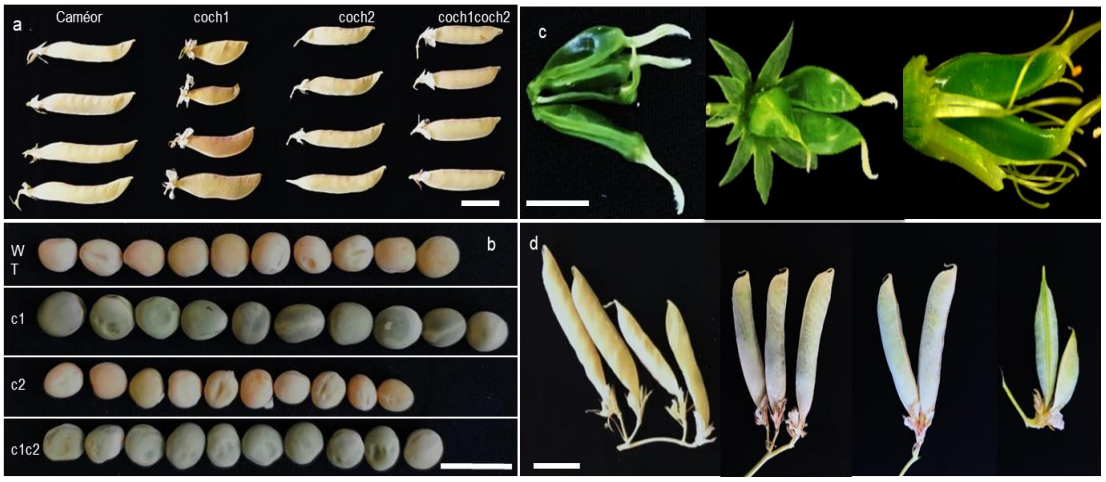

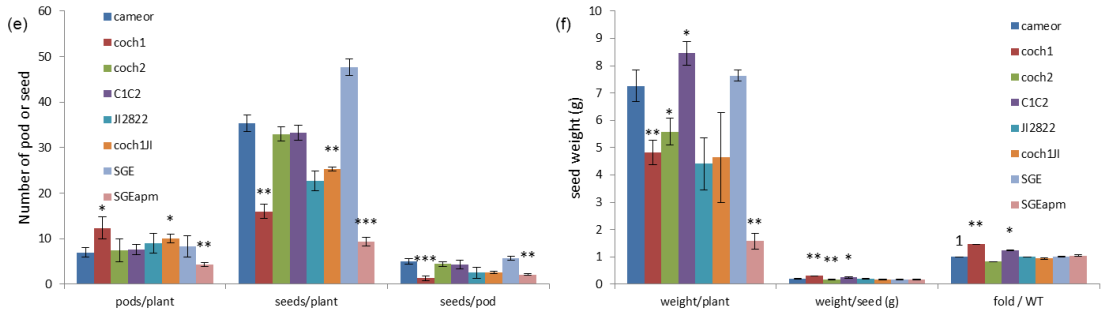

Figure 8. Pod and seed phenotype of *P. sativum coch1, coch2* and *coch1coch2* mutants.

a. Global views of wild-type Caméor (left), *coch1* single mutant (middle left), *coch2* single mutant (middle right), and *coch1coch2* double mutant (right) pod. **b**. Global views of wild-type Caméor (top), *coch1* single mutant (upper middle), *coch2* single mutant (lower middle), and *coch1coch2* double mutant (bottom) seeds. The coch1 show abnormal pod and *coch2*, *coch1coch2* displayed norm pod compares to wild type, the *coch1coch2* double mutant with more pods in one inflorescence, 2 to 4 pods resulting from the fertilization of two to four pistils due to flowers fusion (**c**) or on a single flower stalk (**d**). **e-f,** detail describes the pod and seed phenotype. Scale bars **a-d**: 1 cm. Results represent means ± SE. Star representative p-value, one *=p<0,05, two ** =p<0,01 and three *** =p<0,001.

Altogether, the results suggest that the *NBCLs* are important for pod and seed development, although some variations were observed between *M. truncatula* and pea. *NBCL2* seems to positively control seed size while the *NBCL1* negatively regulate seed size.

PsCOCH2 participates to the symbiotic organ development and functioning (this part from Kevin Magne PhD thesis)

In *M. truncatula*, the *Mtnoot2* single mutant has no symbiotic phenotype (Magne *et al.*, 2018a). By contrast, the double mutant *Mtnoot1noot2* has exacerbate *Mtnoot1* nodule to root phenotype leading to a complete loss of nodule identity and the loss of the nitrogen fixation ability (Couzigou *et al.*, 2012; Magne *et al.*, 2018a). To study the role of the *PsCOCH2* gene in the symbiotic process, the mutant line *Pscoch2* Ps1178 was used. *Pscoch2* Ps1178 homozygous mutants were nodulated using *R. leguminosarum P221* and nodule phenotypes were compared to Caméor. Twenty-seven days after inoculation with rhizobia, the *Pscoch2* mutant nodules presented a typical wild-type indeterminate nodule shape and were not different from wild-type Caméor (Fig. 9a, b).

Pscoch1 single mutant is known to already present a very strong nodule to root phenotype (Couzigou *et al.*, 2015) which does not impair the symbiotic performance

of pea (Ferguson & Reid, 2005). In order to know if the *Pscoch2* mutation increases the *Pscoch1* nodule to root phenotype and if it affects the nodulation process, we generated the double mutant *Pscoch1coch2*. Nodulation experiments on Caméor, *Pscoch1*, *Pscoch2*, and *Pscoch1coch2* mutants showed that 90 % of the *Pscoch1* nodules are pink hybrid nodule-root structures as described in Fergusson and Reid, 2005 and (Fig. 9c,e). *Pscoch1coch2* also develops hybrid nodule-root structures in a similar proportion than *PsCOCH1* (≈90 %, Fig. 9d,e) but these hybrid nodule-root structures remain clearly smaller (three times) with faint pink to white coloration indicating a defect in development and nitrogen fixation efficiency (Fig. 9d). Furthermore big pink converted or not nodules as shown in Fig. 9a, b, c, were not observed in *Pscoch1coch2*. The nodule number formed in the different *Pscoch* mutants indicates that Caméor, *Pscoch1,* and *Pscoch2* formed in average hundred nodules per plant that are mostly converted in *Pscoch1* (Fig. 9f). Surprisingly, while Caméor and *Pscoch2* produced on average forty nodule primordia per plant, very few nodule primordia were observed in *Pscoch1* (Fig. 9f). In contrast, *Pscoch1coch2* double mutants present supernumerary nodules and nodule primordia, one hundred of each, that is twice as much as Caméor, *Pscoch1,* and *Pscoch2* (Fig. 9f). The symbiotic performance was assessed in the mutants using the ARA test and normalized by the plant. This revealed that all the mutants were fix+, however once normalized per nodule, the experiment showed that the *Pscoch1coch2* nitrogen fixation is significantly reduced relative to wild-type (Fig. 9g, h). These results suggest that the nodule to root conversion takes place earlier in the double mutant and results in non-functional nodules. They also show that *PsCOCH2* participates in the symbiotic process.

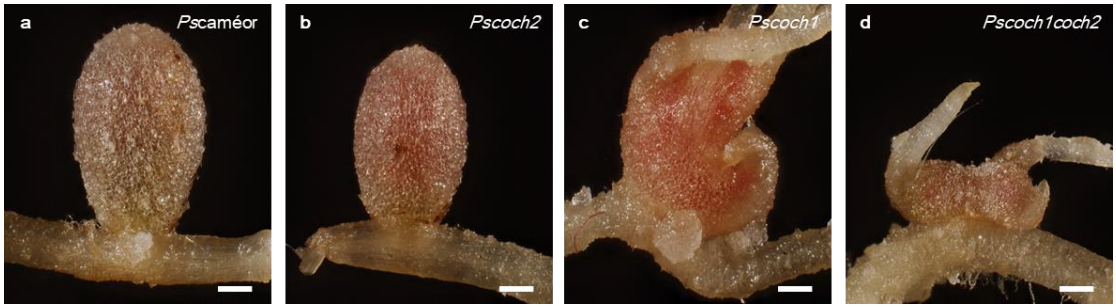

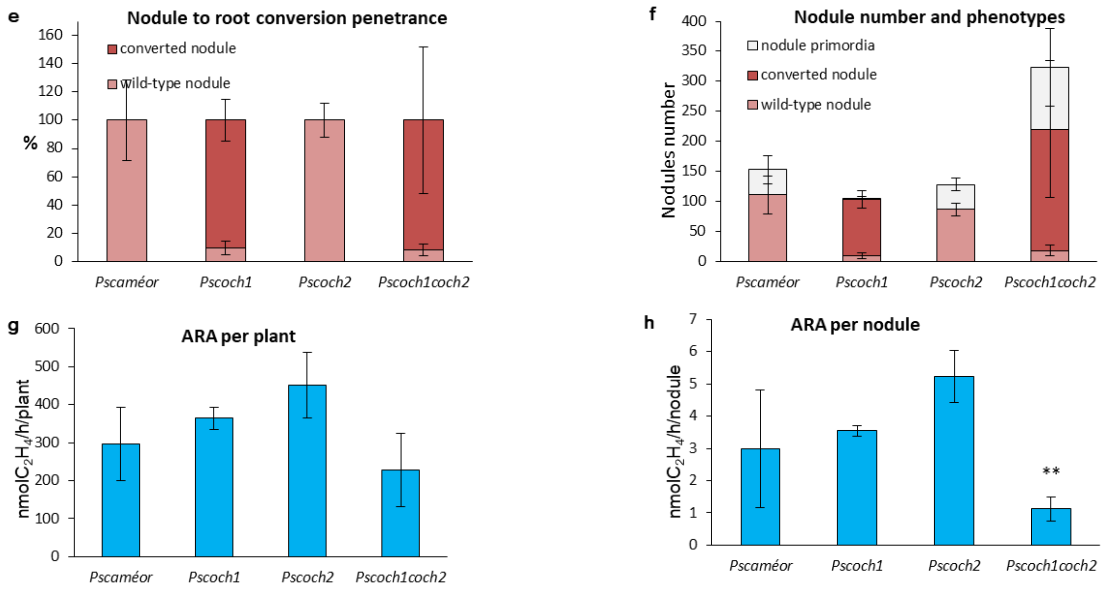

Figure 9. *Ps*caméor, *Pscoch1*, *Pscoch2 and Pscoch1coch2* nodule phenotypes and nitrogen fixation ability.

a-d, Nodule from flowering *P. Sativum* plants inoculated with *R. leguminosarum* strain P221 at 35 dpi. **a**, *P*scaméor shows a wild-type pink indeterminate nodule phenotype. **b**, *Pscoch2* shows a wild-type pink indeterminate nodule phenotype. **c**, *Pscoch1* shows pink nodules converted to root. **d**, *Pscoch1coch2* double mutant nodules from four independent crosses show tiny white or pink nodules that convert to root, big pink nodule as shown in **a,b,c**, is not found in *Pscoch1coch2*. **e,** Nodule to root conversion penetrance in the *Pscoch* mutants relative to wild-type. Results represent the mean percentage ± SE of wild-type (pink bars) and converted nodules (red bars). *P*scaméor present only wild-type nodule and *Pscoch1* and *Pscoch1coch2* present 90 % of converted nodules, nodule primordia are not represented. **f,** Number and phenotype of nodules present in *Pscoch* mutants relative to wild-type. *P*scaméor and *Pscoch2* show only wild-type nodules and nodule primordia, *Pscoch1* show almost only nodules converted to root with few wild-type nodules and few nodule primordia and *Pscoch1coch2* show an increased number of the nodule with twice more converted nodule than *Pscoch1* and twice more nodule primordia than *P*scaméor or *Pscoch2* genotype. **g,h**, Nitrogen fixation in *Pscoch* mutants relative to wild-type, expressed per plant (**g**) and per nodule (without nodule primordia) (**h**). Asterisks indicate a significant difference compared to the *Ps*caméor control (** indicate a p-value < 0,01; Mann and Whitney test). Results in (**e, f, g ,h**) represent means ± SE of one biological experiments containing 4 plants for *P*scaméor, *Pscoch1*, *Pscoch2* and 16 plant from four independent crossing for *Pscoch1coch2* representing 612 *P*scaméor nodules, 422 *Pscoch1* nodules, 511 *Pscoch2* nodule and 5172 *Pscoch1coch2* nodules. Scale bars **a-d,** 500 µm.

DISCUSSION

PsCOCH2 is orthologous to *MtNOOT2*

In this work, we report the identification and the characterization of a new member of the legume specific NBCL2 clade, the *PsCOCH2* gene of *P. sativum*, orthologous to the *MtNOOT2* gene. Using TILLING-NGS technology we identify the first KO mutant allele of the *PsCOCH2* gene in pea. The preliminary studies of this mutant allele showed that *Pscoch2* has no symbiotic phenotype in pea. These findings support the results obtained in the legume model *M. truncatula* in which *Mtnoot2* single mutant shows no phenotype. This also indicates that despite the presence of the transcripts of both *MtNOOT2* and *PsCOCH2* in the indeterminate nodule of *M. truncatula* and *P. sativum*, respectively, and their characteristic symbiotic gene expression behavior, it appears that the *NBLC2* genes are not strictly required for normal indeterminate nodule development.

NBCL2 participate to leaves and stipules development and determinacy

Gene expression analysis revealed a strong transcriptional overlap between *MtNOOT1* and *MtNOOT2* in *M. truncatula* and between *PsCOCH1* and *PsCOCH2* in *P. sativum*. The two homologous genes are co-expressed in many aerial organs, especially in leaves and flowers in the two plants suggesting a common role in the regulation of aerial organ development and possible functional redundancy. The *Pscoch2* and *Mtnoot2* single mutants did not present particular aerial patterning defects in pea and *M. truncatula*, respectively, suggesting that the *PsCOCH1* or *MtNOOT1* genes may be sufficient for the development of the different aerial organs and/or that the *PsCOCH2* or *MtNOOT2* genes can be dispensable. This may also reflect functional redundancy between *NBCL1* and *NBCL2* genes in the two plants.

To better evaluate the role of the *PsCOCH2* and *MtNOOT2* genes, we used the double mutants *Pscoch1coch2* and *Mtnoot1noot2*. Our approach relies on the phenotypic comparison between the *Pscoch1* (*Mtnoot1*) and *Pscoch2* (*Mtnoot1*) single and the *Pscoch1coch2* or (*Mtnoot1noot2I*) double mutants. The *Pscoch1* mutant has already been described for stipules and flower developmental alterations. The penetrance of the *Pscoch1* mutation in pea, is strong for the aerial and symbiotic mutant phenotypes (Yaxley *et al.*, 2001; Ferguson & Reid, 2005; Couzigou *et al.*, 2012, 2015). In *Mtnoot1*, defects in the aerial organ, however, were mild, with reduced stipule and occasionally increased petal number. This indicates that *PsCOCH1* plays a more important role in pea than *MtNOOT1* in Medicago for development. Another difficulty we were facing in this study is the variability of the

aerial *Pscoch1* single mutant phenotypes. Taken together, the strong penetrance and the variability of the aerial *Pscoch1* phenotypes make the phenotypic characterization and comparison between the *Pscoch1* single and the *Pscoch1coch2* double mutants particularly difficult. Despite these difficulties, we tried to understand if the *Pscoch2* mutation accentuates or not some *Pscoch1* mutant phenotypes.

Our observation showed that the *Pscoch1coch2* double mutant phenotype is similar to the *Pscoch1* one for stipules and flower modifications. However, in *Pscoch1coch2* we observed occasionally strong leaf morphology alterations characterized by an increase in leaf complexity. At the early stages of development, most of the plants had fused leaves, indicating a defect in the control of leaf development and determinacy. Such leaf alterations were not previously reported for *Pscoch1*. Previous studies described the *Pscoch1* mutant as strictly impacted in the stipule identity and flower morphology. The leaf morphology alterations observed in the double *Pscoch1coch2* mutant suggests that the *PsCOCH2* genes must also play a role in the regulatory network of leaf development and determinacy. In the double *Mtnoot1noot2* Medicago mutant, some additional leaf defects were also observed, including modified leaflets from transformed stipules and enlarged leaf size. These leaf defects were not observed in *Mtnoot1* and/ or *Mtnoot2* single mutants, indicating that *MtNOOT1* and *MtNOOT2* act together in leaf identity. In Arabidopsis, the *NBCLs* (*BOP1/2*) genes play important roles in regulating leaf morphogenesis and patterning (Ha *et al.*, 2003, 2007). The most dramatic developmental effect is on leaf development, with the *bop1-1* dominant-negative and b*op1bop2* null mutant leaves displaying extensive lobe formation and forming ectopic outgrowths of blade tissue along petioles of cotyledons and leaves (Ha *et al.*, 2003, 2007; Norberg *et al.*, 2005; Hepworth *et al.*, 2005). In tomato, three *BOPs* genes (*SlBOP1/2*/3) were involved in the diversity of leaf complexity through repression of the leaflet formation (Izhaki *et al.*, 2018). This suggests that the *NBCL* genes function redundantly to control leaf development in different species.

Stipule modifications in *Pscoch1coch2* appeared similar to those of the *Pscoch1* single mutant. In both mutants, stipules can become compound-leaf, simple leaflets, highly reduced, or absent. However, a detailed node by node analysis of the strength of the stipule morphology alterations clearly indicates that stipule development and identity are significantly more impacted in the pea double mutant relative to the

Pscoch1 single mutant. Indeed, while *Pscoch1* stipules are generally absent in the first five nodes, in *Pscoch1coch2* the absence of a stipule is accentuated and prolonged until the ninth node. These results clearly indicated that the *PsCOCH2* gene is involved in the stipule development and identity and that *PsCOCH2* is functionally redundant with *PsCOCH1* for stipule determinacy. The enhanced *Pscoch1* stipule identity alteration by the *Pscoch2* mutation is in agreement with the enhanced loss of stipule identity observed in the *Mtnoot1noot2* double mutant relative to the *Mtnoot1* single mutant in *Medicago*. In the *Mtnoot1noot2* double mutant, stipule morphology alterations are enhanced and displayed a range of variations. Stipules were highly reduced or absent, have significantly increased length, and conversion of stipules to compound-leaves was also observed. In contrast in the *Mtnoot1* single mutant, stipules display reduced digitation number and reduced size (Couzigou *et al.*, 2012). Together, the results clearly indict that the *NBCL2* subclade genes in legume, *PsCOCH2,* and *MtNOOT2*, play an important role in leaf and stipule development although with varying degrees in different species. The stipule phenotypes of *Mtnoot1noot2* resemble that of the *Mtphan* (*MtPHANTASTICA*) mutant (Zhou *et al.*, 2014), raising the possibility that PHAN and NOOT may interact to regulate stipule development in *M. truncatula*. Furthermore, the *NBCLs* (*BOPs*) in monocots, such as barley, rice, and *Brachypodium*, are required for ligule and auricle development (Tavakol *et al.*, 2015; Toriba *et al.*, 2019; Magne *et al.*, 2020). In total, the *NBCL* function is conserved in eudicot and monocot to regulate the leaf pattern.

NBCL genes function together to control plant architecture

Internode patterning is a key determinant of inflorescence architecture, with variations in the length and pattern of internode elongation contributing to diversity in inflorescence height and organization of secondary branches and flowers on the primary stem (Sussex, 1989). In Arabidopsis, ectopic expression *BOP1* or *BOP2* results in either short plants with floral pedicels pointing downward (Ha *et al.*, 2007) or short bushy plants with irregular internodes (Norberg *et al.*, 2005). In *M. truncatula*, loss-of-function *Mtnoot1* mutant displayed a bit short plant stature while the *Mtnoot2* increased plant height, and the *Mtnoot1noot2* tremendously increased plant height. This increased plant height resulted from an extended internode length in *Mtnoot1noot2* while *Mtnoot1* internodes were similar to the wild type and slightly longer in *Mtnoot2*. This indicates that *MtNOOT1* and *MtNOOT2* have an additive

effect to repress the internode elongation. In pea, the *Pscoch1* mutant is also shorter, with more branches (see chapter II), while *Pscoch2* is WT. As observed for *Mtnoot1noot2*, the *Pscoch1coch2* double mutant has also an increased plant height but this increase was not so important than in Medicago. Interestingly, in *Brachypodium*, the *Bdcul4laxa* double mutant displayed a dwarf phenotype (see *Brachypodium* chapter) although the *Bdcul4* and *Bdlaxa* single mutants show a wild type internode phenotype (Magne *et al.*, 2020). These data suggest that they function together to control the internode elongation but the effect is species dependant.

The architecture of the inflorescence, the shoot system that bears the flowers, is the main component of the huge diversity of forms found in flowering plants (Benlloch *et al.*, 2015). Wild type *M. truncatula*, generally produce one to three flowers on a single inflorescence, whereas the *Mtnoot1* mutant produces mostly only one flower per inflorescence. In contrast to *Mtnoot1*, the *Mtnoot2* increases flower numbers with up to three flowers on a stalk. Because the penetrance of these phenotypes is weak it is difficult to affirm that these two genes are controlling flower numbers. In the *Mtnoot1noot2* double mutant, however, the number of flowers was significantly increased and a range of variations was observed. Moreover, the flower stalk length also greatly increased even if this was not observed in the *Mtnoot1* and *Mtnoot2* single mutants. The *Mtnoot1noot2* inflorescences thus greatly increased the diversity of plant architecture. In pea, apart from shoot branching, the *Pscoch1* mutant also displayed more flower inflorescences, in contrast to the *Mtnoot1* inflorescence phenotype. The flower number and flower stalk length were unchanged in the *Pscoch2* mutant. All these results suggest an additive effect of the *NBCL1* and *NBCL2* sub-clades to control inflorescence architecture. Consistent with our results, in tomato (*Solanum lycopersicum*) three BOPs (*SlBOPs*) genes act together to control inflorescence architecture and flower production (Xu *et al.*, 2016). In addition, the *NBCL* gene *HvLAXATUM-A* (*LAX-A*) in barley (*Hordeum vulgare*) also controls internode length and homeotic changes of the barley inflorescence (Jost *et al.*, 2016). In contrast, the deletion of the second *NBCL* gene *Uniculme4* (*HvCul4*) in barley did not impact spike architectural traits (Tavakol *et al.*, 2015). Unfortunately, there is no double mutant for these two genes to study their role in the inflorescence structure. In contrast, the *Brachypodium BdCUL4* and *BdLAXA*, homologs of *HvCUL4* and *HvLAX-A*, are important for inflorescence development and control the spikelet

determinacy (Magne *et al.*, 2020). In addition, the *Bdcucl4laxa* double mutant displayed a stronger spikelet phenotype resulting in sterility (see chapter III). The differences between *Arabidopsis* and other plants, including *M. truncatula*, pea, and barley and *B. distachyon* may result from an increasing sub-functionalization of *BOP1/2* homologs in the different species. Although some inflorescence defects are shared among the three species (e.g., elongated internodes and abnormal pedicel orientation), it is striking that the elimination of the BOP activity in Arabidopsis results in a weak loss of IM determinacy, whereas the double legume mutants show an enhanced IM indetermination.

NBCL2 participates to the regulation of the floral patterning in *M. truncatula* and pea

Flower modification is subtle in *Mtnoot1* even if additional organs (petals and stamens) were observed, suggesting a reduced penetrance of the mutation in *M. truncatula* (Couzigou *et al.*, 2012). The *Mtnoot2* single mutant is WT but the *Mtnoot1noot2* double mutant displayed important modifications of flower development resulting in supernumerary petals and increased sepal size. The early opened flower results in exposed stamens and premature senescence of the anthers. In addition, the central carpel was significantly longer and separated from the stamens. In this mutant, the defective carpels developed to abnormal pod-like structures resulting in decreased self-fertility (nearly sterile) or low pod set and reduced seed number per pod. This was never observed in *Mtnoot1* single mutant, suggesting that the *MtNOOT2* gene plays an important role in floral organ development. Taken together, these phenotypes indicate that *MtNOOT1*and *MtNOOT2* function redundantly in the control of the floral organ identity, and stamens and carpels development in *M. truncatula*.

BOP1 and BOP2 act redundantly during reproductive development to control bract suppression, floral patterning, floral organ number, and also gynoecium formation (Ha *et al.*, 2007). Typical *coch1* flowers are dorsalized with enlarged floral bracts and supernumerary organs in all whorls (Yaxley *et al.*, 2001; Kumar *et al.*, 2011; Couzigou *et al.*, 2012; Sharma *et al.*, 2012). As previously mentioned, the *Pscoch2* single mutant does not present any particular floral anomaly. Thus, to determine if *PsCOCH2* is also involved in the floral patterning and identity acquisition in pea, we have compared the *Pscoch1coch2* double mutant flowers to the

Pscoch1 single mutant flowers. Our observations revealed that *Pscoch1coch2* and *Pscoch1* display similar floral patterning defects leading to an open floral structure and reduced self-fertility. Again, because of the strong and high variability of the floral phenotypes of the *Pscoch1* mutant, it was particularly difficult to distinguish if the *Pscoch2* mutation accentuated *Pscoch1* mutant phenotypes. The detailed analysis of the floral defect occasionally shows a novel and recurrent floral patterning alteration that was not observed nor described in the *Pscoch1* single mutant. This mutant phenotype consists of the presence of supernumerary organs in the flower. Wild-type peas have ten anthers fused into a tube and one central carpel completes the flower (Yaxley *et al.*, 2001). The *Pscoch1coch2* mutant form flowers with supernumerary sepals, petals, and anthers. Most of the *Pscoch1coch2* mutant flowers have two central carpels and occasionally three or four. These flowers conserved a strong open structure that often leads to sterility. We can thus hypothesis a role for *PsCOCH2* in the early stages of the young pea floral primordia, probably in redundancy with its paralog PsCOCH1. Scanning electron microscopy analysis of *Pscoch1coch2* inflorescence meristems could allow us to better understand what happens during these early stages of floral development and confirm the involvement of *PsCOCH2* in the genetic network controlling the floral primordia establishment. Such role in frontiers establishment between organs is well known and described for the Arabidopsis *AtBOP1* and *AtBOP2* genes which are the closest orthologs of *PsCOCH1* and *PsCOCH2* genes. Thus a similar role for the pea *NBCL* genes in organ boundaries and organ size establishment and regulation make sense. The absence of floral defects in the *Pscoch2* mutant suggests that this gene is not essential for the floral patterning in pea and that *Pscoch1* gene can perfectly compensate the *PsCOCH2* loss of function, indicating also a partial functional redundancy between the two pea *NBCL* genes. We can hypothesize that *PsCOCH2* has evolved from the more ancient and polyvalent *PsCOCH1* gene to assume other roles in plant development and/or to create additional regulatory steps to better regulate plant developmental processes such for example the establishment of the nodule root organogenesis and/or better regulation of the nodule symbiotic performances. Loss-of-function *bop* mutations in Arabidopsis, *coch1* in pea, and *noot1* in *M. truncatula* all increase the number of floral organs and perturb dorsal-ventral growth patterns, altering flower symmetry (Yaxley *et al.*, 2001; Ha *et al.*, 2003; Norberg *et al.*, 2005;

Hepworth *et al.*, 2005; Xu *et al.*, 2010; Couzigou *et al.*, 2012). The mutation of the *NBCL2* sub-clade gene in pea and *M. truncatula* increased this phenotype.

Like *BOP* genes in other species, the *NOOT1/ NOOT2* or *COCH1/COCH2* seems to have unequal redundant functions in vegetative and reproductive development. For example, whereas Arabidopsis *BOP1* seems to have a more prominent role in leaf development, *BOP2* functions more during reproductive growth (Khan et al. 2014). The *MtNOOT2* and *PsCOCH2* genes belong to the completely unexplored legume-specific *NBLC2* sub-clade. *PsCOCH2* and *MtNOOT2* represent now the first characterized members of the legume *NBCL2* sub-clade and their corresponding mutant alleles represent original genetic tools that can significantly help to increase our knowledge concerning the role of the *NBCL2* genes in legume plants. We have shown that *MtNOOT2* and *PsCOCH2* participate in the regulation of the development and the determinacy of the stipules and leaves and we highlight that *MtNOOT2* and *PsCOCH2* are likely involved in the regulation of the floral patterning in pea. Thus our study provides novel elements significantly improving our understanding of the roles of this *NBCL2* clade. Pea *NBCL* single and double mutants represent important genetic tools of interest to study the role of legume *NBCL* genes and their precise functions in the genetic networks underlying nodules, stipules, leaves and flowers development, patterning and identity determinacy in legumes, as it has been the case for the *Atbop1bop2* double mutant in Arabidopsis in the past decade.

In *Arabidopsis*, *BOP1/2*, *LFY*, and *AP1* activities converge in blocking the continued expression of inflorescence meristem identity genes to maintain floral meristem determinacy at late stage 2 (Liu *et al.*, 2009; Xu *et al.*, 2010). The pea *PIM*, the ortholog of *AP1* (Taylor *et al.*, 2002), expression was slightly upregulated in *Pscoch1* and *Pscoch1coch2* mutant flower primordia and significantly increased in developed flowers. Consistent with this, DET, which acts to maintain the indeterminacy of the apical meristem during flowering (Foucher *et al.*, 2003), was significantly upregulated in *Pscoch1* and *Pscoch1coch2* mutant flower primordia and decreased in developed flower. This suggests that *PsCOCH1* promotes floral meristem determinacy.

The *NBCL* clade shares conserved function governing fruit architecture

Plant organs, such as seeds, are primary sources of food for both humans and animals. Seed size is one of the major agronomic traits that have been selected in crop plants during their domestication (Linkies *et al.*, 2010; Li & Li, 2014, 2016). Legume seeds are a major source of dietary proteins and oils (Ge *et al.*, 2016). Preliminary evidence suggests that *BOP1/2* activities also govern the architecture of fruits. In fruits, *BOP1/2* and *KNAT6/2* function in the same genetic pathway as evidenced by the rescue of the replum formation in *pny* mutants by either *bop1 bop2* or *knat2 knat6* loss of functions (Ragni *et al.*, 2008; Khan *et al.*, 2012b). Given the functions of BOP1/2 acting via KNAT6-ATH1 in the stem and abscission zones, this same module is likely to pattern the fruit (Benlloch *et al.*, 2015).

In *M. truncatula*, the *Mtnoot1* mutant has a bigger pod size, resulting in larger seed size. In contrast, in the *Mtnoot2* mutant, pod and seed size were reduced but the plant produced an increased pod number in a single inflorescence. In the *Mtnoot1noot2* double mutant, the pod size was also reduced and the pod number was even more reduced, with only a few pods per plant. Similar phenotypes were observed in pea *coch1* and *coch2* mutant. In agreement with previous studies, the seeds number is reduced in the *Pscoch1* due to the flower sterility (Yaxley *et al.*, 2001). Besides, we found that the seed size was increased in this mutant. However, as each pod produces only one or two seeds, this can result in larger seeds. Thus a direct implication of *PsCOCH1* on seed size cannot be confirmed. To do this, we also measured the seed size in *Pscoch2* and *Pscoch1coch2* and surprisingly the seed size and weight were reduced in *Pscoch2*. As observed in *Pscoch1*, the *Pscoch1coch2* displayed similar seed size as *Pscoch1*, indicating a role for *PsCOCH1* on seed size. Furthermore, the *NBCL* genes in *Brachypodium* also have a role in seed development, where the *Bdcul4* mutant also shows a lager seed but the *Bdlaxa* and *Bdcul4laxa* had reduced seed size (see chapter III). Together, the *NBCL* Clade shares conserved functions governing the architecture of fruits in plants.

***PsCOCH2* is involved in nodule development and identity**

We demonstrated that *PsCOCH2* like *MtNOOT2* is not expressed in root and induced in nodules and *Pscoch2* mutants have no symbiotic phenotype in pea. In *Medicago*, *MtNOOT2* plays a role in nodule development and identity function redundantly with *MtNOOT1*. Thus, it can be hypothesized that *PsCOCH1* shares

redundant functions with *PsCOCH2* that compensate for the loss of function of *PsCOCH2*.

To understand the role of the *PsCOCH2* gene in the nodulation process, we have undertaken a genetic approach in which we constructed and started to characterize the double mutant *Pscoch1coch2*. The preliminary characterization of the *Pscoch1coch2* double mutant showed that the *Pscoch2* mutation does not exacerbate the already strong nodule to root homeosis present in *Pscoch1* single mutant, but considerably impact the development of the nodule and its ability to fix nitrogen. Indeed, the *Pscoch1coch2* double mutant nodules were always tiny, early converted to root, and poorly to not pink colored. *Pscoch1coch2* nodules never reached a substantial size as in the wild-type or the *Pscoch1* background, their nitrogen fixation capacity was reduced and furthermore, the *Pscoch1coch2* mutant nodules were supernumerary compared to WT plants. Together these observations suggested that the *Pscoch1coch2* mutant is impaired in the nodule apical meristem growth, in the nodule identity and in nodule development resulting in a reduced nitrogen fixation that is probably linked to a poor rhizobia colonization. This colonization status of the *Pscoch1coch2* nodules remained to be tested. The *Pscoch1coch2* supernumerary nodules phenotype is typical of the deregulation of the autoregulation of nodulation (AON, Osipova et al., 2012) and it suggests that the nodules formed on the double mutant are not perceived as real and/or functional nodules by the plant. Additional experiments need to be performed to understand why *Pscoch1coch2* displays a hyper-nodulation phenotype and to decipher if the regulation of the nodule central meristem and/or the secretion of *CLAVATA3/EMBRYO-SURROUNDING REGION* (*CLE*) peptides are altered in *Pscoch1coch2*. On the other hand, the first results we obtained on the *Pscoch1coch2* double mutant undeniably revealed that the *PsCOCH2* gene also plays a role in nodule development and identity conservation in pea, two essential components that are required to properly host the symbiotic rhizobia. Our results may also suggest a role for the *NBCL2* gene clade in nodule central meristem maintenance.

MATERIALS AND METHODS

Plant material

The seeds of wild-type *M. truncatula* ecotype R-108 (Hoffmann *et al.*, 1997) and its corresponding mutants, *MtNOOT1* (Tnk507 and NF2717); *MtNOOT2* (NF5464); *MtNOOT1MtNOOT2* (NF2717 crossed with NF5464); ProNOOT2: GUS; (Magne et al., 2018), Wild-type *P. sativum* var. caméor and *PsCOCH2* (Ps1178, Dalmais et al., 2008, http://urgv.evry.inra.fr/UTILLdb), and wild-type *P. sativum* var. JI2822 and the corresponding fast neutron bombardment full-length deletion mutants lines *Pscoch1JI* (FN3185/1325, Couzigou et al., 2012; John Innes Centre germplasm; www.jic.ac.uk/ GERMPLASM/), *Pscoch1*^{Cam} was use FN3185/1325 back-cross to caméor (back-cross1). Double mutants *Pscoch1coch2* were obtained by crossing Pscoch1^{Cam} (FN3185/1325) with *PsCOCH2* Ps1178 (back-cross 2). SGE wild-type and its corresponding EMS mutant *SGEapm* (Zhukov *et al.*, 2007) were used.

Coch2 mutant isolation

To study the role of *PsCOCH2* using *PsCOCH2* single mutant and to later construct the double mutant *Pscoch1coch2* in a similar *P. sativum* background, TILLING mutations in the *PsCOCH2* genes were screened by TILLING coupled with Next Generation Sequencing technology (TILLING-NGS) using the *P. sativum* var. caméor TILLING mutant collection (Dalmais *et al.*, 2013). 99 % of the coding sequence was screened for *PsCOCH2* genes and 75 TILLING mutants were identified. A summary of the tilling results and detailed lists of the TILLING mutations obtained for *PsCOCH2* was given in Supplementary Table S1. Based on the SIFT score (http://sift.bii.a-star.edu.sg/) which represents the predictive deleterious effect of a mutation on the protein function, two KO lines (SIFT score: 0; Ps1178 and Ps3340) were obtained but Ps3340 line was lost, Ps1178 was chosen for *PsCOCH2* (Supplementary Table S3).

For the *PsCOCH2* gene, homozygous KO mutant was obtained for the family Ps1178 (Supplementary Table S3). Following direct cross-fertilization with wild-type Caméor, the Ps1178 KO mutant line was finally obtained at a homozygous state. This *PsCOCH2* allele was backcrossed 3 times as a single mutant and the plant form backcross 2 were used to construct the double mutant *Pscoch1coch2* (Supplementary Table S3).

Plant growth conditions

Seeds were sacrificed and surface-sterilized by immersion in 5 mL of sodium hypochlorite (one pellet per 1L of sterile water) and 1 droplet of liquid soap for 20 min under agitation. Three successive rinsings with sterile water were done. Seeds were vernalized 2 days at 4°C under darkness on 7g.L^{-1} Kalys Agar plates. Seeds were then transferred to growth chamber 48h at 24°C under darkness for acclimatization and subsequent sowing in soil. For nodulation assays in the pot, a sand/perlite mixture was used (1/2, v/v). For vegetative development and bloom, a loam/peat/sand mixture was used (70/3, 5/7, v/v/v; http://www.puteaux-sa.fr) with expensed clay balls at the bottom of the pot. *P. sativum* plants were grown under 16/8h light-dark cycle, 24/24°C day-night temperature, 60% of relative humidity, and 200 µE of light intensity. Plants were watered three times a week (2 times with water / 1 times with nutritive solution in alternance) with HY N-free nutritive solution for nodulation (For 5 liters of HY N-free solution: 50 mL of stock solutions (KH2PO4, 0,1 M; MgSO4, 0,1 M); 12,5 mL of stock solutions (K2SO4, 0,1 M; CaCl2, 2H2O, 0,1 M); 5 mL of stock solutions (KCl, 50 mM; H3BO3, 23,8 mM; MnSO4, H20, 5 mM; ZnSO4, 7H20, 1 mM; CuSO4, 1 mM; MoNa2O4, 2H20, 0,7 mM; Na-Fe-EDTA, 98mM); pH: 7) or with N+ nutritive solution (Soluplant, NPK16 6 26) for non-nodulated plant.

Genomic DNA extraction

Plant genomic DNA was extracted from leaves as described in Dellaporta et al., (1983) with some modifications. Young leaves were frozen in liquid nitrogen and ground with a ball grinder (Retsch, MM400) two times 30 seconds with a frequency of 25.s-1. 600µL of fresh DNA extraction buffer (NaCl (350mM), Tris-HCl pH: 7,6 (10mM), Urea (7M), N-Lauroyl sarcosine (2%), EDTA (50mM), aqueous phenol pH: 7,9 (6,5%)) were added to the powder. The suspension was vortexed, incubated 5 min at 50°C and shaken 10 min at room temperature. 700 µL of aqueous phenol pH: 7,9; chloroform; iso-amylalcohol (25:24:1) were added. The suspension was vortexed, centrifugated 10min at 14000rpm and aqueous phase was collected. 700 µL of chloroform; iso-amylalcohol (24:1) was added to the aqueous phase. The suspension was centrifuged 10min at 13000rpm and supernatant (800ul) was collected and place on a new 1.5 mL Eppendorf tube. DNA was precipitated using 3M cold sodium acetate: isopropanol (0.1:1). After a 10min centrifugation at 13000rpm, the

supernatant was discarded and the DNA pellet was washed with 1000µL of 70% ethanol. The tube was centrifuged 5min at 13000 rpm, the liquid removed, the DNA pellet dried, and the DNA was re-suspended in 100µL of sterile water and treated with RNase (Roche).

Plant genotyping

The TILLING point mutation in line *PsCOCH2* (Ps1178) was checked by PCR amplification and sequencing. PCR amplifications were carried out using High Fidelity Taq DNA polymerase (EUROBIO GAETHF004D). Detailed information about mutation location is given supplementary table S3 and information concerning oligonucleotides couple used for PCR amplification is providing in supplementary table S2. PCR products were sequenced by Sanger (www.eurofinsgenomics.eu) and analyzed with A plasmid Editor 2.0.49 software. For the *PsCOCH1* line FN3185/1325, the *PsCOCH1* full-length deletion borders are not known and homozygous mutants were selected by phenotyping for the coch1 phenotypes.

Material fixation and X-gluc staining

Samples were pre-fixed in cold acetone 90% during 1h at -20°C. Samples were rinsed twice with phosphate buffer (50mM) and infiltrated 30min under vacuum (≈500mm Hg) in freshly prepared X-gluc staining buffer (phosphate buffer pH: 7,2 (50mM), potassium ferricyanide (1mM), potassium ferrocyanide (1mM), sodium dodecyl sulfate (SDS) 0,1%, EDTA (1mM), 5-bromo-4-chloro-3-indolyl-beta-D-glucuronic acid (X-gluc) containing cyclohexylammonium (CHA) salt (1,25mM). After vacuum, samples were transferred into a wet closed container and incubated in the same X-gluc staining buffer overnight under darkness, at 37°C. After staining, samples were rinsed three times with phosphate buffer (50mM).

RNA preparation and reverse transcription

Plant material was frozen in liquid nitrogen and ground with a mortar in liquid nitrogen in presence of 500 µL of TRIzol reagent (ref# 15596026, AMBION). All the processes of extraction were performed in a clean hood and the samples were kept at 4°C. After 5 min of decreasing, 100 µL of chloroform were added, mix and incubated 10 min. The samples were centrifuged 5 min at 16000 x g and up to 500 µL of the aqueous phases were collected. RNA was precipitated 3h at -20 °C with 250 µL of

isopropanol and 100 µL of sodium acetate (3 M) pH: 5,2. RNA pellets were collected after 10 min centrifugation at 16000 x g and washed with 1 mL of 70 % ethanol. The liquid was discarded after centrifugation of 5 min at 16000 x g and the RNA pellets dried under the hood were resuspended in 30µL of sterile water. RNA samples were treated with the TURBO DNA-free™ Kit (Ambion) according to the manufacturer's recommendations and then quantified with a NanoDrop 1000 (Thermo Scientific) at a wavelength of 260nm. Their integrities were accessed on 2% agarose gel. First-strand cDNA was synthesized from 1 µg of RNA template using SuperScript™ II Reverse Transcriptase kit (ref. 18064-022, Invitrogen) with oligo (dT) primers (Invitrogen) in the presence of Ribolock RNase Inhibitor (Thermo scientific). Samples were diluted ten-fold with RNase free water.

qRT-PCR gene expression analysis

Real-time RT-PCR reactions were performed in triplicate with 1µL of diluted cDNA in each reaction with the 5µL of 2X LightCycler FastStart DNA Master SYBR Green I kit (Ref. 04887352001, ROCHE), 2µL of each primer (2,5µM) in 10µL reaction volumes. The reactions were conducted in a LightCycler®96 (Roche) using the following conditions:1 pre-incubation cycle (95°C, 5 min), followed by 42 cycles of denaturation: 95°C for 15s, hybridization:60°C for 15s, and elongation:72 °C for 15s. 1 melting curve cycle [(denaturation: 95 °C, 10 s), (hybridization: 60 °C, 1 min), (denaturation: 97°C, 1s)], 1 cooling cycle (37°C, 30s).Values were normalized against two housekeeping genes, actin (Medtr2g008050) and RNA recognition motif (Medtr6g034835.1) were used as a reference in relative qPCR experiments. The final threshold cycle (Ct), efficiency, and initial fluorescence (R0) for every reaction were calculated with the Miner algorithm (Zhao & Fernald, 2005). Relative expression levels were obtained from the ratio between R0 of the reference gene and R0 of the target gene. Information concerning primers used for qRT-PCR gene expression analysis is given in Supporting Information Supplementary table 1.

Acetylene reduction assay

Acetylene reduction assays (ARA) were performed on individual plants inoculated with *R. leguminosarum* strain P221 at 35dpi with a protocol modified from Koch & Evans (1966). The nodulated root system of one plant was placed in a 21 mL glass vial sealed with rubber septa in presence of 200 µL of water. Acetylene gas (500

µL) was injected into each vial and 2 h incubation was performed. For each sample, 1 mL of gas was injected. Ethylene production was measured using a Gas Chromatograph (Agilent Technologies, 7820A) equipped with a GS-Alumina column (50 m x 0,53 mm) with hydrogen as the carrier gas. Column temperature and gas flow were adjusted at 120 °C and 7,5 mL.min-1, respectively.

Supplementary table S1. Mutations identified in *PsCOCHLEATA2* gene by TILLING-NGS technology

[a]Position of the mutation in mutants from the starting ATG on the coding sequence. [b]Position of the amino acid substitution in mutants from the starting methionine of the encoded protein. [c]values represent a predictive deleterious score from the SIFT software (http://sift.bii.a-star.edu.sg/). SIFT score ranges from 0 to 1. The amino acid substitution is predicted as damaging the protein if the score is ≤ 0,05 (highlighted in blue) and tolerated if the score is > 0,05. (data from Kevin Magne PhD)

PsCOCHLEATA2			KX821778
Nucleic acid transition [a]	Amino acid substitution [b]	SIFT score [c]	Family
C51T	L17L	1	*Ps697*
C51T	L17L	1	*Ps1641*
C51T	L17L	1	*Ps1073*
C100T	R34C	0	*Ps2431*
G106A	V36I	0,36	*Ps4498*
C113T	A38V	0,34	*Ps1865*
C183T	S61S	1	*Ps3370*
G203A	G68E	0,21	*Ps2874*
C233T	P78L	0,34	*Ps3903*
G246A	P82P	0,68	*Ps575*
G268A	V90M	0,03	*Ps1454*
G282A	L94L	1	*Ps4311*
C320T	P107L	1	*Ps2071*
C348T	C116C	1	*Ps3864*
G354A	E118E	1	*Ps2140*
G366A	W122*	0	*Ps1178*
G372A	T124T	0,75	*Ps4616*
C398T	A133V	1	*Ps1527*
G469A	A157T	0,2	*Ps1698*
G507A	M169I	0,43	*Ps3161*
C564T	S188S	0,64	*Ps3495*
C589T	P197S	0,33	*Ps1004*
C594T	P198P	0,49	*Ps3949*
G604A	A202T	0,33	*Ps3693*
G625A	V209I	0,38	*Ps2143*
G645A	E215E	1	*Ps1747*
C662T	S221F	0,04	*Ps737*
C663T	S221S	1	*Ps984*
C670T	R224C	0,02	*Ps3607*
C675T	R225R	1	*Ps3940*
C677T	S226F	0,02	*Ps2078*
C685T	P229S	0,2	*Ps1014*
C690T	L230L	1	*Ps2960*
C690T	L230L	1	*Ps4407*
A695G	H232R	0,69	*Ps4108*
C751T	R251W	0,02	*Ps466*
G753A	R251R	1	*Ps1742*

PsCOCHLEATA2			KX821778
Nucleic acid transition [a]	Amino acid substitution [b]	SIFT score [c]	Family
C757T	L253F	0,29	*Ps4235*
C767T	S256L	0,01	*Ps1863*
G792A	M264I	0,05	*Ps1873*
G820A	E274K	0,09	*Ps2220*
C830T	A277V	0,05	*Ps1037*
G841A	A281T	0	*Ps1240*
C935T	P312L	0,08	*Ps2892*
G958A	V320M	0,12	*Ps3451*
G976A	A326T	0,64	*Ps1275*
G1013A	R338K	0,73	*Ps1700*
G1025A	G342D	0,02	*Ps3729*
C1033T	P345S	0,36	*Ps3698*
C1034T	P345L	0,16	*Ps1406*
G1081A	A361T	0,05	*Ps4699*
C1082T	A361V	0,05	*Ps4332*
G1091A	G364E	0,08	*Ps3918*
C1099T	H367Y	0,01	*Ps500*
G1105A	E369K	0,6	*Ps3274*
C1135T	L379F	0,17	*Ps1808*
C1141T	Q381*	0	*Ps3340*
C1165T	R389C	0,03	*Ps3552*
C1188T	N396N	1	*Ps2974*
G1198A	A400T	0,03	*Ps2112*
C1211T	A404V	0,02	*Ps1748*
C1225T	P409S	0	*Ps2701*
C1228T	P410S	0	*Ps4485*
G1240A	D414N	0	*Ps3515*
G1250A	S417N	0	*Ps1414*
G1300A	D434N	1	*Ps1747*
G1312A	V438M	0	*Ps4679*
G1330A	A444T	0	*Ps4168*
C1331T	A444V	0	*Ps1343*
G1346A	G449D	0	*Ps1349*
G1348A	G450S	0	*Ps568*
G1354A	G452S	0	*Ps2270*
G1384A	E462K	0	*Ps3825*
G1403A	G468E	0	*Ps1970*
G1421A	G474E	0	*Ps3335*

Supplementary table S2. Oligonucleotides used for TILLING-NGS screen, SNP detection assay and genotyping

Gene	Gene ID	Family and generation	Forward primer (5'-3')	Reverse primer (5'-3')	Amplicon length
PsCOCHLEATA2	KX821778 KX821779 KX821780 KX821781	*Ps1178* M3, M4	PsCOCH2_Ex1_F2 TTCCCTACACGACGCTCTTCCGATC TATCTCTCTCCCTTGACTACC	PsCOCH2_Ex1_R1 AGTTCAGACGTGTGCTCTTCCGATCT ACATAAAAACCTGAGTGAGC	498 bp
		-	PsCOCH2_Ex2_1_F1 TTCCCTACACGACGCTCTTCCGATC TTCTTATCTAACTCTCATTGC	PsCOCH2_Ex2_1_R1 AGTTCAGACGTGTGCTCTTCCGATCT TTCCGGAGACACCATCTCGG	615 bp
		Ps3340 M3	PsCOCH2_Ex2_2_F3 TTCCCTACACGACGCTCTTCCGATC TCGGCTGGCAAAACTCCGCTT	PsCOCH2_Ex2_2_R1 AGTTCAGACGTGTGCTCTTCCGATCT CTAGCTAGGCTTAGAAATCG	604 bp
			NGS-M13_F CACGACGTTGTAAAACGAC.TTCCC TACACGAC	NGS-M13_R GGATAACAATTTCACACAGG.AGTTC AGACGTGT	
			M13F700 CACGACGTTGTAAAACGAC	M13R800 GGATAACAATTTCACACAGG	

na: no seed available for this line; . 5' 26 bp illumina adaptators

Supplementary table S3.| Characteristics of the *coch* mutant lines used in this study

Characteristics of the *coch* mutant lines used in this study

Gene mutated	Type of mutation	Name in this study	Accession ID	Mutagen	Background	References
PsCOCHLEATA1	CGA:TGA>Arg:STOP69	SGEapm	*SGEapm*	EMS	SGE	Zhukov et al. (2007)
	Full-length deletion	coch1JI	*FN3185/1325*	FNB	JI2822	Couzigou et al., 2012
	Full-length deletion	coch1Cam	*FN3185/1325*	FNB(backcross)	Caméor	This study
PsCOCHLEATA2	G366A>W122*	coch2Cam	*Ps1178*	EMS	Caméor	This study
PsCOCHLEATA1 *PsCOCHLEATA2*	————	coch1coch2	(*FN3185/1325*) *X* (*Ps1178*)	Cross	Caméor	This study

EMS, ethyl methanesulfonate; FNB, Fast Neutron Bombardment. * indicate stop mutation

Supplementary table S4 | Schematic representation of the stipule morphology alterations in *Pscoch* mutants relative to wild-type *Pscaméor* .

Stipules morphology is reported from node 1 to 13 (left axis) in *Ps*caméor, *Pscoch1*, *Pscoch2* and *Pscoch1coch2*. Morphology alteration of stipules is ordered from low to high severity, classed in four categories and a color code was assigned: wild-type peltate stipules (Wt, green), leaflet-like or compound leaf-like stipules (Lf, light red), thread-like stipules (Th, red) and absence of stipule (Ab, dark red). Figures represent mean percentage of each category of stipule modifications. For each genotype, at each of the first 13 nodes, the stipule category which is the most represented is highlight in the corresponding color. n, number of stipules analyzed per node. *Ps*caméor, 7 plants; *Pscoch1*, 7 plants; *Pscoch2*, 5 plants; *Pscoch1coch2*, four lines from independent crossing, 28 plants. (data from Kevin Magne PhD)

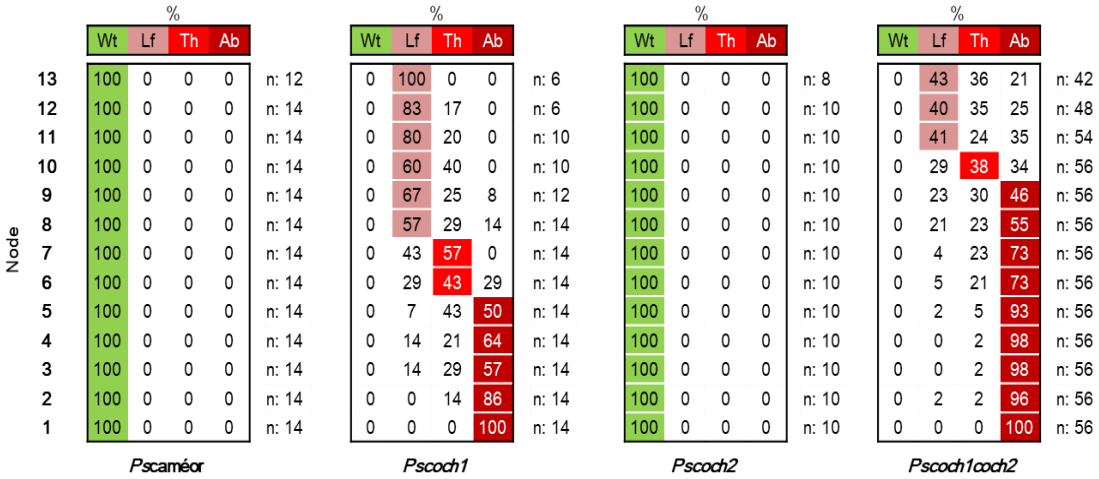

Supplementary table S5. Primers used for qPCR

Gene	Purpose	Primer names	Primer sequences (5' to 3')	Source
PsACTIN	qRT-PCR	PsACT-F PsACT-R	CTCAGCACCTTCCAGCAGATGTG CTTCTTATCCATGGCAACATAGTTC	Azarakhsh et al. 2015
PsBETA-TUBULIN3	qRT-PCR	PsBTUB3_F PsBTUB3_R	TTGGGCGAAAGGACACTATACTG CAACATCGAGGACCGAGTCA	Saha et al., 2012
PsCOCH1	qRT-PCR	PsCOCH1qpcrD PsCOCH1qpcrR	TCATCCTTATCACGCCGCTC TGCAACTCTCAACCGCGTAA	This study
PsCOCH2	qRT-PCR	PsCOCH2qpcrD PsCOCH2qpcrR	AGACCCCACAGTAAGAACCG TTCACGTGAGAGAACAAGAGC	This study
DET (TFL1a)	qRT-PCR	PsDET-F PsDET-R	CCACCATCAACACCAAACC TCTCTTTCCCAAATGTAGCATC	This study
PIM	qRT-PCR	PsPIM-4F PsPIM-6R	GCTTCAGAGTTTGGAACAGC GACTCCATGGTGGTTTGG	Liew et al., 2011
MtACTIN11	qRT-PCR	MtACT-F MtACT-R	TGGCATCACTCAGTACCTTTCAACAG ACCCAAAGCATCAAATAATAAGTCAACC	Plet et al., 2011
MtRNA RECOGNITION MOTIF	qRT-PCR	MtRRM-F MtRRM-R	AGGGGCAAGTTCCTTCATTT GGTAGAAGTGCTGGCTCAGG	Plet et al., 2011
MtNODULE ROOT1	qRT-PCR	MtNOOT1-F MtNOOT1-R	TATGAATGAAGATCACCACCATAG TCATGACCATGAGAGTGATGATG	Couzigou et al., 2012
MtNODULE ROOT2	qRT-PCR	MtNOOT2-F MtNOOT2-R	TTACCCTCCAATGAGCGAAG CCAGATCCCTAGGCTTAGAAGTCA	Magne et al., 2012

CHAPTER II.

The *COCHLEATA1* gene controls branching and flowering time in pea

The *COCHLEATA1* gene controls branching and flowering time in pea

Shengbin Liu[1, 2], Kévin Magne[1, 2] and Pascal Ratet[1, 2]

[1]Institute of Plant Sciences Paris-Saclay IPS2, CNRS, INRA, Université Paris-Sud, Université Evry, Université Paris-Saclay, Bâtiment 630, 91405 Orsay, France.

[2]Institute of Plant Sciences Paris-Saclay IPS2, Paris Diderot, Sorbonne Paris-Cité, Bâtiment 630, 91405, Orsay, France.

ORCIDs:

(SL): 0000-0001-7512-4225; (KM): 0000-0002-6779-5683; (PR): 0000-0002-8621-1495

Author contributions

SL, KM, PR, conceived the research plans. SL, KM designed the experiments, performed the research experiments, and analyzed the data. SL and PR wrote the article.

Abstract

Plant architecture is mostly determined by shoot branching patterns, which result from the spatiotemporal regulation of axillary bud outgrowth. Numerous endogenous, developmental, and environmental factors are integrated at the bud and plant levels to determine numbers of growing shoots. Strigolactones (SLs) are well known for their role in repressing shoots branching. Here, we provide evidence that *NBCL1* (*PsCOCH1*, *MtNOOT1*) inhibits pea and *Medicago* branching, respectively, and that *PsCOCH1* may act as a new component of the strigolactone-dependent branching inhibition pathway. The *nbcl1* mutants exhibit increased shoot branching with reduced plant height like the previously characterized highly branched SL deficient (*ramosus1* (*rms1*) and *rms5*) and SL response (*rms3* and *rms4*) mutants. Grafting studies indicate that the *PsCOCH1* gene is necessary for long-distance signaling. The pea *coch1* mutant is not able to synthesize SL and respond to the SL application. The *PsCOCH1* gene expressed in the axillary buds and roots and is transcriptionally down-regulated by direct application of the synthetic SL GR24. An increased transcript leave of SL biosynthesis genes, *RMS1* and *RMS5*, is observed in the *coch1* mutant. Besides, the CK biosynthesis gene *IPT1* was up-regulated in *coch1*, and the mutant responds to BAP application and decapitation by increasing axillary bud length, implicating that *PsCOCH1* may have a role in integrating SL and CK signals and that SLs act directly within the bud to regulate its outgrowth. Moreover, *PsCOCH1* is up-regulated by auxin indole- 3-acetic acid (IAA) application in internode segments as *RMS1* and *RMS5*. We further conclude that *PsCOCH1* regulates the flora transition by promoting the *PsFTa1* and repress *PsTFLc*, and the flowering time change may involve SL. This study presents new interactions between *RMS* and *PsCOCH1* genes in shoot branching and provides further elements in the control of flowering time in pea.

Keywords: *NBCL1*, branching, Strigolactones, auxin, cytokine, flowering time

INTRODUCTION

The multitude of plant forms observed in nature is the result of the activities of different meristems during postembryonic development. In seed plants, the primary axis of growth, together with the primary shoot and root apical meristems, is laid down during embryonic development. A major aspect of post-embryonic plant development is the formation of secondary axes of growth: vegetative branches, inflorescence branches, or flowers. In vegetative development, axillary meristems initiate the formation of several leaf primordia, resulting in an axillary bud. The pattern of vegetative shoot branching depends not only on the initiation of axillary meristems in the leaf axils but also on the regulation of bud outgrowth (Shimizu-Sato & Mori, 2001). During reproductive development, lateral meristems play a crucial role in the establishment of different inflorescence structures that ultimately lead to the formation of flowers. Axillary meristems are thus major determinants of the architecture and the reproductive success of a plant (Schmitz & Theres, 2005).

The initiation of axillary buds appears to be exclusively genetically regulated without any implication of other contributing factors (Kebrom *et al.*, 2013). Currently, only a few genes have been identified, including *Lateral suppressor* (*Ls*) and its orthologs [*LATERAL SUPPRESSOR* (*LAS*), *MONOCULM1* (*MOC1*)] (Schumacher *et al.*, 1999; Li *et al.*, 2003; Cheng *et al.*, 2006; Gallavotti *et al.*, 2008) and *LAXPANICLE1* (*LAX1*) and its orthologs [*BARREN STALK1* (*BA1*)] (Komatsu *et al.*, 2003b; Gallavotti *et al.*, 2004; Yang *et al.*, 2012). In contrast, the axillary bud outgrowth has been well characterized due to the identification of many mutations related to bud outgrowth (Gomez-Roldan *et al.*, 2008; Domagalska & Leyser, 2011; Costes *et al.*, 2014). These intensive studies regarding the outgrowth of buds have revealed a global and complex regulation network of genetic, hormonal, and environmental factors (McSteen, 2009; Domagalska & Leyser, 2011; Wang & Li, 2011; Guo *et al.*, 2013; Kebrom *et al.*, 2013).

In some plant species, the outgrowth of axillary buds can be suppressed by the primary shoot, a phenomenon known as apical dominance (Sachs & Thimann, 1964; Cline, 1991; Barbier *et al.*, 2017). The phytohormones auxin and cytokinin (CK) have long been implicated in the process, in which auxin from the apex inhibited the outgrowth of axillary buds by affecting its supply in CK while CK coming from the

roots promoted bud outgrowth (Sachs & Thimann, 1967; Eklöf *et al.*, 2000; Li & Bangerth, 2003; Nordström *et al.*, 2004; Tanaka *et al.*, 2006).

Strigolactones (SLs) have long been recognized as responsible for the induction of seed germination of root parasitic plants and as branching factors for symbiotic arbuscular mycorrhizal (AM) fungi (Cook *et al.*, 1966; Akiyama *et al.*, 2005). Recently, genetic and physiological evidence demonstrated that SLs represent a new class of phytohormones that repress shoot branching (Gomez-Roldan *et al.*, 2008; Umehara *et al.*, 2008). Their existence as a novel branching inhibitor signal was suggested through grafting experiments with high-branching mutants deficient in SL biosynthesis or signaling in diverse species including *Arabidopsis thaliana* (more axillary shoot [*max*]), *Pisum sativum* (*ramosus, rms*), *Oryza sativa* (dwarf [*d*] or high tillering dwarf [*htd*]), and *Petunia hybrida* (decreased apical dominance [*dad*]) (Napoli, 1996; Beveridge *et al.*, 1996, 1997, 2000, 2009; Stirnberg *et al.*, 2002; Turnbull *et al.*, 2002; Sorefan *et al.*, 2003; Booker *et al.*, 2004, 2005; Snowden *et al.*, 2005; Zou *et al.*, 2005, 2006, Arite *et al.*, 2007, 2009; Beveridge & Kyozuka, 2010; Domagalska & Leyser, 2011). The mutants, such as *ramosus* (*rms*) are recessive and relatively non-pleiotropic.

In pea, the branching phenotype is also influenced by the gibberellin status and photoperiod. Mutant plants deficient in gibberellin, such as the widely used *le* dwarf cultivars, have a greater tendency to produce lateral shoots from the basal nodes than tall WT counterparts (Murfet & Symons, 2000). Dwarfism is also often associated with increased shoot branching, hence genes regulating internode elongation also affect shoot branching (Silverstone *et al.*, 1997; Lo *et al.*, 2008). Interestingly, branching pattern (basal, aerial, rosette type), and morphology (branch angle, width, number of branches per node) differ according to the gene involved.

Shoot branching is strongly influenced by developmental processes such as flowering. In Arabidopsis, *BRC1* interacts with FLOWERING LOCUS T (*FT*)/and *TSF* (*TWIN SISTER OF FT*, a paralog of *FT*) proteins interact with *BRC1* to repress the floral transition. The *brc1-2* mutant is highly branched, and its lateral branches flower earlier (Niwa *et al.*, 2013). This crosstalk between flowering and branching is complex as floral initiation and branching are both controlled by similar environmental (photoperiod) and endogenous (plant growth regulators) factors, suggesting common regulatory pathways between the two processes. Late-flowering

mutants often exhibit modified branching patterns. In *Arabidopsis*, *FLOWERING LOCUS C* (*FLC*) and *FRIGIDA* (*FRI*), two floral repressors in the vernalization pathway (Andrés & Coupland, 2012), also regulate stem branching (Huang *et al.*, 2013). In forage pea lines, the dominant *hr/elf3* allele is late flowering and associated with increased branching under short-day conditions (Lejeune-Hénaut *et al.*, 2008; Weller *et al.*, 2012). In several species, dormant axillary buds below the flowering node are frequently released from dormancy at floral transition.

The *FT* /*TFL1* (TERMINAL FLOWER1) gene family is involved in the control of floral induction, but also in plant architecture through the control of determinate and indeterminate growth (McGarry & Ayre, 2012; Pin & Nilsson, 2012). The floral activator *FT*, a mobile signal that promotes flowering and the floral repressor *TFL1* are components of the florigen and anti-florigen pathways, respectively. The florigen pathway also stimulates shoot branching. The *FT/TFL1* balance might be a regulator of branching: a high ratio leads to increased branching and a low ratio to decreased branching, as shown in rice (Tamaki *et al.*, 2007), rose (Randoux *et al.*, 2014), or tomato (Lifschitz, 2008) by using mutants or transgenic plants that over-expressed *FT/TFL1* genes.

BOP1 and *BOP2* are also involved in flowering-time regulation by repressing the expression of *FD* in the shoot meristem and may also have a role in controlling floral initiation (Andrés *et al.*, 2015). A delayed flowering is observed in the *bop1bop2* mutants despite that this delay is to a large extent caused by a slower leaf initiation rate in *bop1bop2* (Norberg *et al.*, 2005) or gain-of-function *BOP1/2* plants which display delayed flowering.

The mutant of *P. sativum*, *cochleata* (*coch1*), was first reported as having altered flower and leaf phenotypes (Wellensiek, 1959). The phenotype of the *coch* mutant is homeotic in that stipules assume leaf-blade-like compound morphology (Blixt, 1967). *PsUNI* repression by the *PsCOCH1* gene confers the stipule identity (Gourlay *et al.*, 2000; Kumar *et al.*, 2009). *PsCOCH1* was shown as required for the *P. sativum* inflorescence development and flower organ identity acquisition. The flowers of *coch* exhibit supernumerary and mosaic organs, in addition to abnormally fused parts and reduced fertility (Yaxley *et al.*, 2001; Couzigou *et al.*, 2012; Sharma *et al.*, 2012). The nodules are typically dichotomously branch show root structures emerging from their meristems (Ferguson & Reid, 2005). The molecular characterization

showed that the *PsCOCH1* gene is orthologous to the *Medicago truncatula NODULE-ROOT1* (*MtNOOT1*) gene and to the *Arabidopsis thaliana AtBLADE-ON-PETIOLE1/2* (*AtBOP1*/2) genes (Ha *et al.*, 2004; Norberg *et al.*, 2005; Hepworth *et al.*, 2005), which form together a new gene clade called *NOOT-BOP-COCH-LIKE* (*NBCL*). The *NBCL* clade groups proteins that carry BTB/POZ (BROAD COMPLEX, TRAM TRACK, and BRICK A BRACK/POXVIRUSES and ZINC FINGER) and ANKYRIN repeat domains and belongs to the defense-related *NON-EXPRESSOR OF PATHOGENESIS-RELATED PROTEIN1-LIKE* (*NPR1-LIKE*) family (Couzigou *et al.*, 2012).

Plants overexpressing *AtBOP1/2* show a branching phenotype, producing extra para-clades in leaf nodes (Ha *et al.*, 2007). Loss-of-function *bop1bop2* also causes subtle defects in floral-meristem identity signified by enlarged floral bracts, a delay in the node of the first flower, the occasional absence of cauline leaves at the base of lateral branches, and branched flowers (Norberg *et al.*, 2005; Ha *et al.*, 2007; Xu *et al.*, 2010). Branching complexity and misexpression of inflorescence identity genes is dramatically enhanced in *bop1 bop2 ap1* and *bop1 bop2 lfy* triple mutants with phenotypes suppressed by loss-of-function *agl24*. These genetic interactions suggest a role for BOP1/2 in maintaining determinacy through repression of *AGL24* (Xu *et al.*, 2010). Furthermore, enlarged floral bracts and branched flowers are also found in *coch* mutants, indicating a conserved function in pea (Yaxley *et al.*, 2001; Couzigou *et al.*, 2012). The pea ortholog of *AP1* is *PROLIFERATING INFLORESCENCE MERISTEM* (*PIM*) (Taylor *et al.*, 2002). Flowers in *pim coch* double mutants are similarly replaced by highly branched leafy shoots. Recently, it was reported that the maize *BOP* ortholog *tassels replace upper ears1* (*TRU1*) is directly activated by teosinte branched (*tb1*) to regulate axillary bud growth in maize (Dong *et al.*, 2017). The BOP-Like gene *UNICULME4* controls tillering in barley (Tavakol *et al.*, 2015), in *Brachypodium* the *BdUNICULME4* and *BdLAXATUM*-A act antagonistically to control branching (Magne *et al.*, 2020). Previous studies using highly branched mutants of pea, *Arabidopsis*, and rice have demonstrated that strigolactones, a group of terpenoid lactones, act as a new hormone class, or its biosynthetic precursors, in inhibiting shoot branching.

Here, we reported the new roles for *NBCL1* (*PsCOCH1*, *MtNOOT1*) inhibiting pea and *Medicago* branching, respectively, and we propose that *PsCOCH1* may act as

a new component of the strigolactone-dependent branching inhibition pathway. The phenotype of *nbcl1* mutants is similar to highly branched SL deficient (*ramosus1* (*rms1*) and *rms5*) and SL response (*rms3* and *rms4*) mutants. Grafting studies indicate that the *PsCOCH1* gene is necessary for long-distance signaling. The pea *coch1* mutant is not able to synthesize SL and respond to the SL application. The *PsCOCH1* gene is expressed in the axillary buds and roots, and is transcriptionally down-regulated by direct application of the synthetic SL (GR24) and by CK but up-regulated by auxin (IAA). The expression levels of SL biosynthesis genes *RMS1* and *RMS5* and CK biosynthesis gene *IPT1* were increased in the *coch1* mutant. This suggests that *PsCOCH1* may have a role in integrating SL and CK signals. Furthermore, *PsCOCH1* regulates the floral transition by promoting the *PsFTa1* expression and repressing *PsTFLc*, and this flowering time change may involve SL. This study highlights new roles for the *PsCOCH1* gene, in shoot branching and flowering time in pea.

RESULTS

Mutations in the pea *COCH1* gene increase shoot branching

Branch development (shoot branching) is a key determinant of plant architecture which affects important plant functions like light acquisition, resource use and ultimately impacts biomass yield. The primary branch arising from the main shoot produces secondary, then tertiary, and even higher-order branches. To evaluate the role of the *PsCOCH* genes in pea branching, the phenotypes of *Pscoch1*^{Cam}, *Pscoch2*^{Cam,} and *Pscoch1*^{Cam}*Pscoch2*^{Cam} homozygous mutants were first compared with their wild-type progenitor Caméor. The *Pscoch1*^{Cam}, *Pscoch2*^{Cam} and *Pscoch1*^{Cam}*Pscoch2*^{Cam} mutants do not form buds at the cotyledonary node in Caméor background 4 days post-germination (dpg; Fig.1a, b, c). The phenotypic difference between Caméor WT and mutants were almost qualitative until 8 dpg, with the parental line Caméor and the *Pscoch2*^{Cam} mutant showing little tendency to branch (Fig. 1 h) while mutants *Pscoch1*^{Cam} and *Pscoch1*^{Cam}*Pscoch2*^{Cam} produced a total of 1 to 3 lateral shoots from nodes 1 and/or 2 (Fig. 1i, j). Only a few *coch1* plants produced buds at node 0 at this stage. To confirm this result, we checked the effect of the *coch1* mutation in JI2822 (*coch1JI*) and SGE (*SGEapm*) backgrounds. Contrary to the Caméor background, buds already form on the basal nodes in the *coch1JI* (Fig. 1e,

l) and *SGEapm* (Fig. 1g, n) mutants. They show increased branching from basal nodes and a tendency for buds forming at the cotyledonary node to grow into lateral shoots in JI2822 and SGE background. In the WT cotyledonary node of JI2822 (Fig. 1 d, k) and SGE (Fig. 1f, m) buds remained dormant unless the main shoot was damaged during seedling emergence. Interestingly, two or three buds were present at the cotyledonary node (or form directly from the seed) in the *coch1* mutants and they were growing into lateral shoots or secondary stems in JI2822 and SGE backgrounds (Fig. 1i, n). In contrast to the mutant, JI2822 and SGE parental lines never branched from the cotyledonary node. When the plants grow older, two weeks post sowing (wps), strong basal branching (more than 1cm length) at nodes 1 and 2 was observed in the *Pscoch1*^{Cam} mutants (Fig. 2a, e), with often more than three (average 3.3) branches at node 1 and 2 (supplemental Fig. S1a), whereas the *coch2* mutants (Fig. 2a), which displayed a wild-type Caméor phenotype sometimes showed only a single (average 1.5) branch at node 1 and 2 (Fig. 2a, supplemental Fig. S2a). Moreover, a striking feature of *Pscoch1*^{Cam} mutant plants was the increased number (average 1.5 branches) of cotyledonary branches that appeared about 10 days after germination (Fig. 1j), and that is rarely seen for *Pscoch2*^{Cam} and Caméor wild type. Only approximately half of *Pscoch1*^{Cam}*Pscoch2*^{Cam} double mutants branched at this cotyledonary node (Fig. 2a, f). Interestingly, the *Pscoch1*^{Cam}*Pscoch2*^{Cam} double mutants displayed reduced branching compared to *Pscoch1*^{Cam} either at cotyledonary node (average 0.5 branches) or node 1 and or 2 (average 1.7 branches) but still had a higher branching than wild type (Fig. 2a, supplemental Fig. S2a). This suggests that *COCH1* and *COCH2* might have opposite branching effects.

Figure 1. Phenotype of the *coch* mutant.

Caméor plant (**a**), *coch1* (**b**), *coch1coch2* (**c**) ; **d**, wild-type JI2822 and *coch1*^{JI} mutant (**f**) ; **h**, wild-type SGE and *SGEapm* mutant (**g**) at 4 days post geminatation (dpg); comparison of a wild-type Caméor plant (**h**) with *coch1* (**i**) and *coch1coch2* (**j**) mutants at 8 dpg in Caméor background. **k**, wild-type JI2822 and *coch1*^{JI} mutant (**l**) and wild-type SGE (**m**) and *SGEapm* mutant (**n**) at 8 dpg.

To investigate whether the pea *PsCOCH1* perform similar functions in shoot branching regulation, we analyzed the branching phenotypes of single pea *coch1*^{JI} and *SGEapm* mutants, which were generated by FNB and EMS approaches from the genotype JI2822 and SGE backgrounds, respectively (see "Materials and Methods"). The different *coch1* mutant lines always had a strong branching phenotype and similar to *Pscoch1*^{Cam}, the *coch1*^{JI,} and *SGEapm* mutant plants display a thin stem with a strong branching phenotype (Fig. 2b, d, g, h), at the cotyledonary node, with an average of 2.3 and 1.3 branches, for *coch1*^{JI} and *SGEapm* respectively. In addition, these lines often produce more than three (average 3.1 and 4.5, respectively) branches (supplemental Fig. S1a) at nodes 1 and 2. In contrast the wild-type plants produce only few small branches (average 1.4 and 1.8, respectively) (Fig. 2b, d; supplemental Fig. S1a). Moreover, the *coch1* mutant, in three backgrounds, show similar and high number of lateral shoots (supplemental Fig. S1a). These data strongly suggest that the mutation in the *PsCOCH1* gene in different backgrounds was the cause of the high-branching phenotype.

Figure 2. Phenotype of the *coch* mutants.

a, comparison of a wild-type (WT) Caméor plant (left) with *coch2* (middle left); *coch1* (middle right) and *coch1coch2* (right) mutants in Caméor background, **b**, wild-type JI2822 and $coch1^{JI}$ mutant (**c**). **d**, wild-type SGE (left) and *SGEapm* mutant (right), **e-f**, inclose obsevation of *coch1* mutant in Caméor (**e**), JI288 (**g**), SGE (**h**) background, and *coch1coch2* (**f**).

More precise phenotyping was performed on $Pscoch1^{Cam}$, $Pscoch2^{Cam}$, $Pscoch1^{Cam}Pscoch2^{Cam}$, or $Pscoch1^{JI}$ and *SGEapm* when the plants began flowering. We measured the lateral shoots or bud length at each node in all the mutant lines and their corresponding WT (supplemental Fig. S1b-d). As observed previously, either at the basal node or at the upper nodes, all the *Pscoch1* ($Pscoch1^{Cam}$, $Pscoch1^{JI,}$ and *SGEapm*) allelic lines were significantly more branched than WT plants (supplemental Fig. S2a-h). In addition, the shoots branching took place at the basal part of the plants, generally below node 3. Branching was very rare at upper nodes (above node 3; supplemental Fig. S1b-c). Interestingly, we found that in the SGE background, bud outgrowth was absent from node 5 to node 9 or reduced but after node 9 shoots appeared again (supplemental Fig. S1d). In addition, mutants were shorter than their WT (especially the *coch1JI*) before flowering. However, after flowering, the *SGEapm* and $Pscoch1^{Cam}Pscoch2^{Cam}$ mutants will continue to grow and were finally much higher than the corresponding wild type (supplemental Fig. S1e; S2a-h). In contrast, the $Pscoch2^{Cam}$ mutant was not significantly more branched than the WT Caméor at these nodes and showed also no differences in the total lateral branching length (supplemental Fig. S1b, e; S2a, d). At node 1 and 2, the total branch length was similar in the $Pscoch1^{Cam}$ and $Pscoch1^{Cam}Pscoch2^{Cam}$, whereas, at the cotyledonary node, branching of $Pscoch1^{Cam}Pscoch2^{Cam}$ double mutant plants was significantly shorter than all *coch1* single mutant lines (supplemental Fig. S1b-d). Consequently, it appeared that at the basal nodes, a transgressive phenotype was observed in the $Pscoch1^{Cam,}$ $Pscoch^{JI}$, *SGEapm,* and $Pscoch1^{Cam}coch2^{Cam}$ mutants (Supplemental Fig. S3a-d), where some small branches can continue to grow even when the wild types were already dry.

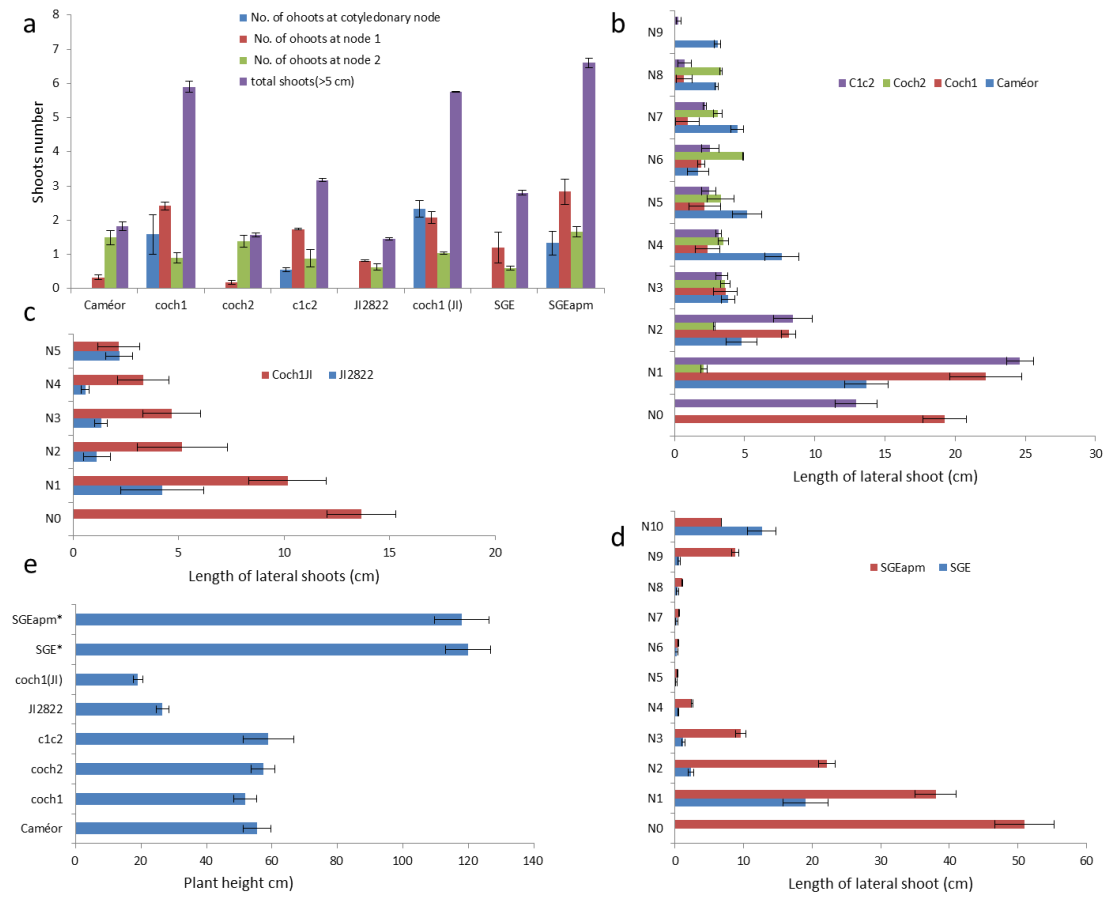

Supplemental Figure S1. Plant phenotype and branching length at different nodes.

a, Shoots numbers at the base part of the *coch* mutant lines and the corresponding wild type. **b-d.** Lateral shoots length of *coch* mutants and wild type at different nodes in Caméor background (**b**), JI2822 background (**c**), and SGE background (**d**). **e.** plant height of *coch* mutant lines and their corresponding wild type. Data are means ± SE with n=10; star indicts that SGE lines are taller genotype. N0: cotyledonary node; N1-N10: node 1 to node 10.

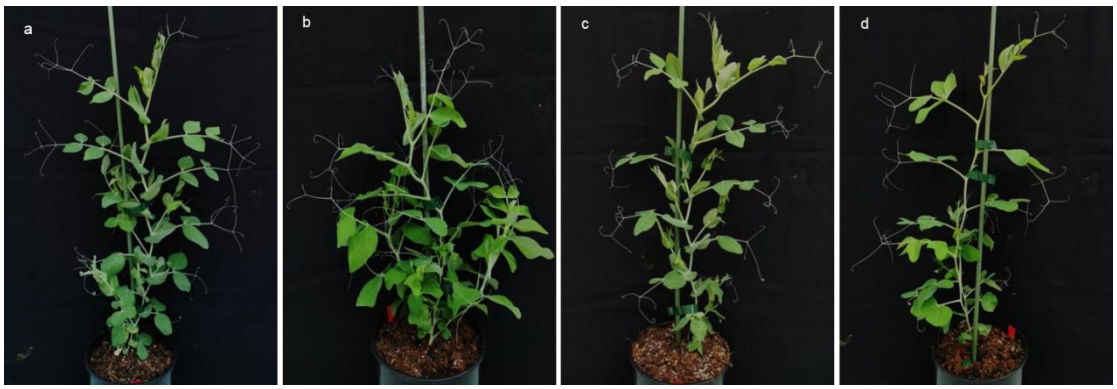

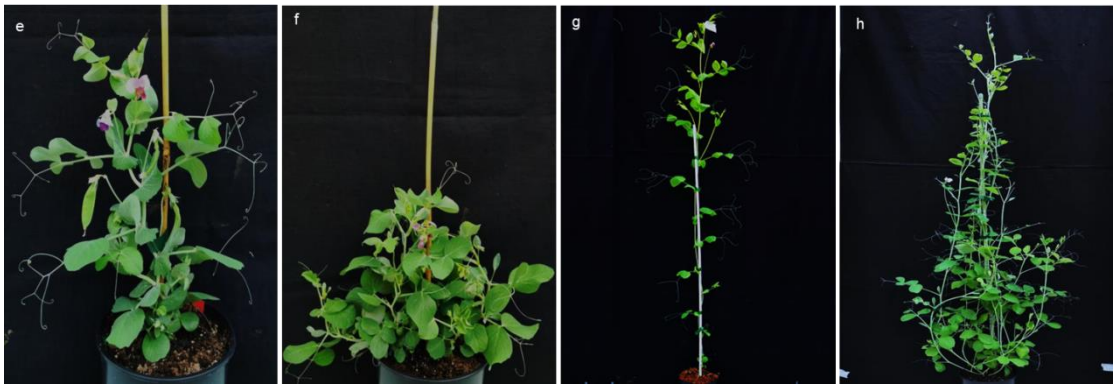

Supplemental Figure S2. The branching phenotype at the initial in *coch* mutant lines and their corresponding wild type.

a, wild-type Caméor plants have just one main shoot and a few small branches, *coch1* mutants in Caméor background displayed an increased branching with several lateral shoots as the main shoot (**b**), *coch2* (**c**) shows similar branches to wild type Caméor; *coch1coch2* (**d**) mutants in also increased the branching compare to wild type Caméor but less than *coch1* single mutants. *coch1* mutants in JI2822 and SGE background show an exaggeratively increased branch (**f**, **h**), especially in SGEapm (**h**), in contrast, the corresponding wild type JI2822 (**e**) and SGE (**g**) have only one main shoot. All the plants were just beginning to flowering or close to the flowering.

In *Medicago Mtnoot1* and *Mtnoot2* play opposite roles in lateral branching

In order to know if the *coch1*-dependent branching phenotype observed in pea could also exist in the corresponding mutants in *M. truncatula*, we analyzed the branching phenotype of the *Mtnoot1 and Mtnoot2* mutants.

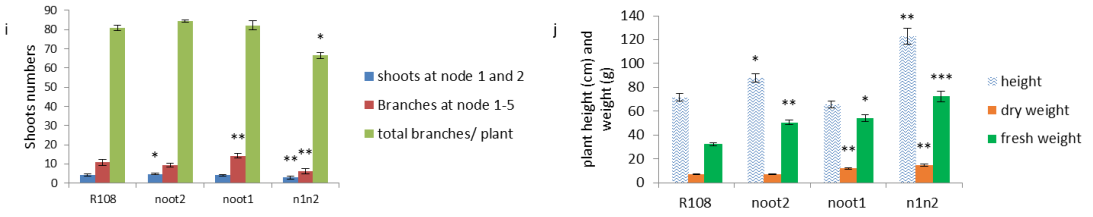

Figure 3. Branching phenotype of the *noot* mutant at the base part of the plant.

a, comparison of a WT *Medicago trunctula* R108 plant (**a**, **e**) with *noot2* (**b**, **f**); noot1 (**c**, **g**) and *noot1noot2* (**d**, **h**) mutants in the different stage; **i**, the average branches of all genotypes. n1n2, *noot1noot2*; Data are means ± SE (n = 12). Star representative p-value, one *=p<0,05, two ** =p<0,01 and three *** =p<0,001.

The *Mtnoot2* mutant showed wild type branch development patterns throughout its life cycle (Fig. 3a-b; e-f, sup. S4a-b). The *Mtnoot1* and *Mtnoot1Mtnoot2* mutants showed no obvious difference during very early plant development stages (sup. S4c-d). In contrast the *Mtnoot1* mutant began to form more branches than control plants (ecotype R108) four weeks after sowing (Fig. 3a, c). The difference became more significant after 6 weeks with the formation of additional secondary and tertiary branches in the *Mtnoot1* mutant (Fig. 3c, g). To analyze in detail this time dependant branching phenotype, we investigated the development of primary, secondary and tertiary branches when the plants had nearly 50% of their flowers open. We also counted the total branches when the plants were completely dried. This study showed that the *Mtnoot1* mutants had about 10 % more primary branches than WT plants, and over 25% more lateral branches (secondary + tertiary). In addition, we found that branches were mainly formed at the lower part (node 1-5) of the shoots (Fig. 3i) but the total number of branches was similar in the *Mtnoot1* mutant due to shorter plant height (Fig. 3j). In contrast to *Mtnoot1*, the *Mtnoot1Mtnoot2* mutants displayed a reduced branching phenotype (Fig. 3d, h) especially at nodes 1 and 2 and a reduction of nearly 50% at node 1-5. The double mutant plants had an average reduction of 15% and 20% in primary and lateral (secondary+tertiary) branches, respectively (Fig. 3d, h, i) compared to the simple *noot1* mutant. The total branches also had an 8% reduction in the double mutants compared with WT. Despite showing no differences in branching, the *noot2* mutant had a bit higher plant height and fresh biomass than WT. As a consequence of its increased branching, the *Mnoot1* mutants displayed more than 60% and a 47% increase in fresh biomass yield and dry biomass, respectively, (Fig. 3j). Despite its reduced branching capacity, the *noot1noot2* double

mutant had a higher (more than 2 times) fresh and dried biomass than all the other genotypes due to the distinct plant height, maybe as a consequence of its reduced fertility (data not shown). These results suggest that the *Mtnoot1* mutation enhanced branching while the combination of the two mutations in the *Mtnoot1Mtnoot2* mutant reduced branching during development, and thus that similarly to what we observed in pea, these two genes have antagonist roles in the *M. truncatula* branching behavior.

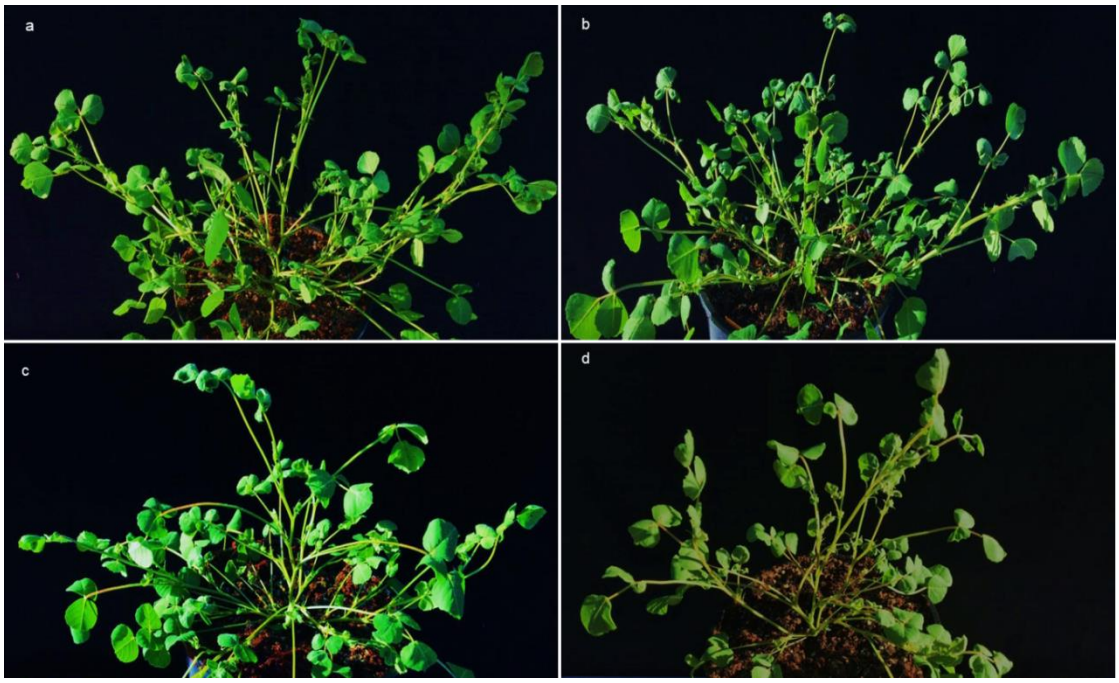

Supplemental Figure S4. Branching phenotype at an early stage.

a-d. branches at 30 days after sowing in the soil of wild type *Medicago trunctula* (*Mt*) R108 (**a**), Mtnoot2 mutant (**b**), Mtnoot1 mutant, and Mtnoot1noot2 double mutants. The Mtnoot2 show a wildtype and Mtnoot1 mutants also no more difference to wild type at this stage, Mtnoot1noot2 show a reduced branch.

The *COCH1* gene is necessary for long-distance signaling

The *Pscoch1*^{Cam}, *Pscoch1*^{JI}, and *SGEapm* mutations cause the extensive release of vegetative axillary buds and lateral growth in comparison to their wild type parental lines (Caméor, JI2822, SGE respectively), in which axillary buds are normally not released under the growth conditions utilized. The results of reciprocal grafts between mutant lines and their WT counterparts show that the branching phenotype of the *coch1* mutant in the shoot is dependent on the genotype of the rootstock. Mutant *coch1* scions exhibited a mutant phenotype only when self-grafted. In contrast, WT scions on *coch1* rootstocks or *coch1* scions grafted to a WT rootstock

did not stimulate outgrowth of basal lateral buds (Supplemental Table. 2). This result suggested the existence of a graft-transmissible signal produced in WT rootstock able to repress bud outgrowth in the mutant scion. These reciprocal grafts demonstrated that the *COCH1* gene may control the level of a mobile repressive substance produced in the root. As cotyledonary lateral buds below the graft union were excised during the first 7-10 days after grafting, our results cannot reveal any effect of scion genotype on the release and growth of buds in the cotyledonary axils of the rootstock. The same grafting test was performed in *Pscoch2*^{Cam} and *Pscoch1*^{Cam}*coch2*^{Cam}. The bud out-growth of mutants was inhibited when either grafted to wild-type rootstocks or WT scions in the mutant rootstocks, except the *Pscoch1*^{Cam} *coch2*^{Cam} self-grafted that exhibited a weak mutant phenotype (Supplemental Table. 2). These grafting studies allowed these mutants (*Pscoch1*^{Cam}, *Pscoch1*^{JI}, and *SGEapm*) to be characterized as long-distance signaling mutants controlling the level or transport of a long-distance signal repressing aerial bud outgrowth.

Supplemental Table 2. The phenotype of the different graft combinations between WT and corresponding *coch* mutants.

Genotype of rootstock / scion	Caméor	coch1	coch2	coch1coch2	JI2822	coch1DL	SGE	SGEapm
Caméor	Non Br	Non Br	Non Br	Non Br				
coch1	Non Br	Br	Non Br	Br				
coch2	Non Br	Non Br	Non Br	Non Br				
coch1coch2	Non Br	Br	Non Br	Br				
JI2822					Non Br	Non Br		
coch1DL					Non Br	Br		
SGE							Non Br	Non Br
SGEapm							Non Br	Br

Caméor, JI2822, SGE are wild type ; Br : branching scions ; Non Br : non branching scions

PsCOCH1 is deficient in the SL signaling pathway

Transcripts of *PsCOCH1* and *PsCOCH2* genes were previously detected in nodules, leaves, stems, flowers, and seeds. To test whether *PsCOCH1* and *PsCOCH2* were expressed in root and axillary buds, transcript levels were quantified by real-time PCR, and higher (2.5 fold) *PsCOCH1* expression was found than for *PsCOCH2*, which the expression level was very low in axillary buds (Fig. 4a). In addition, both *PsCOCH1* and *PsCOCH2* were expressed in the roots where the *PsCOCH1* expression level was still higher than *PsCOCH2* (Fig. 4a).

SLs are widely recognized as shoot branching regulators, and the loss-of-function pea mutants of critical components in the SL signaling pathway, *rms1* throughout *rms6* mutants show increased branch numbers, similar to the phenotype observed with *Pscoch1*. Therefore, we tested whether the altered branching phenotype in the *coch1* mutant alleles was regulated by SLs. The response to SL was analyzed by application of the synthetic SL analog GR24 (0.5µM; 1µM) by vascular supply between nodes 3 and 4 of WT Caméor and the *Pscoch1*^{Cam}, *Pscoch1*^{Cam}*coch2*^{Cam} and *PsCOCH2*^{Cam} mutants. The outgrowth of the buds was measured 7d and 10d after treatment (Fig. 4b). The inhibitory effect of GR24 was not observed for the wild-type Caméor and the *Pscoch2*^{Cam} mutant, in which axillary buds are very small at the nodes. In contrast, the axillary bud outgrowth was strongly inhibited in the *Pscoch1*^{Cam}, and *Pscoch1*^{Cam}*coch2*^{Cam} mutants and the effect of GR24 was more important using 1µM GR24 (Fig. 4b). Furthermore, we also tested the inhibition using the same treatment to the axillary bud at node 4 of Caméor and JI2822 mutant lines. Similar inhibition was observed in *coch1*^{Cam}, *coch1*^{Cam}*coch2*^{Cam}, and *coch1*^{JI} (sup. S5a). This indicates that SL can repress branching in these *coch1* mutants similarly to the grafting of WT rootstock.

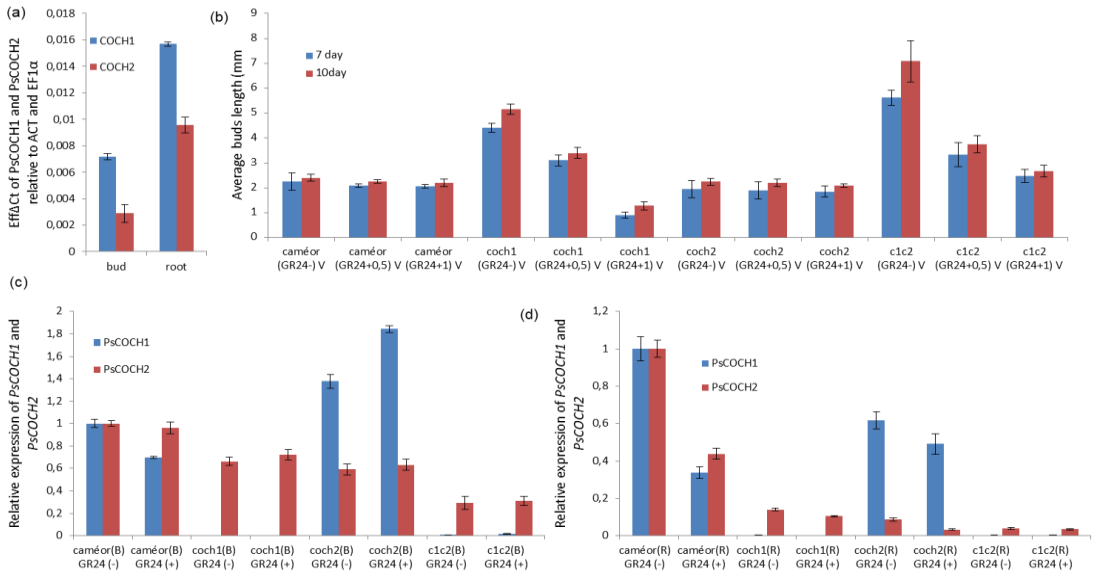

Figure 4. Transcript levels and effects of GR24 application on bud growth.

a, expression of *COCH1* and *COCH2* in axillary bud and root; **b**, bud length at node 3 of wild-type Caméor, *coch1*, *coch2*, *coch1coch2* was measured 7 (blue bars) and10 d (red bars) after treatment was applied by vascular supply with a solution containing 0, or 0,5, or 1 µM GR24, data are means ± SE (n =9). **c-d**, *PsCOCH1*, and *PsCOCH2* transcript levels were determined relative to *EF1α* and *PsACT* in

axillary buds at node 4 after GR24 application or mock treatment (**c**) and in roots (**d**) incubated without or with GR24 for 4 h. RNA was extracted from dissected buds from pools of 10 plants or roots and quantified by real-time PCR. The data are representative of two to three independent experiments.

To further characterize the effect between SL and the *coch1* mutation, the plants of the loss-of-function *Pscoch1*, *Pscoch2*, and double mutant lines and their respective wild types were germinated in vermiculite for 6d and then cultured in hydroponic complete nutrient solution for two weeks supplemented with 0 or 3 µM GR24. The branching phenotype of *Pscoch1*^{Cam}, *Pscoch1*^{JI} and *Pscoch1*^{Cam}*coch2*^{Cam} growing in 3 µM GR24 hydroponic solution was significantly reduced compared to the control (Supplemental Fig. S5b-d). This confirms that the *coch1* mutant backgrounds were sensitive to SLs and are thus probably SL deficient in roots. This suggests that COCH1 participates in the regulation of the SL production in the roots.

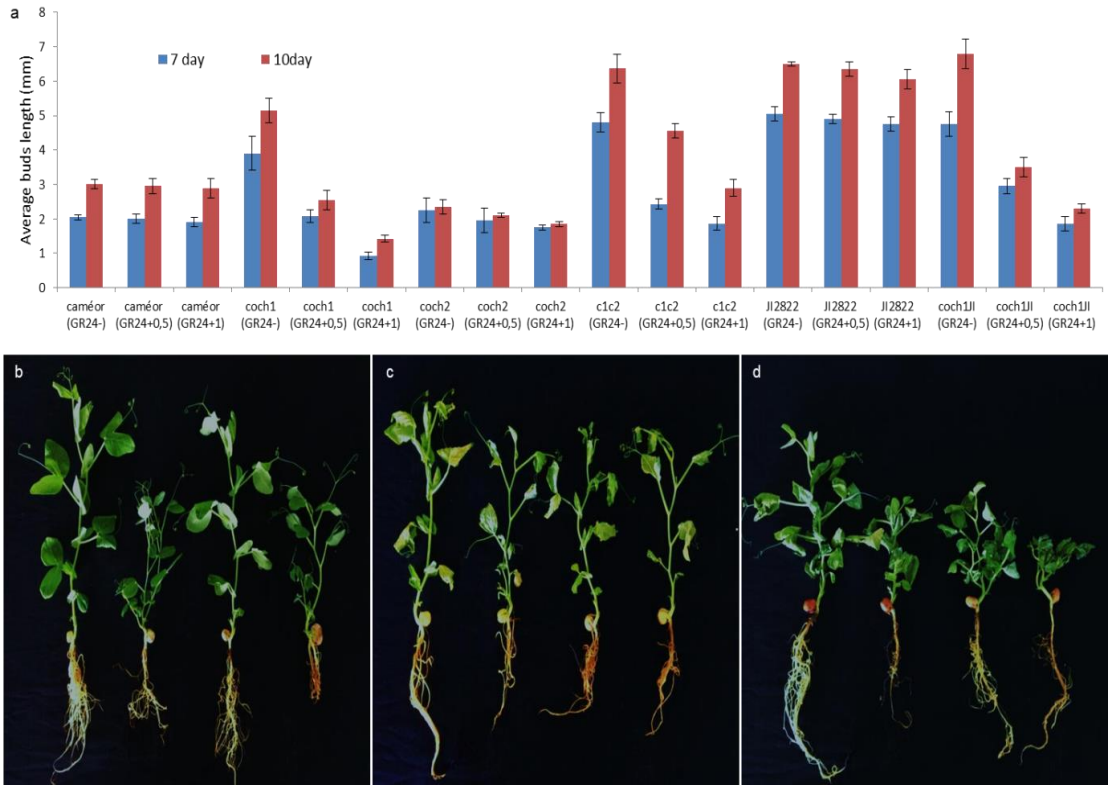

Supplemental Figure S5. Effects of GR24 application on bud growth.

a, bud length at node 3 of wild-type Caméor, *coch1*, *coch2*, *coch1coch2*, and wild-type JI2822, and *coch1*^{JI} was measured 7 and10 d after treatment was applied to buds directly with a solution containing 0, or 0,5, or 1 µM GR24. **b-d**, plant growth in hydroponic solution with or without 3 µM GR24. **b-c**, comparison of WT Caméor plant (left), *coch2* (middle left), *coch1* (middle right) and *coch1coch2* (right) mutants in Caméor background growth in hydroponic solution without 3 µM GR24 (**b**) or with 3 µM GR24 (**c**). **d**, wild type JI2822 growth in hydroponic solution without (left) or with (middle left) 3 µM GR24 and *coch1*^{JI} mutant growth in hydroponic solution without (middle right) or with (right) 3

µM GR24. The experiment was performed three times and each time with at least 3 plants for each genotype.

To test whether *PsCOCH1* and *PsCOCH2* expression could be controlled by SL, the transcript levels *PsCOCH1* and *PsCOCH2* were analyzed 24h after GR24 (1µM) application to axillary bud (Fig. 4b) in wild-type and *Pscoch1*, *Pscoch2*, and *Pscoch1coch2* mutant lines. *PsCOCH1* expression significantly decreased in wild type and increased in *Pscoch2* mutants following GR24 application (Fig. 4b), whereas *PsCOCH2* expression is not modified following GR24 application (Fig. 4b) in the different backgrounds tested. The results were confirmed in *JI2822* and *coch1JI*, in which the *PsCOCH1* expression decreased nearly 70% following GR24 treatment (Fig. S5a). The *PsCOCH1* transcripts were not detectable or very low in *Pscoch1*^{Cam}, *Pscoch1*^{JI}, and *Pscoch1coch2* due to the deletion nature of the *coch1* mutation in these lines (Fig. 4c, sup. s5a). In addition, we also tested the *COCH1* gene expression in root following 4 h incubation with GR24 *in vitro* (Fig. 4d, sup. Fig. S5b) in the caméor and SGE backgrounds. A similar expression level of *PsCOCH1* and *PsCOCH2* was observed compared to axillary buds but the repressing effect of GR24 was stronger in root (Fig. 4c-d) and on both genes (Fig. 4c-d , sup. Fig. S5b). All these results indicate that only *PsCOCH1* transcription was repressed by SL in buds while both genes were repressed in root and thus that the *COCH* genes are direct targets of the SL signaling.

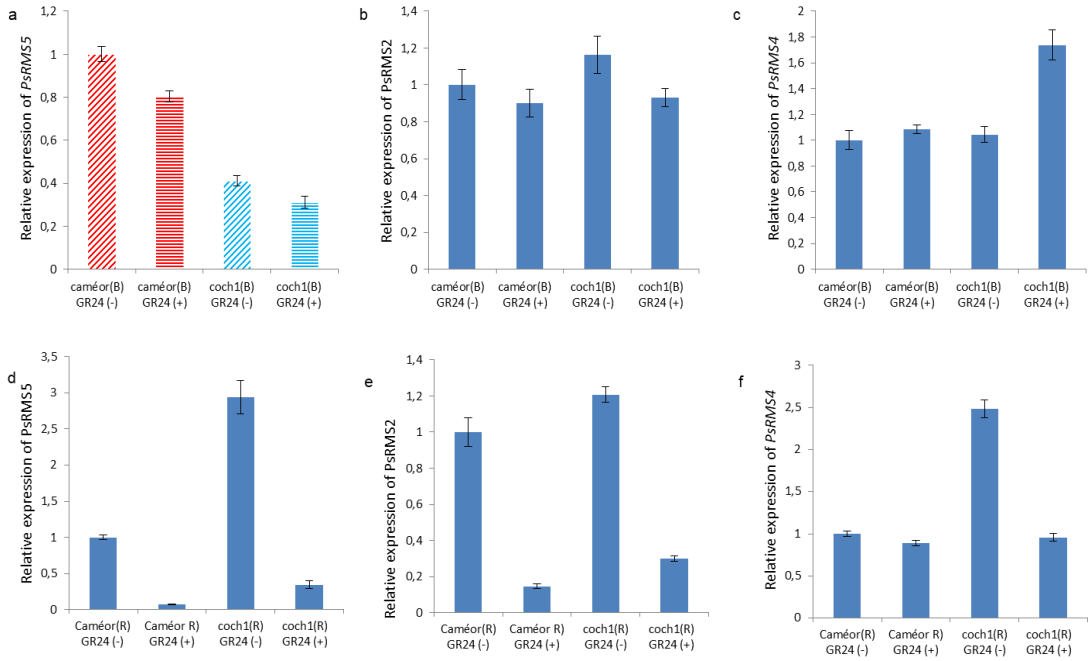

Figure 5. Transcript levels of SL-related genes.

a-f. Expression of *RMS5* (**a, d**), *RMS2* (**b, e**) and *RMS4* (**c, f**) in axillary buds at node 4 (**a-c**) and roots (**d-f**) of WT Caméor and coch1 mutants respectively. Transcript levels were determined relative to *EF1α* and *PsACT* in axillary buds at node 4 after GR24 or mock treatment and in roots incubated without or with GR24 for 4 h. RNA was extracted from dissected buds from pools of 10 plants or roots and quantified by real-time PCR. The data are representative of two to three independent experiments.

To explore how *COCH1* is involved in SL responses, we measured the expression of the known SL-related genes, including *RMS1*, *RMS2*, *RMS4*, *RMS5*, *PsBRC1* and *PsD27* in *coch1* and WT lines. Only WT and the *coch1* mutant lines showing a branching phenotype were analyzed. The transcript levels of the different SL-related genes were followed 24h after GR24 application in axillary buds or in GR24 incubated roots segments (Fig. 5a-f; sup.S5c-h). We observed that the transcript levels of *RMS5* and *RMS2* decreased in axillary buds in WT and *coch1* mutant following GR24 application (Fig. 5a, b). In contrast, the RMS4 expression only increased significantly in the *coch1* mutant following GR24 treatment (Fig. 5c). Similar to *RMS5*, *RMS1* expression also significantly decreased in the WT and *coch1* Caméor (sup. S5c). In addition, *PsBRC1* acting downstream of strigolactones was downregulated in the *coch1* mutant (sup. S5d), and upregulated following GR24 treatment. Moreover, the SL biosynthesis gene *PsD27*, expression is repressed by GR24 application in WT background and induced by GR24 treatment in the *coch1* background. In root, the expression of the *RMS5*, *RMS2* and *RMS4* genes was induced in the *coch1* background and generally repressed following GR24 treatment both in Caméor and SGE backgrounds (Fig. 5d-f and sup. Fig. S5 f-h). From these results, we can conclude that bud and root regulation of these genes is different with a positive effect of the *COCH1* gene on expression in the buds and a negative effect in the root. Importantly the expression of the *RMS4* gene, a repressor of the SL signaling pathway is induced in the *coch1* mutant, suggesting a positive role for COCH1 in SL production in roots. However the repressing effect of the GR24 treatment on the expression of these biosynthetic genes is *coch1* independent.

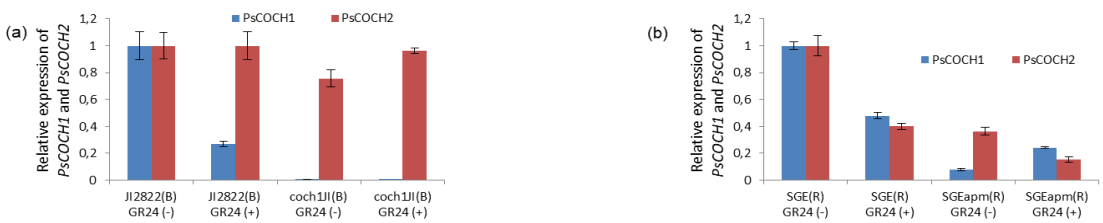

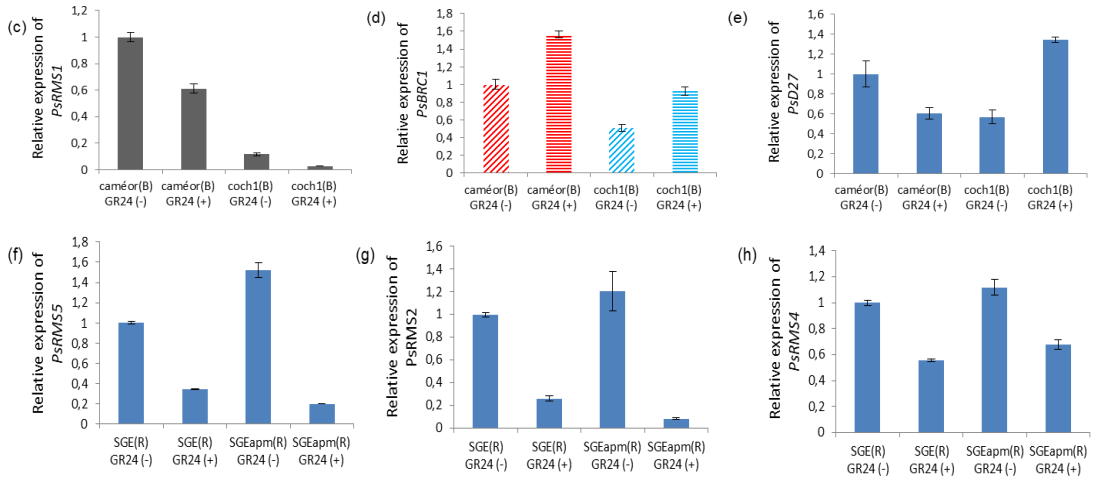

Supplemental Figure S6. Transcript levels of *COCH1* and *COCH2* and SL-related genes in axillary bud and root.

a-b, *PsCOCH1* (blue bars) and *PsCOCH2* (red bars) transcript levels were determined relative to *EF1α* and *PsACT* in axillary buds (**a**) at node 4 after GR24 application or mock treatment in JI2822 and *coch1JI* mutants and in roots (**b**) incubated without or with GR24 for 4 h in SGE and *SGEapm*. **c-e**, *RMS1* (**c**), *PsBRC1* (*d*) and *PsD27* transcripts abundant in axillary buds at node 4 after GR24 application or mock treatment in Caméor and *coch1* mutants. f-h, expression of PsRMS5 (f), PsRMS2(g) and *RMS4* (**h**) in roots incubated without or with GR24 for 4 h in SGE and *SGEapm.* RNA was extracted from dissected buds from pools of 6 plants or roots and quantified by real-time PCR. The data are representative of two independent experiments.

PsCOCH1 expression is downregulated by CK and responds to exogenous CK application independently of SL

SLs negatively regulate the expression of CK biosynthesis genes in the shoot (Dun *et al.*, 2012) and this control participates to shoot branching control. To investigate whether CK regulates the transcription of *PsCOCH1*, axillary buds at node 4 of *Pscoch1*^{Cam}, *Pscoch2*^{Cam,} and *Pscoch1*^{Cam}*Pscoch2*^{Cam} mutants and their corresponding wild types were harvested 6h after direct application of the synthetic CK 6-benzylaminopurine (BAP; 50mM) to analyze *PsCOCH1* expression (Fig. 6a). In wild type plants, the BAP application led to a strong reduction of *PsCOCH1* expression (Fig. 6a). *PsCOCH1* expression in the *coch2* background was similar to WT (Fig. 6a) but the CK treatment on *COCH1* expression was less pronounced. The CK effect on *PsCOCH1* expression in buds of *Pscoch1* and *Pscoch1Pscoch2* lines was not detectable due to the deletion nature of the *coch1* mutation. Thus CK negatively controls *COCH1* expression.

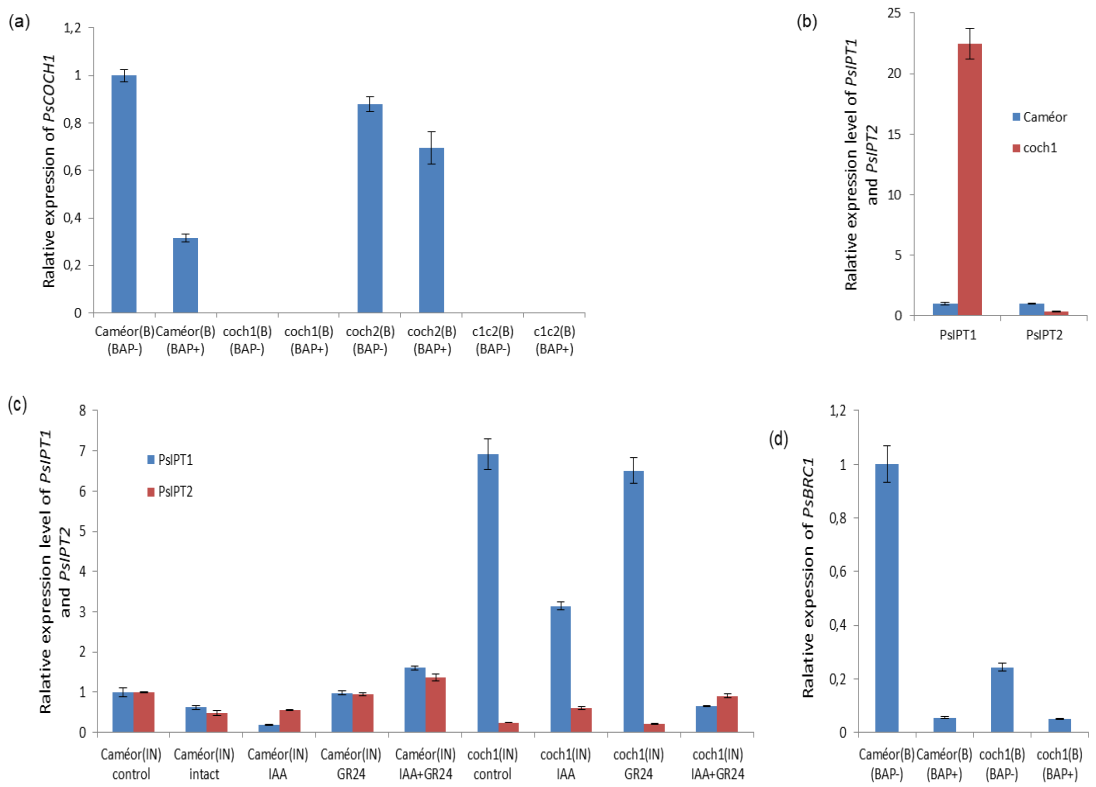

Figure 6. Effects of BAP on *PsCOCH1* and *PsCOCH2* transcript levels and bud growth.

a, PsCOCH1 (blue bars) and PsCOCH2 (red bars) transcript levels were determined relative to *EF1a* and *PsACT* in axillary buds at node 4 after BAP (50 mM) application in wild-type Caméor, $Pscoch1^{Cam}$, $Pscoch2^{Cam}$, $Pscoch1^{Cam}Pscoch2^{Cam}$ RNA was extracted from the dissected buds of 10 plants at the six-node stage and quantified by real-time PCR. The data are representative of three independent experiments. **b**, Effects of BAP (50 mM) treatment on bud growth at node 4 in wild-type Caméor, $Pscoch1^{Cam}$, $Pscoch2^{Cam}$, $Pscoch1^{Cam}Pscoch2^{Cam}$, wild-type JI2822, and $coch1^{JI}$. Measurements were done 5 and 7d after treatment. Data are means ± SE (n = 12).

To analyze the link between *COCH1* and CK, the expression level of the CK biosynthesis genes, *ISOPENTENYL TRANSFERASE1* (*IPT1*) and *IPT2*, was measured in tissue containing internode and node 3 (including bud) from wild-type and *coch1* mutant plants. Interestingly, the expression of *PsIPT1* was strongly increased in the *coch1* background (Fig. 6b) while *PsIPT2* expression was down-regulated. To determine if this overexpression could result from a reduced SL content, we tested if GR24 can regulate the expression of *PsIPT1* or *PsIPT2* by *in vitro* incubating isolated internodes with or without 1µM GR24 and/or 20 µM IAA for 4 h (Fig. 6c). Auxin (IAA) was used as a control, as it is known to reduce the expression of *PsIPT1* and *PsIPT2* in intact, decapitated, and *in vitro* studies (Tanaka *et al.*, 2006). As expected, the expression of *PsIPT1* and *PsIPT2* was slightly increased in WT (both genes) and

strongly increased only for *PsIPT1* in *coch1* isolated segments incubated in control buffer when compared to intact plants, as the segments have no apical source of auxin (Fig. 6c). Incubation with IAA reduced the expression of *PsIPT1* and *PsIPT2* in segments relative to incubation in a buffer, returning their expression to levels similar to those observed in intact plant samples. The synthetic SL, GR24, did not affect within the 4-h time frame on the expression of *PsIPT1* or *PsIPT2*. When combined to IAA it slightly increased the expression of the two *IPT* genes. In the *coch1* background, the high expression of the *PsIPT1* gene decreased in the presence of IAA and was not affected by GR24 treatment. In contrast, the *PsIPT1* expression returned to the WT level in the IAA+GR24 combined treatment (Fig. 6c). This experiment shows that BAP represses *COCH1* expression, that COCH1 represses *PsIPT1* expression, and that IAA plus GR24 represses also represses *PsIPT1* expression in *coch1* background.

To further test the relation between CK and *PsCOCH1*, BAP (50mM) was applied to bud 3 of *Pscoch1*^{Cam}, *Pscoch1*^{JI}, *SGEapm*, and *Pscoch1*^{Cam}*Pscoch2*^{Cam} mutants and their corresponding wild types and bud lengths were measured 7 and 10d after application (sup. 7a). For all lines, axillary buds did not grow much without CK treatment, while CK treatment resulted in a moderated bud/branch lengths increase in all genotypes, particularly for *coch1*^{Cam}, *coch1*^{JI,} and SGEapm mutants (Sup. 7a). In addition, we test another way to respond to CK by decapitation, which, by depleting the source of auxin. Decapitation of *coch1* and *coch1coch2* mutants and their corresponding wild types resulted in increased branch lengths in all genotypes (sup. 7b). These results show that bud elongation in pea is repressed by the GR24 application and activated by decapitation (CK/IAA ratio) in WT and *coch1* mutant indicating that COCH1 act on shoot branching independently or upstream of the hormone control.

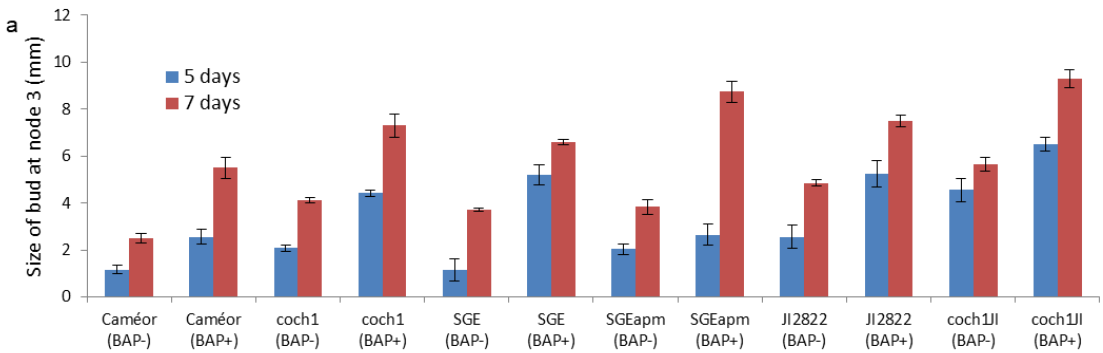

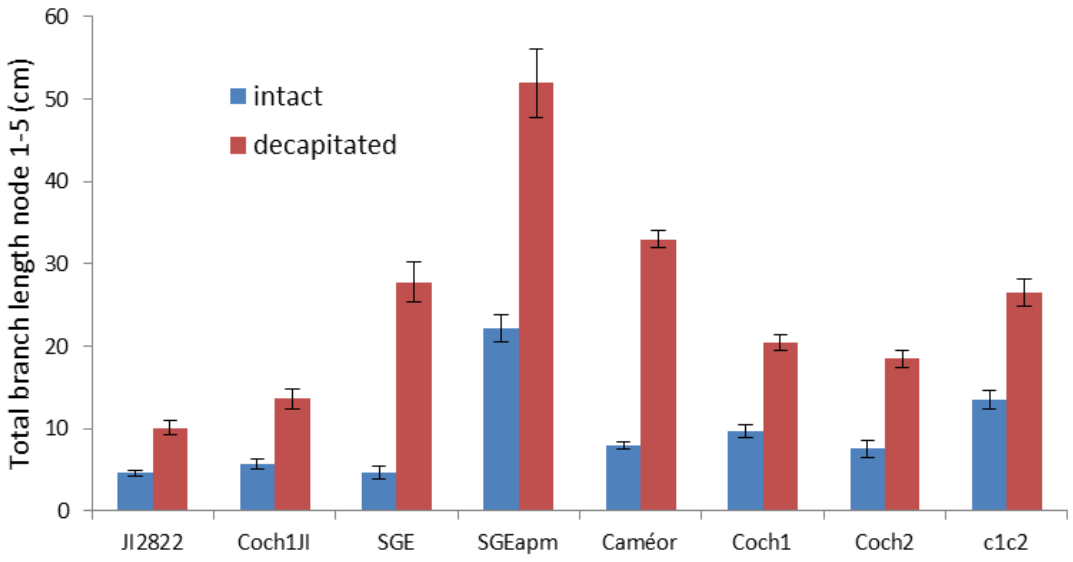

Supplemental figure 7. Effects of BAP on *coch* mutant and corresponding wild type and the decapitation effect on shoots growth.

a. Effects of BAP (50 mM) treatment on bud growth at node 4 in wild-type Caméor, *Pscoch1*, wild-type JI2822, and *coch1*^{JI}, wild type SGE and SGEapm. Measurements were done 5 and 7d after treatment. **b**. the length of the shoot decapitated compared to intact in different genotypes. Data are means ± SE (n = 12). c1c2: *coch1coch2*.

IAA stimulates *PsCOCH1* expression

To also investigate the role of IAA in the branching phenotype observed in the *coch1* mutant, we analyzed the expression of the *COCH1*, *RMS1*, and *RMS5* in isolated segments (internode 3) of young pea seedlings treated with 20 µM IAA for 4 h (Fig. 7). The *COCH1* expression was upregulated in IAA treated segments as compared to control and was slightly higher than in intact samples than in non-treated segments. This suggests that *COCH1* expression is induced by IAA. Similarly and in agreement with previous results, *RMS5 and RMS1* expression increased after auxin application (Foo *et al.*, 2005; Johnson *et al.*, 2006). The increased expression of the two SL biosynthesis genes after treatment with IAA was stronger in *coch1* that in WT internodes. Interestingly the auxin treatment partly restored the expression observed in intact internodes (Fig. 7b) and their expression pattern was higher in the *coch1* mutant treated or not with IAA. These results suggest that the expression of *PsCOCH1*, *RMS1*, and *RMS5* is stimulated by IAA, confirm that *COCH1* negatively controls the *RMS* genes and that the induction of the *RMS* genes by IAA is independent of *COCH1*.

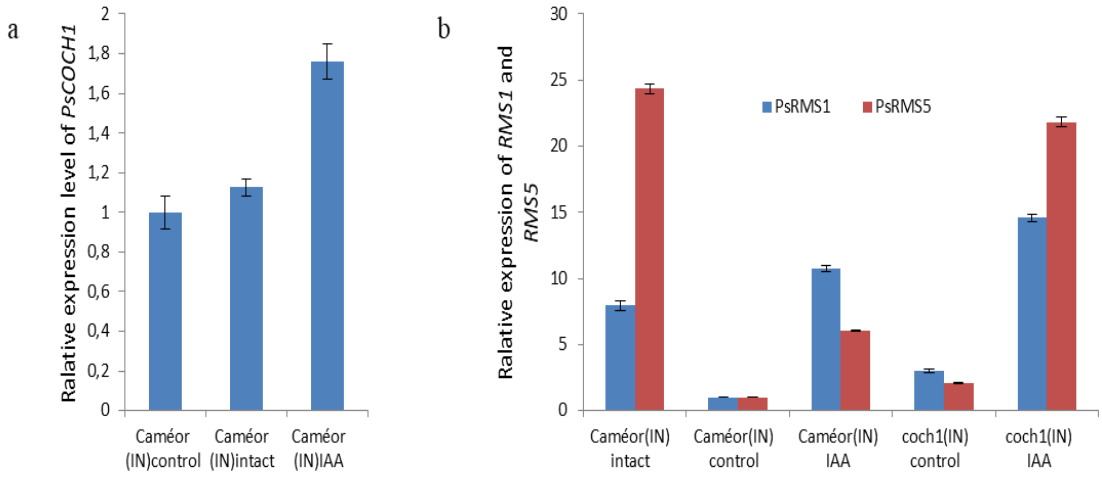

Figure 7. Effects of IAA on PsCOCH1, *RMS1* and *RMS5* transcript levels.

a. *PsCOCH1* transcript levels were determined relative to *EF1a* and *18S* in internode after IAA (20 µM) application in wild-type Caméor. **b.** Transcripts of *RMS1* and *RMS5* in *coch1* mutant and also in wild type. RNA was extracted from the dissected internode of 3 plants at the six-node stage and quantified by real-time PCR. The data are representative of three independent experiments.

The legume *NBCLs* participate in flowering time determination

Yaxley *et al.*, (2001) reported that the flowering time and flowering node were not significantly affected in the *Pscoch1* mutant. In contrast, in our experimental setup, the flowering time was delayed about 8 days in *Pscoch1*^{Cam} and *SGEapm* compared to their respective wild type. In the two WT, the first flower appeared on average 29 days after sowing while they appear on average 37 days after sowing in the mutant backgrounds. This delay is less important (3-4 days) between the JI2822 and *Pscoch1*^{JI} lines. The *Pscoch2*^{Cam} mutant flowers nearly at the same time as the WT. In *Pscoch1*^{Cam}*Pscoch2*^{Cam}, the flowering time is also delayed for about 5-6 days (Fig. 8a). These results suggest that *PsCOCH1* promotes flowering to varying degrees according to the backgrounds.

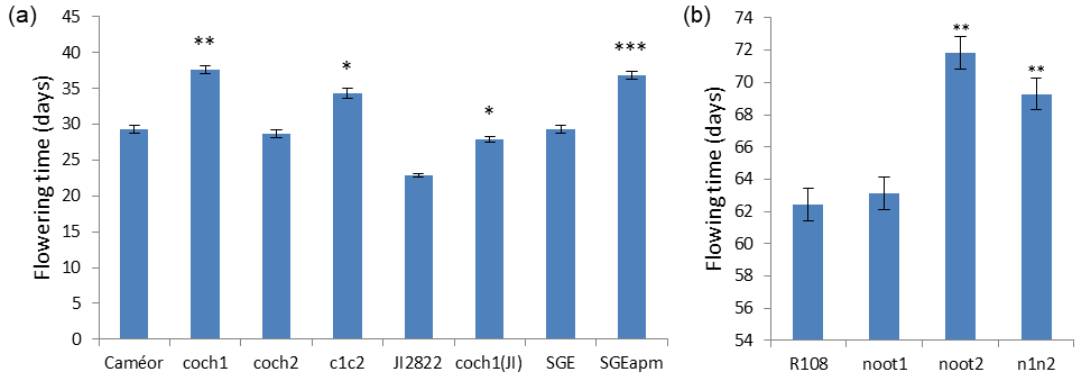

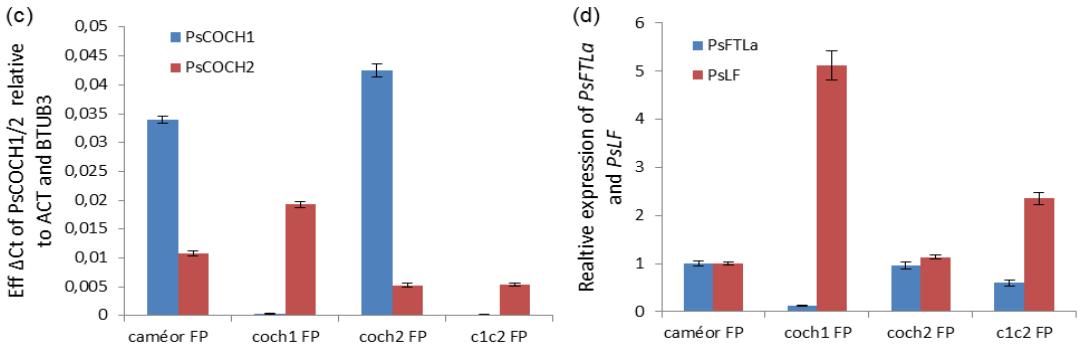

Figure 8. Flowering time and flowering time genes expression.

a-b.The average flowering time of wild-type Caméor, *Pscoch1*, *Pscoch2*, *c1c2*, wildtype JI2822, SGE, and the respective mutant, *coch1*^{JI,} and *SGEapm* in pea and noot mutant lines in *M. trunctula*. Measurements were done when the first flower was opened for plants and grown under the same conditions. Data are means ± SE (n = 9). **c, d.** Transcripts of *PsCOCH1* and *PsCOCH2* (**c**), *PsFTa1* and *PsLF* (**d**) in wild-type Caméor, *coch1*, *coch2*, *c1c2*, transcript levels were determined relative to *PsTUB3* and *PsACT*. RNA was extracted from the dissected of flower primordia of 3 plants and quantified by real-time PCR. The data are representative of three independent experiments. *coch1*: *Pscoch1*^{Cam}, *coch2*: *Pscoch2*^{Cam}, *c1c2*: *Pscoch1*^{Cam}*Pscoch2*^{Cam} , *n1n2*: *Mtnoot1noot2*.

In order to know if a similar situation exists also in *M. truncatula*, we analyzed the flowering time in the *noot1* and *noot2* mutants. The flowering of the legume *M. truncatula*, like winter annual Arabidopsis, is promoted by long day (LD) photoperiod and vernalization. Under non-vernalized growth condition, the wild type, as well as *Mtnoot1* mutants, will flower about 9 weeks after sowing and no significant delay was observed while the first flower of the *Mtnoot2* and *Mtnoot1Mtnoot2* mutant will appear after 10 weeks and showed on average 10 days delay of flowering time compared with wild type (Fig. 8b). These results show that the role of the two genes is different in these two legume plants and that *NOOT2* in controlling flowering time in *Medicago*.

To further understand the role of the *PsCOCH* genes in flowering time, the expression of the *PsCOCH1* and *PsCOCH2* genes was measured in pea young flower primordia. *PsCOCH1* was more expressed in these flower buds than *PsCOCH2* in WT Caméor and its expression further increased in the *coch2* background. Due to the deletion nature of the mutation, the *COCH1* expression was not detected in the *coch1* or *coch1coch2* mutants (Fig. 8c). Similarly to the increased expression of *PsCOCH1* in *coch2* background, *PsCOCH2* expression increased in the *coch1* mutant. The *COCH2* lower expression in *coch2* and *coch1coch2* mutant (Fig. 8c) may reflect the

instability of the mutant transcript. Similar expression patterns of *PsCOCH1* and *PsCOCH2* were observed in JI2822 and SGE backgrounds and their corresponding mutant *coch1*^{JI} and *SGEapm* (sup.8a). This suggests the existence of a regulatory loop between these two genes in this tissue.

In pea, the *FTLa/GIGAS* gene (*PsFTLa*) is an important target of vernalization and promotes flowering, whereas the *LATE FLOWERING* (*LF*) gene, corresponding to *PsTFL1c*, delays the induction of flowering. In agreement with the observed flowering time phenotype, the expression level of *PsFTLa* was down regulated in *Pscoch1*^{Cam} and *Pscoch1*^{Cam}*Pscoch2*^{Cam}, with the strongest down expression observed in the *Pscoch1*^{Cam} line (Fig. 8d). The *PsFTLa* expression also decreased in *Pscoch1*^{JI} and was strongly reduced in *SGEapm* (sup.8b). In contrast, the expression of the *PsLF1c* gene was up-regulated in both *coch1* and *coch1coch2* mutant and with the highest expression observed in the *coch1* line (Fig. 8d, sup.8b). In the *coch2* line the expression of both genes was unchanged compared to WT (Fig. 8d). The expression of these genes in the *coch1* mutant is thus consistent with the flowering time observed in the mutant backgrounds.

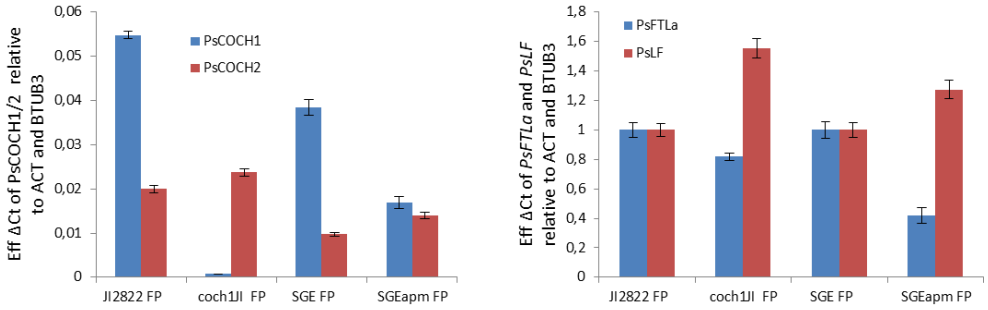

Supplemental figure 8. Transcript levels of *PsCOCH1*, *PsCOCH2*, *PsFTa1* and *PsLF*.

a, b. Transcripts of *PsCOCH1* and *PsCOCH2* (**a**), *PsFTa1*, and *PsLF* (**b**) in wild type JI2822, SGE, and the respective mutant, *coch1JI* and *SGEapm* in pea. Transcript levels were determined relative to *PsTUB3* and *PsACT*. RNA was extracted from the dissected of flower primordia of 3 plants and quantified by real-time PCR. The data are representative of three independent experiments.

DISCUSSION

A novel role for *NBCL* genes in plant development

The *NBCL* genes were reported as key regulators, involved in many aspects of plant development. In Arabidopsis, BOP1/2 act as a co-transcript factor, redundantly regulating the root, leave, flower, seeds development (Ha *et al.*, 2003, 2004; Xu *et al.*,

2010; Khan *et al.*, 2012b,a, 2015; Woerlen *et al.*, 2017; Yu, 2019a). Plants overexpressing *AtBOP1/2* show a branching phenotype, producing extra para-clades in leaf nodes (Ha *et al.*, 2007). Loss-of-function *bop1bop2* double mutants also cause a delay in the node of the first flower and branched flowers (Norberg *et al.*, 2005; Ha *et al.*, 2007; Xu *et al.*, 2010). Similarly, the *NBCL* genes in legume, such as *NOOT* in *Medicago, COCH* in pea and *LjNBCL1* in lotus also affected multiple aspects of plant development. In addition, the *NOOT* and *COCH* genes are key regulators in nodule organ identity (Couzigou *et al.*, 2012, 2015, Magne *et al.*, 2018a,b). The *P. sativum cochleata* (*coch*) mutant, was first reported as having altered flower and leaf phenotypes (Wellensiek, 1959). The *coch1* mutant phenotype is homeotic in that stipules assume leaf-blade-like morphology (Blixt, 1967). The mutant nodules are typically dichotomously branched and root structures emerge from vascular tissue meristems (Ferguson & Reid, 2005). In our work, we describe two novel roles for the legume *NBCL* genes. We show that COCH1 is a negative regulator of shoot branching and plays a role in the signal cross talk regulating this shoot branching.

The *Pscoch1* mutant lines analyzed here showed a strong branching phenotype in comparison to their wild-type progenitors, particularly at basal nodes. The *Pscoch1* mutant displayed few long branches at upper nodes and the branches at the base are similar to the main shoot. The *coch2* mutant had a WT phenotype but the *coch1coch2* mutant also show a similar but less pronounced phenotype compared to *coch1*. This indicates that *COCH2* plays an opposite role to *COCH1* in the branching phenotype. Furthermore, the height of *coch1coch2* was not affected compared with WT Caméor and other *coch1* mutants, which are relatively increased. In Medicago, we observed a similar but less strong branching phenotype for the orthologous mutants. Additional branches appeared at the base of the *noot1* but not the *noot2* mutant. Interestingly, the *noot1noot2* double mutants show a strong reduction in node 1-5, with even fewer main shoots than the WT R108. The plant height was greatly increased compared to WT and also noot1, its height was less affected but noot2 mutants displayed a higher plant stature than WT. Our study suggests opposite roles for the two *NBCL* genes in legume plants with *COCH1/NOOT1* inhibiting branching and *COCH2/NOOT2* activating branching. The roles for SL in plant architecture, other than shoot branching, have been suggested for dwarfism (Lin et al., 2009) and root architecture (Koltai et al., 2009; Kapulnik et al., 2011; Ruyter-Spira et al., 2011). The relative

dwarfism of SL mutants is not yet understood, but it is very likely that SL controls stem growth. In pea, surprisingly, total branch length was strongly enhanced in the *coch1* mutant plants, mainly because of the strong development of the cotyledonary branches. When branching was quantified according to the position along the stem, branching in *SGEapm* was lost at upper nodes (node 4 to 9) but transgressive at basal nodes (cotyledonary node and node 1 or 2), forming up to 6 shoots at the same node. Notably, the branching appeared again above node 9. These results suggest a possible specific regulation of branching at basal nodes in pea. These buds are differentiated very early in the embryo at the axils of particular leaves (cotyledons and scale leaves) and their development generally occurs below the soil surface. In addition, two or three branches can be observed directly from the seeds just after germination. In pea, the *RMS6* gene has been shown to control bud outgrowth only at these nodes (Rameau *et al.*, 2002), and might be related to the *COCH* regulation described here.

PsCOCH1 **is necessary for long-distance signaling and deficient in the SL signaling pathway**

Legumes are useful for shoot-branching researches because of several features that facilitate studies of axillary buds and long-distance signaling. They have long internodes separating axillary buds and the shoot tip, are easy to graft, are amenable to root xylem-sap extraction, and their axillary buds are accessible for hormone applications, growth measurements, and other related analyses. Additionally, for many pea varieties, most axillary buds are dormant but have the potential for release throughout development.

The result that *coch1* scion only shows a mutant phenotype when grafted on its rootstock, suggests that COCH1 is required for the production of a long-distance signal repressing bud outgrowth. In addition, because only *coch1* grafted on *coch1* rootstock show increase branching, it also shows that COCH1 participates in the perception of the branching signal. In addition, the fact that the *Pscoch1* mutant responds to SL application suggests that *PsCOCH1* act upstream of the SL signaling. In support of this, we showed that *PsCOCH1* expression in axillary buds and roots was rapidly reduced by SL treatment, especially in the root. The expression of *PsCOCH1* in the *Pscoch1* (*coch1*^{Cam} and *coch1*^{JI}) mutant was difficult to compare to the wild type due to the full-length deletion and its expression nearly undetectable. But an increase of *PsCOCH1* expression after GR24 application was not observed in

SGEapm, corresponding to a point mutation. In addition, either vascular supply or direct application of SL inhibited strongly the growth of the axillary buds. These data indicate that *PsCOCH1* was negatively regulated by SL and correlate with the repression of bud growth with the same treatment. As described previously (Foo et al., 2005), SL biosynthesis *RMS1* and *RMS5* genes are also downregulated by the SL treatment. Because the expression of these genes is repressed by SL treatment in the *coch1* background, the highest expression observed in the mutant might reflect a reduced SL content in the *coch1* background. Similar to previous *RMS1* expression data, *RMS5* has the characteristic acropetally expression profile, greatest in the roots (Johnson *et al.*, 2006).

PsCOCH1 participates in hormone cross talk to control plant architecture

Our results showed that *coch1* is an SL-defective mutant, like *rms1* and *rms5*. Thus, *PsCOCH1* could also involve in hormone regulate loop, combination transcript level and hormone treatment, indeed, *PsCOCH1* as a new actor player in regulating loop to control shoot branching. In rice and pea, CKs downregulate the *FINE CULM1/PsBRANCHED1* (*FC1/PsBRC1*) gene specifically expressed in axillary buds (Minakuchi *et al.*, 2010; Braun *et al.*, 2012), which acts as a negative regulator of shoot branching and as an integrator of multiple pathways (Aguilar-Martínez *et al.*, 2007). In pea, CKs also appear to act independently of *PsCOCH1* because the *Pscoch1* mutant responds to CK application.

Our results showed that *PsCOCH1* transcription levels decreased after the direct application of CK to the axillary bud. In addition, the expression of *PsIPT1* was strongly increased in the coch1 background while *PsIPT2* expression was down-regulated. We tested the phenotypic response of CK application on axillary buds at node 4 of *Pscoch1*, *Pscoch2*, *Pscoch1coch2*, and their corresponding wild-type progenitors. CK treatment-induced bud outgrowth for all genotypes, including *Pscoch1*. This response indicates that CK may promote axillary bud outgrowth and/or growth independently of the SL signaling pathway and from *PsCOCH1*. The phenotypic response to decapitation was consistent with the CK response of *Pscoch1*. Furthermore, either *PsIPT1* or *PsIPT2*, the transcription was downregulated with exogenous auxin but was minimally affected by SL deficiency. The insensitivity of the stem *PsIPT* expression to SL defects is consistent with the failure of exogenously supplied SL to modify *PsIPT* expression (Dun *et al.*, 2012). These results demonstrate

that CK controls *PsCOCH1* expression independently of the SL pathway. Thus, *PsCOCH1* expression could integrate the SL and CK pathways at the transcriptional level within the bud and bud outgrowth would occur where *PsCOCH1* falls below a certain transcription level (Fig. 9).

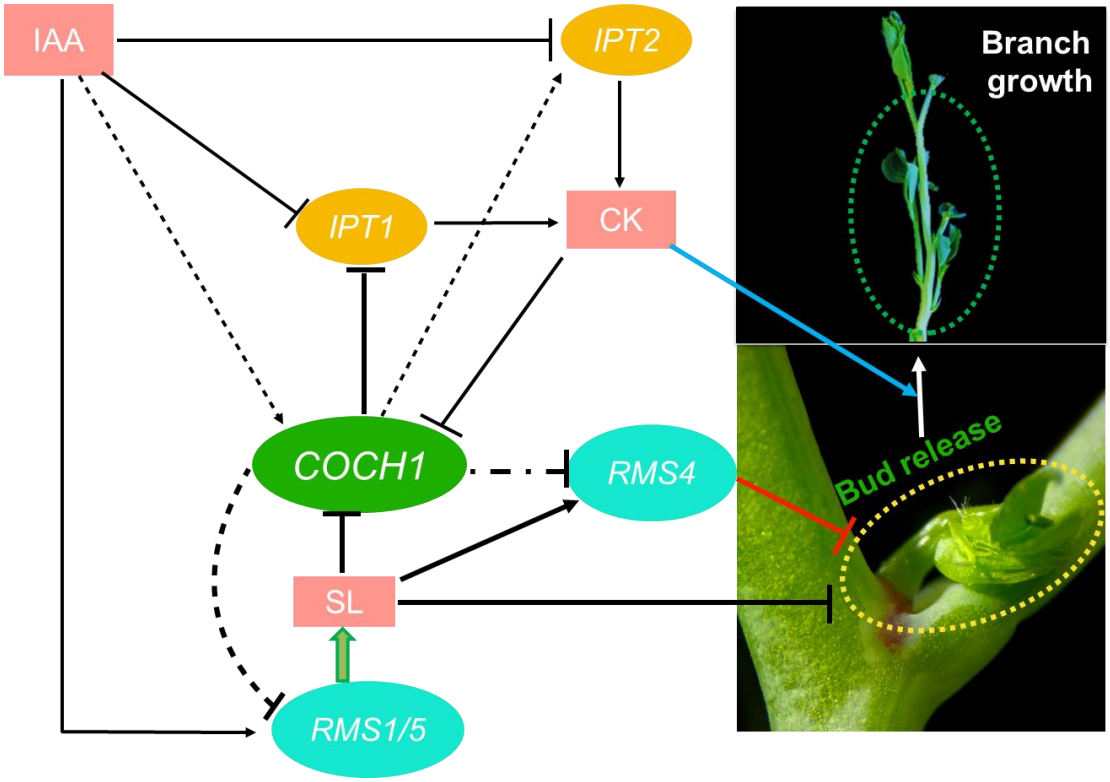

Figure 8. Schematic representation for the hormonal control of branching in pea integrating the function of *PsCOCH1* in the axillary bud.

PsCOCH1 integrates the SL and CK and also IAA pathways to control bud outgrowth. CK also increases bud growth via a PsCOCH1-independent pathway. Auxin maintains *RMS1* and *RMS5* transcript levels, and hence SL synthesis, and down-regulates CK biosynthesis genes *IPT1* and *IPT2*. CK repress *PsCOCH1*, which repress PsIPT1 in CK pathway. Auxin active *PsCOCH1* thus inhibit bud out growth. SL represses *PsCOCH1* via active *RMS4*, and down-regulate SL biosynthesis *RMS1* and *RMS5*.

In several species, auxin up-regulates genes encoding two carotenoid cleavage dioxygenases (*CCD7* and *CCD8*; (Foo *et al.*, 2005; Johnson *et al.*, 2006; Zou *et al.*, 2006; Arite *et al.*, 2007; Hayward *et al.*, 2009). *CCD7* and *CCD8* convert together with the β-carotene isomerase D27, all-trans-β-carotene into carlactone, a key intermediate in the SL biosynthesis pathway (Lin et al., 2009; Alder et al., 2012). The *COCH1* expression was upregulated in IAA treated segments as compared to control and was slightly higher than in intact samples than in non-treated segments. This

suggests that *COCH1* expression is induced by IAA. Similarly and in agreement with previous results, *RMS5 and RMS1* expression increased after auxin application, and was stronger in *coch1* than in WT internodes (Foo *et al.*, 2005; Johnson *et al.*, 2006). These results suggest that the expression of *PsCOCH1, RMS1,* and *RMS5* is stimulated by IAA, confirm that *COCH1* negatively controls the *RMS* genes, and that the induction of the *RMS* genes by IAA is independent of *COCH1*.

These findings support a model in which the *PsCOCH1* plays a role in SL, CK, and auxin regulation in shoot branching. In this regulatory loop, *PsCOCH1* positively responds to auxin while act as a negative player to SL and CK. In relation to CK biosynthetic genes *IPT1/2* and SL marker gene *RMS1/5* and *RMS4*, it can be deduced that *PsCOCH1* regulates CK biosynthesis independently of the SL level.

NBCL genes are involved in flowering-time regulation

Flowering time is a major adaptive trait in the life strategy of flowering plants, which have to synchronize their reproduction with favorable environmental conditions. The transition from vegetative growth to flowering, termed floral induction, is controlled by physiological signals and genetic networks that integrate environmental (photoperiod and temperature) and endogenous (stage of the plant) conditions (Levy & Dean, 1998; Colasanti & Sundaresan, 2000; Srikanth & Schmid, 2011; Ietswaart *et al.*, 2012; Romera-branchat *et al.*, 2014). *BOP1* and *BOP2* are expressed in lateral organs close to boundaries of the SAM during vegetative development (Ha *et al.*, 2004, 2007; Norberg *et al.*, 2005; Hepworth *et al.*, 2005; Karim *et al.*, 2009; Xu *et al.*, 2010; Couzigou *et al.*, 2012). Floral induction in Arabidopsis by *FT* requires direct repression of *BOP* genes by the homeodomain protein *PENNYWISE* (*PNY*), which binds to the promoters of *BOP1* and *BOP2* (Andrés *et al.*, 2015). Ectopic *BOP* gene expression in the *pny* mutant or the gain-of-function bop1-6d mutation strongly reduced *FD* transcription, confers the late flowering of *pny* and *bop1-6d* mutants (Andrés *et al.*, 2015).

In legume, the *NBCLs* genes are also involved in flowering-time regulation. Mutation of *PsCOCH1* and *MtNOOT2* result in late flowering, although the *Pscoch2* and *Mtnoot1* are not delay for flowering. The *nbcl1nbcl2* double mutant also displayed delay flowering in both species. Consequently, the *PsFTa1* (former *FTLa*) expression level was extremely downregulated in *Pscoch1* and *Pscoch1coch2* mutant. In contrast, the *PsLF* (*PsTFL1c*) expression was greatly upregulated in *Pscoch1* and

Pscoch1coch2 mutant. In the *coch2* mutant, *PsFTa1* and *PsLF* have a WT expression level. In addition, The *PsCOCH1* transcription was increased in the *coch2* mutant and the *PsCOCH2* transcription was elevated in the *coch1* mutant. This indicates that these genes repress each other and that *PsCOCH1* activate *FTa1* and repress *PsLF* expression. Interestingly, the *FT* gene regulation model for *PsCOCH1* gene in pea is opposor to the one described for *BOPs* in Arabidopsis, where *BOPs* repress the *FT* expression through reduced *FD* transcription (Andrés *et al.*, 2015). Indeed, there are several differences between Arabidopsis and legumes concerning the flowering time control, with evolutionary and genetic data indicating the likely involvement of legume-specific genes and mechanisms. For example, legumes lack a clear ortholog of the key Arabidopsis vernalization-responsive gene, *FLC* (Hecht *et al.*, 2005) and the ability to respond to vernalization has likely evolved independently in legumes and other plant families (Bouché *et al.*, 2017). A mode of action was recently proposed in Arabidopsis, where FT and TSF proteins interact with BRC1 in axillary buds to inhibit floral induction. The *brc1-2* mutant is highly branched, and its lateral branches flower earlier (Niwa *et al.*, 2013). To confirm that the FT module is different between Arabidopsis and pea and better understand our results, the expression of *PsBRC1* in *Pscoch1* could be tested.

Extending the concept of strigolactone in floral transition and nodule identity

The following key question appears: what is the relationship between branching, the SL network, and controlling flowering? Previous report indicate that a mobile signal was specifically required for the transition to flowering. Recessive mutants at the *GIGAS* (*GI*) locus can show a photoperiod response in flowering node but show a large delay in flowering under short days (SD), and flower late or not at all under long days (LD). GI is proposed to have a role in long-distance signaling because flowering can be partially restored to *gi* mutant scions by grafting to a WT stock (Beveridge & Murfet, 1996). Development of *gi* mutant plants in LD proceeds relatively normally until around the time of flower initiation in WT, after which the mutants appear to lose apical dominance and become highly branched at aerial nodes (Beveridge *et al.*, 2003). Recently, Zhang *et al.*, (2019) have shown that the *Arabidopsis* mutants, *d14*-1 and *max4 - 1*, compromised in either SL synthesis or signaling, flower earlier due to higher melatonin (MT) content in both mutants than in wild types. In *Arabidopsis*

thaliana, strigolactone inducing floral transition in an FLC-dependent manner through repression of the synthesis of melatonin. These results suggest SL plays a role in floral transition, supporting our results that *coch1* is deficient in SL and delayed in flowering.

Apart from the role in shoot and root architecture, strigolactones were originally identified through their activities as root exudates in the rhizosphere(Cook *et al.*, 1966), most notably, exudation of SL from roots is important for the recruitment of arbuscular mycorrhizal (AM) fungi (Akiyama *et al.*, 2005). Recently, Foo & Davies, (2011) reported that endogenous SLs are positive regulators of nodulation in pea, required for optimal nodule number but not for nodule formation. The *rms1* mutant root exudates and root tissue are almost completely deficient in SLs, and *rms1* mutant plants have significantly reduced nodules number. In addition GR24 treatment increases nodule number. *PsCOCH1* is a key regulator for nodule development and shows highly aerial branching similar to *ram1* mutants. Therefore, it could worth testing whether the SLs alter the *coch1* nodule phenotype. This study will be enhancing the understanding between the SLs and nodule identity.

MATERIAL AND METHODS

Plant material, growth conditions and scoring methods

Wild-type *P. sativum* var. caméor, the corresponding ethyl methanesulfonate (EMS) tilling mutants lines *Pscoch2* (*Ps1178*, Dalmais *et al.*, 2008), and *Pscoch1* use pre-existing full-length deletion mutant (FN3185/1325) in the background JI2822 (a progeny line from JI399 CENNIA and JI15 WBH1458) close to caméor (Jing et al., 2010) back-cross to caméor (back-cross1), double mutants *Pscoch1coch2* [*Pscoch1* FN3185/1325 (back-cross1) crossing with *Pscoch2 Ps1178* (back-cross2)], and wild-type *P. sativum* var. JI2822 and the corresponding fast neutron bombardment full-length deletion mutants lines *Pscoch1* (Couzigou *et al*., 2012; John Innes Centre germplasm; www.jic.ac.uk/ GERMPLASM/), SGE wild-type back-ground and its corresponding EMS mutant SGEapm (Zhukov *et al.*, 2007) were used. Seeds of wild-type *P. sativum* and the corresponding mutant lines (see supplemental table 1) were surface-sterilized 10 min with sodium hypochlorite and washed three times with sterile water and placed between two filter papers on agar plates (Kalys Biotech, HP696-5, 7g.L^{-1}). Seeds were vernalized for 4 days at 4°C and germinated 48h at 24°C under darkness for acclimatization before sowing. For vegetative development and bloom, a loam/peat/sand mixture was used (70/3.5/7, v/v/v; http://www.puteaux-sa.fr) with expensed clay balls at the bottom of the pot. *P. sativum* were grown under 16/8h light-dark cycle, 24/24°C day-night temperature, 60% of relative humidity, and 200 µE of light intensity. Plants were watered three times a week (2 times with water/1 times with nutritive solution in alternance) (Soluplant, NPK16626).

The branching phenotype scoring methods was done according to Rameau *et al.*, (2002). Node counts commenced from the first scale leaf as node 1. The cotyledonary node is referred to as node 0, and day 0 as the day of planting. Nodes 0-3 are referred to as basal nodes whereas upper stem nodes are referred to as aerial nodes. First-order lateral shoot arises from nodes on the main stem and second-order laterals from a node on a first-order lateral. More than one lateral shoot may arise from one node. Lateral shoot lengths were measured from the base of the lateral to the lateral apex. Basal lateral shoots that grew stronger as rivals of the main stem were referred to as secondary stems.

Grafting studies

Grafting has long been used to study long-distance transport and signaling between different plant tissues. Grafts were performed prior to any macroscopic sign of bud release as described by Beveridge et al. (1994). The seedlings were 7d old at the time of grafting, and scions (shoot) and stocks (roots and cotyledons) were joined at the epicotyl by a wedge connection. This grafting procedure requires that lateral buds at the cotyledonary node are removed to enable the formation of new vascular connections and growth of the scion without competition with cotyledonary shoots (Rameau *et al.*, 2002). Only vigorous plants (usually more than 90% of grafted plants) were included in the analysis.

Strigolactone application

The synthetic SL, GR24 (gifted by xx), was shown to inhibit bud outgrowth to the level seen in wild type and was active down to 10 nM when supplied directly to the xylem stream in the internode (Gomez-Roldan et al., 2008; Umehara et al., 2008). The response of the *Pscoch* mutant to SL was performed on 10-day-old plants. For direct application on pea buds, GR24 was supplied in a solution (10 mL) containing 50% ethanol, 1% polyethylene glycol 1450 (Sigma), 0.1% dimethyl sulfoxide (Sigma), and 0.1% acetone containing or not (mock treatment) 1µM GR24. Axillary buds at node 4 were treated with 10 µL of 0 or 1µM GR24 of *Pscoch1*, *Pscoch2,* and *Pscoch1Pscoch2* mutants and their respective wild types. The Bud length was measured 7d and 10d later. For vascular supply, a thread submerged in GR24 (0.5µM or 1µM) solution was passed through the stem between nodes 3 and 4 using a needle; the outgrowth of the bud at node 5 was measured 7d and 10 d later.

For hydroponics treatments, culture was as described by Braun et al. (2012). Pea plants were germinated in vermiculite for 6 d and then transferred to aerated hydroponic complete nutrient solution culture, with 12 plants in 6 L of the solution in a growth cabinet. Acetone or GR24 (dissolved in acetone) was added to the hydroponic culture solution to give a final concentration of 0 or 3 µM GR24 and 0.01% acetone. The hydroponic culture solution was replaced weekly.

Exogenous auxin studies

To investigate whether CK regulates the transcription of *PsCOCH*, the synthetic CK 6-benzylaminopurine (BAP; Sigma) was applied to axillary buds at node 4 as 10 µL of a solution containing 50% ethanol, 1% polyethylene glycol 1450 (Sigma), and

0.5% dimethyl sulfoxide (Sigma) containing or not (mock treatment) 50µM BAP. After 6 h and 24 h treatment, the buds of *Pscoch1*, *Pscoch2,* and *Pscoch1Pscoch2* mutants and their respective wild types were harvested and the transcript levels were quantified using real-time PCR. To test whether *PsCOCH* is needed for axillary bud growth, the same treatment was done and buds were measured 5 and 7 d after CK application.

The *in vitro* IAA treatment of isolated internodes was adapted from Theologis *et al.*, (1985). Internodes 3 was harvested from 16-d-old plants and incubated 0.5 h in 100 ml of incubation buffer (1mM-citrate, 1mM-PIPES, 15mM-sucrose, 1mM KCl, 50µg of chloramphenicol/ml, pH 6.0) to deplete segments of endogenous auxin. They were then kept in the fresh incubation buffer supplemented with or without 20µM IAA with gentle shaking in the light for 4 h. The internodes were collected for RNA extraction (3 biological repeats of 6 internodes).

RNA extraction and cDNA synthesis

RNA extraction and cDNA synthesis were adapted from Magne *et al.*, (2018). Total RNA was isolated from pea internodes or 20 to 30 buds using TRIZOL reagent (Invitrogen) following the manufacturer's protocol. RNA samples were treated with the TURBO DNA-free™ Kit (Ambion) according to the manufacturer's recommendations. RNA was quantified using NanoDrop 1000 and migrated on gels to check RNA non-degradation. Total cDNA was synthesized from 1µg of total RNA using the SuperScript™ II Reverse Transcriptase kit (Invitrogen) in presence of Ribolock RNase Inhibitor (Thermo scientific) and cDNA was diluted 10 times before subsequent analysis.

Quantitative reverse transcription-PCR analyses were adapted from Magne *et al.*, (2018). Three biological repeats were analyzed in duplicate. To calculate relative transcript levels, the final threshold cycle (Ct), efficiency, and initial fluorescence (R0) for every reaction were calculated with the Miner algorithm (Zhao & Fernald, 2005). Transcript levels for the different genes were expressed relative to the expression of the PsACTIN, PsBETA-TUBULIN3 genes for flower, EF1a gene (Johnson et al., 2006) for axillary buds and 18S for internode. Detailed information concerning oligonucleotides used for qRT-PCR analysis was provided in the supplementary Table S3.

Supplemental Table1. Characteristics of the *coch* mutant lines used in this study

Gene mutated	Type of mutation	Denote	Accession ID	Mutagen	Background	References
	CGA:TGA>Arg:STOP69	SGEapm	*SGEapm*	EMS	SGE	Zhukov et al. (2007)
PsCOCHLEATA1	Full-length deletion	coch1JI	*FN3185/1325*	FNB	JI2822	Couzigou et al., 2012
	Full-length deletion	coch1Cam	*FN3185/1325*	FNB(backcross)	Caméor	This study
PsCOCHLEATA2	G366A>W122*	coch2Cam	*Ps1178*	EMS	Caméor	This study
PsCOCHLEATA1 *PsCOCHLEATA2*	———	coch1coch2	(*FN3185/1325*) *X* (*Ps1178*)	Cross	Caméor	This study

EMS, ethyl methanesulfonate; FNB, Fast Neutron Bombardment.

Supplemental Table3. Primers used for qPCR.

Gene	Purpose	Primer names	Primer sequences (5' to 3')	Source
PsACTIN	qRT-PCR	PsACT-F	CTCAGCACCTTCCAGCAGATGTG	Azarakhsh et al. 2015
		PsACT-R	CTTCTTATCCATGGCAACATAGTTC	
PsBETA-TUBULIN3	qRT-PCR	PsBTUB3_F	TTGGGCGAAAGGACACTATACTG	Saha et al., 2012
		PsBTUB3_R	CAACATCGAGGACCGAGTCA	
FTa1	qRT-PCR	PsFTLa-6F	GCCCAAGCAACCCTACTTTT	Liew et al., 2011
		PsFTLa-2R	CCATCCTGGAGCGTAAACCC	
DET (TFL1a)	qRT-PCR	PsDET-F	CCACCATCAACACCAAACC	This study
		PsDET-R	TCTCTTTCCCAAATGTAGCATC	
PIM	qRT-PCR	PsPIM-4F	GCTTCAGAGTTTGGAACAGC	Liew et al., 2011
		PsPIM-6R	GACTCCATGGTGGTTTGG	
PsTFL1c	qRT-PCR	cF3	CCACATTTGGAAAAGAGTTGACAAGC	Foucher et al., 2003
		cR3	GCGTCTTCTAGGAGCCGTTGC	
PsCOCH1	qRT-PCR	PsCOCH1qpcrD	TCATCCTTATCACGCCGCTC	This study
		PsCOCH1qpcrR	TGCAACTCTCAACCGCGTAA	
PsCOCH2	qRT-PCR	PsCOCH2qpcrD	AGACCCCACAGTAAGAACCG	This study
		PsCOCH2qpcrR	TTCACGTGAGAGAACAAGAGC	
EF1a	qRT-PCR	EF1a-F	GATGCACCTGGACATCGTGAC	Johnson et al., 2006
		EF1a-R	CTTAGGGGTGGTAGCATCCATCT	
RMS4	qRT-PCR	RMS4-F	GCATAGCAATGGTAACAGTAGCGG	Johnson et al., 2006
		RMS4-R	CCGGTTTCGGTTGCCCT	
PsBRC1	qRT-PCR	PsBRC1-F	AGGCAAGAGAAAGAGCAAGG	Braun et al., 2012
		PsBRC1-R	TTGCATTGCTTTGAGTTTGA	
PsRMS5	qRT-PCR	PsRMS5-forward	TGACCGACGGTTGTGATTTGG	Ligerot et al., 2017
		PsRMS5-reverse	GCGGCATCTTAAAGACTCCGTAC	
PsAFB4/5	qRT-PCR	For-PsAFB4/5	GGATGAGGGTTTTGGTGCTA	Ligerot et al., 2017
PsRMS2		Rev-PsAFB4/5	ACAGGACGACATCCAAAGGA	
RMS1	qRT-PCR	PsRMS1 forward	TCCATTCCTTCCCTGTTACTC	This study
		PsRMS1 reverse	CCACACTTGCCACAATCTTTC	
18S	qRT-PCR	18S forward	ACGTCCCTGCCCTTTGTACA	Ozga et al., 2003
		18S reverse	CACTTCACCGGACCATTCAAT	
PsIPT1	qRT-PCR	PsIPT1 forward	ACCGTCTTGATGCTACGGAGGTTGTGC	Tanaka et al., 2006
		PsIPT1 reverse	TCTAATGGGTTACCCCTGCCACAGACG	
PsIPT1	qRT-PCR	PsIPT2 forward	TGGCAGCAACATCATCCTCTGCCTGC	Tanaka et al., 2006
		PsIPT2 reverse	ACCTGTGGCCCCCATTATCACTAC	
DRAWF	qRT-PCR	PsD27_F3	CTACCGTGGCTTCAAAGAAA	
		PsD27_R3	ATTTTGATGGTGGCATCACT	
RMS1	qRT-PCR	PsRMS1F	GGAATGGTCCGGGCATGTG	
		PsRMS1R	TGAGACTCGATCTGCCGGTGA	
PsMAX1	qRT-PCR	PsMAX1-A12_F3	AAAAACTAGGCGGACGTCTT	
		PsMAX1-A12_R3	TCCGAAACAGCTTTTGATTC	

CHAPTER III.

The *Brachypodium distachyon BLADE-ON-PETIOLE-Like* proteins *UNICULME4* and *LAXATUM-A* are redundantly required for plant development

The *Brachypodium distachyon* BLADE-ON-PETIOLE-Like proteins *UNICULME4* and *LAXATUM-A* are redundantly required for plant development

Shengbin Liu[1,2], Kévin Magne[1,2], Richard Sibout[3,4] and Pascal Ratet[1,2]

1 : Institute of Plant Sciences Paris-Saclay IPS2, CNRS, INRA, Université Paris-Sud, Université Evry, Université Paris- Saclay, Bâtiment 630, 91405 Orsay, France

2 : Institute of Plant Sciences Paris-Saclay IPS2, Paris Diderot, Sorbonne Paris-Cité, Bâtiment 630, 91405, Orsay, France

3 : Institut Jean-Pierre Bourgin, UMR 1318, INRA, AgroParisTech, CNRS, Université Paris-Saclay, RD10, Versailles Cedex 78026, France.

4 : UR1268 BIA (Biopolymères Interactions Assemblages), INRA, 44300, Nantes, France.

Short summary

BdCUL4/BdLAXA loss-of-function affects ligule, leaf and spikelet formation, tillering, internode elongation, seed yield and lignin content but not seed shattering.

FOOTNOTES

Funding information

This work was supported by the CNRS and by the grant from the Agence National de la Recherche (ANR-14-CE19-0003-01) to Pascal Ratet. This work has benefit from the support of the LabEx Saclay Plant Sciences (ANR- 10-LABX-0040-SPS, LabEx SPS and ANR-17-EUR-0007, EUR SPS-GSR) which is managed by the French National Research Agency under the program “Investissements d’avenir” (ANR- 11-IDEX-0003-02). S. Liu is supported by Chinese scholarship council (CSC) with 48 months.

The plant journal policy aprovement

The author responsible for the distribution of materials integral to the findings presented in this article in accordance with the policy described in the instructions for authors is Pascal Ratet (pascal.ratet@cnrs.fr).

Summary

In cultivated grasses, tillering, leaf and inflorescence architecture, as well as abscission ability, are major agronomic traits. In barley, maize, rice, and *Brachypodium*, *NOOT-BOP-COCH*-LIKE (*NBCL*) genes are essential regulators of the grass vegetative and reproductive development.

Monocot species generally possess two-to-four copies of *NBCL* genes and until now only one study on the rice model plant showed that the disruption of all *NBCL* genes strongly impacts rice development.

To improve our understanding of the role of *NBCL* genes in grasses, we studied the impact of the simultaneous loss-of-function of the two *NBCL* copies *BdUNICULME4* (*BdCUL4*) and *BdLAXATUM-A* (*BdLAXA*), using TILLING and Crispr-Cas9 *nbcl* double mutants in the non-domesticated grass *Brachypodium distachyon*.

The single *Bdlaxa* Crispr-Cas9 knock out mutant confirmed the previous result obtained using missense mutants. *BdLAXA* indeed negatively affect tillering and positively contributes to floral organ identity but also promotes primary root growth and seed yield. In addition, we show that *BdCUL4* and *BdLAXA* are not essential for seed shattering in *B. distachyon* but are essential for *B. distachyon* development and flowering. *BdCUL4* and *BdLAXA* redundantly contribute to internode elongation, leaf and spikelet architecture and are also required for the stem lignification.

Keywords:

Brachypodium distachyon, Crispr-Cas9, Boundary, Grass development, Ligule formation, Inflorescence determinacy, Leaf morphogenesis, *NBCL* genes, Tillering, Lignin content.

INTRODUCTION

Plant organogenesis is assured by pools of dividing pluripotent cells called the plant stem cell niches that reside in the meristems (Žádníková & Simon, 2014). The shoot apical meristem (SAM) is a continuous source of founder cells for the initiation of aerial lateral organs throughout the life cycle. The SAM is organized into a central zone, composed of slowly dividing stem cells, a peripheral zone where lateral organs initiate, and a rib zone that provides cells for internodes (Aichinger *et al.*, 2012). The initiation of organs from the peripheral zone requires the creation of meristem-to-organ boundaries that separate these two cell groups with very distinct gene expression programs and morphologies (Žádníková & Simon, 2014). Boundaries are characterized by a specific genetic program which aims to repress cell proliferation and to promote initiation and differentiation of adjacent lateral organs (Aida & Tasaka, 2006a,b; Barton, 2010; Žádníková & Simon, 2014; Hepworth & Pautot, 2015; Wang *et al.*, 2016). Previous researches have revealed a network of genes and hormone pathways participating in boundary regulation. Among these molecular actors, the members of the *NOOT-BOP-COCH*-LIKE (*NBCL*, Couzigou *et al.*, 2012) clade encode highly conserved key developmental co-transcription factors containing BTB/POZ (BROAD COMPLEX, TRAM TRACK, and BRICK A BRACK/POXVIRUSES and ZINC FINGER) and ANKYRIN domain repeats.

In dicots, through their roles in boundary regulation, *NBCL* genes are associated with multiple aspects of developmental processes, such as differentiation and patterning of stipules and leaves (Yaxley *et al.*, 2001; Ha *et al.*, 2003, 2004, 2007; McKim *et al.*, 2008; Couzigou *et al.*, 2012), floral meristem identity acquisition, internode elongation, and flower patterning and identity (Yaxley *et al.*, 2001; Ha *et al.*, 2003, 2004, 2007; Norberg *et al.*, 2005; Xu *et al.*, 2010; Couzigou *et al.*, 2012; Khan *et al.*, 2012a, 2015). They also play a role in the establishment and functioning of abscission zones (Norberg *et al.*, 2005; Hepworth *et al.*, 2005; McKim *et al.*, 2008; Ietswaart *et al.*, 2012; Couzigou *et al.*, 2015; Frankowski *et al.*, 2015), as well as in inflorescence architecture and fruit patterning (Hepworth *et al.*, 2005; Khan *et al.*, 2012a; Xu *et al.*, 2016). In addition, *NBCL* genes were recently shown to be involved in photo/thermo-morphogenesis and root development (Woerlen *et al.*, 2017; Zhang *et al.*, 2017) and may help to restrict fungal susceptibility of the rosette core (Dai *et al.*, 2019). Plants overexpressing *Arabidopsis BLADE-ON-PETIOLE* (*BOP*) show a

branching phenotype, producing extra paraclades in leaf nodes (Ha *et al.*, 2007) and also *BOP1/2* function downstream of BREVIPEDICELLUS- PENNYWISE (*BP-PNY*) in the stem and have a reciprocal function associated with lignin biosynthesis (Khan *et al.*, 2012b).

In monocotyledon, *NBCL* genes are also conserved but their roles were less studied. Two *NBCL* genes (*HvUniculme4* (*HvCul4*) and its paralog *HvLaxatum-a* (*HvLax-a*)) are present in barley (*Hordeum vulgare*). The *HvCul4* gene acts at axil and leaf boundary regions to control axillary bud differentiation as well as the development of the ligule and the *HvLax-a* gene controls internode length, floral organ identity, and rachis development (Tavakol *et al.*, 2015; Jost *et al.*, 2016). By contrast to barley, the modern maize (*Zea mays* ssp. *mays*) possesses four *NBCL* paralogs: *tassels replace upper ears1* (*ZmTRU1*) and *tassels replace upper ears1-like1* (*ZmTRU1*-like, *TRL1*) are homologous to *HvCul4* and *ZmTRU2* and *ZmTRU2*-like are putative homologous to *HvLax-a* (Dong *et al.*, 2017). Maize which was domesticated from teosinte (*Z. mays* ssp. *parviglumis*) is characterized by the suppression of axillary branching through an increase in apical dominance. Branch suppression in maize was achieved through the selection of a gain of function allele of the *TEOSINTE BRANCHED1* (*TB1*) transcription factor and its loss of function mutants overproduce tillers and have long aerial branches tipped by male tassels that replace the normally female ears (Doebley *et al.*, 1995). *ZmTB1* functions as a repressor of both axillary bud growth and inflorescence sexual fate (Hubbard *et al.*, 2002), which encodes a class II TB1, CYCLOIDEA, PCF1 (TCP) transcription factor that is orthologous to *Arabidopsis thaliana BRANCHED1* (Doebley *et al.*, 1997; Aguilar-Martínez *et al.*, 2007). The *NBCL* gene *ZmTRU1* is directly activated by *ZmTB1* to mediate axillary branch suppression (Dong *et al.*, 2017). In rice, there are three *NBCL* genes (*OsBOPs*). *OsBOP1* is homologous to *HvCUL4* and *OsBOP2*/*3* are homologous to *HvLAX-A*. They act as the main regulators of proximal-distal patterning through activation of proximal sheath differentiation and suppression of distal blade differentiation. They control temporal changes in the sheath-blade ratio of rice leaves and are also essential for ligule and auricle differentiation (Toriba *et al.*, 2019). The mutant phenotypes of the *HvCul4*, *Zmtru1* and *OsBOPs* suggest that the roles of *NBCL* genes might be different for tillering and for the development of ligule and auricles at the sheath-blade boundary region (Tavakol *et al.*, 2015; Jost *et al.*,

2016; Dong *et al.*, 2017; Toriba *et al.*, 2019). The grasses (*Poaceae*) have complex inflorescences, such as maize (*Zea mays*) tassels and the rice panicles, which comprise spikelets and branches generated from spikelet and branch meristems, respectively. The spikelets can be divided into determinate spikelets (DS) and indeterminate spikelets (IDS) (Ren *et al.*, 2013; Whipple, 2017; Bommert & Whipple, 2018). The DS species such as rice and maize form a fixed number of florets and grains in a single spikelet, while IDS species such as *Brachypodium* and wheat (*Triticum* sp.), produce variable numbers of florets, resulting in more than two grains per spikelet (Malcomber *et al.*, 2006; Koppolu & Schnurbusch, 2019). *B. distachyon*, like wheat and barley, forms unbranched spike inflorescences (Bonnett, 1935, 1936; Koppolu & Schnurbusch, 2019). The inflorescence meristem (IM) in *B. distachyon* and wheat terminate into a terminal spikelet meristem (SM), which produces 10-12 floret meristems (FMs) in a distichous manner on the indeterminate rachilla (Bonnett, 1936; Draper *et al.*, 2001; Derbyshire & Byrne, 2013; Kellogg *et al.*, 2013; Koppolu & Schnurbusch, 2019). In contrast, the barley IM is indeterminate and no terminal spikelet is formed, each SM produces one FM, always resulting in three single-flowered spikelets per rachis node that produce one or three florets in two-rowed and six-rowed barley, respectively (Bonnett, 1935; Babb & Muehlbauer, 2003; Kellogg *et al.*, 2013; Koppolu *et al.*, 2013).

Although some developmental differences can reasonably be explained by functional redundancy, our knowledge concerning the roles of *NBCL* genes in grasses remains limited and unfortunately restricted to domesticated crops. The selection pressure that was applied during domestication may bias our interpretations of the roles of some developmental gene regulators in cultivated crops.

Brachypodium distachyon (*B. distachyon*) is a non-domesticated model diploid monocot grass that has a small genome, a short life cycle, a small stature, is amenable to genetic transformation and is related to wheat and barley (Draper *et al.*, 2001; Vogel *et al.*, 2006; Opanowicz *et al.*, 2008; Brkljacic *et al.*, 2011; Scholthof *et al.*, 2018). The *B. distachyon UNICULME4* (*BdCUL4*) and *LAXATUM-A* (*BdLAXA*) genes are orthologous to *HvCul4* and *HvLax-a*, respectively, and were named according to the barley literature (Babb & Muehlbauer, 2003; Dahleen *et al.*, 2007; Franckowiak & Lundqvist, 2010; Tavakol *et al.*, 2015; Jost *et al.*, 2016)). By studying TILLING *nbcl* mutants in *B. distachyon*, we have previously shown that the *BdCUL4*

and *BdLAXA* genes are important for plant development (Magne *et al.*, 2020). The loss-of-function of *BdCUL4* causes reduced tillering, ligule and auricle developmental defects as well as the loss of spikelet determinacy, while *BdLAXA* loss-of-function causes increased tillering, modified spikelet architecture and floral mis-organization.

Unfortunately, the *Bdlaxa* TILLING mutants (*Bdlaxa*^{TI}) were missense mutants and not knock-out (KO) mutants leaving the possibility that the mutations were leaky. To confirm the mutant phenotype of the previously published *Bdlaxa* missense mutant, we generated 4 KO single mutants alleles for *BdLAXA* by clustered regularly interspaced short palindromic repeats and CRISPR-associated protein9 (CRISPR-Cas9) with *B.distachyon* wild type Bd21-3 as background (*Bdlaxa*^{CR}). We also constructed KO double mutants *Bdcul4Bdlaxa* through *BdLAXA* inactivation by CRISPR-Cas9 with *Bdcul4* (*Bd4982*) KO mutant as background. In parallel, we also produced a double mutant by crossing *Bdlaxa* (*Bd3615*) missense allele with a different *Bdlaxa*^{TI} (*Bd7965*) KO mutant line. Here, we report that *BdCUL4* and *BdLAXA* are redundantly essential for *Brachypodium* development and that the *Bdlaxa*^{CR} loss-of-function mutants have a similar but stronger phenotype than the *Bdlaxa*^{TI} missense mutant alleles. The *Bdcul4Bdlaxa*^{CR} loss-of-function double mutants are dwarf with curly leaves and aberrant flower development, and consequently infertile. Fortunately, the double mutant, obtained by crossing a KO *Bdlaxa*^{TI} with a missense *Bdlaxa*^{TI} can produce few seeds even if plants had strongly modified inflorescences and a dwarf phenotype similar to the *Bdcul4Bdlaxa*^{CR} double mutants. As *B. distachyon* naturally loses its seeds after ripening, we studied the role of these *NBCL* genes in seed shattering. Our results indicate that none of the single and double mutants were altered in abscission ability but the double mutant is strongly affected in cellulose and lignin content. Our results reveal an essential role of *BdCUL4* and *BdLAXA* in a broad spectrum of developmental processes, suggesting a central role in pooideae.

RESULTS

Generation of *Bdlaxa* Crispr-Cas9 null alleles and of *Bdcul4laxa* double mutants

In order to create *Bdlaxa* null alleles and *Bdcul4laxa* double mutants, we used the Crispr/Cas9 technology in *B. distachyon*. To do so, we used two sequence-specific guides RNA (sgRNA) located in the two exons of the *BdLAXA* gene (Fig.1a and

Supplementary Table 1) and targeted the *BdLAXA* gene in *Brachypodium* inbred line *Bd21-3* (wild type) and *Bdcul4* KO mutant (*Bd4982*-Q127* called $Bdcul4^{Q127*}$ see below) backgrounds in order to produce KO *Bdlaxa* single mutant and *Bdcul4Bdlaxa* double mutant, respectively. In order to distinguish between the two types of mutants, we set the *Bdcul4* and *Bdlaxa* TILLING mutants as $Bdcul4^{TI}$ ($Bdcul4^{Q127*}$ or $Bdcul4^{W203*}$) and $Bdlaxa^{TI}$ ($Bdlaxa^{T381I}$ or $Bdlaxa^{L365F}$) and the *Bdlaxa* Cripsr-Cas9 alleles as $Bdlaxa^{CR}$. Four and three independent T0-generation transgenic lines were obtained for *Bd21-3* and $Bdcul4^{Q127*}$ lines to generate $Bdlaxa^{CR}$ and $Bdcul4^{Q127*}Bdlaxa^{CR}$ single and double mutants respectively. In total, we obtained six different types of mutations in *BdLAXA* (Fig.1b, c) in these Cripsr-Cas9 transgenic plants.

In the wild type background, we obtained a single base pair (bp) deletion in the first exon and a four bp deletion in the second exon (Fig.1a, c). The entire progeny of these two $Bdlaxa^{CR}$ alleles presented similar phenotypes consisting of shorter spikelets and increased tillering phenotypes reminiscent of the $Bdlaxa^{TI}$ missense mutant phenotypes described previously (Magne *et al*., 2020; see detailed phenotyping in the section below, Fig.2c-d).

In the $Bdcul4^{Q127*}$ background, the T0 transgenic plants contain mixtures of $Bdlaxa^{CR}$ mutations in the different tillers and some tillers contain bi-allelic mutations. This suggested that the Cripsr-Cas9 machinery was operating during plant regeneration, creating independent mutations in the different tillers of a single plant. In total, we isolated up to five different types of mutations in one plant (Fig.1b, see also the chimeric plant Sup. 1c). These five different mutations correspond to one bp addition or one, two, three, or four bp deletions (Fig.1b). The plant with the three bp deletion in the *BdLAXA* gene shows no additional phenotype as compared to the $Bdcul4^{Q127*}$ parent indicating that it is an in-frame deletion of one amino acid without phenotype. In contrast, the progeny lines containing one, two, and four bp deletions in the first exon of the *BdLAXA* gene generated premature stop codons and the independent homozygous plants had similar extreme dwarf phenotype and were sterile. These double mutant lines had thus a dramatically different phenotype compared to the $Bdcul4^{Q127*}$ parent line (see below). The different Crispr-Cas9 KO alleles obtained in this work show identical phenotypes and the mutations were named $Bdlaxa^{CR}$ through the rest of this study independently of the KO allele used.

The phenotypes of the *Bdcul4*^{Q127*}*Bdlaxa*^{CR} double mutant lines (4 alleles) were so strong that the plants were sterile and did not produce seeds (sup.1d, h). Therefore, viewing the impossibility to work with the double KO mutants, we generated weaker double mutants by crossing the *Bdcul4*^{W203*} KO mutant line, different from the allele used in the Crispr-Cas9 experiment above, with the missense *Bdlaxa*^{T381I} mutant line (Fig. 1a). Note that these two *Bdcul4* alleles have identical phenotypes (Magne *et al*., 2020). We succeeded to generate one single F1 line and to retrieve six *Bdcul4*^{W203*}*Bdlaxa*^{T381I} homozygous double mutant plants within a progeny of 137 individuals that segregated both *cul4* and *laxa* single mutant phenotypes. The segregation of the F2 lines followed the correct segregation ratio 9:3:3:1 (Supplementary table 1b). The double mutant lines obtained by crossing are less affected than the double KO, produced seeds, and unable to pursue the study.

(b)

Mutation	target site	PAM		phenotype
WT	CCGGCGGCGGAGGAGGCTGTGTTGGGCCAGTTGAGGGGCGGCGG	WT		Bdcul4^{TI}
TY1	CCGGCGGCGGAGGAGGCTGTGTTGGGCCAG-TGAGGGGCGGCGG	Δ1		Bdcul4^{TI}Bdlaxa^{CR}
TY2	CCGGCGGCGGAGGAGGCTGTGTTGGGCC--TTGAGGGGCGGCGG	Δ2		Bdcul4^{TI}Bdlaxa^{CR}
TY3	CCGGCGGCGGAGGAGGCTGTGTTGGGCC---TGAGGGGCGGCGG	Δ3		Bdcul4^{TI}
TY4	CCGGCGGCGGAGGAGGCTGTGTTGGGCC----GAGGGGCGGCGG	Δ4		Bdcul4^{TI}Bdlaxa^{CR}
TY5	CCGGCGGCGGAGGAGGCTGTGTTGGGCCAGTTtGAGGGGCGGCG	+1		Bdcul4^{TI}Bdlaxa^{CR}

(c)

Mutation	target site	PAM		phenotype
WT	CCGGCGGCGGAGGAGGCTGTGTTGGGCCAGTTGAGGGGCGGCGG	WT		Bd21-3
TY2	CCGGCGGCGGAGGAGGCTGTGTTGGGCCAG-TGAGGGGCGGCGG	Δ1		Bdlaxa^{CR}
WT	GTCTTCCCCGTCGGGCCCGCACGCGAGTTCACGTCGGCGGCGCC	WT		Bd21-3
TY6	GTCTTCCCCGTCGGGCCCGCACGCGAG----CGTCGGCGGCGCC	Δ4		Bdlaxa^{CR}

Figure 1. Genome editing by Cas9 nucleases in *Brachypodium BdLAXA* gene and location of *Bdcul4* and *Bdlaxa* mutations.

(a) Schematic representation of *BdCUL4* (green) and *BdLAXA* (blue) proteins. Unhatched and hatched blocks represent BTB/POZ domains and ankyrin repeat domains, respectively. *Bdcul4* (*Bd4982*, *Bd7965*) TILLING mutant alleles and *Bdlaxa* (*Bd5998*, *Bd3615*) TILLING and CRISPR mutant alleles used in the study and their corresponding amino acids substitutions are indicated by asterisks (KO mutations) or by black triangles (missense mutations). (**b**, **c**) The mutations in *BdLAXA* with *Bdcul4* background (**b**) and wild type background (**c**), and the corresponding phenotypes were listed on the right side. The original sequence of the target site for *BdLAXA* in Bd21-3 are indicated with green

letters and the protospacer adjacent motif (PAM) site is red. The dashed line replace the deleted nucleotides in the mutant plant, the "t" marked with blue color was the addition in the KO plant.

Bdlaxa^{CR} and Bdlaxa^{TI}, and Bdcul4^{Q127*}Bdlaxa^{CR} and Bdcul4^{W203*}Bdlaxa^{T381I} mutants present similar phenotypes

To confirm the functions of *BdCUL4* and *BdLAXA*, we compared the phenotypes of the TILLING and Crispr-Cas9 mutants. The *Bdcul4* mutants had reduced tiller numbers compared to wild type (Fig. 2a, b, f). We found that the phenotype of the *Bdlaxa^{CR}* single KO mutants was similar to the *Bdlaxa^{TI}* (missense) mutants but slightly stronger in spikelets and tiller numbers (Fig. 2c, d, g; sup. 1b). The *Bdlaxa^{CR}* or *Bdlaxa^{TI}* mutants have twice more secondary or tertiary tillers than the wild type plant, while there was no difference for the primary tillers. As described previously (Magne *et al*., 2020), *Bdcul4^{TI}* single mutants showed a reduced number of tillers as compared to the wild type plants, and this reduction of the number of tillers was even stronger in the double mutants (Fig. 2e, g). Strikingly, this reduced number of tillers was accentuated in the *Bdcul4^{Q127*}Bdlaxa^{CR}* double mutant when compared to the *Bdcul4^{W203*}Bdlaxa^{T381I}* Tilling double mutant (Fig. 2e, f, g).

In *Bdlaxa^{CR}* mutants, the spikelets phenotype was similar to the previously described *Bdlaxa^{TI}* mutants, however, the *Bdcul4^{Q127*}Bdlaxa^{CR}* and *Bdcul4W203*BdlaxaT381I* double mutants show spikelet differences, (see below). The *Bdlaxa^{CR}* and *Bdlaxa^{L365F}* show a similar plant height with the wild type (Fig. 1c, d, h) but *Bdlaxa^{T381I}* was shorter (data not shown). The reduced size observed in the *Bdlaxa^{T381I}* TILLING mutant was not observed in the *Bdlaxa^{L365F}* allele or in the Crispr-cas9 mutants and probably resulted from other mutations in this background. Although there was no significant difference in plant height between control and *Bdcul4^{TI}* lines, *Bdcul4^{Q127*}Bdlaxa^{CR}* and *Bdcul4^{W203*}Bdlaxa^{T381I}* lines were significantly shorter with a dwarf phenotype (Fig. 2e, f, h). Furthermore, the total weight of the above-ground part at complete senescence and the biomass of double mutants were significantly reduced compared to wild type and the *Bdcul4^{TI}* and *Bdlaxa^{CR}* mutants (Fig. 2i). To determine at which developmental stage the growth of the double mutant was affected, we observed their development from seed germination until plants were fully mature. One week after germination, the *Bdcul4^{W203*}Bdlaxa^{T381I}* lines had a wild type stature but phenotypically diverged when internodes began to elongate (Sup. 1e-h). In contrast, the dwarf phenotype of the

Bdcul4^{Q127*}*Bdlaxa*^{CR} double mutants was visible soon (at one leaf stage) after germination and remained remarkable throughout the life cycle of the plant (Sup. 1i-l). Moreover, in the *Bdcul4*^{W203*}*Bdlaxa*^{T381I} mutant leaves were partly curled while all the *Bdcul4*^{Q127*}*Bdlaxa*^{CR} mutant leaves started to curl after germination. This indicates that the Crispr/Cas9 double mutant phenotype was stronger.

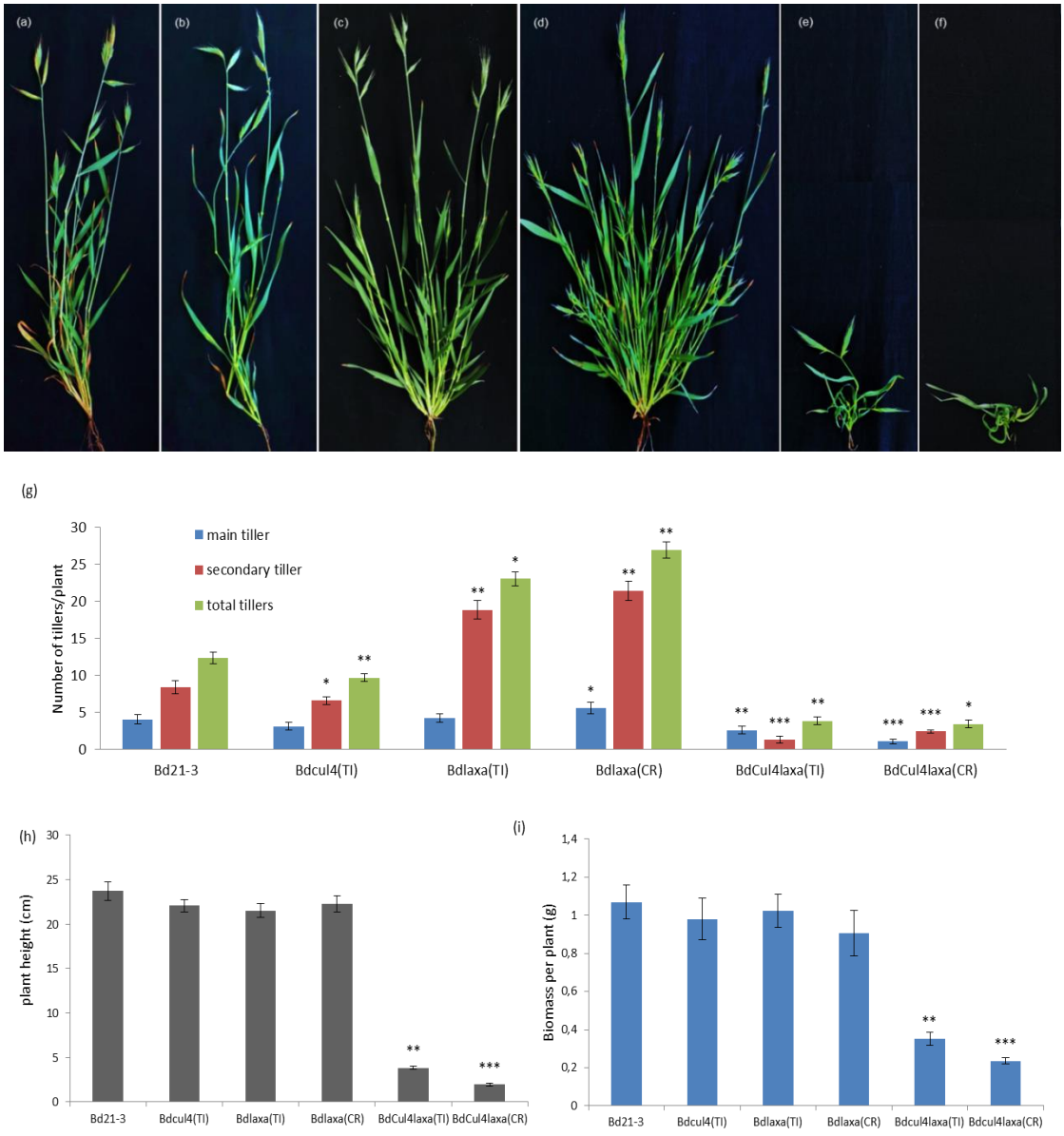

Figure 2. Whole plant phenotype of *Bdcul4*, *Bdlaxa* and *Bdcul4Bdlaxa* mutants.

(**a**)-(**f**), phenotype of developing *Brachypodium* wild type Bd21-3 (**a**), *Bdcul4* KO mutant (**b**), *Bdlaxa* missense (**c**) and CRISPR KO mutant plant (**d**), *Bdcul4Bdlaxa*^{TI} (*Bd7965Bd3615*; **e**), and *Bdcul4Bdlaxa*^{CR} (*Bd4982Bdlaxa*^{CR}; **f**), respectively. The tillers were counted for different genotypes (**g**), Numbers of primary (blue bars), secondary (red bars), and total tillers (green bars) per plant in completely mature wild type, *Bdcul4*, *Bdlaxa*, and *Bdcul4Bdlaxa* mutants. *Bdcul4* present less secondary tillers, *Bdlaxa*^{TI} and *Bdlaxa*^{CR} both present more secondary tillers compared to wild type.

The *Bdlaxa*^{CR} also displayed a stronger phenotype with more secondary tillers than the *Bdlaxa*^{TI} missense mutant. The double mutants, *Bdcul4Bdlaxa*^{TI} and *Bdcul4Bdlaxa*^{CR}, show reduced tillers and the CRISPR KO double mutants (**f**) always cannot form a real tiller. The average plant height (**h**) and the biomass of the above-ground part (**i**) of different genotypes were measured when the plant was totally dry. Error bars represent standard deviation. Wild type, n: 20; Bdcul4, n: 18; BdlaxaCR, n: 22 and Bdlaxa Bd5998, n: 15. Scale bars: a-k, 1 cm. Asterisks indicate significant difference compared to the Bd21-3 control one *=p<0,05, two ** =p<0,01 and three *** =p<0,001; Mann and Whitney test).

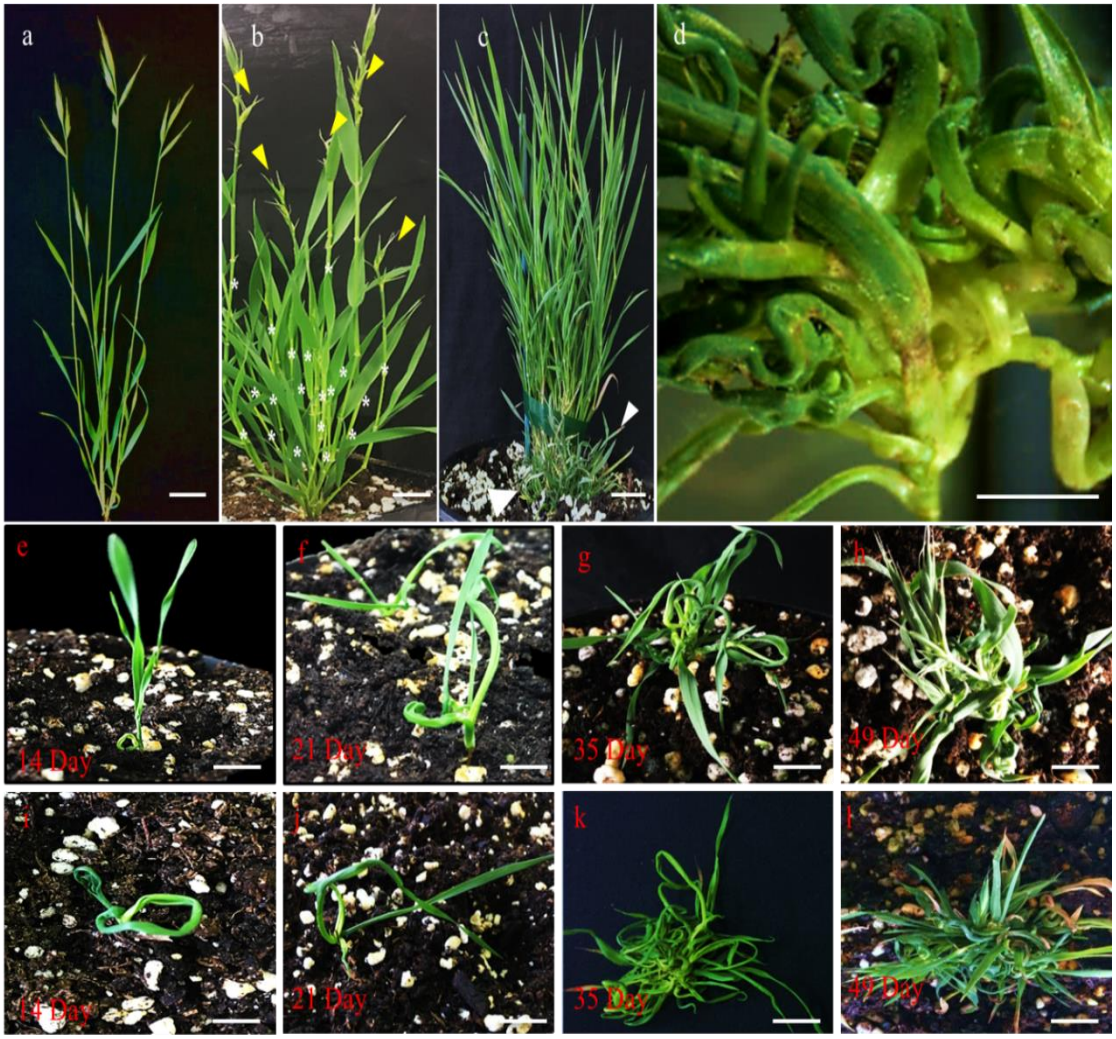

Supplementary Figure 1. Tiller phenotype of Bdlaxa and Bdcul4laxa.

(**a**)-(**d**), the phenotype of developing *Brachypodium* wild-type Bd21-3 (**a**), CRISPR *Bdlaxa*^{CR} KO single mutant (**b**), CRISPR KO Bdcul4BdlaxaCR(Bd4982BdlaxaCR) double mutant heterozygous plant and the homozygous mutant (white arrowheads) with higher magnification (**d**) respectively. *Bdlaxa*^{CR} presents more tillers (**b**) compared to wild type (**a**), the BdlaxaCR also displayed a stronger impact on spikelet phenotype. The Bdcul4BdlaxaCR double mutants show highly curly leaves and always cannot form a real (**d**). **(e)-(l).** Different growth stages of CRISPR *Bdcul4Bdlaxa*^{CR} (*Bd4982Bdlaxa*^{CR}) KO double mutant (**a-d**) and *Bdcul4Bdlaxa*^{TI} (**e-h**) from one week after sowing in the soil to the spikelet have appeared. **e**, i. at 14 days post sowing (dps), f, j. at 21 dps, g, k. at 35 dps

and h, l. at 49 dps. Scar bar: 1cm. Asterisks indicate more tillers compared to Bd21-3 control. White arrowheads indicate small CRISPR KO double mutant and yellow arrowheads show the impacted spikelet in CRISPR single and double mutants.

The loss-of-function of *BdCUL4* and *BdLAXA* affects internode cells elongation

Due to the significant difference in plant height of the *Bdcul4Bdlaxa* double mutant lines compared to wild type plants, we investigated the cause of this phenotype. Nodes and internodes numbers were unchanged in the single and double mutant lines compared to control (Fig. 3a). However, the dissection of the *Bdcul4*^{W203*}*Bdlaxa*^{T381I} and *Bdcul4*^{Q127*}*Bdlaxa*^{CR} double mutant stems revealed a drastic reduction of the internode elongation. This indicates that the extremely dwarf phenotype is due to a defect in internode elongation rather than to the change in internode numbers (Fig. 3a). To estimate this internode size difference, we measured the length of the first three internodes from the apex for each genotype as well as the average length of the internodes for each internode position. The average length was measured for WT, *Bdcul4*, and three *Bdlaxa* mutant lines (*Bdlaxa*^{L365F}, *Bdlaxa*^{T381I,} and *Bdlaxa*^{CR}) and showed that line *Bdlaxa*^{T381I} is smaller than *Bdlaxa*^{L365F}and *Bdlaxa*^{CR} (data not shown). This might result from unrelated mutations present in this TILLING mutant line. For the following, we thus used the *Bdlaxa*^{CR} line as control. In the *Bdcul4*^{W203*}*Bdlaxa*^{T381I} double mutant, the internode length was tremendously reduced (Fig. 3a, f) as compared to the wild type (Fig. 3a, f). Possible explanations for the short internode observed in the double mutants may include shorter cells, fewer cells, or both. To test these possibilities, we next examined toluidine blue-stained longitudinal sections from the first internodes and nodes, using bright-field microscopy (Fig. 3b-e). Microscopic observation of the internode and node longitudinal sections indicated that the cell length was significantly decreased in the *Bdcul4*^{W203*}*Bdlaxa*^{T381I} double mutant compared to wild type (Fig. 3b, e, f, g). In contrast, the length of the internode and node cells in *Bdcul4*^{TI} (Bd7965) and *Bdlaxa*^{L365F} single mutants were not significantly different from the wild type (Fig. 3c, d, f, g).

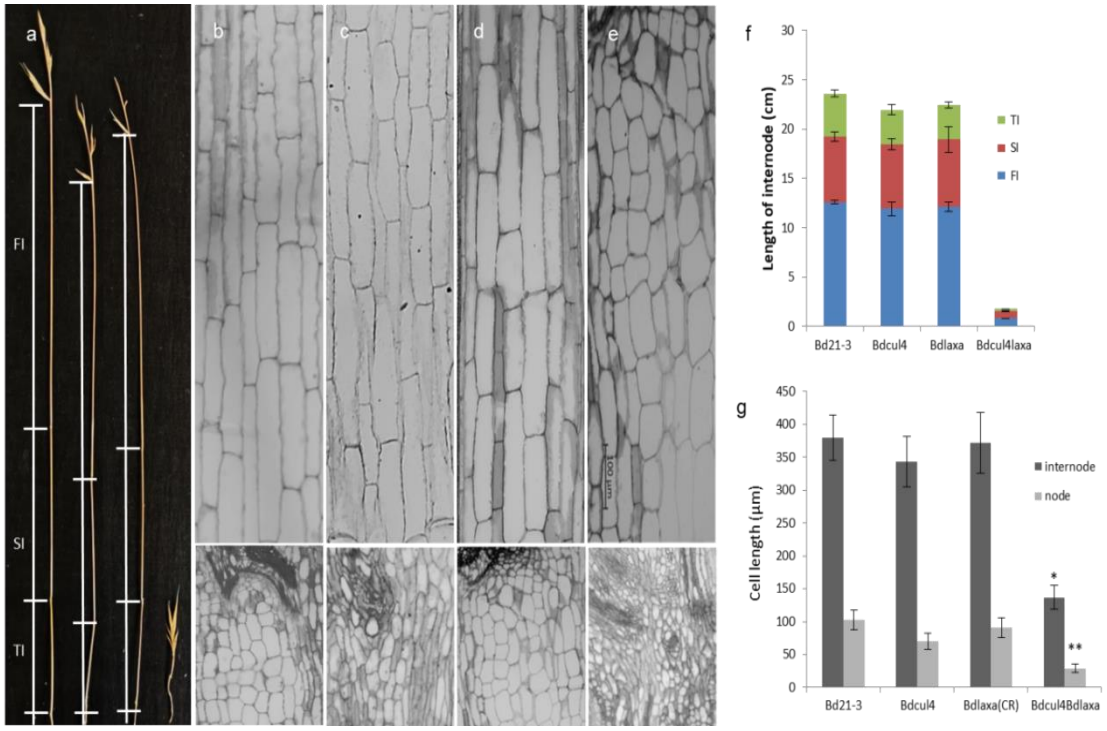

Figure 3. The length of the internode and the stem cells in *Bdcul4, Bdlaxa* and *Bdcul4Bdlaxa*.

(**a**) Internode phenotype of tallest stem, from left to right is Bd21-3 (left), *Bdcul4* (middle left), *Bdlaxa*^{CR} (middle right), *Bdcul4Bdlaxa*^{TI} (right), respectively. Between the spikelets and the node from the top as first internode (FI), the length of the first three internodes were measured (**f**). Length of first internode (blue bars), secondary internode (SI, red bars), third internode (TI, green bars) in completely elongated wild type, *Bdcul4*, *Bdlaxa*^{CR,} and *Bdcul4BdlaxaTI*. Ten shoots of each line were measured for each experiment. (**b-k**) Microscopic images of toluidine blue-stained longitudinal stem sections of the first internode of flowering stems illustrating the cell length of the first internode (top) and node (bottom) in control (**b**), *Bdcul4* (**c**), *Bdlaxa*^{CR} (**d**) and *Bdcul4BdlaxaTI* (**e**). Scale bar = 100 µm. (**m**) cell length of the first internode and node of flowering stems (30 cells for each replicate. Cell lengths and counts are means ± SEM, Star representative p-value, one *=p<0,05, two ** =p<0,01. Error bars represent standard errors.

BdCUL4 is required for ligule and represses *BdLAXA* in auricle formation

In monocots, the leaf is composed of a basal sheath, a distal blade, and the junction between the two called the "laminar joint" (Yu, 2019). The sheath and leaf blade are separated and articulated by two wedge-like structures called auricles, which act as a hinge allowing the leaf blade to project at an angle from the vertical stem. In the *Bdcul4*^{Q127*} and *Bdcul4*^{W203*} mutant lines, the ligule and auricles do not develop and only a fringe of differentiated tissue is visible (Fig.4b, f, j), showing that *BdCUL4* is required for ligule and auricle development (Magne *et al.*, 2020). By contrast, in

Bdlaxa^{L365F} and *Bdlaxa*^{T381I}, ligule and auricles are present (Magne *et al.*, 2020). The presence of ligule and auricles in the *Bdlaxa*^{CR} null mutant supports our previous results (Fig.4c, g, k), and confirms that *BdLAXA* is not essential for the blade-sheath boundary differentiation.

Interestingly, in the *Bdcul4*^{W203*}*Bdlaxa*^{T381I} double mutant, the ligule is absent however auricles developed normally (Fig.4d, h, i). We hypothesized one possible action model for the *BdCUL4* and *BdLAXA* to regulate the auricle formation (Fig. 4m), in which, *BdCUL4* may repress the *BdLAXA* and indirectly inhibited the auricle formation and this can be supported by the gene expression in the mutant (below). In the *Bdcul4*^{Q127*}*Bdlaxa*^{CR} double mutant, the auricle is difficult to observe because the leaves intensively curled and the plant does not form a real stem. We also tested the expression level of *BdLAXA* and *BdCUL4* genes in the sheath, the blade, and the lamina joint. qRT-PCR results showed that *BdLAXA* and *BdCUL4* genes were highly expressed in the sheath and lamina joint while very low expression was detected in the blade. The highest expression for *BdCUL4* was found in the lamina joint while for *BdLAXA* it was found in the sheath (Fig.4n). These results are in agreement with those previously reported for sheath-blade boundary and blade organs (Magne *et al.*, 2020). The accumulation of *BdCUL4* and *BdLAXA* transcripts in these organs is consistent with the mutant phenotypes.

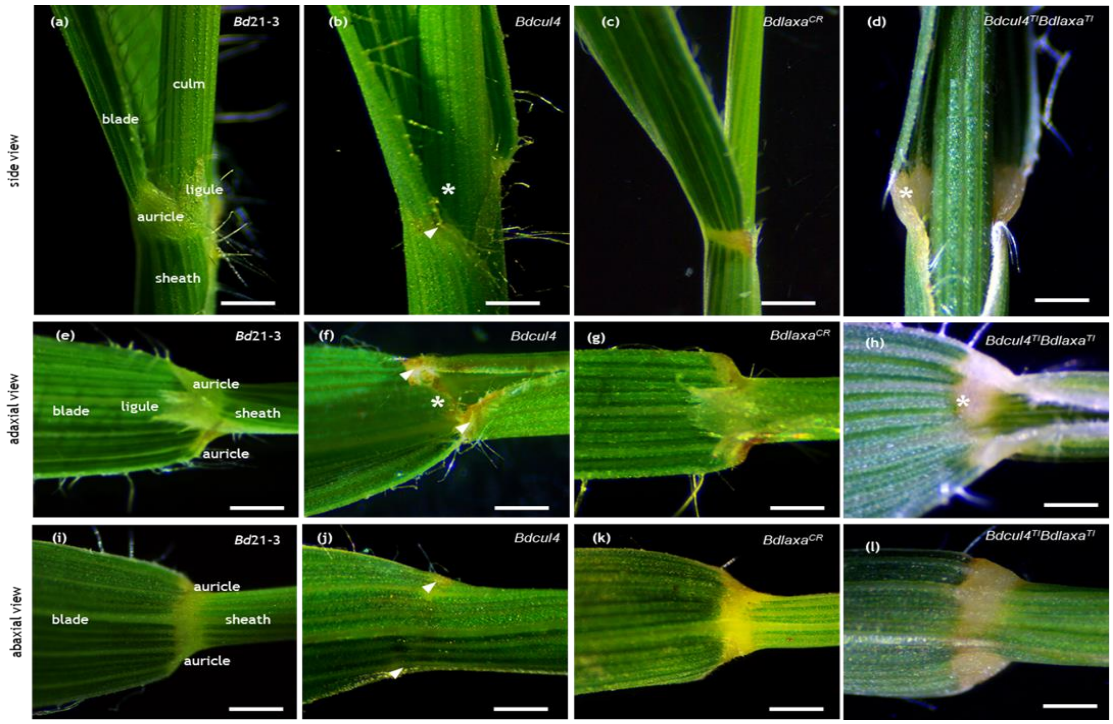

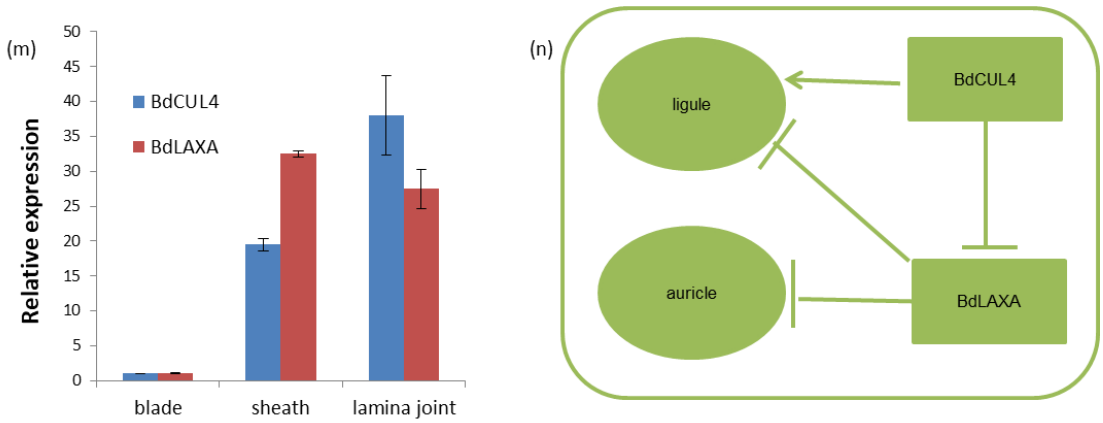

Figure 4. *Bdcul4* mutants lack ligules and auricles but the double mutant *Bdcul4xBdlaxa* lacks only ligules.

Blade-sheath boundary region of 40 days-old Bd21-3 (**a**,**e**,**i**,); *Bdcul4 Bd7965* (**b**,**f**,**g**), *Bdlaxa*^{CR}(**c**,**j**,**k**), *Bdcul4Bdlaxa Bd7965Bd3615* (**d**,**h**,**l**). The first, second, and third rows represent side, adaxial and abaxial views, respectively. Bd21-3 blade-sheath boundary region presents two auricles and one ligule (**a**,**e**,**i**,). In *Bdcul4 Bd7965*, auricles and ligule are missing (**b**,**f**,**g**) and instead of a ligule, only a fringe of tissues remains (**f**). In the *Bdlaxa*^{CR} blade-sheath boundary region organization is similar to Bd21-3 and auricles and ligule are properly developed (**c**,**j**,**k**). In Bdcul4Bdlaxa *Bd7965Bd3615*, the ligule still missing but the auricles appear again (**d**,**h**,**l**), In pictures e,f,g,h, the culms have been removed to display the ligule. White arrowheads indicate missing auricles and white asterisks indicate missing ligules. Scale bars: 1 mm. (**m**), *BdCUL4* (blue bars) and *BdLAXA* (green bars) gene expression profiles in Bd21-3 leaf, transcripts accumulation in 40 days-old. Gene expression analysis was performed leaf blade, sheath, and lamina joint, by qRT-PCR. *BdCUL4* and *BdLAXA* gene expression were normalized against the constitutively expressed *BdPOLYUBIQUITIN 4* and *BdUBIQUITIN-CONJUGATING ENZYME E2 18* reference genes. Results represent the means ± SEM of three biological repeats and three technical replicates. Primers used for qRT-PCR analysis are given in Supporting Information Table S1. (**n**), the possible model for *BdCUL4* and *BdLAXA* regulating the ligule and auricle formation. Arrow indicates activation.

BdCUL4 and *BdLAXA* present antagonistic roles in leaf positioning

In grasses, the plant architecture is important and can impact the crop yield. Leaf angle (LA), is an important parameter of the grass architecture and it is determined by the development of the lamina joint connecting the leaf blade and leaf sheath (Kong *et al.*, 2017; Zhou *et al.*, 2017). In this study, we identified that the *Bdcul4*^{TI} mutants exhibited an erected leaf phenotype probably caused by a defect in the lamina joint development resulting from a complete absence of the auricles and ligules (Fig. 4b, f, j). The mutant lines exhibited a reduced leaf angle and more compact plant architecture compared to wild type Bd21-3 (Fig. 5a, b, e, f). We

measured the flag leaf angle between the midrib of the flag leaf and the internode below the spike in the *Bdcul4*^{TI} mutants and Bd21-3 and found that the means of flag leaf angle was 13.50° and 28.23°, respectively (Fig. 5i). Similarly, the second and third LAs in the *Bdcul4*^{TI} mutant are smaller than wild type (Fig. 5a, b). In contrast, in both the *Bdlaxa* single mutant and *Bdcul4*^{TI}*Bdlaxa*^{TI} double mutant the leaf angle was increased compared to wild type, especially for the double mutant which showed horizontal-type leaves (Fig.5c, d, g, h, i). These results indicate that *Bdcul4*^{TI}, *Bdcul4*^{Q127*}*Bdlaxa*^{CR}, and *Bdcul4*^{W203*}*Bdlaxa*^{T381I} mutants are altered for lamina joint development and that *BdCUL4* and *BdLAXA* are antagonistic participating in leaf angle determination.

Strikingly, the leaves of the *Bdcul4*^{Q127*}*Bdlaxa*^{CR} double mutants are distorted at almost 180° and looks like helices (Fig. 5d). In addition, the sheath of the double mutant is separate from the stem while the sheath of the *Bdcul4* and *Bdlaxa* single mutants surrounds the stem (Fig.5 f, g).

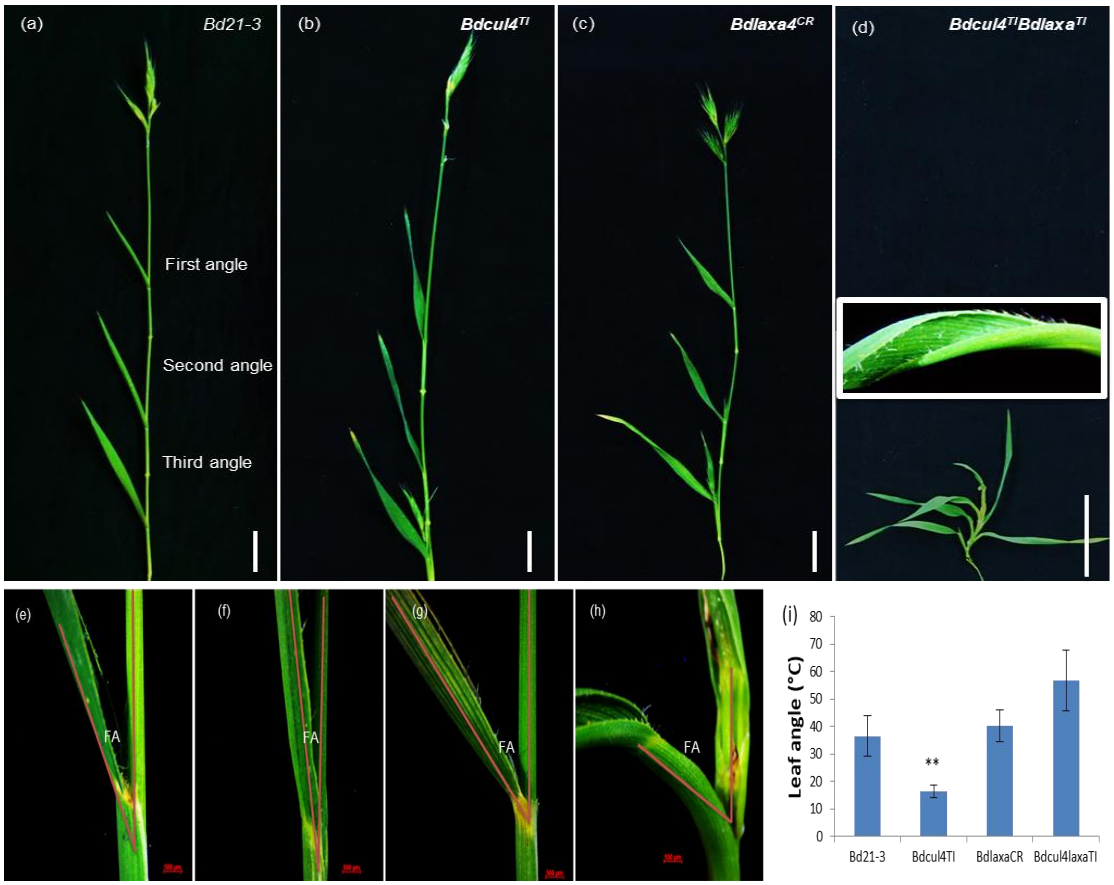

Figure 5. *Bdcul4* and *Bdlaxa* mutants present leaf architecture modifications.

(**a-d**), Photographs of Brachypodium leaf architecture at the flowering stage in wild type (**a**), Bdcul4(**b**), *Bdlaxa*^{CR} (**c**), and *Bdcul4*^{TI}*Bdlaxa*^{TI} (**d**), The curly leaf was magnified in the white box. (**e-h**),

Morphologies of the flag leaf and showing Leaf angle (LA) between the leaf blade and the vertical culm (marked by red lines) at the flowering stage in wild type (**e**), *Bdcul4* (**f**), *Bdlaxa*^{CR} (**g**) and *Bdcul4*^{TI}*Bdlaxa*^{TI} (**h**). (**i**), the average of the first three leaf angles in different genotypes, first LA. 10 seedlings for each replicate experiment. The asterisk represents significant differences determined by the two-tailed Student's t-test at P<0.01. Error bars = SD (n = 10)

BdCUL4 and *BdLAXA* are required for spikelet architecture and determinacy

BdCUL4 and *BdLAXA* were previously shown to be involved in *B. distachyon* spikelet architecture and determinacy (Magne *et al.*, 2020). *Bdcul4*^{TI} *mutants* showed exaggerated spikelet length while *Bdlaxa*^{TI} missense mutants showed an opposite short-spikelet phenotype with bent floret rachises (Fig. 6a-c, and 6h-i). Similarly, *Bdlaxa*^{CR} showed a short-spikelet phenotype and this result confirmed the previous *laxa* missense phenotype (Fig. 6c-d, and 6h-i). Notably, the defects were stronger and fewer seeds can be formed in *Bdlaxa*^{CR} (Fig. 6d) although the mutant lines produced more florets per spikelet compared to *Bdlaxa*^{TI}.

In *Bdcul4*^{W203*}*Bdlaxa*^{T381I}, spikelets were longer than those of the *Bdlaxa* and wild type plants and appeared similar to the *Bdcul4*^{TI} ones although spikelet was a bit shorter (Fig. 6b, e, and 6h-i). In addition, most florets were empty in *Bdcul4*^{W203*}*Bdlaxa*^{T381I}, suggesting that the filling of the grain was incomplete and partial sterility.

The *Bdcul4*^{Q127*}*Bdlaxa*^{CR} double mutant grew slowly and produced short and extremely aberrant inflorescences (Fig. 6f, h). This *Bdcul4*^{Q127*}*Bdlaxa*^{CR}, presented spikelet-like organs with the presence of a modified and thicker lemma in between the lemma and the palea (Fig. 6g). Compared to wild type, *Bdcul4*^{Q127*}*Bdlaxa*^{CR} possesses all floral organs, although it dried prematurely (Fig. 6f, g). Under our growing conditions the *Bdcul4*^{Q127*}*Bdlaxa*^{CR} did not produce seeds at all (Fig. 6h), indicating that *BdCUL4* and *BdLAXA* are essential for fertility in *B. distachyon*. These results suggest that one of the roles of *BdCUL4* is to restrict the length of the spikelet maybe through the repression of the spikelet meristematic activity. On the other hand, *BdLAXA* seems to promote both the relaxation of the spikelet architecture and the length of spikelet. Together with the phenotype in the double mutant, it suggests that *BdCUL4* and *BdLAXA* are both required for spikelet architecture and determinacy and that they also control fertility. For these characters, these two genes show additive effects.

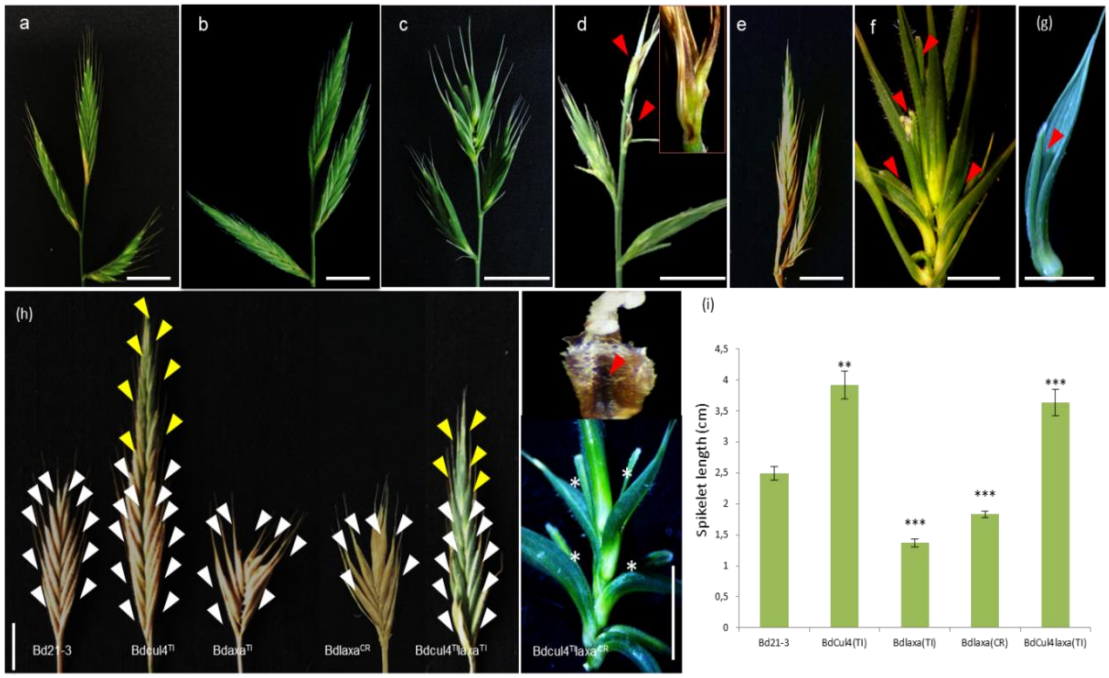

Figure 6. *cul4*, *laxa* and *cul4laxa* mutants present modified spikelet architecture and an altered number of florets per spikelet.

(**a**)-(**g**)**.** Phenotypes of developing spike of wild type (**a**), *Bdlcul4*^{TI} (**b**), *Bdlaxa*^{TI} (**c**), *Bdlaxa*^{CR} (**d**), double mutant *Bdcul4Bdlaxa*^{TI} (Bd7965Bd3615; **e**) and *Bdcul4Bdlaxa*^{CR} (**f, g**) at 49 days after sowing. The spike of *Bdcul4* show loss of determinacy and the *laxa* spike was relaxed, some spike in the *laxa*^{CR} were necrotic (red box) and the *Bdcul4*^{TI}*Bdlaxa*^{CR} show a leaf-like spike (marked with red arrowheads). (**h**). Spikelet phenotype, from left to right is *Bd*21-3, *Bdcul4*, *Bdlaxa*^{TI}, *Bdlaxa*^{CR}, *Bdcul4*^{TI}*Bdlaxa*^{TI}, and *Bdcul4*^{TI}*Bdlaxa*^{CR} at 60 days after sowing. The *Bdcul4* and *Bdcul4*^{TI}*Bdlaxa*^{TI} mutants show an exaggerated spikelet growth with an increased number of florets per spikelet and increasing spikelet length compared to wild type (**h, i**) while the *Bdcul4*^{TI}*Bdlaxa*^{CR} show a leaf-like spikelet (marked with white asterisks). Wild-type and supplementary florets are indicated by white and yellow arrowheads, respectively. *Bdlaxa*^{TI} and *Bdlaxa*^{CR} mutants show a short spikelet phenotype with a reduced number of florets (white arrowheads) per spikelet compared to wild type (**h, i**). Values represent means and asterisks indicate significant differences relative to wild type (two ** =p<0,01 and three *** =p<0,001; Mann and Whitney test). For *Bd*21-3, *Bdcul4*, *Bdlaxa*^{TI}, *Bdlaxa*^{CR} and *Bdcul4*^{TI}*Bdlaxa*^{TI} spikelets, n: 200, 150, 180, 190, and 120, respectively. Scale bars =1cm. Error bars = SE

BdLAXA is inhibited by *BdCUL4* in the control of floral organ number and identity

The *B. distachyon* floral organization consists of a feathery stigma, an ovary, two abaxial lodicules, and two adaxial stamens (Fig. 7a, b). In a previous study, we showed that in the *Bdcul4*^{TI} KO lines the floral organization was not altered while in the *Bdlaxa*^{TI} missense mutant lines additional stamens were formed and partial

lodicule-to-stamen identity switch called stamenoid lodicules were observed. These results suggested that the floral organ identity was altered in this mutant (Magne *et al.*, 2020).

In this study, we further describe the floral organization of *Bdlaxa*^{CR}, *Bdcul4*^{W203*}*Bdlaxa*^{T381I} and *Bdcul4*^{Q127*}*Bdlaxa*^{CR} mutants. We found that *Bdlaxa*^{CR} and *Bdlaxa*^{T381I} presented similar floral organization defects. Indeed, *Bdlaxa*^{CR} also showed additional floral organs at the adaxial position which displayed partial-to-complete stamen-like identity (Fig. 7d). In addition, at the abaxial side of the flower, *Bdlaxa*^{CR} also presented thicker, narrower, and partially yellowish lodicules similarly to the previously described *Bdlaxa*^{L365F} mutants (Fig. 7c).

Interestingly, in *Bdcul4*^{W203*}*Bdlaxa*^{T381I} and *Bdcul4*^{Q127*}*Bdlaxa*^{CR} mutants, flowers were not modified and look-like wild type flowers (Fig. 7e-h). This suggests that *BdLAXA* represses *BdCUL4* for normal flower development. However, in *Bdcul4*^{Q127*}*Bdlaxa*^{CR} the stamen is abnormal, and dried in an early stage (Fig. 7i-j). This may explain that the *Bdcul4*^{Q127*}*Bdlaxa*^{CR} cannot succeed in grain filling.

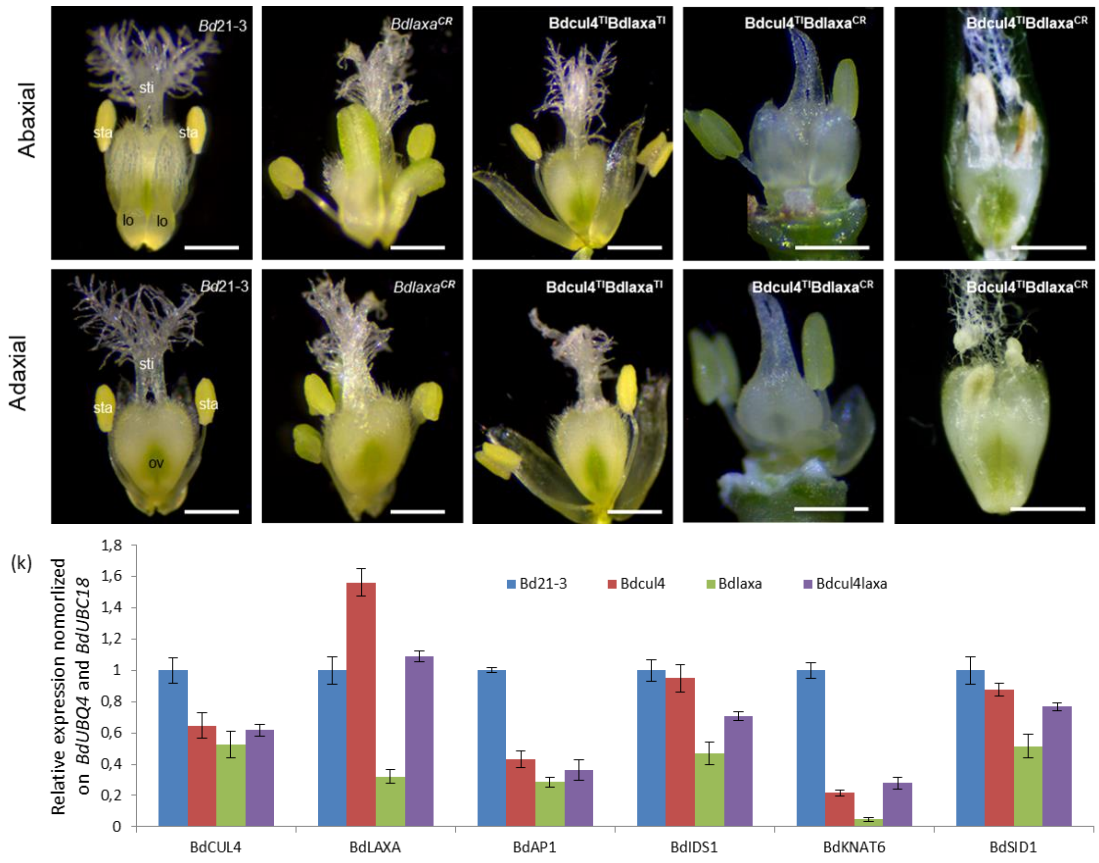

Figure 7. *Bdlaxa* mutants present modifications in reproductive organ identity.

(**a-j**) Reproductive organ organization in *Bd*21-3 (**a**,**b**), *Bdlaxa*^{CR} (**c**,**d**), *Bdcul4Bdlaxa* (*Bd*7965*Bd3615*) (**e**,**f**) and *Bdcul4Bdlaxa*^{CR} (**g-j**) during anthesis on 40 days-old plants. Pictures (**a**,**c**,**e**,**g**,**i**) and pictures (**b**,**d**,**f**,**h**,**j**) represent the abaxial and adaxial floral sides, respectively. *Bd*21-3 presents a feathery stigma, an ovary, two abaxial lodicules, and two adaxial stamens (**a**,**b**). *Bdlaxa*^{CR} presents floral organ number and identity modifications (**c**,**d**). *Bdcul4Bdlaxa* (*Bd*7965*Bd3615*) and the very early stage of *Bdcul4Bdlaxa*^{CR} floral organization is similar to wild type (**e-h**) but the flower was sterile in the later stage in *Bdcul4Bdlaxa*^{CR} (**i**,**j**). In abaxial position, *Bdlaxa*^{CR} presents narrow lodicules with aberrant yellow tissues (black asterisks, **c**) suggesting partial stamen identity. In the adaxial position, *Bdlaxa*^{CR} presents additional stamen-like organs (white asterisks, **d**). The number of flowers dissected for *Bd*21-3, *Bdlaxa*^{CR}, *Bdcul4Bdlaxa,* and *Bdcul4Bdlaxa*^{CR}, *n:* 102, 120, 50, 20, respectively. sti, stigma; sta, stamen; lo, lodicule; ov, ovary. Scale bars: a-j, 500 µm. (**k**), Transcripts level of *BdCUL4*, *BdLAXA*, *BdAP1*, *BdIDS1*, *BdKNAT6* and *BdSID1* in Bd21-3 (blue bars), *Bdcul4* (red bars), *Bdlaxa*^{CR} (green bars), and *Bdcul4*^{TI}*Bdlaxa*^{TI} (purple bars), respectively. Gene expression analysis was performed on spikelet by qRT-PCR when the inflorescence just appeared from flag leaves and gene expression was normalized against the constitutively expressed *BdUBQ4* and *BdUBC18* reference genes. Results represent the means ± SEM of three biological repeats and three technical replicates. Primers used for qRT-PCR analysis are given in Supporting Information Table S1.

To better understand the role of the *BdCUL4* and *BdLAXA* genes during flower development, we quantified the accumulation of transcripts in the young spikelets of the *B. distachyon* wild type and mutants by qRT-PCR. In, addition, the expression of *BdCUL4* and *BdLAXA* was compared with the expression of marker genes known to be sequentially induced or repressed during flower development. These genes include the key regulator of the floral meristem identity *BdAPETALA1* (*BdAP1*), two *BdAPETALA2-LIKE* floral identity repressors, *BdIDS1*, *BdSID1* and *BdKNAT6*, a downstream effector of *BOP* important for inflorescence formation. The abundance of the *BdCUL4* transcripts is significantly decreased in all the mutant lines *Bdlaxa*^{CR}, *Bdcul4*^{W203*}, and *Bdcul4*^{W203*}*Bdlaxa*^{T381I} mutants compared with wild type (Fig. 7k). In contrast, the expression level of *BdLAXA* has significantly increased in the *Bdcul4*^{W203*} mutants and slightly increased in the double mutant. We also observed a significantly decreased in the *Bdlaxa*^{CR} loss-of-function mutant compared with the control Bd21-3 (Fig.7k). The results suggest that the *CUL4* and *LAXA* transcript levels do not correlate with the flower identity phenotypes but eventually to a retro-control between these genes.

Similarly to *BdCUL4*, the expression level of the *BdAP1* and *BdKNAT6* were significantly decreased in all mutant lines compared with control (Fig. 6k). The expression of the *BdIDS1* and *BdSID1* genes was slightly downregulated in *Bdcul4*^{W203*} and significantly reduced in the *Bdlaxa*^{CR} and moderately decreased in the *Bdcul4*^{W203*}*Bdlaxa*^{T381I} double mutant (Fig. 7k). The results suggest that *AP1* and *KNAT6* are positively controlled by *CUL4* and *LAXA* while *IDS1* and *SID1* are controlled by *LAXA*. The results in the *Bdcul4*^{W203*} background shows that the *CUL4* transcript is unstable (reduce expression) and that *CUL4* require *LAXA* for full expression. The results in the *laxa* backgrounds indicate that the transcript is unstable in the KO mutant and that both *CUL4* and *LAXA* repress *LAXA* expression. These results indicate a role for BdCUL4 and BdLAXA in the expression of flower regulatory gene expression.

BdLAXA is required to maintain seed size and roots growth

Plants with erected leaves have an increased capacity to intercept light and a higher photosynthetic efficiency, which results in improved grain filling (Sinclair & Sheehy, 1999). In *Bdcul4* mutant lines the LA is reduced while it increases in the *Bdlaxa* and *Bdcul4Bdlaxa* mutant lines. To check if these modifications of the LA could have consequences on seed size and yield we measured them in different backgrounds. Our results show that *Bdcul4*^{TI} loss-of-function mutants had a larger seed size, seeds being longer and wider. Moreover, the total weight of 1000 seeds is also higher than in the wild type (Fig. 8a, b). In contrast, the *Bdlaxa*^{CR}, *Bdlaxa*^{TI} and *Bdcul4*^{Q127*}*Bdlaxa*^{T381I} mutant lines show a significantly reduced seed size (shorter and narrower) and the total weight of 1000 seeds was nearly reduced by 50% compared to wild type (Fig. 8a, b). These results suggest that *BdLAXA* is involved in *Brachypodium* seed development through the control of the seed size, which results in yield reduction in the *Bdlaxa* mutant backgrounds. In contrast, *Bdcul4*^{TI} loss-of-function has an antagonist effect and increases seed yield.

Due to the multiple aspects of the developmental defect of the mutants in the aerial part, we also measured the length of the root *in vitro* two weeks after germination (WAG) for plants grown on half MS medium. The *Bdcul4*^{TI} showed no significant difference in root growth compared to WT. In contrast, the single *Bdlaxa*^{CR} or *Bdlaxa*^{TI} mutant lines showed a reduction in root growth (Fig. 8c, d). In addition,

the average root length of the *Bdcul4*^{Q127*}*Bdlaxa*^{CR} double mutant was reduced by about 40% as compared to wild type (Fig. 8c, d). These phenotypes suggested that *BdLAXA* plays a significant role in *Brachypodium* root development.

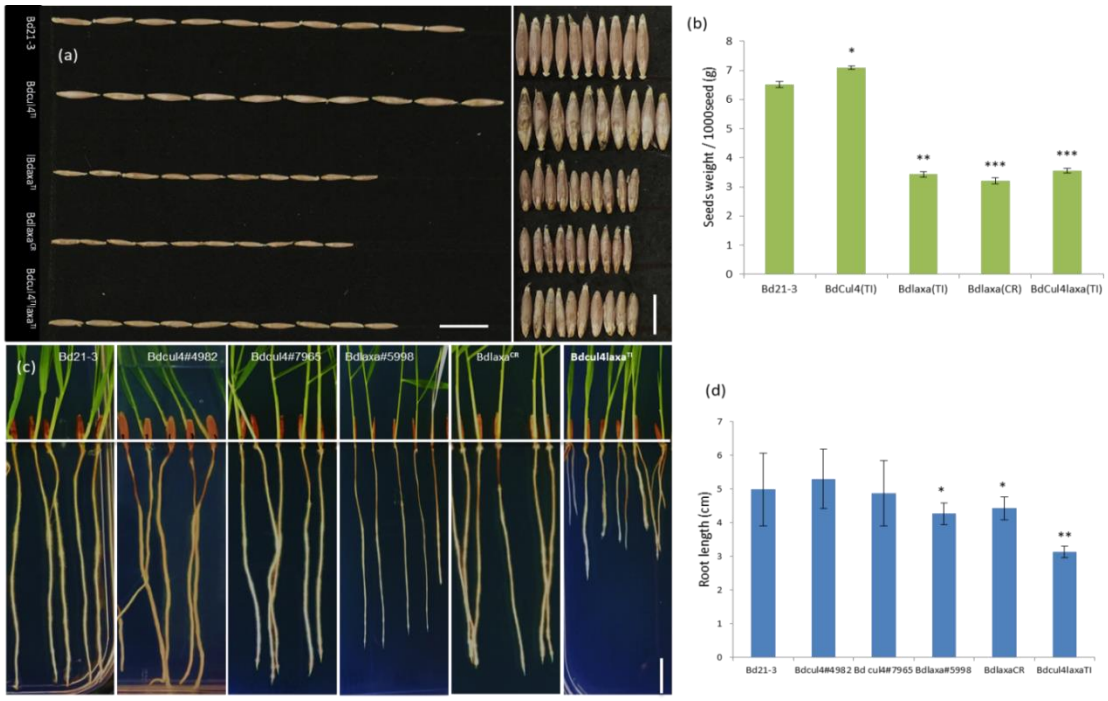

Figure 8. *BdLAXA* is required to maintain seed size and root development.

(**a, b**). Phenotypes of seeds, from top to bottom is *Bd*21-3, *Bdcul4*, *Bdlaxa*^{TI}, *Bdlaxa*^{CR} and *Bdcul4*^{TI}*Bdlaxa*^{TI} (**a**), and the corresponding average seeds weight (1000 seeds) were measured (**b**). The seed size and weight were significantly reduced in *Bdlaxa* and *Bdcul4laxa* mutants. (**c**) The global view of Brachypodium roots growth in-vitro on half MS medium at 14 days, from left to right is wild type Bd21-3, *Bdcul4* KO mutant (Bd4892 and Bd7965), Bdlaxa missense (Bd5998) and CRISPR KO mutant plant, *Bdcul4Bdlaxa*^{TI} (Bd7965Bd3615), respectively. The roots length was measured for different genotypes (**d**). The *Bdlaxa* single mutants and *Bdcul4Bdlaxa* double mutants show reduced roots length. Error bars represent standard deviation. Wild type, n: 80; *Bdcul4*, n: 78; *Bdlaxa*^{CR}, n: 92 and *Bdlaxa* Bd5998, n: 85. Scale bars: 1 cm. Asterisks indicate significant difference compared to the Bd21-3 control one *=p<0,05, two ** =p<0,01 and three *** =p<0,001; Mann and Whitney test).

BdCUL4 and *BdLAXA* are not necessary for seed abscission

The dicot *NBCL* genes are involved in aerial organ abscission in Brassicaceae, Solanaceae, and Papilionoidaceae (McKim *et al.*, 2008; Wu *et al.*, 2012; Couzigou *et al.*, 2016). In order to know if the *BdCUL4* and *BdLAXA* genes play a similar role in monocots, we analyzed seed abscission in the single and double mutant backgrounds. In a previous study (Magne *et al.*, 2020), we reported that *BdCUL4* and *BdLAXA* are

not altered in seed abscission in *Bdcul4*^{TI} KO mutant and *Bdlaxa*^{TI} missense mutant independently. To ascertain that these genes do not participate in seed shattering, we tested abscission in the *Bdlaxa*^{CR} KO and double mutants. Our results show that *Bdlaxa*^{CR} and *Bdcul4*^{W203*}*Bdlaxa*^{T381I} still presented a wild-type seed shedding. The seed morphology was not altered and seed abscission zones presented sharp scars without mis-formation sign (Fig. 9a-f). Histological analysis of *Bd*21-3, *Bdlaxa*^{CR}, *Bdcul4*^{W203*}*Bdlaxa*^{T381I} seed abscission zones clearly showed small differentiated cell layers corresponding to the abscission zone (Fig. 9g-i). These results suggest that *BdCUL4* and *BdLAXA* either independently or together are not essential for seed abscission zone establishment in *Brachypodium*.

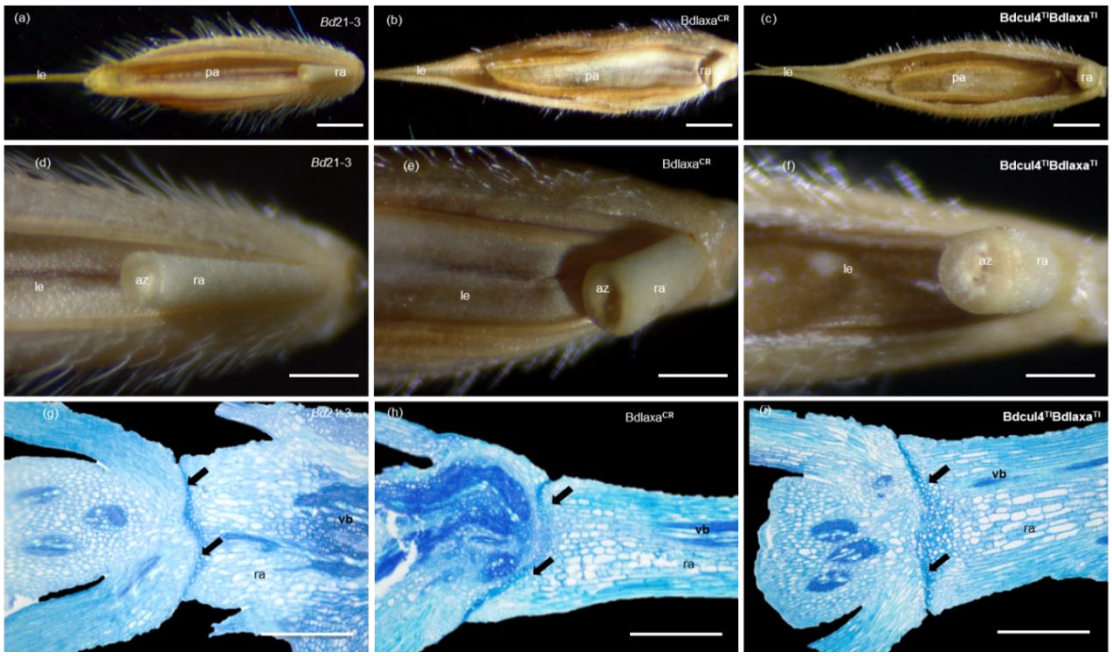

Figure 9. Shattering phenotypes of *Bdlaxa*^{CR} *and Bdcul4*^{TI} *Bdlaxa*^{TI} mutants.

Magnification of mature dry seed abscission zones in *Bd*21-3 (**a**), *Bdlaxa*^{CR} (**b**), *Bdcul4*^{TI} *Bdlaxa*^{TI} (**c**). Seed abscission zones shown in d-f are presented in sepia to focus on the shapes of the abscission zones. Longitudinal sections of *Bd*21-3 (**g**), *Bdlaxa*^{CR} (**h**), *Bdcul4*^{TI} *Bdlaxa*^{TI} (**i**) seed abscission zones in 40 days-old spikelets stained with toluidine blue. Abscission cell layers are indicated by black arrows. le, lemma; az, seed abscission zone; pa, palea; ra, rachilla; vb, vascular bundle. Scale bars: **a-f**, 1 mm; **g-i**, 100 µm. Section thickness: 7 µm. For abscission zone sections, *Bd*21-3 n: 15; *Bdlaxa*^{CR} n: 12; *Bdcul4*^{TI} *Bdlaxa*^{TI} n: 20.

BdCUL4 and *BdLAXA* regulate secondary cell wall lignification and composition

Lignin is a principal component of secondary cell walls and one of the major factors in determining the woodiness of higher plants. In Arabidopsis, the *BOP* genes have a role in regulation of lignin biosynthesis. In a dominant activation tagging allele of *BOP1* (*bop1-6D*) mutant, the expression of four lignin biosynthesis genes was dramatically up-regulated and this resulted in lignification of boundaries specialized for floral organ abscission and pod shatter (Khan *et al.*, 2012b; Hepworth & Pautot, 2015). To further investigate the function of *BdCUL4* and *BdLAXA*, stem cross-sections were analyzed using bright field light microscopy for changes in vascular patterning and composition. Vascular bundle shape and arrangement appeared similar in all *Bdcul4* and *Bdlaxa* mutant lines. However, a striking difference was observed in the cells between the vascular bundles when stained with the lignin-indicator dye, phloroglucinol- HCl (Fig. 10a-h). The interfascicular fiber regions in *Bdcul4* and *Bdlaxa* single mutant sections were bright red like in the wild type plants (Fig. 8a-g). In contrast, the *Bdcul4Bdlaxa* double mutant sections were yellow or white relative to the control sections, indicating very low lignin content (Fig. 10d, h). The striking change in histochemical staining led us to investigate the lignin content in these lines. Fully senesced, grounded stem tissue was assayed for acetyl bromide soluble lignin content. There was a slight increase in lignin content in *Bdlaxa*^{T381I} stems and a significant decrease in *Bdcul4*^{W203*}*Bdlaxa*^{T381I} (Sup. 2a).

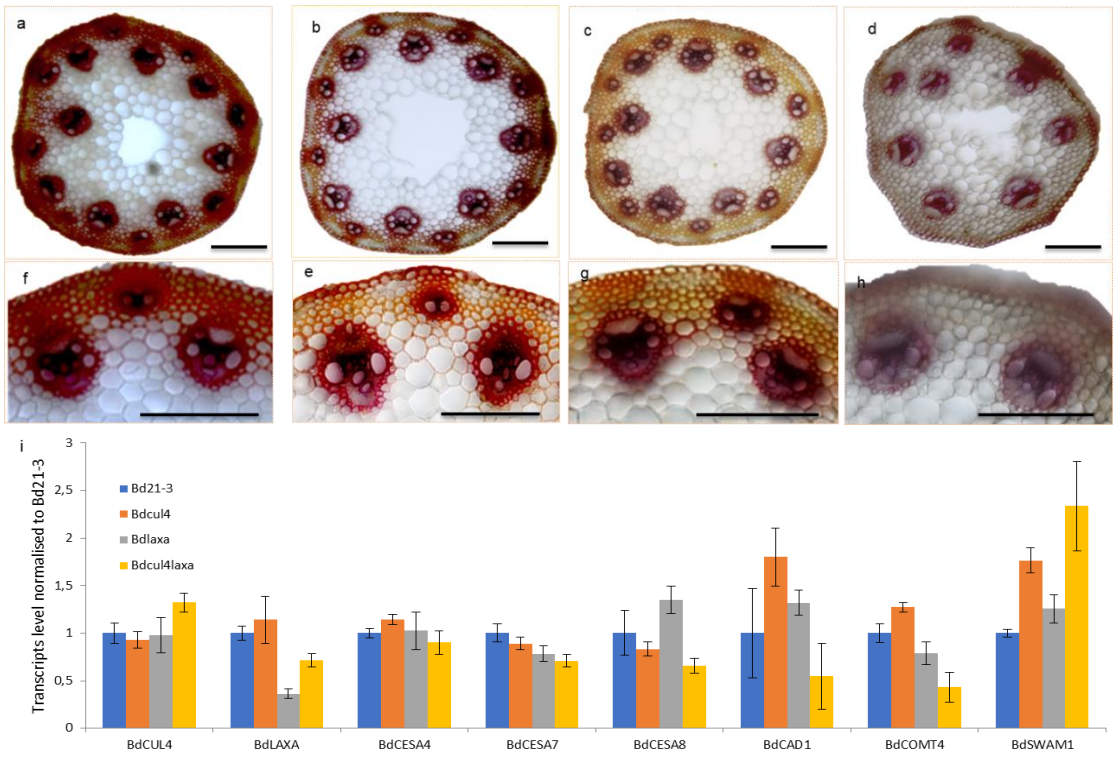

Figure 10. Phloroglucinol-stained stem cross-sections and transcripts of lignin marker genes. (**a–h**). First internodes of fully senesced plants were sectioned and stained with phloroglucinol-HCl to visualize lignin (red coloration) and representative images are illustrated. Whole stem (**a-d**) and higher magnification (**e-h**) of *B. distachyon* cross-sections of wild type Bd21-3 (**a**, **e**), *Bdcul4* (**b**, **f**), *Bdlaxa*^{CR} (**c**, **g**) and *Bdcul4laxa*^{TI} (**d**, **h**). Compared with the control (**a**, **e**) *Bdcul4* (**b**, **f**) and *Bdlaxa* stem sections (**c**, **g**) stained an orange-red color and show no significant difference with wild type, but *Bdcul4laxa* stem sections (**d**, **h**) were stained yellow in the interfascicular region and a less intense red color in the vascular bundles. Images were taken using bright-field microscopy. Scale bars = 0.1 mm. (**i**). Transcript abundance of *BdCUL4*, *BdLAXA*, and lignin marker genes *BdCESA4/7/8*, *BdCAD1*, *BdCOMT4*, and *BdSWAM1* in Bd21-3 (blue bars), *Bdcul4* (red bars), *Bdlaxa*^{CR} (gray bars), and *Bdcul4*^{TI}*Bdlaxa*^{TI} (yellow bars), respectively. Gene expression analysis was performed on the stem by qRT-PCR when the inflorescence just appeared from flag leaves and gene expression was normalized against the constitutively expressed *BdUBQ4* and *BdUBC18* reference genes. Results represent the means ± SEM of three biological repeats and three technical replicates. Primers used for qRT-PCR analysis are given in Supporting Information Table S1.

In addition, we found that the insoluble cell wall compounds were significantly decreased in the *Bdcul4*^{W203*}*Bdlaxa*^{T381I} double mutant while *Bdcul4* and *Bdlaxa* single mutant lines had a wild type insoluble cell wall composition (Sup. 2b). Similarly, the sugar composition, including glucose (mainly from cellulose) is significantly affected in the double mutants while the rhamnose, fucose, mannose, and galactose are only poorly detected in all the genotypes. Apparently, xylans (mainly from hemicellulose) are also impacted in the double mutants. The uronic acids (pectins), the content was very low in all genotypes (Sup. 2c) as expected in grasses.

These results suggest that changes in the secondary cell wall may account for the overall differences observed in stem area and above-ground biomass (Fig. 2i) and that *BdCUL4* and *BdLAXA* play an important role in secondary cell wall lignification and composition in Poaceae.

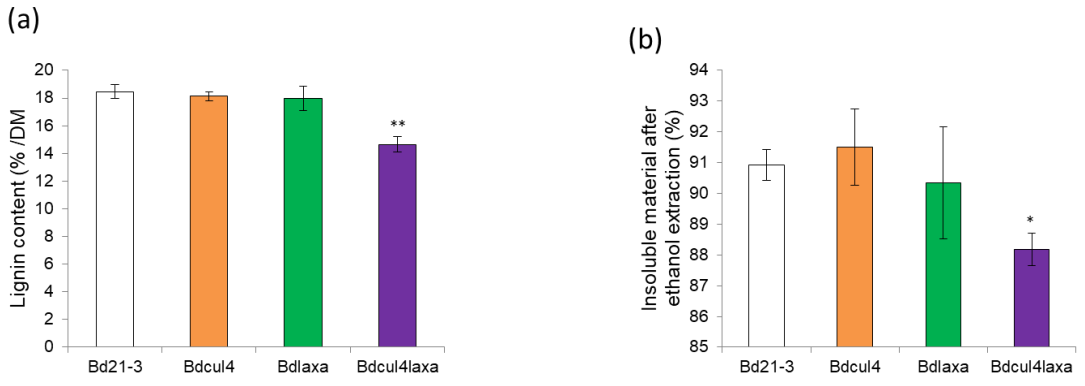

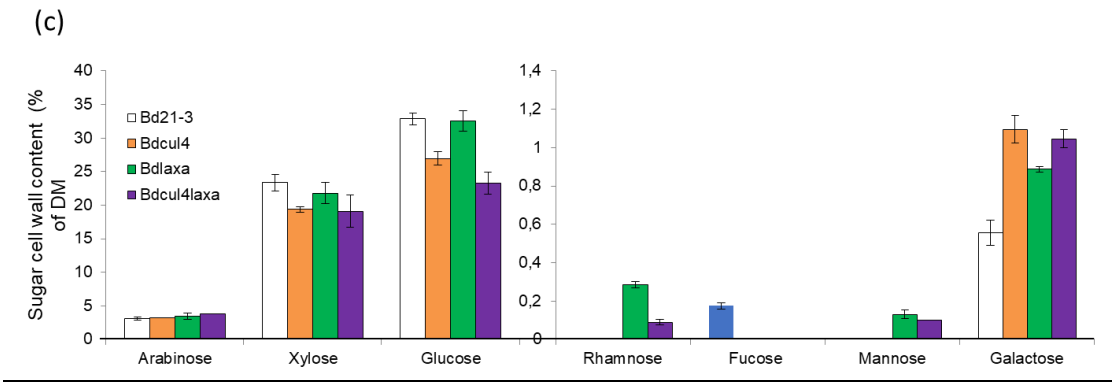

Supplementary figure 2. Cell wall composition of *Bdcul4* and *Bdlaxa* mutants.

(**a**) Insoluble material after ethanol extraction (%), (**b**) Acetyl bromide soluble lignin content, and (**c**) Sugar cell wall content (% of DM) of completely senesced stem tissue in Bd21-3, *Bdcul4*, *Bdlaxa*, and *Bdcul4laxa*. Data represent Means ± SEM. Pulverized stem tissue from six to sixteen individuals from three independent events was analyzed for each line.

BdCUL4 and *BdLAXA* regulate cellulose and lignin associated gene expression

To better understand the role of the *NBCL* genes in cell wall composition, genes involved in cell wall formation were analyzed in WT and mutant backgrounds. In *Brachypodium*, the *CELLULOSE SYNTHASE A* (*BdCESAs*) genes involved in secondary cell wall synthesis were generally enriched in stems, which are abundant in secondary cell walls, and transcripts were specifically abundant in stem vascular tissue and the surrounding tissue (Handakumbura *et al.*, 2013; Petrik *et al.*, 2016; Le Bris *et al.*, 2019). Cinnamyl alcohol dehydrogenase (*CAD*) and Caffeic acid O-methyltransferase (*COMT*) catalyze key steps in the pathway of lignin monomer biosynthesis (Bouvier D'Yvoire *et al.*, 2013; Trabucco *et al.*, 2013) and *SECONDARY WALL ASSOCIATED MYB1* (*BdSWAM1*) act as a positive regulator of secondary cell wall biosynthesis (Handakumbura *et al.*, 2018). The expression level of all three *CESA* genes was significantly down-regulated in *Bdcul4*^{TI}*Bdlaxa*^{TI} double mutant while *BdCESA4* transcripts slightly increase in *Bdcul4* and *BdCESA7* was down-regulated in *Bdlaxa* (Fig. 10i). Interestingly, the *BdCESA8* transcripts were slightly down-regulated and increase in *Bdcul4* and *Bdlaxa* single mutant, respectively. The expression of *BdCAD1* was up-regulated in either *Bdcul4* or *Bdlaxa* single mutants. The transcript abundance of the other lignin gene, *BdCOMT4*, increased in *Bdcul4* and decreased in the *Bdlaxa* single mutant. However, the transcript level of both *BdCAD1* and *BdCOMT4* significantly decreased in the *Bdcul4*^{TI}*Bdlaxa*^{TI} double mutant. Notably, the expression of *BdSWAM1*, a cell wall thickening regulator gene,

was significantly up-regulated in the *Bdcul4*^{TI}*Bdlaxa*^{TI} double mutant and showed a slight increase in both *Bdcul4* and *Bdlaxa* single mutants (Fig. 10i). In the same tissues, the *BdCUL4* transcripts significantly increased in double mutants and slightly decreased in *Bdcul4* single mutant. In contrast, the abundance of the *BdLAXA* transcripts significantly decreases in *Bdlaxa* single and double mutants and slightly increased in *Bdcul4* single mutant (Fig. 10i).

These results suggest that *BdCUL4* and *BdLAXA* influence the expression of cellulose, cell wall, and lignin gene expression. Changes in *BdCESA4*/7/8, *BdSWAM1*, *BdCOMT4*, and *BdCAD1* transcript levels along with the changes observed in cell wall composition and lignin content suggest that *BdCUL4* and *BdLAXA* activate the transcription of secondary cell wall biosynthetic genes.

DISCUSSION

BLADE-ON-PETIOLE1/2 (AtBOP1/2) are transcription co-factors in *Arabidopsis* regulating plant architecture through modulation of growth and meristem activity. Constitutive overexpression of *BOP1* or *BOP2* inhibits stem elongation, resulting in short plants (Norberg *et al.*, 2005; Khan *et al.*, 2012a, 2015). Analogously, the *BOP-like* gene *NtBOP2* in tobacco (*Nicotiana tabacum*) also regulates cell elongation (Wu *et al.*, 2012). Moreover, the overexpression of *Populus trichocarpa BPL1/2* (*PtrBPL1/2*) in *Arabidopsis* produced dwarf bushy plants with clustered flowers similar to overexpression of *AtBOP1* or *AtBOP2* (Devi, 2014). In our study, we have shown that *BdCUL4* and *BdLAXA*, homologs of *Arabidopsis BOP1/2* genes, are involved in multiple aspects of development in the non-domesticated grass *Brachypodium distachyon*. We generated the KO mutant alleles for *BdLAXA* by CRISPR-CAS9 and also produced *Bdcul4Bdlaxa* double mutants by CRISPR-CAS9 or by crossing using different *Bdcul4* alleles. In contrast to previous studies, our results show that the loss-of-function of both *Bdcul4* and *Bdlaxa* genes (double mutants) results in dwarf plants with compact stature. In these plants, the cell elongation of the stems was severely inhibited while the *Bdcul4* and *Bdlaxa* single mutants show no significant difference to WT for cell size. This suggests that the *NBCL* genes have antagonistic roles on plant growth in monocot and dicot plants.

The shoot apical meristem(SAM) initiates a series of repetitive units called phytomers, each consisting of a leaf, a node, an internode, and an axillary meristem

(AXM) located in the axil between the leaf and the shoot axis (Sussex, 1989). AXMs control shoot development, effectively influencing lateral branch and leaf formation. Leaves and tillers, the vegetative branches, are key determinants of grass shoot architecture in cereals that directly contribute to grain yield (Kebrom *et al.*, 2013). Tillers develop from axillary meristems located in the leaf axils at the base of many kinds of grass and undergo three distinct morphological stages: (1) initiation of an axillary meristem in the leaf axil; (2) development of leaf primordia on the axillary meristem to form an axillary bud; and (3) elongation of internodes into a tiller with the potential to form a grain-bearing spike (Schmitz & Theres, 2005; reviewed in Okagaki *et al.*, 2018). In our previous work (Magne *et al.*, 2020), the *BdCUL4* loss-of-function affected secondary tiller formation resulting in reduced tillering. *BdCUL4* and *HvCul4* share similar functions in the tillering by promoting AXM outgrowth. In barley, *HvLax-a* loss-of-function does not show any tillering phenotype (Jost *et al.*, 2016). In contrast, either the TILLING-NGS $Bdlaxa^{TI}$ missense or CRISPR/CAS9 $Bdlaxa^{CR}$ KO mutant alleles show increased tillering in the non-domesticated model *B. distachyon*. Thus, the KO alleles described in our work confirm our previous results with the missense mutants showing the opposite role of the two *NBCL* paralogs in plant architecture. Interestingly, the double mutants, $Bdcul4^{Q127*}Bdlaxa^{CR}$ and/or $Bdcul4^{W203*}Bdlaxa^{T381}$, are extremely reduced in the tiller formation especially for the $Bdcul4^{Q127*}Bdlaxa^{CR}$ CRISPR double KO mutant developing almost without secondary tillers. The possible explanation is the compact stature with curly leaves in the double mutants. In addition, the *Bdcul4Bdlaxa* tillers were often bent and distorted, possibly as a result of difficulties in emergence from the leaf sheaths that enclosed them. Our mutant analysis indicates that *BdCUL4* and *BdLAXA* seem to have opposite roles in tillering, by promoting and repressing AXM outgrowth, respectively. Interestingly, the double mutation resulted in a further decrease in the tillering.

Plants overexpressing *Arabidopsis* BLADE-ON-PETIOLE (*BOP*) show a branching phenotype, producing extra para-clades in leaf nodes (Ha *et al.*, 2007). Grass leaves develop from the flanks of the SAMs and AXMs are composed of a proximal sheath and distal blade separated by the ligular boundary. The ligular region is composed of the ligule, an outgrowth of an epidermal tissue flap, and the auricle (Becraft *et al.*, 1990; Sylvester *et al.*, 1990). In modern maize, the molecular actors such as *Zmliguleless1*/*2*/*3*(*Zmlg1*/*2*/*3*), *Zmliguleless narrow* (*Zmlgn*) and its redundant

Zmsister of liguleless narrow (*Zmsln*) participating in blade-sheath boundary establishment, and in ligule and auricle formation are beginning to be well characterized (Sylvester *et al.*, 1990; Moreno *et al.*, 1997; Muehlbauer *et al.*, 1997; Walsh *et al.*, 1998; Bolduc *et al.*, 2012; Moon *et al.*, 2013). The maize *NBCL* genes such as *Zmtru1* and its paralog *Zmtru1-like* are expressed in developing ligules, leaf axils, and axillary meristems (Johnston *et al.*, 2014), but their involvement in ligule or auricle formation has not yet been demonstrated. The barley *UNICULME4* (*CUL4*) gene is the barley *BOP* homolog (Tavakol *et al.*, 2015), and plants carrying mutations in *CUL4* are defective in both axillary meristem and ligule development. Moreover, *CUL4* is expressed in developing ligules, leaf axils, and axillary meristems and defines the boundaries of ligule and axillary bud development like the maize *BOP* homolog (Tavakol *et al.*, 2015). In addition, the barley *uniculm2* (*cul2*) mutation blocks axillary meristem development, and mutant plants lack lateral tillers (Babb & Muehlbauer, 2003). *ELIGULUM-A* (*ELI*-A), the suppressors of *CUL2*, mutations in ELI-A produce shorter plants with fewer tillers and disrupt the leaf blade-sheath boundary, producing liguleless leaves and reduced secondary cell wall development in stems and leaves (Okagaki *et al.*, 2018). In the *Bdcul4* mutant, ligule and auricle were absent while the *Bdlaxa* (KO line) did not result in any ligule and auricle defects. Interestingly, in the loss-of-function *Bdcul4Bdlaxa* double mutant, the auricle but not the ligules are present. One possible explanation is that *BdCUL4* is necessary for ligule formation and is a repressor of the *BdLAXA* gene, which acts as a direct repressor of ligule and auricle formation in *Brachypodium*.

Leaf angle (LA), defined as the inclination between the leaf blade midrib and the stem and is influenced by leaf development, particularly at the laminar joint. LA directly influences canopy structure and consequentially affects yield. Classical *liguleless* (*lg*) mutants, such as *lg1*, *lg2*, *lg3*, and *lg4* in maize (Zea mays) and *Oslg1* in rice (Oryza sativa) are deficient in the formation of the ligule and auricles, resulting in smaller leaf angles (Mantilla-Perez & Salas Fernandez, 2017). In agreement with the results obtained in rice, loss-of-function *BdCUL4* and *BdLAXA* exhibited LA modification. The *Bdcul4* reduced and the *Bdlaxa* slightly increased leaf angle while the double mutant leaves grow horizontal and are distorted at nearly 180 °C. In addition, the sheath is no longer wrapped around the stem but separated from it. Leaf auricle has a crucial effect on LA in a large population of maize inbred lines, and the

diversity of auricle development contributes to LA in maize (Kong *et al.*, 2017). Consistent with our results, reduced development of the auricle resulted in narrow LA, as observed in the *lg1* and *lg2* mutants (Moreno *et al.*, 1997; Walsh *et al.*, 1998). Erected leaves result in increased grain yield in grass crops (Sakamoto *et al.*, 2006; Liu *et al.*, 2019; Yu, 2019b). In agreement with this, the seeds yield is slightly increased in the *Bdcul4* mutant lines while significantly decreased in *Bdlaxa* and *Bdcul4Bdlaxa* mutants showing increase LA. Thus our results suggest that an increased leaf angle also reduces yield in *Brachypodium*.

In dicot, the leaf defects were observed in Arabidopsis *bop1/2* mutants (Ha *et al.*, 2003, 2004; Norberg *et al.*, 2005; Hepworth *et al.*, 2005) and also in loss-of-function mutants of *BOP* orthologs in pea and *Medicago truncatula* (Couzigou *et al.*, 2012). The phenotypic effects in the *Bdcul4* mutant more closely resembled the leaf alterations in *Arabidopsis bop1/2* mutants. Phenotypic defects in dicot bop mutants and monocot *Bdcul4* and *Bdcul4Bdlaxa* indicate that the corresponding genes are required for the correct morphogenesis of the proximal region of the leaf. This suggests at least a partial conservation of the *BOP* gene function in leaf development between dicots and monocots. Consistent with a role in the tiller and leaf development, both *BdCUL4* and *BdLAXA* have significantly higher expression in the lamina joint and sheath than the leaf blade.

Inflorescence architecture is the most prominent part of small-grain cereal plants, has a direct effect on yield, and was a selection target in breeding for yield improvement. Mutation of *HvLax-a* causes a pleiotropic phenotypic alteration in the barley inflorescence development, resulting in an elongated spike rachis conferring a more relaxed inflorescence, thinner grains exposed at spike maturity due to reduced marginal growth of the palea and lemma, homeotic conversion of lodicules into stamenoid structures and broadened base of the lemma awns (Jost *et al.*, 2016). In *B. distachyon*, the wild-type lodicules are generally wide, flat, and translucent organs while in $Bdlaxa^{CR}$, approximately 13% lodicules were homeotically transformed into stamenoid organs and 10% with additional stamens in the abaxial position where only lodicules should develop. This is a bit different from *HvLax-a*, in which, the florets did not exhibit supernumerary organs. Our results confirmed the previous study in $Bdlaxa^{TI}$ missense mutant alleles. Interestingly, there is no lodicule-to-stamen homeosis and/or additional stamens observed in the *Bdcul4Bdlaxa* double mutants.

Once again this suggests possible antagonist actions for *BdCUL4* and *BdLAXA* in flower organ formation. In Arabidopsis, BOP1/2-regulated expression of *AP1* leads to the down-regulation of *AGAMOUS-LIKE24*, a homolog of *AGAMOUS* (Xu *et al.*, 2010). Ectopic expression of *OsMADS3*, the rice ortholog of *AG* (Kyozuka & Shimamoto, 2002), also leads to the homeotic transformation of lodicules into stamens. Therefore, the conversion of lodicules into stamens in *Bdlaxa* could potentially be explained by a lack of *AG* down-regulation in lodicules. Notably, the stamens were dry in the early stage of development and resulted in sterility in the $Bdcul4^{Q127*}Bdlaxa^{CR}$ CRISPR double mutant. Together, these results suggest that *BdLAXA* is involved in floret patterning by repressing male sexual fate and controlling the number of stamens independently.

In barley, *HvCul4* loss-of-function does not affect spike or spikelet development (Tavakol *et al.*, 2015; Jost *et al.*, 2016). However, in *B. distachyon*, *BdCUL4* loss-of-function showed an exaggerated and continuous production of florets on the terminal and lateral spikelets resulting in longer spikelets than wild type (Magne *et al.*, 2020) suggesting that *BdCUL4* is involved in the control of spikelet determinacy. By contrast, the *Bdlaxa* mutants produce short spikelets with a reduced number of florets. The $Bdlaxa^{CR}$ mutants produced here have similar but stronger defects compared with the previously described $Bdlaxa^{TI}$ alleles suggesting that they were leaky mutants. In addition, the floret rachilla in $Bdlaxa^{CR}$ is bent and tends to grow perpendicularly to the abaxial/adaxial floret axis leading to a more compact, opened spikelet architecture with most of the florets being sterile. The spikelet architecture in $Bdcul4^{W203*}Bdlaxa^{T381}$ and $Bdcul4^{Q127*}Bdlaxa^{CR}$ double mutants are different. In $Bdcul4^{W203*}Bdlaxa^{T381}$, the spikelet architecture more closely resembled the *Bdcul4* spikelets, but a bit shorter, while the $Bdcul4^{Q127*}Bdlaxa^{CR}$ shows strong modifications and the spikelet are separated with a modified lemma, which looks like a thicker leaf structure. This double mutant is consequently sterile and cannot give seeds.

In grasses, *APETALA2*/*Ethylene Response Factor* transcription factors (*AP2/ERF* TFs) are important for spike architecture maintenance and control the number and the development of spikelets, as well as the floret meristem fate. Loss-of-function in this AP2/ERF TFs such as Zmbranched silkless1(*Zmbd1*; Chuck *et al.*, 2002), *Zmids1/sid1* (Chuck *et al.*, 2008), TaFRIZZY PANICLE (*TaFZP*; Dobrovolskaya *et al.*, 2015), *HvCompositum2* (Poursarebani *et al.*, 2015), *OsFRIZZY*

PANICLE/BRANCHED FLORETLESS1 (Komatsu *et al.*, 2003a), and *BdMORESPIKELETS1* (*BdMOS1*; Derbyshire & Byrne, 2013), trigger spikelet-to-branch homeosis and each branch looks like an entire spike. We investigated the expression pattern of some floral meristem regulator genes including two AP2/ERF TFs, *BdIDS1* and *BdSID1*, and also the *BdAP1*, and *BdKNAT6* in the different *Brachypodium* backgrounds. The expression level of the *BdAP1* and *BdKNAT6* was significantly decreased in all mutant lines compared with control as the *BdCUL4* expression pattern. The *BdIDS1* and *BdSID1* were significantly reduced in the $Bdlaxa^{CR}$ and moderately decreased in $Bdcul4^{W203*}Bdlaxa^{T381I}$ double mutant, suggesting that *IDS1* and *SID1* were controlled by *LAXA* and that *BdCUL4* and *BdLAXA* have an antagonistic role in floral meristem formation.

Seed shattering is an agronomically important trait. While easy shattering causes a reduction in yields when the seed is lost prior to harvest, non-shattering also affects those yields by hampering the process of harvesting (Ji *et al.*, 2006). In dicot plants, *NBCL* genes are involved in abscission zone formation and functioning (Hepworth *et al.*, 2005; McKim *et al.*, 2008; Wu *et al.*, 2012; Ichihashi *et al.*, 2014; Couzigou *et al.*, 2015; Frankowski *et al.*, 2015). In grasses, a role for the *NBCL* genes in seed shattering was not investigated yet but cultivated grasses were selected for a non-shattering phenotype. In contrast, *B. distachyon* has not been selected for a non-shattering phenotype and represents an ideal model to determine whether *NBCLs* genes participate in the abscission ability in grasses.

In the previous study, *Bdcul4* KO and *Bdlaxa* missense mutants did not show any defect in seed abscission zone establishment and functioning. In this study, *Bdlaxa* KO mutants and *Bdcul4laxa* double mutants also did not show any defect for seed shattering. Thus, our work suggests that *BdCUL4* and *BdLAXA* are not participating in seed abscission in *Brachypodium* and that the role of *NBCLs* genes in abscission is not conserved in grasses.

Lignin is a principal component of secondary cell walls and one of the major factors in determining the woodiness in higher plants (Rogers & Campbell, 2004). Arabidopsis plants that overexpress *BOP1/2* are late-flowering with short internodes containing excessive lignin. Several lignin biosynthetic genes are up-regulated in the stems of *BOP* overexpressing lines. These data reveal a promotive role for *BOP* genes in lignin production, a characteristic of secondary growth in plants (Khan *et al.*,

2012b, 2014; Khan, 2013). We examined the pattern of lignin deposition in stem cross-sections and the lignin content was measured in loss-of-function *Bdcul4* and *Bdlaxa* single and double mutant. Our results suggest that in the loss-of-function *Bdcul4* and *Bdlaxa* single mutants just a slight alteration in lignin content in whole stems is observed but the simultaneous inactivation of the two genes (double mutants) resulted in a significant decrease of the lignin content. The phloroglucinol-HCl staining revealed a profound impact on the interfascicular fiber cell wall lignification and a moderate to a minimal effect on the vascular bundle lignification in the double mutant. Furthermore, in *Bdcul4* and *Bdlaxa* mutant the expression level of *BdCAD1*, *BdCOMT4* and *BdSWAM1* were up-regulated while the CESAs were slightly decreased. In *Bdcul4Bdlaxa* double mutant, the *BdCAD1, BdCOMT4,* and *CESAs* transcripts were down-regulated while the *BdSWAM1* transcription was significantly up-regulated. These results suggest the BdCUL4 and BdLAXA function as potential activators for secondary wall biosynthesis.

CONCLUSION

In this work, we studied the roles of two grass *NBCL* genes, *BdCUL4* and *BdLAXA*, in the non-domesticated model plant *B. distachyon.* Based on our previous work, an analysis of the loss-of-function *Bdlaxa* and *Bdcul4Bdlaxa* mutants enabled us to unravel new roles for these two genes in grass development.

The CRISPR technology in *Brachypodium* was successful and we got KO mutants for *BdLAXA*. The phenotype of $Bdlaxa^{CR}$ CRISPR single mutants on tillering and spikelet was similar to observed in the TILLING missense mutants, which confirmed our previous results. Moreover, we found *BdLAXA* showing a positive effect on roots growth and seed yield. These effects on other agronomically relevant characters were not described for the barley ortholog. We also found that *BdCUL4* is an activator for ligule formation but represses the *BdLAXA* gene to inhibit the auricle formation. This results in the modification of the leaf angle and also the leaf architecture.

Seed abscission is another major character of interest in agriculture. Here we attempted to determine if *NBCL* genes play a role in grass abscission, as previously shown for dicots. In *B. distachyon, BdCUL4* and *BdLAXA*, either independently or together, were not essential for floret abscission, which suggests that these proteins do not participate in abscission processes in grasses.

The plant growth status is very important for the crop, it is the key factor to determine whether we can get seeds. Our results suggest that the *Bdcul4Bdlaxa* double mutants are dwarf and severely impact the seed formation and also the lignin content and secondary cell wall composition. Due to the absence of described double mutants for the barley orthologs, our work uncovers the new functions for *BdCUL4* and *BdLAXA.*

The discovery of new molecular actors involved in grass architecture, spike formation, and organ abscission may facilitate the domestication of new species and provide new tools for breeding strategies.

ACKNOWLEDGMENTS

The IPS2 benefits from the support of the LabEx Saclay Plant Sciences-SPS (ANR-10-LABX-0040-SPS).
CSC financing for S. Liu with 48 months, CNRS financing for Pascal.

Author contributions

P.R. and S.L. conceived the project. S.L. performed the CRISPR, the gene expression analysis, the mutant genotyping, the segregation analysis, and the histological analysis. K.M. performed the TILLING mutant isolation and the crossing for the double mutant. R.S. performed the lignin and cell wall content measurement. S.L. K.M. and P. R. wrote the article.

Thanks, Oumaya Bouchabké-Coussa for in vitro culture and transformation advice.
Thanks to the peoples who provided the vectors for the CRISPR.

MATERIALS AND METHODS

Plant material

The community standard diploid inbreed Bd21-3 was used for transformation and as a control in all experiments The TILLING mutant alleles used in this work (Supplementary Table 1) were described in Magne *et al*., (2020).

Growth conditions

After the removal of lemma and palea, *B. distachyon* wild type and mutant seeds were surfaces sterilized in a solution of sodium hypochlorite (half a pellet, 1.5g, per 1 l of sterile water; NOTILIA group, ref:156104) with 1 droplet of liquid soap for 10 min, shaking at room temperature. Surface sterilized seeds were washed three times with sterile water before placement on 7% Kalys Agar plates in water. Sealed plates were stratified for 7 days at 4 °C under darkness and then transferred to 19$^{\circ C}$ for 48 h under darkness for acclimatization. Seedlings were transferred in 1.5 l pots in a loam-sand-perlite mixture (2:1:1; v/v/v) or in a sand-perlite mixture (1/2, v/v) in a controlled growth chamber with a 20 h light/4 h dark cycle, 19/17 °C day-night temperature, relative humidity 60 % and photosynthetic photon flux density (200 µmol m^{-2} s^{-1} at 10 cm above the ground). Plants were watered three times per week.

Plasmid construction and transformation of Agrobacterium strains

Due to the absence of a specific binary vector that can accommodate the CRISPR-Cas9 system for Agrobacterium-mediated *Brachypodium* stable transformation, we used the Gateway^{TM} binary T-DNA vectors designed for rice transformation and that can co-express both CAS9 and guide RNA (Miao *et al.*, 2013). The guide RNAs were designed using the http://crispor.tefor.net/ web site. The guide RNAs were expressed from the pol III type promoter of U3 snRNA and the CAS9 coding sequence was express from the maize Ubiquitin (Ubi) promoter (Miao *et al.*, 2013). To inactivate the *BdLAXA* gene, we designed two guide RNA sequences from two exons of the *BdLAXA* gene. The two annealed oligos containing BsaI restriction sites were inserted cloned into the BsaI-digested pOssgRNA gateway plasmid. The bar genes with pOssgRNA were sequence confirmed and then combined into vector pH-Ubi-cas9-7. The verified constructs were transformed into *Agrobacterium tumefaciens* strain AGL1 via electroporation. Each construct was then

transformed into *Brachypodium* embryo-derived calli using *A. tumefaciens* followed by regeneration of T0-generation transgenic plants on hygromycin selection media.

Callus culture

Tissue culture was performed according to standard procedures as described (Bragg *et al.*, 2015). Embryos (<0.3 mm) were dissected out of sterilized seeds from Bd21-3 wild type and *Bdcul4*^{Q127*}mutant approximately 14 days after anthesis (Draper *et al.*, 2001) using fine forceps and a dissecting microscope in a laminar flow hood. The embryo was then placed with the scutellar surface in contact with the callus induction medium [CIM: 4.4g/l Murashige and Skoog (MS) minimal organics and Skoog medium including vitamins (Duchefa Biochemie, M0222.0050), 0.07% Solution MES (+BCP) and 0.0008% Solution BCP, 30 g/l sucrose, 0.6mg/l CuSO4, 2.5 mg/l 2,4-D, pH 5.7 and 0.2% Phytagel (Sigma P8169)]. Seal plates were incubated at 28 °C in the dark for 3-4 weeks. Calli were then transferred to a fresh callus induction medium and cultured for an additional 2 weeks. The embryogenic calli from the second subculture were grown for 1 additional week before being used for transformation.

Transformation of *B. distachyon*

The *Brachypodium* transformations were performed essentially as described (Christiansen *et al.*, 2005; Bragg *et al.*, 2015) with the following modifications. For the *Agrobacterium* and callus co-culture, the CIM based medium was supplemented with 60 mg/l acetosyringone and 0.1% pluronic (F-68 solution, Sigma-life science, CAS: 9003-11-6). The transformants for the Crispr-Cas9 *BdLAXA* knock out construct in Bd21-3 and *Bdcul4* backgrounds were selected on the CIM medium with 200 mg/L hygromycin (Sigma H3274-1g) and 250 mg/L Timentin (Duchefa T0190.0025). For regeneration, the medium was based on the selection medium, contained 0.2mg/l Kinetin (Sigma, K3378) and no 2,4 D (Sigma D7299-100G), and the sucrose was replaced by maltose. Plates were incubated in the light at 28 °C and calli started to turn green and shoots should appear in 2-4 weeks. Finally, shoots were transferred to rooting medium containing 2.5mg/l AIB (Indole-3-butyric acid, Sigma I5386) and 10g/l saccharose based on CIM but without 2,4 D.

***B. distachyon* genomic DNA extraction**

B. distachyon DNA of individual plants was isolated from young leaves using a phenol/chloroform procedure (Theologis *et al.*, 1985). DNA was precipitated using 3M cold sodium acetate: isopropanol (0.1:1) and washed by 70% ethanol. DNA samples were dried, resuspended in sterile water and RNase treated (Roche).

Genotyping of the transgenic plants and *Bdcul4Bdlaxa* mutants

The genotyping was performed by PCR using AccuPrime™ GC-Rich DNA Polymerase (Invitrogen) and goTaq DNA polymerase (Promega) with specific primers (Supporting Information Tables S2a). The AccuPrime™ GC-Rich DNA Polymerase was used to amplify the GC rich region of the first exon. With other enzymes, the PCR products were mixtures of deletions and impossible to sequence. PCR products were sequenced by Sanger (http://www.eurofinsgenomics.eu) and analyzed with 'A plasmid Editor 2.0.50' software. Information concerning primers used for mutants genotyping is given in Supporting Information Table S2a. To confirm that hygromycin selected *B. distachyon* plants were transgenic we also did the PCR with the oligos designed from the selection marker and CAS9 genes of the vector. DNA was separated by electrophoresis and visualized on an ethidium bromide-stained agarose gel. Four independent regeneration events were generated and tested for the presence of $Bdlaxa^{CR}$ mutant phenotypes, and three events with the most similar transgene expression profiles were selected for functional characterization in $Bdcul4^{TI}$ $Bdlaxa^{CR}$ mutants.

qRT-PCR gene expression analysis

The transcripts accumulations of the genes were assessed in different organs of 40 days old wild type *B. distachyon* cv. Bd21-3 and different genotype of mutants. These genes include: *BdCUL4* (*Bradi*2g60710.1); *BdLAXA* (*Bradi*4g43150.1); the marker genes relate to *Brachypodium* development, such as KNOTTED1-LIKE HOMEOBOX GENE 6 (*BdKNAT6*: *Bradi2g11540*), Indeterminate spikelet 1 (*BdIDS1*: *Bradi1g03880*), Sister of indeterminate spikelet 1 (*BdSID1*: *Bradi1g53650*), APETALA 1 (*BdAP1*: *Bradi1g08340*); and the marker genes associated to cellulose production: *CELLULOSE SYNTHASE A* (*BdCESA4*, *Bradi4g28350*; *BdCESA7*, *Bradi2g30540*; *BdCESA8*, *Bradi2g49912*), to the lignin content, such as cinnamyl alcohol dehydrogenase1 (*BdCAD1*, *Bradi3g17920*) and caffeic acid O-methyltransferase 4 (*COMT4*, *Bradi3g16530*); the regulator of secondary cell wall

thickening in *B. distachyon*: *SECONDARY WALL ASSOCIATED MYB1* (*SWAM1*, *Bradi2g47590*). Total RNA was isolated using Trizol© reagent, (http://www.invitrogen.com) from three independent collects of leaves, nodes, internodes, stems, and young spikelets. Young spikelets were collected and flash-frozen when the inflorescence was just visible from the flag leaf of the tallest stem with equivalent development. Transcript abundance was examined by qRT-PCR with specific primers. RNA samples were treated with the TURBO DNA-free™ Kit (Ambion) according to the manufacturer's recommendations. First-strand cDNA was synthesized from 1 µg of RNA template using Superscript II reverse transcriptase with oligo (dT) primers (Invitrogen) in the presence of Ribolock RNase Inhibitor (Thermo scientific). Samples were diluted ten-fold with RNase free water. Real-time RT-PCR reactions were performed in triplicate with 1 µL of diluted cDNA in each reaction with the LightCycler FastStart DNA Master SYBR Green I kit (Ref. 04887352001, ROCHE) in 10 µL reaction volumes. The reactions were conducted in a LightCycler®96 (Roche) using the following conditions:1pre-incubation cycle (95°C, 5 min), followed by 42 cycles of denaturation: 95°C for 15s, hybridization: 60°C for 15s, and elongation: 72 °C for 15s.1 melting curve cycle [(denaturation: 95 °C, 10 s), (hybridization: 60 °C, 1 min), (denaturation: 97°C, 1s)], 1 cooling cycle (37°C, 30s). Values were normalized against two housekeeping genes, *BdPOLYUBIQUITIN 4* (Bd3g04730.3) and *BdUBC18* (UBIQUITIN-CONJUGATING ENZYME 18, *Bd4g00660.1*) served as reference transcripts. The final threshold cycle (Ct), efficiency, and initial fluorescence (R0) for every reaction were calculated with the Miner algorithm (Zhao & Fernald, 2005). Relative expression levels were obtained from the ratio between R0 of the reference gene and R0 of the target gene. Information concerning primers used for qRT-PCR gene expression analysis is given in Supporting Information Supplementary Table 1.

Histochemical staining of lignin

Sections were stained with 1% phloroglucinol for 2 minutes followed by a wash in 50% HCl and were mounted onto microscope slides for observation. All the histochemical staining was performed on sections cut in the middle of the second internode from the base of developmentally equivalent transgenic and control plants. Samples were hand-sectioned or embedded in 4% agarose before being transversely sectioned at a thickness of 70 µm using a vibratome (Leica VT1200S, Leica). Total

lignin content and localization in the stem were visualized by Wiesner staining (Phloroglucinol-HCl) (Wiesner & Von Wiesner, 1878; Pradhan Mitra & Loqué, 2014). All sections were observed under a Zeiss Apotome II microscope system with automatic exposure times.

Lignin content measurement

All main stems of each plant were collected and ground after removing spikelets and leaves. Ground samples were sequentially extracted at 60 °C with 50 mL of ethanol, water, and ethanol. At each step, the samples were vortexed. These steps were repeated twice before the sample drying. The extracted and dried samples, referred to as extract-free samples, were used for lignin analyses (Le Bris *et al.*, 2019). Lignin content was measured by the Klason method and the acetyl bromide method according to (Dence, 1992).

Monosaccharide Composition and Linkage Analysis of Polysaccharides

Neutral monosaccharide composition was determined on 5 mg of dried alcohol-insoluble material after hydrolysis in 2.5 M trifluoroacetic acid for 1.5 h at 100°C as described (Harholt *et al.*, 2006). To determine the cellulose content, the residual pellet obtained after the monosaccharide analysis was rinsed twice with 10 volumes of water and then hydrolyzed with H_2SO_4 as described (Updegraff, 1969). The released Glc was diluted 500-fold and then quantified using high-performance anion-exchange chromatography-pulsed-amperometric detection as described by Harholt *et al.* (2006).

Imaging, light microscopy and sample preparation

Pictures of whole organs were acquired using a ZESS stemi305 stereomicroscope. Sample sections embedded in Technovit resins were treated essentially as described in Van De Velde *et al.* (2006). In brief, fixed samples were infiltrated 15 min under vacuum (≈ 500 mm of Hg) in sodium cacodylate buffer (0.05 M, pH: 7), 1% glutaraldehyde and 4% formaldehyde and incubate at 4 °C overnight. Once dehydrated by successive ethyl-alcohol bathes, samples undergo three successive Technovit stock solutions (3:1, v/v), (1:1, v/v) and (1:3, v/v) bathes and three 100% Technovit stock solution bathes at 4°C under agitation. Samples were included in Technovit resin thanks to a Teflon Histoform S embedding mould (Heraeus Kulzer). Technovit sections were carried out using a microtome RM 2165

(LEICA) and tungsten disposable blade (TC-65, LEICA), 8 µm thickness sections were stained 10 min by immersion in toluidine blue (0.02 %) and observed with an Apotome II microscope (Zeiss) and acquired using ZEN (blue edition) software.

Supplementary Table 1. Primers used for mutant genotyping.

(a)

Genes	Gene ID	Familly	Forward primer (5'-3')	Reverse primer (5'-3')	Amplicon length
BdCUL4	*Bd*2g60710.1	*Bd4982*	BdCUL4Ex1_F1 TTCCCTACACGACGCTCTTCCGATCTTAGGAG GTGCCAGATTAAGG	BdCUL4Ex1_R3 AGTTCAGACGTGTGCTCTTCCGATCTTTAC CTGGGTGAGGAGAGCG	602 bp
		Bd7965	BdCUL4Ex2.1_F1 TTCCCTACACGACGCTCTTCCGATCTTCTTGA TCTGTCTGGCATGC	BdCUL4Ex2.1_R1 AGTTCAGACGTGTGCTCTTCCGATCTCGG CAGGCCCTGCCGGGTGG	591 bp
BdLAXA	*Bd*4g43150.1	guides RNA (sgRNA)EX1	GGCTGTGTTGGGCCAGTTGAGGG	CCCTCAACTGGCCCAACACAGCC	23 bp
		guides RNA (sgRNA)EX2	GCCCGCACGCGAGTTCACGTCGG	CCGACGTGAACTCGCGTGCGGGC	23 bp
		gRNAEX1	BdLAXA_Ex1_L GTGTCAAGCGCGAGATCAAC	BdLAXA_Ex1_R GTTGATCTCGCGCTTGACAC	330 bp
		gRNAEX2	BdLAXA_Ex2_L CTCCACCATCATCCCTCGTG	BdLAXA_Ex2_R CACAGCTACCTCCCCATGAC	498bp
		Bd3615	BdLAXA_Ex2.2_F1 TTCCCTACACGACGCTCTTCCGATCTCCACTG CAACCGGGACGTTG	BdLAXA_Ex2.2_R1 AGTTCAGACGTGTGCTCTTCCGATCTACGA CGACCAGTCGATATCA	625 bp

Underlined sequences represent 5' 26 bp illumina adaptators.

(b)

Locus	distribution	wild type	heterozygous	homozygous	ratio (wt:hetero:homo)
BdCUL4 Bd7965 *BdLAXA Bd3615*	theoric	68,5	137	68,25	1:2:1
	observed	67(21+46)	144(79+65)	63(37+26)	0.5:2.3:1.3
	phenotypes	67 wild-type		6 double mutant	

number of F1 lines: 1; number of F2 plants: 137; df: 1; pvalue: 0.05; X^2: 4.5 < critical X^2: 5.99

Supplementary Table 2. Primers used for qRT-PCR gene expression analysis.

Genes	Gene ID	Forward primer (5'-3')	Reverse primer (5'-3')	Origins
BdPOLYUBIQUITIN 4	*Bd*3g04730.3	BdUBQ4_D TGACACCATCGACAACGTGA	BdUBQ4_R GAGGGTGGACTCCTTCTGGA	Zhu *et al.*, 2015
BdUBIQUITIN-CONJUGATING ENZYME E2 18	*Bd*4g00660.1	BdUBC18_D GGTCATTTTCCTCAACCCGG	BdUBC18_R GCGGCAGTTCCTAACATAGC	Hong *et al.*, 2008
BdUNICULME4	*Bd*2g60710.1	BdCUL4_D ACAATAGCAACAATCCTGCG-	BdCUL4_R CAAGTTCAGATACACCATCC	Magne *et al.*, 2020
BdLAXATUM-A	*Bd*4g43150.1	BdLAXA_D GGGGAGGAATAAAGCCAGCA	BdLAXA_R TCATCAGCACCGTGGAATGG	Magne *et al.*, 2020
BdSECONDARY WALL ASSOCIATED MYB1	*Bd*2g47590.1	BdSWAM1_D AGGAAACAGGTGGTCGCAGATTG	BdSWAM1_R GCTTCTTCTTGAGGCAGCTGTTCC	Handakumbura *et al.*, 2018
BdCINNAMYL ALCOHOL DEHYDROGENASE 1	*Bd*3g06480.1	BdCAD1_D AGGATAGAATGGGCAGCATCGC	BdCAD1_R ATCTTCAGGGCCTGTCTTCCTGAG	d'Yvoire *et al.*, 2013
BdCAFFEIC ACID O-METHYLTRANSFERASE4	*Bd*3g16530.1	BdCOMT4_D TGGAGAGCTGGTACTACCTGAAG	BdCOMT4_R CGACATCCCGTATGCCTTGTTG	Trabucco *et al.*, 2013
BdCELLULOSE SYNTHASE A4	*Bd*3g28350.1	BdCESA4_D GCGTTTCGCATACACCAACACC	BdCESA4_R ACTCGCTAGGTTGTTCAGTGTGG	Handakumbura *et al.*, 2018
BdCELLULOSE SYNTHASE A7	*Bd*4g30540.1	BdCESA7_D GCGATTCGCCTACATCAACACC	BdCESA7_R GGCTGGCAAATGTGCTAATCGG	Handakumbura *et al.*, 2018
BdCELLULOSE SYNTHASE A8	*Bd*2g49912,1	BdCESA8_D CAAAGCACAAGTTCCGCCTGTG	BdCESA8_R TGGCTCGTATGCATCTGTCAAATC	Handakumbura *et al.*, 2018
BdKNOTTED1-LIKE HOMEOBOX GENE 6	*Bd*2g11540,1	BdKNOT6_D TCTCGACCCGAAGCAGATCAAC	BdKNOT6_R TATCGAAGTAGAGCGTCGTCCC	This study
BdINDETERMINATE SPIKELET1	*Bd*1g03880.1	BdIDS1_D AACCAAACGCTCACGACTCC	BdIDS1_R ACTGCTGTGCCATGCTGATG	This study
BdAPETALA 1	*Bd*1g08340,1	BdAP1_D GCTGAAGCGGATCGAGAACAAG	BdAP1_R TGGAGAAGATGATGAGCGCGAC	This study
BdSISTER OF INDETERMINATE SPIKELET1	*Bd*1g53650.1	BdSID1_D GCTGTTCGCTTCAATGGAAGGG	BdSID1_R AGCCAGTCAGGATGTCATCACC	This study

CHAPTER IV.

Characterization of potential *MtNODULEROOT1* and *MtNODULEROOT2* interacting partners participating in nodule and aerial organ development

Characterization of potential *MtNODULEROOT1* and *MtNODULEROOT2* interacting partners participating in nodule and aerial organ development

Shengbin Liu[1,2] , Kevin Magne[1,2], Jiangqi Wen[3] Kirankumar S. Mysore[3] and Pascal Ratet[1,2]

[1] Institute of Plant Sciences Paris-Saclay IPS2, CNRS, INRA, University Paris-Sud, University Evry, University Paris-Saclay, Bâtiment 630, 91405 Orsay, France.
[2] Institute of Plant Sciences Paris-Saclay IPS2, Paris Diderot, Sorbonne Paris-Cité, Bâtiment 630, 91405, Orsay, France.
[3] Noble Research Institute, 2510 Sam Noble Parkway, Ardmore OK73401, USA.

Author contributions

SL, PR, KM, conceived the research plans. SL designed the experiments, performed the research experiments and analyzed the data. SL and PR wrote the article.

Abstract

NBCL genes encode plant-specific co-transcriptional factors containing BTB/POZ domains and are key regulators for legume nodule development. They also participate in different aspects of plant development. The ALOG (*Arabidopsis LSH1* and *Oryza G1*) proteins represent plant-specific proteins, which contain a DNA-binding domain and a weak transcriptional activity. This transcriptional activity is enhanced by interaction with *BLADE-ON-PETIOLE* (*BOP*) transcriptional cofactors. Here, we identify a novel function for a *Medicago truncatula* ALOG family member, *MtALOG1*, involved in negatively regulating nodulation. *MtALOG1* is highly expressed in nodules and stems and its expression pattern in nodule is similar to the nodule identity markers *MtNOOT2* and *MtNIN*. The *Mtalog1* mutant had significantly more multi-lobed nodules compared to wild type. In addition to the nodule phenotype, *Mtalog1* also shows an increased branching and flower number. To further investigate the role of the *MtALOG1* gene and its genetic relationship with the *MtNOOT* genes in nodule formation and in the aerial development, the *Mtnoot1alog1* and *Mtnoot2alog1* double mutants were investigated and shows that in *Mtnoot1alog1,* the number of multi-lobed nodules and the shoots branching was increased. In addition, using a *KNOX3::GUS* fusion, we studied the class II KNOX TFs (*MtKNOX3*) expression in the *noot* mutant context. Similarly to *MtKNOX9* in *Mtnoot1* and *Mtnoot1noot2* nodules, the *MtKNOX3* expression pattern also changed in *Mtnoot1* and *Mtnoot1noot2* nodules and highlights the role of the class II KNOX TFs in nodule development.

Key words: *NBCL*, ALOG, nodule, KNOX, DUF640, interacting partner.

INTRODUCTION

Uncharacterized proteins with Domain of Unknown Function 640 (DUF640) are found in plant proteins playing various roles in stress responses and plant development (Yoshida *et al.*, 2009, 2013; Takeda *et al.*, 2011; Iyer & Aravind, 2012; MacAlister *et al.*, 2012). The *ALOG* family of proteins is present in multiple copies in land plants. Members of the plant *ALOG* family are characterized by a highly conserved *ALOG* domain region (DUF640), whereas the N- and C-termini are highly diverse in monocots and eudicots (Dong *et al.*, 2014; Peng *et al.*, 2017). A nuclear localization signal, KKRK, was identified in the C-terminal flanking region after the *ALOG* domain (Nan *et al.*, 2018). There are ten *ALOG* genes named *LSH1* to *LSH10* present in *Arabidopsis* and rice (Zhao *et al.*, 2004; Yoshida *et al.*, 2009; Cho & Zambryski, 2011). ALOG proteins are absent in green algae but exist in all land plants analyzed as well as in some Charophycean algae the closest relatives of land plants. ALOG proteins emerged before the evolution of land plants and exhibit functional conservation and diversification during the evolution of land plants (Naramoto *et al.*, 2020). From genome-wide identification and characterization, the *ALOG* domain genes were first identified from 7 species, including four monocotyledons (*Oryza sativa*, *Zea mays*, *Sorghum bicolor*, and *Brachypodium distachyon*), two dicotyledons (*Arabidopsis thaliana*, *Populus trichocarpa*), and moss (*Physcomitrella patens*) (Li *et al.*, 2019). In many instances, duplications appeared to have occurred very late, such as within Brassicaceae or legumes. Within dicots, only 5 lineages namely, *LSH1/2*, *LSH3*, *LSH4*, *LSH7/8*, and *LSH10* can be confidently recognized as being present in the common ancestor of the legumes and Brassicales, corresponding to the rosid and malvid clades of eudicots.

The *Arabidopsis LIGHT-DEPENDENT SHORT HYPOCOTYLS1* (*LSH1*) and *Oryza G1* (*ALOG*) were the first identified plant-specific gene family members that encode proteins with a previously uncharacterized domain (corresponding to DUF640 in Pfam; (Zhao *et al.*, 2004; Yoshida *et al.*, 2009). *LSH1* is functionally dependent on phytochrome to mediate light regulation of seedling development in Arabidopsis (Zhao *et al.*, 2004). In rice, the long sterile lemma1 (*g1*) mutant plants show empty glumes that transform into lemma-like organs, suggesting that *G1* is involved in the repression of lemma identity to specify the sterile lemma (Yoshida *et al.*, 2009; Hong *et al.*, 2010; Yoshida & Nagato, 2011; Liu *et al.*, 2016). Both *LSH1* and *G1* proteins

localize to the nucleus, and *G1* showed transactivation activity, indicating that *ALOG* proteins are involved in transcriptional regulation (Zhao *et al.*, 2004; Yoshida *et al.*, 2009).

An *ALOG* domain is also found in the N-terminal DNA-binding domains of integrases encoded by a distinct type of *DIRS1-like LTR* (*XerC/D-like*, protelomerase, topoisomerase-IA, and *Flp*) retrotransposon found in several eukaryotes (Poulter & Goodwin, 2005; Iyer & Aravind, 2012). *ALOG* domains help to establish organ identity and differentiation by binding specific DNA sequences and act as transcription factors or recruiters of repressive chromatin. They are also found in certain plant defense proteins, where they are predicted to function as DNA sensors (Iyer & Aravind, 2012).

The role of ALOG proteins in meristem maintenance is conserved between monocots and dicots. In rice (*Oryza sativa*) and tomato (*Solanum lycopersicum*), *OsTAWAWA1* (*OsTAW1*) and *TERMINATING FLOWER* (*SlTMF*, the tomato *TAW1* homolog), members of the *ALOG* gene family repress the maturation of meristems during reproductive growth (Kyozuka *et al.*, 1998; Pnueli *et al.*, 2001; Marchler-Bauer *et al.*, 2013). Interestingly, *OsTAW1*, *SlTMF*, and *AtLSH3* are expressed in lateral organ boundaries but not in the apical meristems (Bomblies & Doebley, 2006; Carmona *et al.*, 2007; Marchler-Bauer *et al.*, 2013), suggesting that although the *ALOG* genes act cell-autonomously during the development of lateral organs, they act non-cell autonomously to control meristem development. *Marchantia polymorpha LATERAL ORGAN SUPPRESSOR 1* (*MpLOS1*), a member of the *ALOG* gene family, plays a role in integrating meristem activity by repressing lateral organ differentiation and is thus required for meristem maintenance in *M. polymorpha* (Naramoto *et al.*, 2020).

The establishment of organ boundaries is a fundamental process for proper morphogenesis in multicellular organisms. In plants, the shoot apical meristem (SAM) repetitively forms organ primordia from its periphery, and boundary cells are generated as narrow bands between them to separate their cellular fates. The boundary cells also give rise to the axils, which often act as sites for new shoot meristem initiation (Aida & Tasaka, 2006a,b; Rast *et al.*, 2008; Takeda & Aida, 2011). The genes *CUP-SHAPED COTYLEDON1* (*CUC1*) and *CUC2*, which encode plant-specific NAC transcription factors, play central roles in the establishment of the shoot

organ boundaries in *Arabidopsis thaliana*. In shoot organ boundary cells, *CUC1* protein activates expression of *LIGHT-DEPENDENT SHORT HYPOCOTYLS 3* (*LSH3*) and *LSH4*, also known as *ORGAN BOUNDARY1* (*OBO1*) and *OBO4* (Takeda *et al.*, 2011). Expression of *LSH4* and *LSH3* is detected in the boundary of the SAM and lateral organs, such as cotyledons, leaves and floral organs (Cho & Zambryski, 2011; Takeda *et al.*, 2011), and requires the activity of *CUC1* and *CUC2*, which is similar to the expression pattern of *TMF* in tomato (MacAlister *et al.*, 2012). Constitutive expression of *LSH4* and *LSH3* in the SAM and organ primordia resulted in severe developmental defects, indicating that their normal expression is strictly restricted to boundary cells and excluded from the SAM and organ primordia. Dominant mutants of the paralogous *LSH3* and *LSH4* genes suppress differentiation of leaves and disrupt the normal boundary regions between different floral organs (Zhao *et al.*, 2004; Takeda *et al.*, 2011). However, knocking out *LSH3* and *LSH4* does not result in an obvious phenotype (Takeda *et al.*, 2011). This indicates that the functions of the *LSH* genes are masked by other redundant factors.

The transition to flowering is a major determinant of plant architecture, and variation in the timing of flowering can have profound effects on inflorescence architecture, flower production and yield. Variation in plant reproductive success and agricultural productivity is largely determined by differences in shoot architecture. Reproductive shoots known as inflorescences show extensive diversity in both branch and flower number. Vegetative shoots produce inflorescences when endogenous and environmental signals coincide to induce groups of pluripotent cells called SAMs to transition to flower-producing inflorescence meristems (Kobayashi & Weigel, 2007; Turck *et al.*, 2008).

Flowering plants have evolved a remarkable diversity of inflorescence branching patterns, which is largely governed by developmental decisions that take place in inflorescence meristems and their derived meristems between maintenance of indeterminacy and commitment to the floral fate. Regulation of inflorescence architecture is mediated by flowering time genes, ALOG family genes, and the interaction between the auxin pathway and floral meristem regulators. Previous studies in Arabidopsis have suggested that an antagonistic interaction between the shoot identity gene *TERMINAL FLOWER 1* (*TFL1*) and floral meristem identity genes, such as *LEAFY* (*LFY*) and *APETALA1* (*AP1*), regulates the inflorescence

branching pattern (Bradley *et al.*, 1997; Liljegren *et al.*, 1999; Ratcliffe *et al.*, 1999). Molecular genetic evidence suggests that *AP1* and *LFY* are two upstream repressors of *TFL1* in floral meristems (Liljegren *et al.*, 1999; Ratcliffe *et al.*, 1999; Ferrándiz *et al.*, 2000; Parcy *et al.*, 2002). A set of MADS-box transcription factors, namely *SUPPRESSOR OF OVEREXPRESSION OF CONSTANS 1* (*SOC1*), *SHORT VEGETATIVE PHASE* (*SVP*), *AGAMOUS-LIKE 24* (*AGL24*), and *SEPALLATA 4* (SEP4), act redundantly and directly to suppress *TFL1* in emerging floral meristems (Liu *et al.*, 2013) and they are indispensable for the well-known function of AP1 and *LFY* in repressing *TFL1*. Thus, these MADS-box genes have redundant roles in regulating *TFL1* expression in different genetic backgrounds.

SVP, *SOC1*, and *AGL24* have crucial and persistent roles in mediating several successive developmental programs during the floral transition, including flowering time control, floral meristem specification, and floral organ patterning, all of which contribute to different extents to shaping the inflorescence architecture. In rice, enhanced panicle branching with an increased number of higher-order branches is observed (Liu *et al.*, 2013) when the rice orthologs of *SOC1* and *SVP/AGL24* are downregulated in the panicle phytomer2-1 mutant, in which a rice ortholog of SEP4 is knocked out (Kobayashi *et al.*, 2010). These observations suggest that the interaction of flowering time genes with *TFL1-like* genes could be a conserved mechanism for regulating inflorescence architecture in dicots and monocots.

Members of the *ALOG* gene family are important regulators that affect inflorescence architecture by mediating the phase transition of IMs due to their roles in the maintenance of undifferentiated cells, such as *LSH1*, *TMF*, *TH1*/*BSG1*, and *TAW1* (Yoshida *et al.*, 2009, 2013; Kyozuka *et al.*, 2014; Teo *et al.*, 2014; Peng *et al.*, 2017). *TAWAWA1* (*TAW1*) encodes an *ALOG* family protein in rice and regulates inflorescence architecture, partly through promoting the expression of *SVP*-like genes (Yoshida *et al.*, 2013). Tomato *TMF*, like rice *TAW1*, affects inflorescence organization (MacAlister *et al.*, 2012), possibly by preventing the early expression of orthologous genes of *Arabidopsis UNUSUAL FLORAL ORGANS* (*UFO*), *LFY*, *APETALLA* 1 (*AP1*) and *SEP*, which contribute to promoting floral fate (Teo *et al.*, 2014). Loss of *TMF*, one of 10 *ALOG* genes in tomato, causes much earlier flowering and conversion of primary inflorescences into single flowers (MacAlister *et al.*, 2012). In addition, tomato orthologs of *AP1* and *SEP* genes are upregulated in *tmf* mutant.

TRIANGULAR HULL1/BEAK-SHAPED GRAIN1 (*TH1/BSG1*), determines grain shape and size by regulating cell division and extension of the lemma and palea (Li *et al.*, 2012; Yan *et al.*, 2013). *TH1/BSG1* functions as a transcriptional repressor regulating lemma and palea development in rice (Yan *et al.*, 2013; Ma *et al.*, 2013; Ren *et al.*, 2016; Peng *et al.*, 2017).

Previous studies in inflorescence development in tomato have shown that *TMF* (*LSH6*), which affect vegetative/reproductive transition (Chakrabarti *et al.*, 2013), interacts with three *Solanum lycopersicum BLADE-ON-PETIOLE* genes (*SlBOPs*) and *BOPa* (MacAlister *et al.*, 2012; Xu *et al.*, 2016). *LSH3b* interacts with *BOPa* and also binds to the *PETROSELINUM* (*PTS*) promoter (Kemmeren *et al.*, 2002; Ichihashi *et al.*, 2014), suggesting that *BOPa* can physically interact with *LSH*, and the complex may directly regulate *PTS* expression. Because *PTS* regulates *KNOX* at the protein level (Kimura *et al.*, 2008), *BOPa* might affect *KNOX* targets via regulation of *PTS* expression (Ichihashi *et al.*, 2014). This indicates the potential role of *LSH* genes in regulating both leaf broadness and complexity in this species.

M. truncatula MtNODULE-ROOT 1/2 (*MtNOOT1/2*) are orthologs of *A. thaliana AtBOP1/2* and were described as key regulators for nodule meristem and also participate in aerial part development (Couzigou *et al.*, 2012; Magne *et al.*, 2018a). Thus, the *MtNOOT1/2* may interact with ALOG proteins, but their role in legume is poorly studied with only one recent report showing that one *ALOG* gene has a role in regulating nodulation in *Lotus japonicus* (Lei *et al.*, 2019).

KNOX TFs are grouped into two classes, class I *KNOX* (*KNOXI*) and class II *KNOX* (*KNOXII*) (Hay & Tsiantis, 2010), and encode homeodomain-containing transcription factors. The class I *KNOX TFs* are required for the initiation and the patterning of organs and the meristem establishment and maintenance (Hake *et al.*, 2004; Hay & Tsiantis, 2010). The *KNOXII* were further divided into two subclasses, *KNAT7-like* and *KNAT3/4/5-like* (Mukherjee et al., 2009) and the roles of class II KNOX TFs are less understood but they have been suggested to repress the gametophytic (haploid) developmental program during moss sporophyte (diploid) development. Recently, it was shown that in *Arabidopsis*, *KNAT3/4/5* genes act redundantly to promote differentiation of aerial organs antagonistically to the action of *KNOXI* genes (Furumizu *et al.*, 2015).

In *M. truncatula*, three class II genes (MtKNOX3, MtKNOX5 and MtKNOX9) are constitutively expressed in the root stele including pericycle and endodermis (Di Giacomo *et al.*, 2008, 2016) and up-regulated in nodules (Azarakhsh *et al.*, 2015). Class II KNOX TFs therefore regulate legume nodule development, and as a potential regulator was investigated in the *Mtnoot* context.

Based on the *ALOG/BOP-like* interaction described for plant development, the present study aims to investigate if a similar interaction exists in *M. truncatula* between MtALOG and NOOT to promote nodule development and/or to maintain the symbiotic nodule identity. Here we report the identification of the *AtLSH4* (*ALOG*) closest orthologous gene in *M. truncatula*, which we called *MtALOG1*, as a nodule induced gene. In addition, we characterized the corresponding *Mtalog1 Tnt1* insertional mutant showing increased flower number, shoot branches, and also more nodules. We constructed the *Mtnoot1alog1* and *Mtnoot2alog1* double mutants and initiated their phenotypic and molecular characterization. We suggest that *MtALOG1* might be a potential interacting partner of *MtNOOT1* and *MtNOOT2*.

RESULTS

Identification of the *M. truncatula ALOG* gene

Phylogenetic analysis of the ten *A. thaliana LSH* (*ALOG*) TFs and the 10 *M. truncatula LSH-LIKE* genes revealed relative conservation across the two species. In *M. truncatula*, three members of the class I *MtALOG* family group, includes the two closest members to *AtOBO1/LSH3*, and one close to *AtLSH4* (At3g2290). This later was used in this study and called *MtALOG1* (Medtr1g075990; Fig. 1a). In addition, two members group with class II containing *AtLSH1/2* and two closed to AtLSH5/6 group in class III. In group IV, one is close to *AtLSH7/8*, one is close to *AtLSH9* and one is close to *AtLSH10* (Fig. 1a).

In agreement with the transcriptomic data of Roux et al., 2014 (data not shown), qRT- PCR gene expression analysis of the 10 *M. truncatula ALOG* genes showed that four are expressed in *M. truncatula* R-108 mature nodules (Fig. 1b), four are expressed in the root (Fig. 1c) and six are detected in the aerial part (Fig. 1d). Interestingly, just three genes (MtALOG1, 3, and 5) are expressed in all the tested tissue and their expression level presents a range variation between the tested organs. *MtALOG1* and *MtALOG3* were highly expressed in nodules, internodes, nodes, and

shoot apical meristems but the expression level was very low in leaf and root (Fig. 1b-d). The *MtALOG2* gene is expressed in nodules and aerial parts, but the expression level is very low in all the tested tissues (Fig. 1b, d). *MtALOG4* is expressed in internodes, nodes, and shoot apical meristems (Fig. 1d). *MtALOG5* is mainly expressed in roots, internode, nodes, and shoot apical meristems while its expression is very low in leaves and nodules. *MtALOG8* shows a similar expression pattern with *MtALOG5* but is not expressed in nodules. In contrast, the expression of the *MtALOG6*, *7*, *9*, and *10* genes were not detected in all the tested tissues (Fig. 1b-d). The variation of expression of the different ALOG members in *M. truncatula* indicates that they are tissue-specific and may have different functions in these tissues. The common character of all these *MtALOG* members was that they are not express in leaf or their expression level was extremely low. In addition, most of the *ALOG* genes in *M. truncatula* are highly expressed in the stem, such as in internodes and nodes (Fig. 1d). This expression analysis revealed that *MtALOG1* is well expressed in nodules and stems relative to the other *MtALOG* genes, except *MtALOG3*, which shows a higher expression level in nodule and stem (Fig. 1b, d).

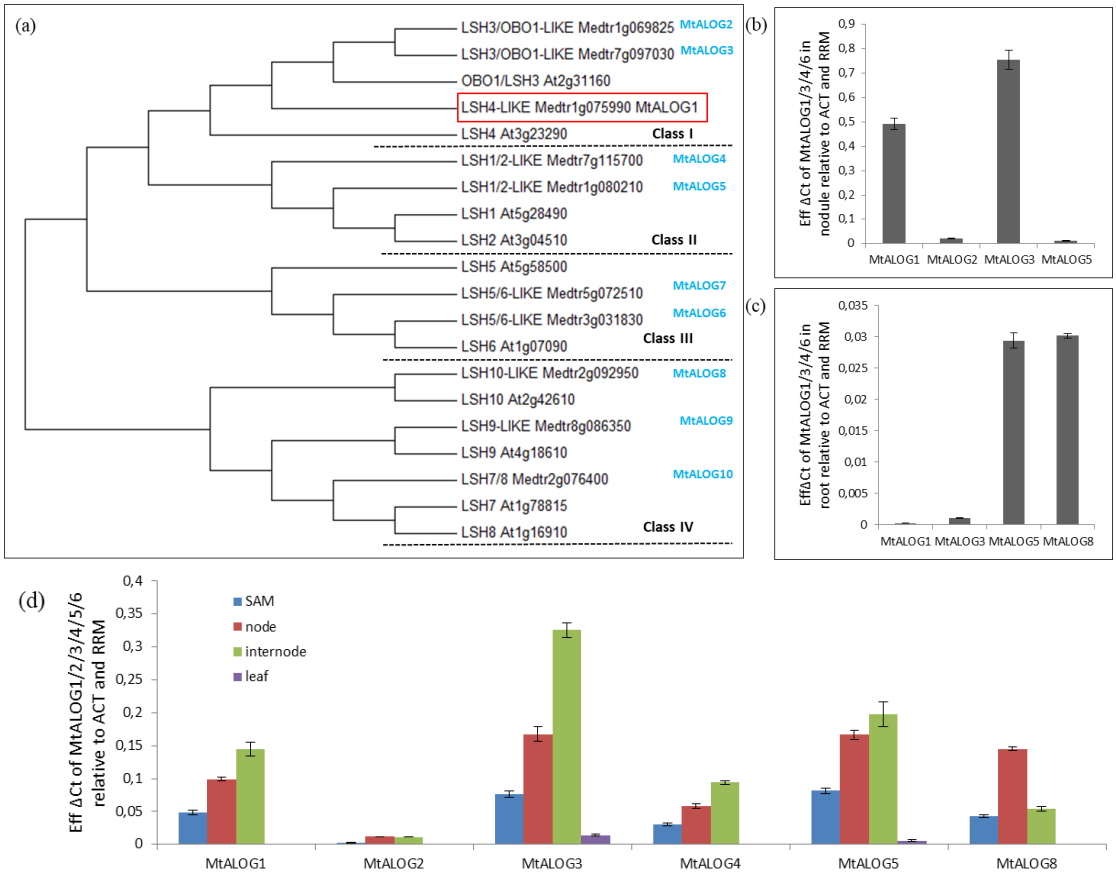

Figure 1. Phylogenetic tree of *M. truncatula* and *A. thaliana ALOG* homologs and gene expression analysis of 10 *M. truncatula LSH-like* (*MtALOG*) genes in R-108 nodules (b) root (c) and aerial part (d).

a. Neighbor-joining phylogenetic tree of full-length *ALOG* from *A. thaliana* (*At*) and *M. truncatula* (*Mt*). *A. thaliana* and *M. truncatula ALOG* group into four classes (I-IV).The MtALOG1 protein is highlighted in red. The phylogenetic tree was built using the neighbor-joining method with the MEGA7 program (Kumar *et al.*, 2016). **b**. qRT-PCR gene expression of 10 *M. truncatula ALOG* genes, *MtALOG1-10* were analyzed in R-108 wild-type nodules at 35 dpi with *S. medicae WSM419* strain; also in the root, leaf, internode, node and shoot apical meristems at 29 days after sowing. The 10 *M. truncatula ALOG* gene expressions were variation in different tissue. Genes with undetectable expression are not shown. Gene expression values were normalized against the constitutively expressed *MtRRM* and *MtACT* reference genes. Results represent means ± SE of three biological repeats and three technical replicates.

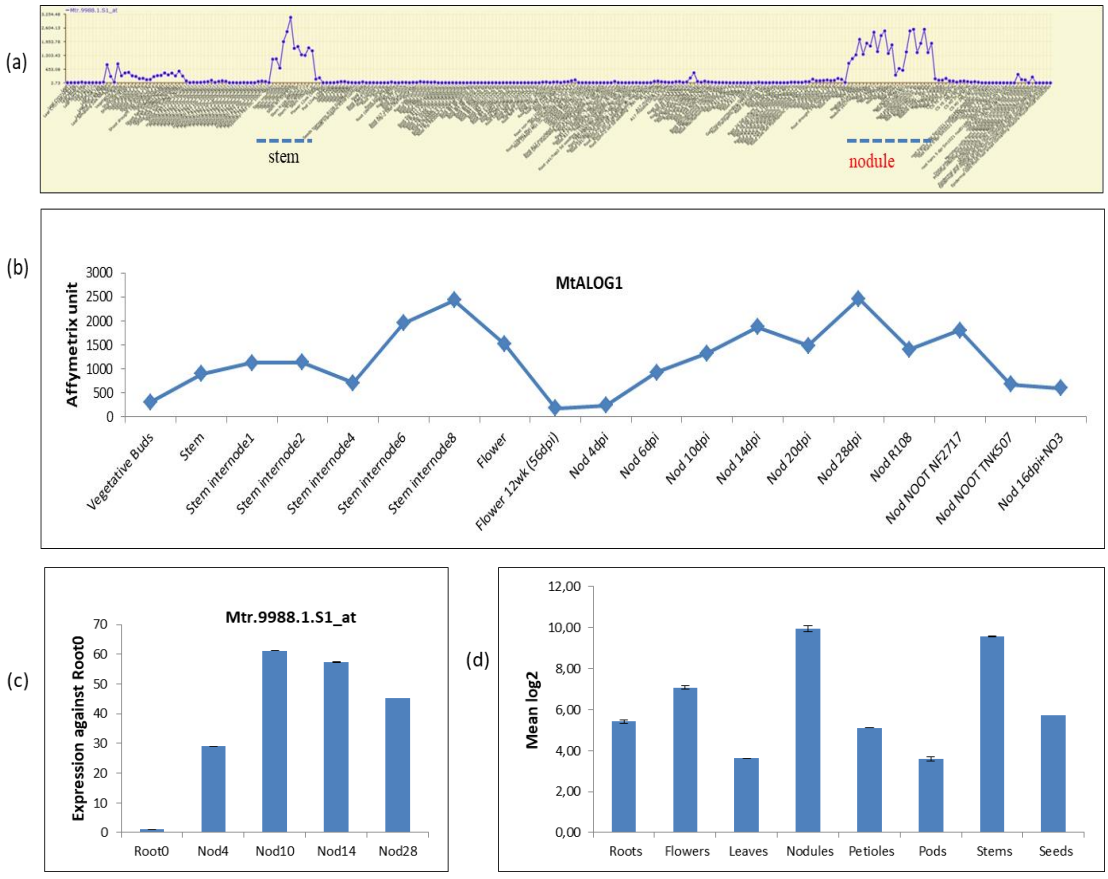

Supplemental Figure 1. *MtALOG1* gene expression profile from *Medicago truncatula* Gene Expression Atlas.

a-b. *MtALOG1* gene expression profile established using 11 specific probes from the Affymetrix *Medicago truncatula* GeneChip. The *MtALOG1* associated probeset Mtr.9988.1.S1_at was used. **a**. Overview of *MtALOG1* gene expression profile using the whole MtGEA dataset available on the *Medicago truncatula* Gene Expression Atlas (MtGEA) and **b**. The detailed expression level of *MtALOG1* in stem and nodule organ, data extracted from (MtGEA). **c-d**. *MtALOG1* gene expression

profile using the Benedito et al., 2008 datasets. Gene expression values are expressed in the Affymetrix unit and are organized by organs. In nodule, the expression was against roots (**c**), and in root and aerial part, the expression was mean log2; dpi, days post-inoculation.

The probeset Mtr.9988.1.S1_at corresponding to the *MtALOG1* gene expression profile on the *M. truncatula* Gene Expression Atlas (MtGEA, https://mtgea.noble.org/v3/) confirmed that *MtALOG1* is highly expressed in nodules and stems (Sup. 1a,b). In addition, which also expressed in *Mtnoot1* mutant lines (NF2717 and TNK507) (Sup. 1b). Furthermore, expression data from Benedito et al., 2008, also indicates that the *MtALOG1* gene is induced during nodulation from 4 to 28 days post-inoculation (dpi, Sup. 1c). In agreement with our RT-qPCR results, the RNAseq data also show that the *MtALOG1* gene is highly induced in stem (Benedito *et al.*, 2008) and flowers (Sup. 1b, d).

The *MtALOG1* gene expression induction during nodulation was confirmed by qRT- PCR analysis. In our experiments, *MtALOG1* expression was detected from 5 to 21 dpi and was the highest at 21 dpi (Fig. 2), in agreement with the expression kinetics from MtGEA (Sup. 1b) and slightly different of RNAseq data (Sup. 1c; Benedito *et al.*, 2008). The *MtALOG1* gene can be considered as an early symbiotic gene since its expression pattern was similar to the *MtNOOT2* and *MtNODULE INCEPTION* (*MtNIN*) gene expressions (Magne *et al.*, 2018a). In contrast to *MtNOOT1*, constitutively expressed in the root and induced from 8 to 21 dpi (Magne *et al.*, 2018a), the *MtALOG1* gene was nearly undetectable in the root (Fig. 2).

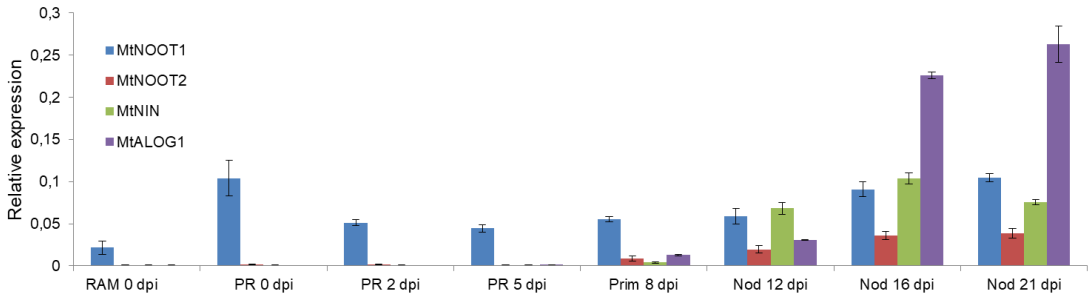

Figure 2. Gene expression in R108 during nodulation.

MtALOG1 gene expression in wild-type M. truncatula R108 uninoculated root apical meristem (0,5 cm, 2 days post vernalization: RAM 0 dpi), in uninoculated primary root devoid of root apical meristem (2 days post vernalization: PR 0 dpi), in inoculated primary root (PR 2, 5 dpi), in nodule primordia (Prim 8 dpi) and in nodules (Nod 12, 16 and 21 dpi) inoculated with Sinorhizobium medicae WSM419 strainand and the expression level compare to MtNOOT1(blue bar), MtNOOT2 (red bar), and MtNIN (green bar) marker genes. The relative expression was normalized against the

constitutively expressed *MtRNA RECOGNITION MOTIF* (*MtRRM*) and *MtACTIN* (*MtACT*) genes and against uninoculated primary root. Results represent means ± SE of three technical replicates and three biological replicates. Prim, primordia; Nod, nodule.

The qRT-PCR and Affymetrix data clearly show that *MtALOG1* was early and highly expressed during nodulation (Sup. 1 and Fig. 2). The laser-capture microdissection (LCM) coupled with RNAseq data, Roux *et al.*, (2014) also show that *MtNOOT1*, *MtNOOT2*, and *MtALOG1* have a similar expression pattern across the different zones analyzed, with a majority of transcripts found for all three genes in the apical part of the nodule (FI and FIId) representing the meristematic zone and the distal region of the differentiation and infection zone, respectively (Sup. 2a, b). These data concerning *MtNOOT1* and *MtNOOT2* gene expression are in agreement with the pMtNOOT1: GUS expression in the nodule vascular bundle and the nodule vascular meristem (NVM) and pMtNOOT2:GUS expression in the nodule central meristem (NCM, Magne *et al.*, 2018). Our preliminary results also show that pMtALOG1:GUS is expressed in the NVM (Sup. 2b,c). *MtNOOT1*, *MtNOOT2*, and *MtALOG1* seem to be expressed at the same time (Fig. 2) and in the same tissues during nodulation (Sup. 2), supporting well our hypothesis in which *MtALOG1* could represent a potential interacting partner for *MtNOOT1* and/or *MtNOOT2*.

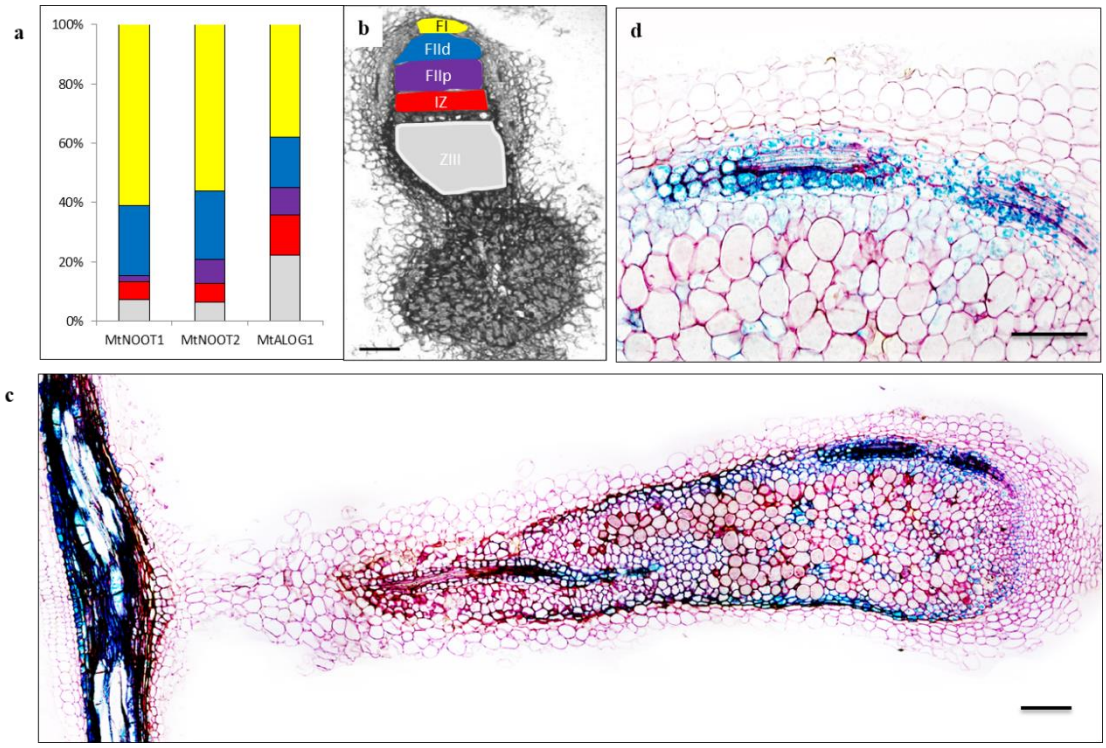

Supplemental Figure 2. Digital in situ localization analysis of *MtNOOT1*, *MtNOOT2* and *MtALOG1* gene expression in the nodule.

a-b. *MtNOOT1*, *MtNOOT2*, and *MtALOG1* gene expression localization based on digital *in situ* analyses performed by Roux et al. (2014). **a**. Values represent the mean percentage of normalized reads recovered in each laser-capture microdissection (LCM) fraction from 3 repetitions. **b**. Representation of the different LCM fractions adapted from Roux et al. (2014). FI, Fraction I, meristematic zone; FIId, Fraction II distal region, differentiation and infection zone; FIIp, Fraction II proximal region, differentiation, and infection zone; IZ, Inter-Zone, inter-zone between zone II and zone III; ZIII, Zone III, nitrogen-fixation zone. Total LCM reads (DESeq normalized) for *MtNOOT1*, *MtNOOT2*, and *MtALOG1* were 602.3, 922.2, and 1437, respectively. **c, d**. promotor MtALOG1 expression in *M. trunctula* R108 background in a nodule (**c**) and magnified nodule apical misterm section (**d**).

Isolation and characterization of *M. truncatula Mtalog1 Tnt1* insertional mutants

In the present study, we have characterized *Mtalog1 Tnt1* insertional mutant lines for their phenotypes in nodule or aerial part and compared them to the *Mtnoot Tnt1* mutants. The *MtALOG1*gene displays only one exon and contains a highly conserved *ALOG* domain. Three insertion lines were isolated for the gene *MtALOG1*, NF13390, NF19406, and NF17903 with *Tnt1* insertions located in the exon (NF13390) and the 3' untranslated region (3' UTR) sequence, (NF19406 and NF17903, Sup. 3c).

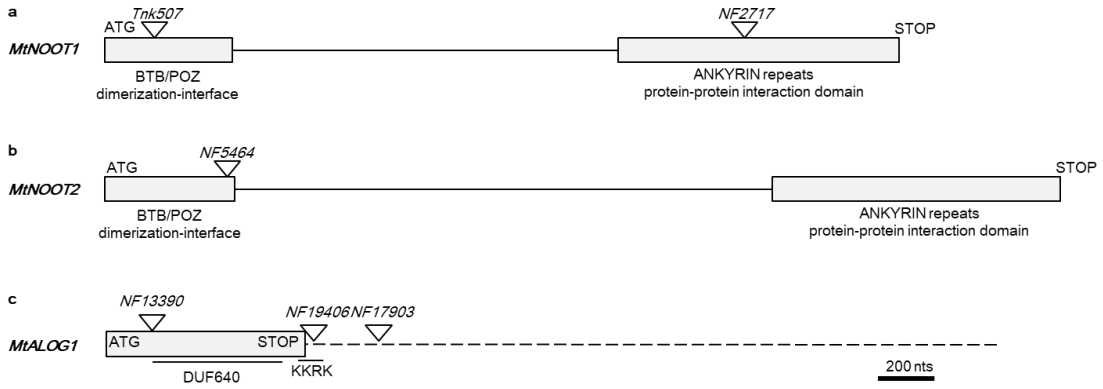

Supplemental Figure 3. *MtNOOT1*, *MtNOOT2* and *MtPAN-LIKE* gene structures and Tnt1 insertions localization.

a-c. Schematic representation of *MtNOOT1*, *MtNOOT2*, and *MtALOG1* gene structures and their respective *Tnt1* retro-element insertions. **a, b.** *MtNOOT1* and *MtNOOT2* encode co-transcriptional factors containing bric-a-brac tram track and broad complex/poxvirus and zinc finger (BTB/POZ) and ankyrin repeats protein domains. BTB/POZ domain serves as a dimerization interface and ankyrin repeat domain serves as a protein-protein interaction interface. *M. truncatula Tnt1* insertion in lines *Tnk507*, *NF2717*, and *NF5464* are localized in the BTB/POZ domains of *MtNOOT1* and *MtNOOT2*, respectively. **c.** *MtALOG1* contains 1 exon, *M. truncatula Tnt1* insertion in lines *NF13390*, *NF19406* and *Nf17903* are localized in the exon and terminal sequence (after stop code), respectively. Exons and

introns are represented by light-grey rectangles and black lines, respectively. The dotted line represented the terminal sequence. Positions of the *M. trunctula Tnt1* insertions are indicated by a triangle.

The nodule phenotype of both *Mtalog1* NF13390 (exonic insertion) and NF19406 (3'UTR) was changed in agreement with the *MtALOG1* expression in nodule (Fig. 2 and Sup. 1). The global observation of nodules at 35 dpi shows more nodules per plant than wild type (Fig. 3a) and the mutant always displayed multi-lobed nodules (Fig. 3b) when the plants were grown in sand-perilite mixture. To confirm this mutant phenotype, we nodulated the plants *in vitro* and similar mutant phenotypes were observed (Fig. 3c, d). The *Mtalog1* mutants produced more nodules per plant relative to wild-type R-108 (Fig. 3c, d) but the numbers of multi-lobbed nodules were slightly reduced or the multi-lobed phenotype was less strong than the plant growth in sand-perilite (Fig. 3a, b). This result suggests that the *MtALOG1* gene plays a role in controlling the nodule number and for nodule identity maintenance.

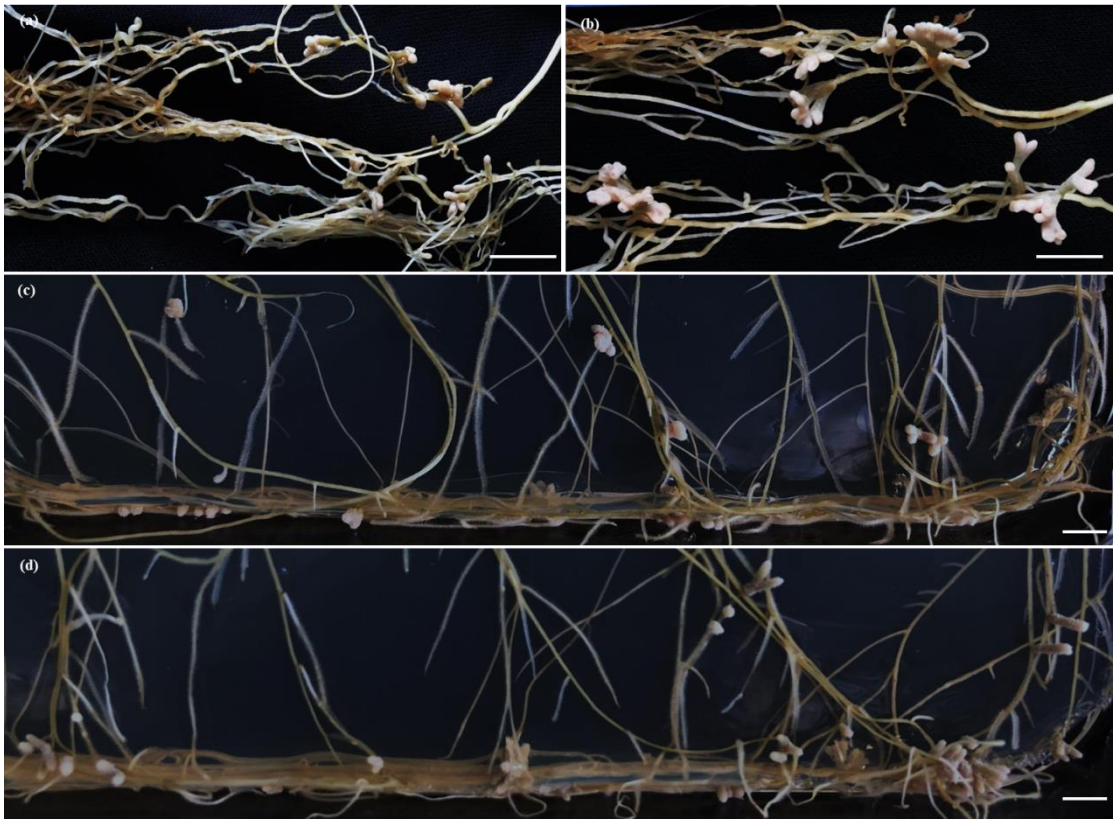

Figure 3. Nodule phenotype of *Mtalog1* mutant.

a-d. nodule phenotype of Mtalog1(b, d) compare to wild type R108 (a, c) in sand/perilite (a,b) and in vitro (c, d) at 35 dpi, respectively.

RT-qPCR gene expression analysis on the Mtalog1 (NF13390, NF19406 and NF17903) mutant lines showed that the Tnt1 insertion impacts the *MtALOG1* transcription relative to R-108 in nodule and indicates that these lines represent the true mutant (Fig. 4a). Because *MtNOOT1* and *MtNOOT2* are key regulators of the symbiotic organ development, the *MtALOG1* gene expression was analyzed in *Mtnoot* single and double mutant backgrounds (Fig. 4b). The *MtALOG1* gene expression was significantly reduced in *Mtnoot1* and *Mtnoot1noot2* mutant nodules while its level of expression in *Mtnoot2* was just slightly decreased relative to R-108 (Fig. 4b). Consistent with the gene expression in *Mtnoot1* (TNK507) mutant background profile from the MtGEA database, this indicates that the *MtALOG1* gene expression is dependent on the nodule identity and that *MtALOG1* may share some functions with *MtNOOT1*. Future experiments will require detailed numeration of the nodule number and measurement of the nitrogen fixation efficiencies of the *Mtalog1* mutants by acetylene reduction assay (ARA; Koch and Evans, 1966) to validate this first observation.

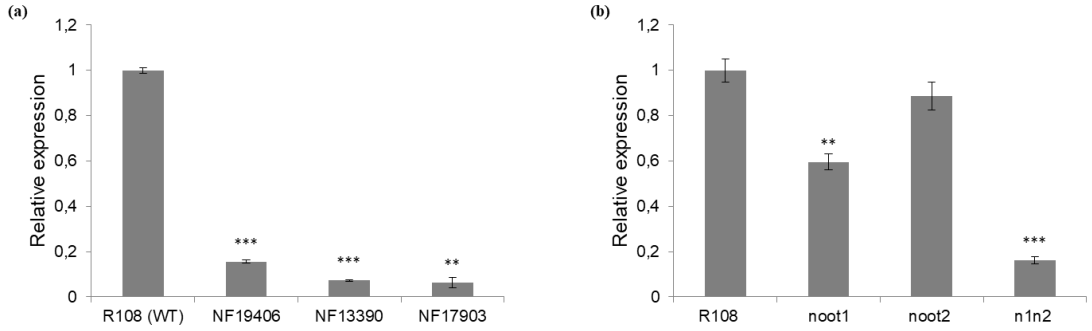

Figure 4 | *MtALOG1* expression level in *Mtalog1* and *Mtnoot* mutant mature nodules.

a-b. qRT-PCR gene expression analysis were performed in *Mtalog1* (*NF13390, NF19406* and *NF17903)* single mutants nodules (a) and noot1, noot2, noot1noot2 mutants relative to R-108 wild-type nodules at 35 dpi with *S. medicae* WSM419 strain. Gene expression data represent relative expression normalized against the constitutively expressed *MtRRM* and *MtACT* reference genes and against R-108 nodules. Results represent means ± SE of three biological repeats and three technical replicates. Asterisks indicate significant differences compared to R-108 nodule (** p-value < 0,001;*** *p*-value < 0,0001; One-way ANOVA). n1n2: noot1noot2.

Construction and preliminary characterization of the *Mtnoot1alog1* and *Mtnoot2alog1* double mutants in nodule

As *MtALOG1* gene expression was significantly downregulated in *Mtnoot* single and double mutant backgrounds we hypothesize that they may interact with

each other (Fig. 4b). To investigate if *MtALOG1* is involved in the *MtNOOT1/2*-dependent nodule identity pathway (Couzigou *et al.*, 2012; Magne *et al.*, 2018a) we initiated a genetic approach to uncover the relationship existing between *MtNOOT1*, *MtNOOT2*, and *MtALOG1*.

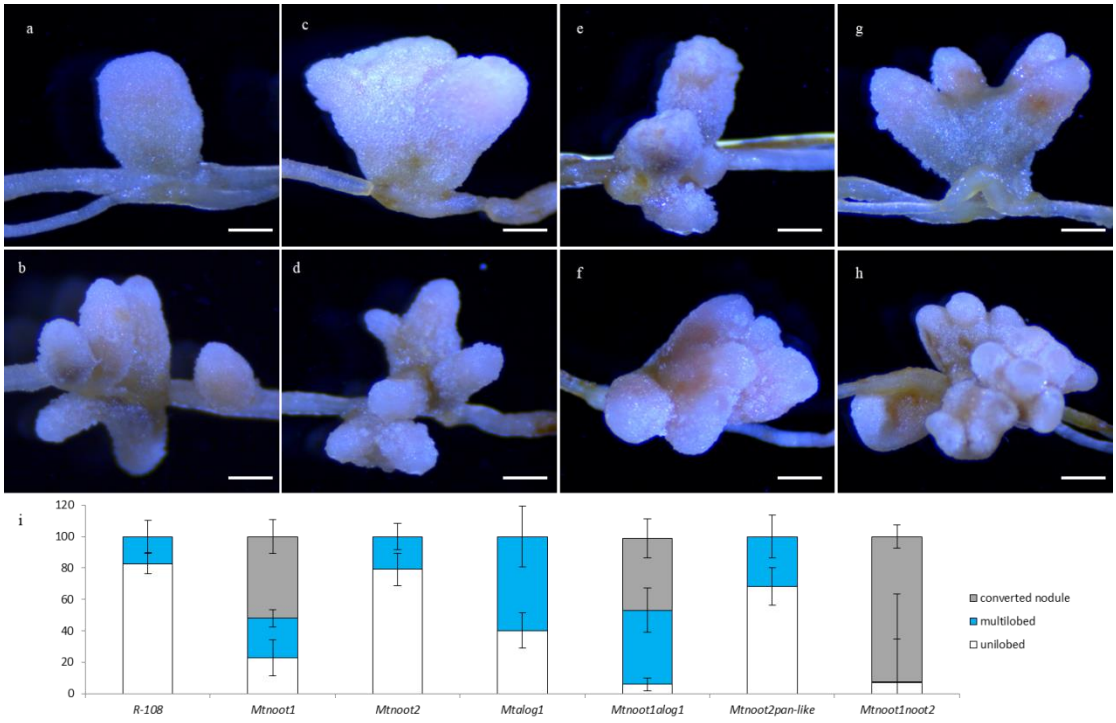

Figure 5. Nodule phenotype of *Mtalog1, Mtnoot1, Mtnoot2, Mtnoot1alog1, Mtnoot2alog1* mutants and R-108

a-h. Nodule phenotype of *Mtnoot2* (**c**) , *Mtalog1*(**e**, **f**) and *Mtnoot1* unconverted nodule (**g**), *Mtnoot2alog1* (**d**), *Mtnoot1alog1* multilobed nodule (**h**) compare to wild type R108 (**b**, **d**) in sand/perilite (**b**, **c**) at 28 dpi, respectively. **i**. The proportion of unilobed nodules (white bars), multilobed nodules (dark blue bars), and converted nodules (grey bars) were assessed in *Mtnoot1*, *Mtnoot2*, *Mtalog1* single mutants and in *Mtnoot1alog1*, *Mtnoot2alog1* and *Mtnoot1noot2* double mutants relative to R-108 wild-type plant control. **b**. Results represent means ± SEM of 3 biological replicates, representing 20 plants for R-108 and Mtnoot1noot2, and 16 plants for Mtnoot1, Mtnoot2, Mtalog1, Mtnoot1alog1 and Mtnoot2alog1 at 28 dpi with S. medicae WSM419. Total number of nodules analyzed for each genotype: R-108, 242; *Mtnoot1*, 189; *Mtnoot2*, 248; *Mtalog1*, 305; *Mtnoot1alog1*, 348; *Mtnoot2alog1*, 315; *Mtnoot1noot2*, 166.

We have constructed the *Mtnoot1alog1* and *Mtnoot2alog1* double mutants. *Mtnoot1*, *Mtnoot2*, *Mtalog1* single mutants, *Mtnoot1alog1*, *Mtnoot2alog1*and R-108 have been characterized for their nodules phenotype 28 dpi with *S. medicae* WSM419. R-108 and the *Mtnoot2* mutant showed similar proportions of wild-type uni-lobed

nodules (≈85 %) and multi-lobed (≈15 %) nodules, while *Mtnoot2alog1* show a slight increase in multi-lobed nodules (≈25 %; Fig. 5a-d, i). The *Mtalog1* mutant showed uni-lobed (≈40 %) and multi-lobed (≈60 %) nodules and the number of lobes was always more than six (Fig. 5e, f). The *Mtnoot1* showed nearly half nodules converted into roots and just about 20% were multi-lobed nodules (Fig. 5g, i). In contrast, *Mtnoot1alog1* showed less (≈40 %) nodules converted into roots and an increased proportion (55%) of multi-lobed nodules showing a significant increase in lobe numbers (Fig. 5h). The remaining nodules were uni-lobed (≈5%; Fig. 5i). *Mtnoot1noot2* showed almost only nodules converted into roots (Fig. 5i) as previously described (Magne et al., 2018). The proportion of nodule types observed in *Mtnoot2alog1* double mutants was similar to the *Mtnoot2* single mutants suggesting that the *Mtnoot2* mutation reduces the multi-lobed phenotype of *Mtalog1* mutation (Fig. 5c, d, i). These results suggest that the *MtALOG1* gene act independently of the *MtNOOT1* gene (additive effect) for nodule identity and that MtNOOT2 is required for the *Mtalog1* phenotype. Notablely, when the plants cultured in vitro, the muti-lobed phenotype were weaker than cultured in sand/perilite for the *Mtalog1*, *Mtnoot1alog1* and *Mtnoot2alog1* mutants (Sup. 4).

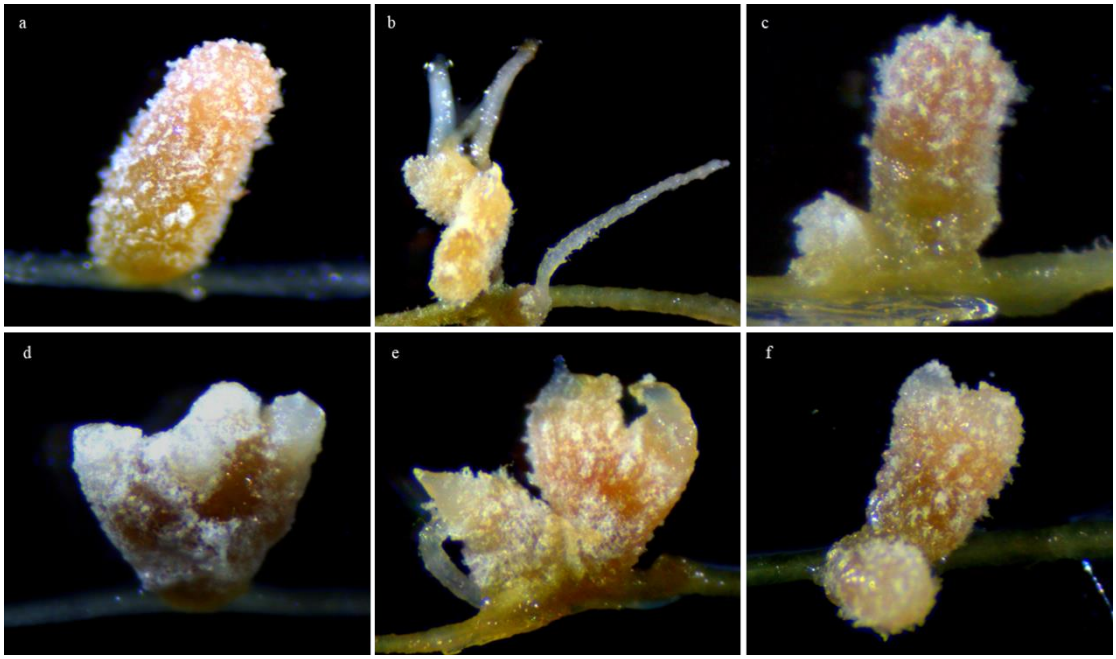

Supplemental Figure 4| nodule phenotype of *Mtalog1*, *Mtnoot1*, *Mtnoot2*, *Mtnoot1alog1*, *Mtnoot2alog1* mutants and R-108.

Comparation of wild type nodule (a), (b), Mtnoot1 converted nodule and Mtnoot2 nodule (c); Mtalog1multilobed nodule (d) and *Mtnoot1alog1* converted multilobed nodule (e), *Mtnoot2alog1* (f) in vitro at 30 dpi, respectively.

The qRT-PCR gene expression analysis were performed in *Mtalog1*, *Mtnoot1* and *Mtnoot2* single and double mutant nodules (Figure 6a). The transcripts of *MtALOG1* were significantly decreased in *Mtalog1*, *Mtnoot1* and *Mtnoot1alog1* and no alteration in *Mtnoot2* and *Mtnoot2alog1*(Fig. 6a). In contrast, the expression level of *MtNOOT1* and *MtNOOT2* were significantly increased in *Mtalog1* while reduced in *Mtnoot1alog1* and *Mtnoot2alog1*, respectively(Fig. 6a).

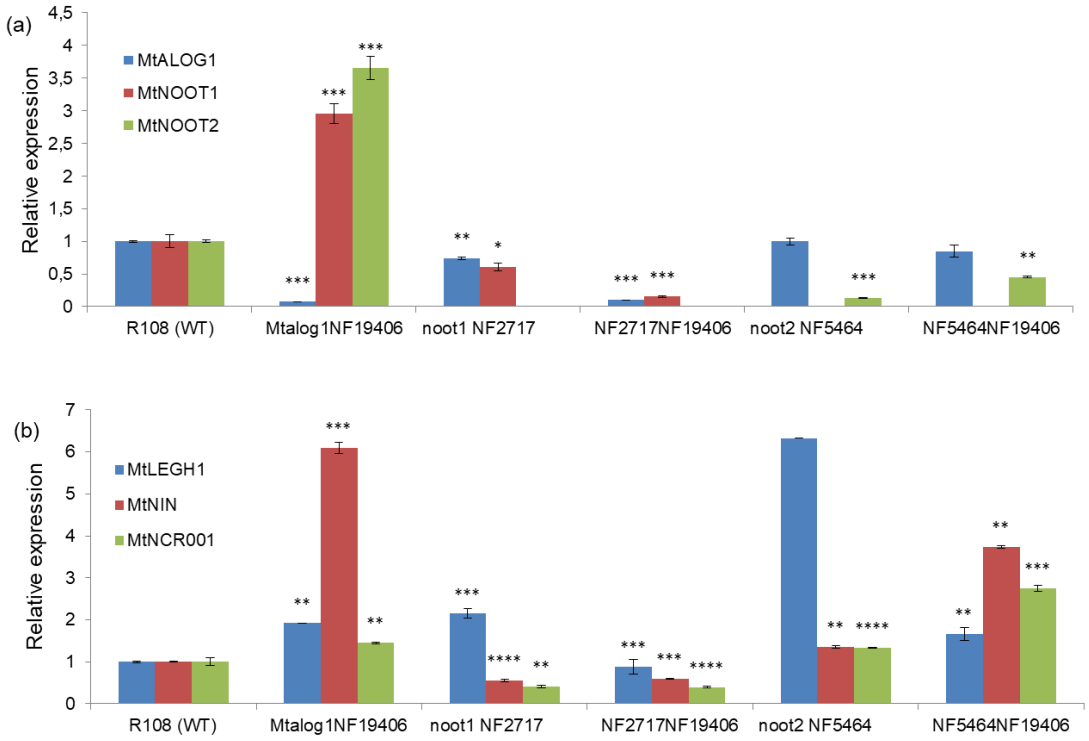

Figure 6 | qRT-PCR gene expression analysis of symbiotic identity marker genes in Mtnoot and Mtalog1 single and double mutant nodules.

a-b. *MtALOG1*, *MtNOOT1* and *MtNOOT2* gene expression (**a**) and qRT-PCR gene expression analysis of the symbiotic marker genes *MtLEGH1* (blue bars), *MtNIN* (red bars) and *MtNCR001* (green bars) (**b**) in wild-type *M. truncatula* R108, *Mtalog1*, *Mtnoot1*, *Mtnoot2*, *Mtnoot1alog1* and *Mtnoot2alog1* nodules inoculated with Sinorhizobium medicae WSM419 strain. The relative expression was normalized against the constitutively expressed *MtRNA RECOGNITION MOTIF* (*MtRRM*) and *MtACTIN* (*MtACT*) genes and against in R-108 nodules. Results represent means ± SE of three technical replicates and three biological replicates. Asterisks indicate significant difference compared to R-108 nodule (* p-value < 0,01; ** p-value < 0,001; *** p-value < 0,0001; One-way ANOVA).

The loss of nodule identity is characterized by a nodule to root homeosis and by drastic molecular shifts such as symbiotic marker gene expression reduction. To better characterized Mtnootalog1 mutants, qRT-PCR expression analysis were performed in mutant nodules using symbiotic marker genes (Fig. 6b). *MtNIN*, *MtNCR001* and *MtLEGH1* symbiotic genes expression analysis showed that all the mutants correctly expressed symbiotic genes (Fig. 6b). We noted that in *Mtnoot1* and *Mtnoot1alog1* mutants showing nodule to root conversions, the expression level of symbiotic gene markers were sinificantly reduced compared to the level observed in *Mtnoot2*, *Mtalog1* and *Mtnoot2alog1* mutants that showed no symbiotic phenotype however except for *Mtnoot1* that *MtLEGH1* transcripts show a significant increased relative to wild-type.Taken together, nodule phenotype analysis and qRT-PCR gene expression analysis of symbiotic marker genes, indicate that the *Mtalog1* mutation alone does not affect symbiosis, however, the symbiosis was affected in association with *Mtnoot* mutations (Fig. 5 and Fig. 6).

Characterization of the *Mtalog1* and *Mtnoot1alog1* double mutants in aerial development

Apart from a function in nodules, *MtALOG1* may also play a role in aerial development due to its stem and flower specific expression (Fig. 1 and Sup.1). As expect, we observed that the *Mtalog1* mutant generally produces three flowers in a single inflorescence (Fig. 7b), similar to previous observation for the *Mtnoot2* mutant (see chapter I), while wild type *M. trunctula* R108 plants mostly produce one and only occasionally two flowers in a single inflorescence (Fig. 7a). Similar to wild type, the *Mtnoot1* mutant produces mostly one flower on a single inflorescence (Fig. 7c). In contrast, the *Mtnoot1alog1* double mutants also show a increased flower number as the Mtalog1 single mutants (Fig. 7d). However, the *Mtnoot2alog1* double just show a *Mtnoot2* or *Mtalog1* single mutant flower phenotype. In addition, the stipule also modified in *Mtnoot1alog1* with reduced or simplified digitations like the *Mtnoot1* (Fig. 7g, h) while the *Mtalog1* single mutant show a wild type stipule phenotype (Fig. 7a, b). Furthermore, the pods phenotype also alterated in *Mtalog1* and *Mtnoot1alog1* double mutants and mostly with three pods in each stalk (Fig. 7j, k), however, the noot1 only one pod on each stalk like wild type (Fig. 7i, k). The pod phenotype in *Mtalog1* and *Mtnoot1alog1* like the flower phenoytype and maybe as the consequence of the increased flower number of *Mtalog1* and *Mtnoot1alog1* mutants (Fig. 7b, d).

Notably, the flower in *Mtnoot1alog1* double mutants were partly sterile. The flower phenotype in *Mtalog1* like the *Mtnoot2* and the *Mtnoot1noot2* double mutants show almostly sterile (see chapter I). It will be thus interesting in the future to study whether *MtALOG1* has a role with *MtNOOT1* and *MtNOOT2* to control the flower development.

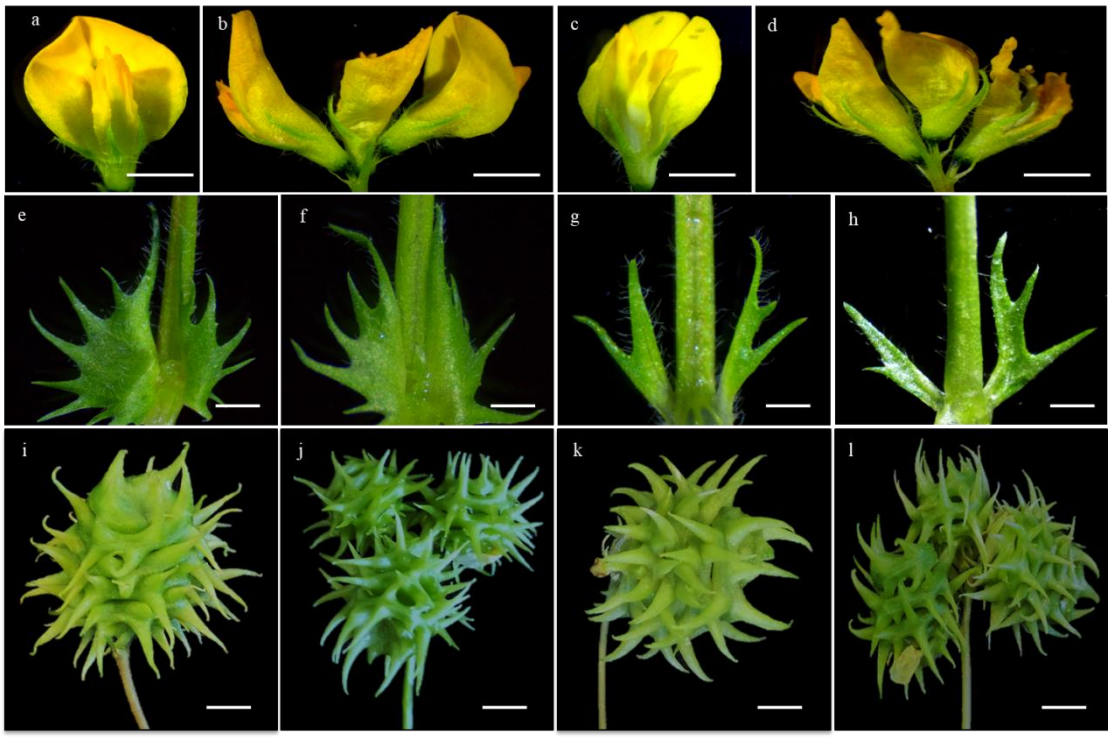

Figure 7 | Flower, stipule and pod phenotype of R-108, *Mtalog1*, *Mtnoot1* and *Mtnoot1alog1* mutants.

Global view of flower (**a-d)**, stipule (**e-h**) and pod (**i-l**) phenotype of wild type *M. trunctula* R108 (a, e, i), *Mtalog1* (b, f, j), *Mtnoot1* (c, g, k) and *Mtnoot1alog1* (d, h, l), respectively. Scare bar: 0,5cm.

The qRT-PCR gene expression analysis were performed in *Mtalog1*, *Mtnoot1* and *Mtnoot1alog1* single and double mutant pods and young flowers (Figure 8). The results show that the transcripts of both *MtNOOT1* and *MtALOG1* were significantly decreased in *Mtalog1*, *Mtnoot1* and *Mtnoot1alog1* single and double mutant, especialy in *Mtnoot1alog1* (Fig. 8a, b). The similar expression pattern were observed in pod and yound flower for *MtNOOT1* and *MtALOG1* except a bit difference in *Mtnoot1* mutant. In addition, we test the flora meristem maker genes, *MtPIM*, *MtAP1* and *MtAGa* and the expression level were significantly increased in all the tested mutants (Fig. 8c). These results indict that the *MtALOG1* realy has a function on control the flower number and also floral misterm formation and function with *MtNOOT1* to control the aerial development.

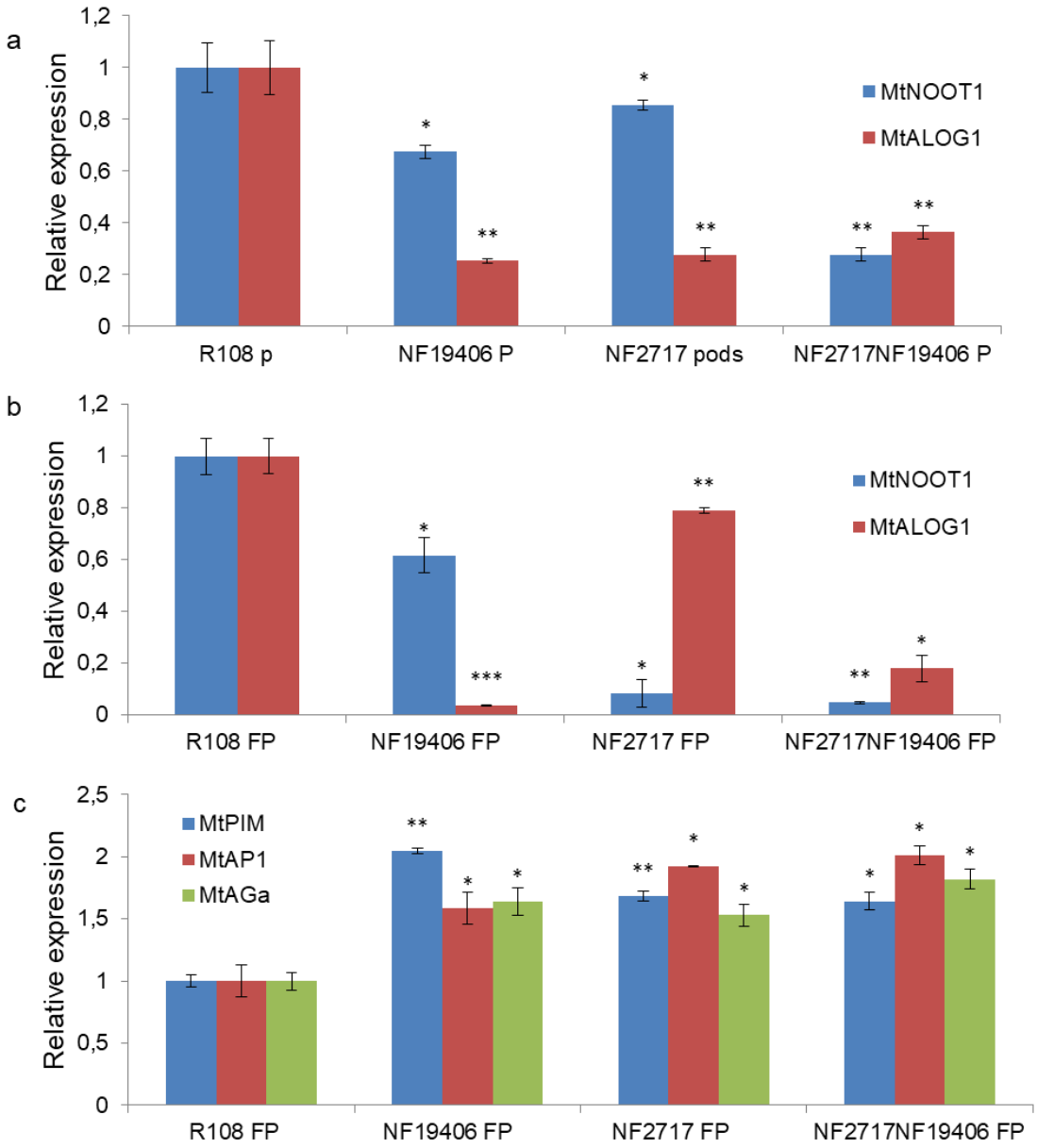

Figure 8 | Gene expression analysis in *Mtnoot* and *Mtalog1* single and double mutant.

a-b. *MtNOOT1* and *MtALOG1* gene expression in pods (**a**) and young flowers (b) and qRT-PCR gene expression analysis of the flora meristem marker genes *MtPIM* (blue bars), *MtAP1* (red bars) and *MtAGa* (green bars) (**c**) in wild-type *M. truncatula* R108, *Mtalog1*, *Mtnoot1* and *Mtnoot1alog1*. The relative expression was normalized against the constitutively expressed *MtACTIN* (*MtACT*) genes and against in R-108 wild type. Results represent means ± SE of three technical replicates and three biological replicates. Asterisks indicate significant difference compared to R-108 nodule (* p-value < 0,01; ** p-value < 0,001; *** p-value < 0,0001; One-way ANOVA).

In addition, our preliminary observations show that the *Mtalog1* mutation increased the branches number at the base of the plant compared to wild type *M. truncatula* R108 (Sup. 5a,b), similarly to the *Mtnoot1* mutation (Sup. 5c; see chapter

II). The *Mtnoot1alog1* double mutant was also investigated for a stronger branching phenotype. At the young stage, the global observation showed an increased branching similar to the *Mtalog1* and *Mtnoot1* single mutants (Sup. 5d). Differences could not be estimated without careful numeration because the single mutants already have increased branches (Sup. 5b-d). As the plants develop, some of the *Mtnoot1alog1* double mutants displayed an exaggerated branching phenotype (Sup. 5e-f) compared to the *Mtnoot1* or *Mtalog1* mutant indicating that *MtNOOT1* and *MtALOG1* may function redundantly to control branching. Indeed, the plant biomass, dry weight or fresh weight, were significantly increased in the *Mtnoot1*, *Mtalog1* and *Mtnoot1alog1* mutants and the double mutants displayed a highter biomass than either *Mtnoot1* or *Mtalog1* single mutants (Sup. 5g). To confirm these phenotypes, more plants have to be analyzed in detail in future experiments.

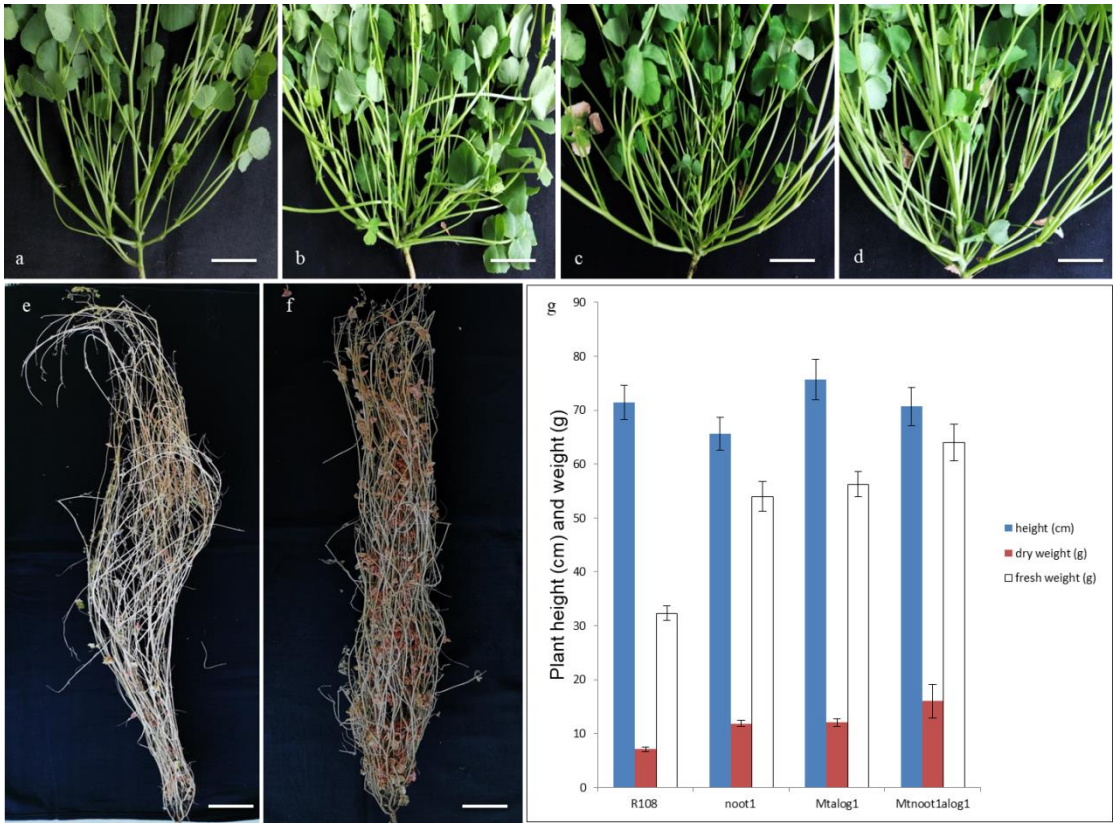

Supplemental Figure 5 | branching phenotype of *Mtalog1*, *Mtnoot1*, *Mtnoot1alog1*mutants and R-108.

a-f. Global view of wild type *M. trunctula* R108 (a), *Mtalog1* (b), *Mtnoot1* (c) and *Mtnoot1alog1* (d) at 35 day after sowing and *Mtalog1* (e), *Mtnoot1alog1* (f) when the shoots were totally dry. **g**. statistic of plant height (blue bars), fresh weight (green bars) and dry weight (red bars). Data presentative means ± SE, n=9.

The *MtNOOT1* gene regulate class II *MtKNOX* gene expression in nodules

In *M. truncatula*, class II *MtKNOX3*, *MtKNOX5*, and *MtKNOX9* genes are constitutively expressed in the root stele, including the pericycle and endodermis, and are up-regulated in nodules (Azarakhsh *et al.*, 2015; Di Giacomo *et al.*, 2016). Moreover, *MtKNOX3* and *MtKNOX9* gene expression were reduced in *Mtnoot1* and *Mtnoot1noot2* nodules relative to R-108 nodules and the *MtKNOX9* gene expression pattern was *Mtnoot1* dependent (Magne *et al.*, 2018a).

Nodules are highly organized organs with several meristematic domains delimited by boundaries. As the expression pattern of *MtKNOX3* and *MtKNOX9* were similar in the *noot* mutants ((Magne *et al.*, 2018a), we hypothesize that their spatial expression patterns could also be *MtNOOT*-dependent. To genetically characterize the role of *MtKNOX3* in the *noot* mutants, we generated *M. truncatula* transgenic plants expressing the promoter MtKNOX3:GUS: terminator (ProKNOX3::GUS) fusion construct and crossed one plant to the *noot1noot2* mutant. The *MtKNOX3* expression pattern was investigated in R-108, *Mtnoot1*, and *Mtnoot1noot2* nodules. In wild type R-108 nodules, strong ProKNOX3::GUS activity was observed in entire developing nodule primordia especially in the parenchyma tissues surrounding the vascular bundles (Fig. 9a, g), in agreement with previous observations (Azarakhsh *et al.*, 2015; Di Giacomo *et al.*, 2016). Similar *MtKNOX3* expression was observed in whole nodule primordia in both *Mtnoot1* and *Mtnoot1noot2* (Fig. 9c, i, e, k) from the very early stages of symbiotic nodule formation. In wild type mature nodules, the pKNOX3::GUS fusion was strongly expressed at the apical part of nodule corresponding to the central meristem and was also detected in provascular bundle tissues (Fig. 9b, h). In contrast, in the *Mtnoot1* and *Mtnoot1noot2* unconverted uni/multi-lobed mature nodules, the pKNOX3::GUS expression was restricted to the vasculature (Fig. 9d, j, f, l, m, o), suggesting that the *MtKNOX3* expression in the nodule apical meristem region is *MtNOOT1*-dependent (Fig. 9c, e). In the *Mtnoot1* and *Mtnoot1noot2* converted nodules, however, the pKNOX3::GUS expression was detected from the nodule vascular bundles to the ectopic root vasculature and lost in the nodule apical region (Fig. 9n, p). It is noteworthy, that in the nodule to root conversions events, the PKNOX3::GUS reporter is expressed in the vasculature of the ectopic root emerging from the mutant nodule, further highlighting the vascular

connection between the nodule vascular bundles and the nodule ectopic root vasculatures (Fig. 9n, p).

Azarakhsh *et al.*, (2015) indicated that the MtKNOX3 promoter activity was also found in lateral root primordia and root tips. This is also consistent with our results because once nodule identity is lost, the converted nodule vascular bundles behave as a root organ, supporting the hypothesis that nodule-root identity can override the nodule identity. These results similar to the *MtKNOX9* expression in the *Mtnoot* mutant contexts suggest that loss of nodule identity observed in *Mtnoot1* and in *Mtnoot1noot2* nodules is associated to both, a decrease in the Class II KNOX (*MtKNOX3* and *MtKNOX9*) gene expression levels and to a drastic shift in the *MtKNOX3* and or *MtKNOX9* spatial expression patterns from the apical meristematic region to the vascular tissues.

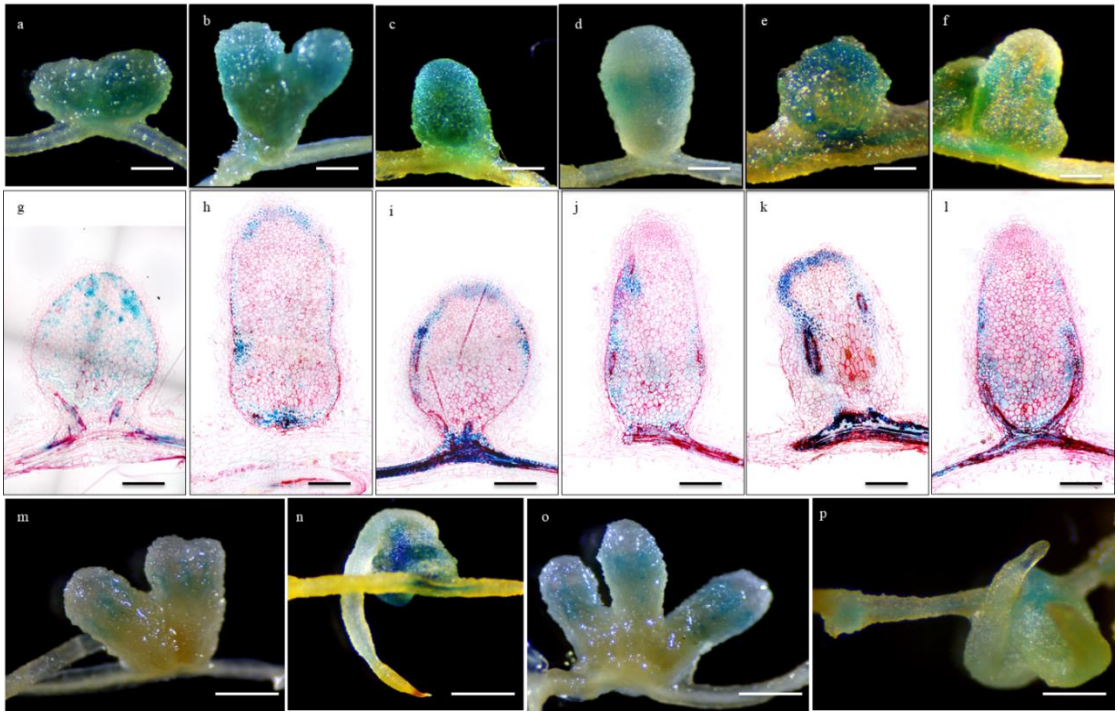

Figure 9. Changes in the expression pattern of the *ProKNOX3:GUS* reporter fusion in R108, *Mtnoot1* and *Mtnoot1noot2* mutant nodules.

(a-f, m-p) global view and longitude sections (**g-l**) show the *ProKNOX3:GUS* expression in wild type (**a**, **b**, **g**, **h**) and *Mtnoot1* (**c**, **d**, **i**, **j**, **m**, **n**), and *Mtnoot1noot2* (**e**, **f**, **k**, **l**, **o**, **p**) nodules. **a, g**. *ProKNOX3:GUS* expression in entire nodule primordia and restricted to the apical meristem zone with weak expression along the vascular bundles of mature (28-35 dpi with S. meliloti in R108 nodules (**b**, **h**). **c, i. e, k,** *ProKNOX3::GUS* expression in whole the nodule primordia in *Mtnoot1*(**c**, **i**) and *Mtnoot1noot2* (**e**, **k**) nodules and in uni-lobed Mtnoot1(**d**, **j**) and Mtnoot1noot2 (**f**, **l**) mature nodule. (**m**) Mtnoot1 unconverted multi-lobed nodules with strong *ProKNOX3::GUS* expression in the vasculature.

(**n**) *ProKNOX3::GUS* expression in Mtnoot1 converted nodules with loss of expression in the apical central meristem region and strong expression in the vascular bundles of the nodule to ectopic root conversions. (**o**) *Mtnoot1noot2* wild-type-looking nodule with *ProKNOX3::GUS* expression with particularly strong expression in the vasculature, similar to the expression pattern in *Mtnoot1*. (**p**) *Mtnoot1noot2* converted nodule with loss of expression in the apical central meristem region and expression in the vascular bundles of the nodule to ectopic root conversions, similar to the Mtnoot1 mutant. Scale bars: a-f, m-p: 1 mm; g-l: 500 µm.

DISCUSSION

Members of the *NODULE-ROOT/BLADE-ON-PETIOLE/COCHLEATA-LIKE (NBCL)* gene family belong to the *NON-EXPRESSOR OF PATHOGENESIS-RELATED PROTEIN1-LIKE (NPR1-LIKE)* family and are key regulators of the symbiotic organ identity (Ferguson & Reid, 2005; Couzigou *et al.*, 2012; Magne *et al.*, 2018a). *NPR1-LIKE* and *NBCL* genes encode plant-specific co-transcriptional factors containing BTB/POZ domains which serve as dimerization interface and are also Cullin-3 adaptors that provide substrate specificity for Cullin-3 based E3 ubiquitin ligases for subsequent ubiquitin-dependent degradation by the 26S proteasome (Pintard *et al.*, 2004; Van Den Heuvel, 2004; Gingerich *et al.*, 2007; Zhang *et al.*, 2017).

The ALOG protein represents a plant-specific protein, which contains a DNA-binding domain and weak transcriptional activity (MacAlister *et al.*, 2012; Yoshida *et al.*, 2013; Xu *et al.*, 2016)(MacAlister et al. 2012; Xu et al. 2018; Yoshida et al. 2013). Its transcriptional activity is enhanced by interaction with BLADE ON PETIOLE (BOP) transcriptional cofactors (Xu *et al.*, 2016). Previous studies in inflorescence development in tomato have shown that TMF (LSH6), which affect vegetative/reproductive transition (Chakrabarti *et al.*, 2013), interacts with three *Solanum lycopersicum BLADE-ON-PETIOLE* members (*SlBOPs*) and *BOPa* (MacAlister *et al.*, 2012; Xu *et al.*, 2016) and the *LSH3b* interacts with *BOPa* and also binds to the PETROSELINUM (PTS) promoter (Kemmeren *et al.*, 2002; Ichihashi *et al.*, 2014), suggesting that BOPa can physically interact with LSH.

Although the precise functions of ALOG (or DUF640) domain proteins remain uncertain, there are five possible roles for these proteins based on the published information. These are: 1) specific transcription factor that regulates inflorescence architecture, 2)transport of RNA, 3) determination of organ identity and

differentiation, 4) sensing of invading DNA, and 5) regulating nodulation (Yoshida *et al.*, 2009, 2013; Iyer & Aravind, 2012; MacAlister *et al.*, 2012; YAN *et al.*, 2013; Teo *et al.*, 2014; Peng *et al.*, 2017; Lei *et al.*, 2019). To better understand the regulation of the *MtNOOT1*/*MtNOOT2*-dependent symbiotic organ identity, the present work aimed to decipher whether one member of the *ALOG* family in *M. truncatula* can be a potential NOOT interacting partner.

Our investigation on the *M. truncatula ALOG* first revealed that, four of the ten *ALOG* members are expressed in nodules and roots and six are expressed in *M. truncatula* aerial organs at different levels. In addition, among the 10 *ALOG* genes, only two were highly induced in nodules and four were not detected in all the tissues tested. In our study, we have identified the closest ortholog of *AtLSH4* in *M. truncatula* and named it *MtALOG1*. RT-qPCR experiments and RNA-seq data show that *MtALOG1* is highly expressed in nodules and also stems, and represents a suitable candidate gene potentially involved in the regulation of *M. truncatula* nodule development. We show that *MtALOG1* is a nodule-induced gene that behaves as an early symbiotic gene similar to *MtNIN* and *MtNOOT2* (Magne *et al.*, 2018a). Furthermore, the *MtALOG1* symbiotic nature was confirmed by testing its expression in the *Mtnoot* mutant backgrounds. It was previously shown that symbiotic genes are downregulated in the *Mtnoot1* and *Mtnoot1noot2* mutant backgrounds (Magne *et al.*, 2018a) and we obtained similar results for *MtALOG1* suggesting that its expression is dependent of the nodule identity. Based on the work of Roux *et al.*, (2014), we highlighted that *MtNOOT1*, *MtNOOT2* and *MtALOG1* shared a similar spatial expression pattern and that their transcripts were mostly found in the apical part of the nodules. The apical localization of *MtNOOT1* and *MtNOOT2* found in Roux *et al.*, (2014) is coherent with the previously described proNOOT1::GUS and the proNOOT2::GUS expression patterns in nodule vascular bundle apex and in the nodule apical meristem, respectively (Couzigou *et al.*, 2012; Magne *et al.*, 2018a). Indeed, the preliminary result shows that proALOG1::GUS is expressed in the nodule vascular bundle apex. In rice, the *TRIANGULAR HULL1* (*TH1*) gene, encoding an ALOG protein, was shown to localize in the nucleus and possess transcriptional repression activity (Peng *et al.*, 2017). In lotus, LjALOG proteins were also predicted to contain nuclear localization sequences (NLS) in their C-termini (Lei *et al.*, 2019). *MtALOG1* is also predicted to contain an NLS in its C-termini

(http://mleg.cse.sc.edu/seqNLS/MainProcess.cgi). As described in the literature for BTB/POZ and ankyrin repeat co-transcriptional factor, MtNOOT1::GFP and MtNOOT2::GFP are both localized in the nucleus and the cytoplasm (Magne et al, unpublished data), indicating that an interaction between the nucleo-cytoplasmic MtNOOT proteins and the nuclear MtALOG is possible. In future work, we will confirm the gene expression pattern by *in situ* hybridization and also by expressing a GFP reporter construct (vector construction already is done) to know the exact localization of this protein. The precise subcellular localization of the MtALOG1 protein could significantly add to the comprehension of the role of this gene. Furthermore, we showed by qRT-PCR that *MtNOOT1*, *MtNOOT2*, and *MtALOG1* genes were simultaneously expressed. These spatial and temporal common gene expression patterns support well our hypothesis of a conserved *NBCL/ALOG1* regulation module in the nodule of *M. truncatula* involving *MtNOOT1/2* and *MtALOG1*.

The analysis of the *Mtalog1* mutant shows an increased nodule number and nodule are multi-lobed. Therefore, future work should test whether these multi-lobed nodules exhibit a nitrogen fixation defect or not. In contrast, it was recently reported that *LjALOG1* in lotus as a positive role during nodulation and increased the nodule number when overexpressed in transgenic hairy roots (Lei *et al.*, 2019). This can be explained by the different nodule types (determinate/indeterminate) in the two plants. In addition, our preliminary results show that the mutation of *MtALOG1* also displayed a role in branching and flower number. Studies suggest that ALOG proteins regulate floral and spikelet organ development as well as the transition from indeterminate to determinate growth in angiosperms (Yoshida *et al.*, 2009; Takeda *et al.*, 2011; Li *et al.*, 2012; MacAlister *et al.*, 2012; Bencivenga *et al.*, 2016; Xu *et al.*, 2016; Peng *et al.*, 2017). The rice *ALOG* family gene, *TAWAWA 1* (*TAW1*), inhibits the maturation of axillary meristems into floral meristems during reproductive growth (Yoshida *et al.*, 2013). Mutation in the tomato TMF induces the simplification of primary inflorescences into single flowers (MacAlister *et al.*, 2012). Overexpression of the Arabidopsis *ALOG* family genes, *LSH4* and *LSH3*, induces extra flower differentiation within a flower (Takeda *et al.*, 2011). However, *lsh4* as well as *lsh3lsh4* do not show obvious phenotypes (Bencivenga *et al.*, 2016), suggesting the existence of functionally redundant genes in this gene family that has undergone

multiple duplications. *MtALOG3* which has a pattern of expression similar to *MtALOG1*, is another *ALOG* member that can be tested for its role in nodule and aerial organ development.

To further investigate the role of the *MtALOG1* gene and its genetic relationship with the *MtNOOT* genes in nodule and aerial organ development, *Mtnoot1alog1* and *Mtnoot2alog1* double mutants were constructed. The phenotypic characterization of the nodule populations showed an increase in multi-lobed nodules in the *Mtnoot1alog1* but not in*Mtnoot2alog1* double mutants compared to the single mutants. This suggests that the *Mtalog1* mutation in association with the *Mtnoot1* mutation may impact the nodule identity. In addition, our preliminary experiments indicate that the branching phenotype of the *Mtnoot1alog1* double mutant is increased compared to the single mutants.

In *A. thaliana*, one of the roles of the *AtBOP* genes in meristem-to-organ-boundary and at the base of the lateral organ is to repress cell proliferation through the repression of class I *AtKNOTTED1-LIKE HOMEOBOX1/2/6* (*AtKNAT1*, *AtKNAT2*, and *AtKNAT6*) genes (Ha *et al.*, 2003, 2004; Žádníková & Simon, 2014). However, class II *KNOX* has an antagonistic role to the class I *KNOX* during development (Furumizu *et al.*, 2015). Recently in *M. truncatula*, class II *KNOX* TFs (*MtKNOX3*, *MtKNOX5*, and *MtKNOX9*) were shown to be functionally redundant and to contribute to the regulation of proper nodule size, boundary, and shape during nodule development (Azarakhsh *et al.*, 2015; Di Giacomo *et al.*, 2016). In *Mtnoot1* and *Mtnoot1noot2* nodules the class II *MtKNOX3* and *MtKNOX9* gene expressions were down-regulated and a drastic rearrangement of the ProKNOX9::GUS expression pattern was observed in the mutant context (Magne *et al.*, 2018a). Similarly, the ProKNOX3::GUS expression pattern in the nodule apical meristematic zone was also lost and a re-activation of the *MtKNOX3* gene expression occurs in nodule vascular tissue recalling the ProKNOX3::GUS pattern in wild-type root. The shift of the ProKNOX3::GUS expression pattern reflects the homeosis event that occurs in *Mtnoot1* and *Mtnoot1noot2* and supports the function of *MtKNOX3* in nodule identity previously proposed for the gene belonging to the *MtKNAT3/4/5-like* genes sub-class (Di Giacomo *et al.*, 2016). This supports that the class II MtKNOX genes expressed in the root have been recruited to build the nodule and define its identity in a MtNOOT1-dependent manner (Magne *et al.*, 2018a).

The present study describes MtALOG1 as the first member of the *ALOG* family in *M. truncatula*, in which it negatively regulates nodulation. Despite that the *Mtalog1* mutant does not show obvious nodule identity defects, this study suggests that MtALOG1 is a potential interacting partner of the MtNOOT proteins in *M. truncatula* indeterminate nodules. We thus provide new elements to better understand the completely misunderstood *ALOG* family in *M. truncatula* or in legume. In addition, the MtKNOX3 study in MtNOOT enhanced the point that the class II MtKNOX genes expressed in the root have been recruited to build the nodule and define its identity in a MtNOOT1-dependent manner.

MATERIALS AND METHODS

Plant material and growth conditions

The seeds of wild-type *M. truncatula* ecotype R-108 (Hoffmann *et al.*, 1997) and its corresponding mutants *Mtalog1*(NF13390, NF19406, NF17903; this study), *Mtnoot1* (Tnk507 and NF2717; Couzigou *et al.*, 2012), *Mtnoot2* (NF5464); *Mtnoot1Mtnoot2* (NF2717 crossed with NF5464); Magne *et al.*, 2018) were scarified and surface-sterilized by immersion in 5 mL of sodium hypochlorite (one pellet per 1L of sterile water) and 1 droplet of liquid soap during 20 min under agitation. Three successive rinsing with sterile water were done. Seeds were vernalized 2 days at 4°C under darkness on 7g.L-1 Kalys Agar plates. Seeds were then transferred to growth chamber 48h at 24°C under darkness for acclimatization. Seedings were cultivated on a perlite and sand mix (3:1, v/v) or sowing in soil or on sterilized Buffered Nodulation Media (BNM) in vitro plates (Ehrhardt *et al.*, 1992) solidified with Kalys agar (7g L^{-} 1) and supplemented with 0.5 µm 2-aminoethoxyvinylglycine (AVG). Plants were grown in a controlled environmental chamber with a 16/8-h light/dark cycle, 24°C/24°C day/night temperature, relative humidity of 60%, and photosynthetic photon flux density (200 µE at 10 cm above the ground). Plants cultivated in the sand-perlite mixture were watered with 1 g L^{-}1 N-free nutritive solution (Plant-Prod NPK 0-15-40).

Transformation of Medicago truncatula

To localize *MtKNOX3* expression during development, we use a construct carrying a 3500 bp putative promoter region of the *MtKNOX3* (Medtr1g012960) gene. The vector construction was described by Di Giacomo et al., (2016). Plasmids were introduced in the *Agrobacterium tumefaciens* EHA105 strain by electroporation and the construct was transformed into *M. truncatula* leaf explants via Agrobacterium-mediated transformation (Cosson *et al.*, 2015).

Crossing between *noot* and *Mtalog1* and *noot* mutant lines and proMtKNOX3::GUS

The *M. truncatula* crossing was performed according to the protocol described by Veerappan et al., 2014. *Mtnoot1*#202 (*Tnk507*), *Mtnoot2*#35 (*NF5464*), and *Mtnoot1Mtnoot2* (*NF2717NF5464*) homozygous mutant plants served as pollen

receiver female and were crossed independently with *Mtalog1* (*NF13390*, *NF17903* and *NF19406*) homozygous lines. The noot mutant lines also served as pollen receiver female and were crossed independently with *M. truncatula proMtKNOX3: GUS* transgenic plants.

M. truncatula DNA extraction and *Tnt1* insertional mutant genotyping

M. truncatula DNA was extracted from young leaves using CTAB. DNA was precipitated using 3M cold sodium acetate: isopropanol (0.1:1) and washed using 70% (v/v) ethanol. DNA samples were dried and resuspended in sterile water and performed RNase treatment finally (Roche).

To confirm that Kanamycin selected *M. truncatula* plants were transgenic for the *pMtKNOX3: GUS* transcriptional fusions, the genotyping was performed by testing the expression of the GUS reporter gene and by doing PCR with high-fidelity polymerase (Phusion, Thermo Fisher Scientific). Primers used for genotyping are indicated in supporting information Table S1. DNA was separated by electrophoresis and visualized on an ethidium bromide-stained agarose gel.

The *M. truncatula Mtnoot1* (*Tnk507* and *NF2717*), *Mtnoot2* (*NF5464*) and *Mtalog1* (*NF13390*, *NF17903* and *NF19406*) Tnt1 insertional lines were genotyped by semiquantitative PCR using goTaq DNA polymerase. *M. truncatula Mtalog1* (NF13390) mutant plants homozygous for a Tnt1 insertion 129 bp after AUG codon on the *MtALOG1* gDNA sequence have been genotyped by semi-quantitative PCR. Four oligonucleotides were used. Amplification of MtALOG1 (NF13390) without insertion using *MtALOG1-F1* and *MtALOG1-R1* gives a product of 426 bp. Amplification on MtALOG1 (NF13390) containing the *Tnt1* insertion was carried out using the oligonucleotides MtALOG1-F1 and LTR4 or MtALOG1-R1 and LTR6 located in the Long Terminal Repeat of the Tnt1 retroelement at the position 5258bp or 78bp, respectively. Mtalog1 (*NF17903*) and (*NF19406*) mutant plants homozygous for a Tnt1 insertion 8bp, 20bp after a terminal (TAA) on the MtALOG1 gDNA sequence, respectively. Amplification on *MtALOG1* (*NF17903* and *NF19406*) containing the Tnt1 insertion was carried out using the oligonucleotides MtALOG1-F2 and LTR4 or MtALOG1-R2 and LTR6 located in the Long Terminal Repeat of the Tnt1 retroelement at the position 167bp or 78bp (NF19406)/ 179bp or 66bp (NF17903), respectively. For *Mtnoot* mutants genotyping see (Magne *et al.*, 2018a).

Information concerning the primers used for Tnt1 insertional mutant genotyping is provided in Supplemental Table S1.

Construction of the overexpression, *MtALOG*-GFP and promoter: GUS plasmids

The full-length open reading frame (OFR: 595bp) and the ORF without termination codon (591bp) of *MtALOG1* was amplified by PCR using cDNA of R108 as the template with primers listed in Table S1, respectively. For the *MtALOG1* overexpression construct, the MtALOG1 ORF sequence was released from the pJET Amp vector using NcoI/ BstE II restriction sites and cloned into the binary vector pCAMBIA1302 (cut GFP fragment) under the control of the 35S-CaMV promoter. For the MtALOG1-GFP fusion, the MtALOG1 ORF (without termination codon) fragment was released from the pJET Amp vector using NcoI/ Bgl II restriction sites and fusion into the binary vector pCAMBIA1302 in pCAMBIA 1302 driven by the CaMV 35S promoter. For the promoter MtALOG1: GUS reporter, the 1955 bp of the MtALOG1 promoter region was amplified with the with Phusion polymerase (Thermo Fisher Scientific) using primers listed in Table S1. The amplified fragment was cloned into the pGEMT Easy vector (Promega) and sequenced from each extremity. The fragment corresponding to this promoter region was cloned into the pCAMBIA1391 vector as a BamH I /BspHI BamH1- BspHI/NcoI fragment and resulted in a translational fusion to the GUS gene. The resulting promoter-GUS region was sequenced for confirmation.

Inoculations of *Medicago*

The Sinorhizobium medicae WSM419 chloramphenicol resistant strain (Howieson & Ewing, 1986) was used to inoculate *M. truncatula* plants. WSM419 CpR was grown during 2 days, at 30°C, under darkness, on YEB Agar plate supplemented with 12,5 µg.mL^{-}1 of chloramphenicol antibiotic. WSM419 CpR liquid culture was then realized using one colony resuspended in 100mL of liquid YEB containing 12.5 µg.mL^{-}1 of chloramphenicol antibiotic. Rhizobia were grown 2 days, at 30°C, under darkness. WSM419 CpR liquid culture was centrifugated 20min at 4000rpm, liquid YEB was discarded and bacteria were resuspended in sterile water. The optical density of the rhizobia suspension was measured using spectrophotometer at 600nm wavelength and suspension was adjusted to an absorbance of 0.1 with sterile water.

Inoculations of *M. truncatula* seedling roots were performed three days after the seedling transfer on BNM plates supplemented with AVG, 2mL of WSM419 liquid suspension per plate was used. The WSM419 liquid suspension was dropped all along the root for two 2h and the excess of the solution was discarded. For the plants which grow in a perlite and sand mix (3:1, v/v), inoculations were performed seven days after the seedling transfer in the pot with 5mL of WSM419 liquid suspension per pot. Then plants were watered three times per week with 1g.L-1 N-free nutritive solution.

Light microscopy and sample preparation

Histochemical GUS staining was performed as described previously by Pichon *et al.*, (1992). Briefly, nodules samples were pre-fixed in cold acetone 90% during 1h at -20°C but for leaves without pre-fix. Two rinsings were done with phosphate buffer (50mM) and infiltrated 30min under vacuum (legume during early stages of the gluc staining buffer and then incubated at 37°C, overnight, under darkness. Freshly X-gluc-stained samples were fixed under vacuum (um (r vacuum (with phosphate buffer (50mM) and infiltrated 30min under vacuum (legume during early stages for 2h.

Sample sections embedded in Technovit resins were treated essentially as described in Van De Velde *et al.* (2006). Fixed samples were infiltrated 15min under vacuum (≈500mm Hg) in 0.05M sodium cacodylate buffer pH: 7 (0.05M), glutaraldehyde 1% and formaldehyde 4%. After infiltration, samples were rotated at 4°C overnight in the same buffer. Once dehydrated by successive ethanol baths, samples undergo three successive ethanol: Technovit stock solutions (3:1, v/v), (1:1, v/v) and (1:3, v/v) bathes and three 100% Technovit stock solution bathes [Technovit 7100 (100mL), HardenerI (1g)] at 4°C under agitation, each time 1h, respectively. Samples were included in Technovit resin using Teflon Histoform S embedding molds (Heraeus Kulzer). For GUS stained samples counter-stained with 0.05% (w/v) Ruthenium Red and for samples stained with 0.02% (w/v) Toluidine Blue, technovit sections with 8 µm thickness were carried out using a microtome RM 2165 (LEICA) and tungsten disposable blade (TC-65, LEICA).

Sections were dispatched on watered glass slides and dried on a dry block at 50°C until complete evaporation. Glass slides holding technovit sections were stained by a 10 min immersion in ruthenium red (0,05 %). Stained technovit sections were washed 20 times in a water bath and 20 times in a new water bath. Underhood, glass slides were dried, included in Eukitt ®mounting medium (R1339, EUKITT) covered

by a lamella and left for drying overnight. Technovit sections were observed thanks to the Apotome II microscope (Zeiss) and acquired using ZEN (blue edition) software. Pictures of whole organs were acquired using a ZESS stemi305 stereomicroscope.

RT-qPCR gene expression analysis

Total RNA extractions were performed from frozen tissues using TRIzol reagent (Ambion). RNA samples were treated with the TURBO DNA-free Kit (Ambion) according to the manufacturer's recommendations. Full-length cDNA was synthesized using the SuperScript II Reverse Transcriptase kit (Invitrogen) in the presence of Ribolock RNase Inhibitor (Thermo Scientific). Real-time RT-PCR reactions were performed in triplicate with 1µL of diluted cDNA in each reaction with the 5µL of 2X LightCycler FastStart DNA Master SYBR Green I kit (Ref. 04887352001, ROCHE), 2µL of each primer (2,5µM) in 10µL reaction volumes. The reaction process and conditions were described in the last chapter. *MtACT* and *MtRRM* reference genes were used for gene expression normalization. The final threshold cycle (Ct), efficiency and initial fluorescence (R0) for every reaction were calculated with the Miner algorithm (Zhao & Fernald, 2005). Relative expression levels were obtained from the ratio between R0 of the reference gene and R0 of the target gene. Information concerning the primers used for RT-qPCR gene expression analyses is provided in Supplemental Table S3.

Phylogeny of *M. truncatula ALOG* genes

Full-length ALOG family protein sequences of *Arabidopsis* and *M. truncatula* were downloaded from TAIR (http://www.arabidopsis.org/) and *M. truncatula* Mt4.0v1 genome via (https://phytozome.jgi.doe.gov) (Goodstein *et al.*, 2012). These sequences were aligned using ClustalW (Thompson *et al.*, 1994) and the phylogenetic tree was built using the neighbor-joining method with the MEGA7 program (Kumar *et al.*, 2016). The bootstrap method was used and set at 10.000 replicates for the phylogenetic analysis.

Accession numbers for all the genes and proteins described in this work are listed in Supplemental Table S1.

Supplemental Table 1. Characteristics of the *Mtalog1* mutant lines used in this study.

Gene mutated	possion of mutation	Name in this study	Accession ID	Mutagen	Background	References
MtALOG1		NF13390	*Medtr1g075990*	Tnt1	M. trunctula R108	This study
		NF19406	*Medtr1g075990*	Tnt1	M. trunctula R108	This study
		NF17903	*FMedtr1g075990*	Tnt1	M. trunctula R108	This study

Tnt1, the transposable element of tobacco (*Nicotiana tabacum*) cell type 1.

Supplemental Table 2. Primers used for qPCR.

Genes used for gene expression analysis	**Gene ID**	**Forward primer (5'-3')**	**Reverse primer (5'-3')**	**Origin**
MtACTIN11	Medtr2g008050	TGGCATCACTCAGTACCTTTCAACAG	ACCCAAAGCATCAAATAATAAGTCAACC	Plet *et al.*, 2011
AtACTIN2	NM_112764.3	CGCTCTTTCTTTCCAAGCTCAT	TCCTGCAAATCCAGCCTTC	Lee et al. 2013
MtRNA RECOGNITION MOTIF	Medtr6g034835	AGGGGCAAGTTCCTTCATTT	GGTAGAAGTGCTGGCTCAGG	Plet *et al.*, 2011
MtNOOT1	Medtr7g090020	TATGAATGAAGATCACCACCATAG	TCATGACCATGAGAGTGATGATG	Couzigou *et al.*, 2012
MtNOOT2	Medtr1g051025	TTACCCTCCAATGAGCGAAG	CCAGATCCCTAGGCTTAGAAGTCA	Magne *et al.*, 2018
MtNODULE INCEPTION PROTEIN	Medtr5g099060	GCAATGTGGGGATTTAGAGATT	GGAAGATTGAGAGGGGAAGCTT	Guan *et al.*, 2013
MtLEGHEMOGLOBIN1	Medtr5g066070	GCTTCTCAACTTCGAGCAACA	AGTTGCCAGTGCATCATAAGCT	Magne *et al.*, 2018
MtNODULE SPECIFIC CYSTEIN RICH PROTEIN 001	Medtr6g463200	CGTAAGCATTTTTCACACCA	TAGCGTCAGAAGTGCAAGGA	tMagne *et al.*, 2018
MtALOG1	Medtr1g075990	CTCTCACGTTGTAGTGGAGCA	CCCAAGCTTGTCGTAGAGGA	This study
MtALOG2	Medtr1g069825	CGGTGCTCATGTGCTTGAAT	TTTGTTTCTGGCTTCCCTCCA	This study
MtALOG3	Medtr7g097030	CATCGTCCACCTCTTTCCCTC	GTGCATCAAGGCTTCCCCAT	This study
MtALOG4	Medtr7g115700	TGGGGTAGCCTTGATGCTCT	GTTGCGGTTAGGTCTCTTCC	This study
MtALOG5	Medtr1g080210	CCACCACTCTCATTAGCCCT	TACCCCACGCTTGACGAAGA	This study
MtALOG6	Medtr3g031830	CCGGGTGTCCGTATTTTGGA	GTAGGCCGCTCTGAGTCTTC	This study
MtALOG7	Medtr5g072510	GAACTCGGGCGGTTAGGATT	GGTCCATTGCTATTCACCGC	This study
MtALOG8	Medtr2g092950	TCAACCTCGCAAGGAATCACA	GAAAGTGGAACGGGTGGTCT	This study
MtALOG9	Medtr8g086350	TCGGAGACTAACCCCTTTGC	GATCCCTCTTGCCTTTTGCTG	This study
MtALOG10	Medtr2g076400	TCCGCTTAGTCGATACGAGTC	CAGGTGGTTCGGTTTGTCCG	This study
MtPROLIFERATING INFLORESCENCE MERISTEM	Medtr8g066260	CAACTTTGAACATGGGTGGC	TGGCAGGTATACAATGGTTCC	Zhu et al., 2018
MtAPETALA1	Medtr8g066260	TTGGAGCGCTATGAAAGGTACTC	CCCTGTGACTCAGAATCATTTGC	Zhao et al., 2019
MtAGAMOUS a	Medtr3g452380	TCAAATGACTGCATTACAACCAAG	CTAGGAAGCAAATTACAGGTCTTTC	Zhu et al., 2018

ALOG: Arabidopsis LIGHT-DEPENDENT SHORT HYPOCOTYLS1 (LSH1) and Oryza G1

Supplemental Table 3. Oligonucleotides used for genotyping and construction.

Gene name and ID	**Mutant allele ID**	**Genomic sequence size**	***Tnt1* position on gDNA from ATG**	**Primer sequence (5'-3')**	**Primer sequence (5'-3')**	**PCR product size**	**Origin**
MtNOOT1 Medtr7g090020	*TNK507*	2804 bp	170 bp	TNK507_D GTTCAGCGACGTTGTTTTCAGC	TNK507_R CTGTGGAAATTCCCAAGACCC	555 bp	Magne et al., 2018 This study
				TNK507_D GTTCAGCGACGTTGTTTTCAGC	LTR4 TACCGTATCTCGGTGCTACA	179 bp	Ratet *et al*., 2010 This study
				LTR6 GCTACCAACCAAACCAAGTCAA	TNK507_R CTGTGGAAATTCCCAAGACCC	547bp	Ratet *et al*., 2010 This study
MtNOOT2 Medtr1g051025	*NF5464*	3374 bp	438 bp	NOOT2geno-D GAGGATCCTCTCGTCAGCCG	NOOT2geno-R ACCCTTTCCCCTTCATCTGC	413 bp	Magne et al., 2018 This study
				NOOT2geno-D GAGGATCCTCTCGTCAGCCG	LTR4 TACCGTATCTCGGTGCTACA	313 bp	Ratet *et al*., 2010 This study
				LTR6 GCTACCAACCAAACCAAGTCAA	NOOT2geno-R ACCCTTTCCCCTTCATCTGC	274 bp	Ratet *et al*., 2010 This study
MtALOG1 Medtr1g075990	*NF13390*	594 bp	123 bp	ALOG1-F1 CAGAAACACAATGCGTTTTTCTGA	ALOG1-R1 GGTGTTAGGACTCCTTTTGGGTGT	703bp	This study
				LTR4 TACCGTATCTCGGTGCTACA	ALOG1-R1 GGTGTTAGGACTCCTTTTGGGTGT	536bp	Ratet *et al*., 2010
MtALOG1 Medtr1g075990	*NF19406*	594 bp	602 bp	ALOG1-F2 CAGAAACACAATGCGTTTTTCTGA	ALOG1-R2 GGTGTTAGGACTCCTTTTGGGTGT	703bp	This study
				LTR4 TACCGTATCTCGGTGCTACA	ALOG1-R2 CAGAAACACAATGCGTTTTTCTGA	387bp	Ratet *et al*., 2010
MtALOG1 Medtr1g075990	*NF17903*	594 bp	616 bp	ALOG1-F2 CAGAAACACAATGCGTTTTTCTGA	ALOG1-R2 GGTGTTAGGACTCCTTTTGGGTGT	703bp	This study
				LTR4 TACCGTATCTCGGTGCTACA	ALOG1-R2 CAGAAACACAATGCGTTTTTCTGA	387bp	Ratet *et al*., 2010
MtALOG1	promotor			CGT AAC AAA TGG GAT CCT AAA AAA C	CAA ATG AAT TCA TGA CTA AAC TAG A	1975bp	This study

GENERAL DISCUSSION

GENERAL DISCUSSION

The *nbcl1nbcl2* double mutants highlight the role of the *NBCL2* genes in the patterning of aerial organs

Our study of the *NBCL* genes was initially focused on their roles in nodule development and identity. The legume *NBCL1*, *MtNOOT1*, *PsCOCH1* and *LjNBCL1*, genes are key regulators of the root nodule symbiosis. Indeed, the *NBCL1* clade is required to maintain the symbiotic organ identity and to repress the NVM root identity in both indeterminate and determinate nodule types (Yaxley *et al.*, 2001; Couzigou *et al.*, 2012; Magne *et al.*, 2018a,b). Apart from the nodule identity, however, the *NBCL1* genes impacted the development of several aerial organs in *Medicago*, pea and *Lotus*. In all three species, *nbcl1* mutations mainly affect the initiation, the development and/or the determinacy of stipules/nectary glands and flowers (Yaxley *et al.*, 2001; Couzigou *et al.*, 2012; Magne *et al.*, 2018b). Magne *et al.*, (2018b) noted that the Lotus *nbcl1* mutant showed stronger alterations of flower development compared to pea and *M. truncatula*, in which, the flower defect was mild (Couzigou *et al.*, 2012). In general, less important effects were observed in leaves but the mutants sow modification of the stipules, such as reduced serration of stipules in *Medicago* (Couzigou *et al.*, 2012) and reduced or absent stipules in pea (Yaxley *et al.*, 2001; Couzigou *et al.*, 2012). *NBCL2* genes are often co-expressed with *NBCL1* genes in aerial organs and both *NBCLs* transcripts accumulated mainly in nodes where stipules/nectaries arise, in leaves, and in flowers. Moreover, in Medicago, the proNOOT2::GUS expression pattern is associated to the frontiers between the different organs similar to the published proNOOT1::GUS gene expression pattern (Couzigou *et al.*, 2015). In addition the proNOOT2::GUS expression pattern overlaps with the proNOOT1::GUS one at the base of young stipules, leaves and leaflets and also at the base of floral organs and pod. However, the *nbcl2* mutants did not display obvious aerial development defects. To understand if *NBCL2* genes are involved in the stipules, leaves, and flower development, the *Medicago* and pea *nbcl1nbcl2* double mutants were characterized for their aerial phenotypes and similar observations were made. As expected, the *Mtnoot1noot2* double mutants showed that the *Mtnoot2* mutation increased the *Mtnoot1* mutant aerial phenotypes, including stipule phenotypes amplification and strong flower alteration leading to partial

sterility. Most of stipules had needle-like structure and some formed leaf-like stipule structures. More complex structures were also observed. In addition, flowers also displayed strong defect on carpel and stamen development forming pod-like structures from aborted floral primordia leading to sterility. Furthermore, the double mutant displayed strong alteration on inflorescences and internode, also changed the leaf size. These modifications were not observed in the *nbcl1* mutant. In pea, similar exaggerations of the *Pscoch1* phenotype in *Pscoch1coch2* were observed, including an increase alteration of stipules identity and additional flower defects despite that the *Pscoch1* mutation is already strong in pea. All these results indicate that the *NBCL2* genes participated in the patterning of aerial organs and act redundantly with *NBCL1*.

NBCL genes redundantly control plant architecture

In Arabidopsis, ectopic *BOP1* or *BOP2* expression results in either short plants with floral pedicels pointing downward (Ha et al., 2007) or short bushy plants with irregular internodes (Norberg et al., 2005). In legumes, *nbcl1* displayed a shorted status while the *nbcl2* mutation only slightly increased the plant height. However, *nbcl1nbcl2* double mutant showed a greatly increased plant height. Interestingly, in the monocot plant *Brachypodium*, the simultaneous mutation of the two *NBCL genes* (*BdCUL4* and *BdLAXA*) in the *Bdcul4laxa* double mutant resulted in plants with a dwarf phenotype (Liu et al, unpublished data) although the *Bdcul4* and *Bdlaxa* single mutants show a wild type internode phenotype (Magne *et al.*, 2020). These data suggest that the *NBCLs* function together to control internode elongation but the effect presents the variation in different species.

The architecture of the inflorescence, the shoot system that bears the flowers, is the main component of the huge diversity of forms found in flowering plants (Benlloch *et al.*, 2015). The *coch1* mutant shows mild alterations with occasionally fused flowers and the *coch2* mutant has wild type inflorescences. In contrast, the *coch1coch2* form inflorescences with more flowers and elongated flower stalk. A similar phenotype is also observed in the *Mtnoot1noot2* double mutant that produces modified inflorescences with up to ten flowers on a single flower stalk. The two corresponding single mutants did not show these modifications. In addition, flowers can form directly from axillary nodes without flower stalks or sepal transformation to leaflet was also observed in the *Mtnoot1noot2* double mutant. Furthermore, in the

double mutant several inflorescences originated from the same node and developed extremely long flower stalk. These results indicate that *NBCL1* and *NBCL2* redundantly control plant architecture. In Arabidopsis, loss-of-function *bop1bop2* mutants show minor defects in inflorescence and floral architecture but in combination with *lfy* or *ap1*, synergistic defects in floral fate and shoot architecture was revealed. BOP1 and BOP2 function in parallel with LFY to control determinacy in floral shoots through the activation of AP1 and the repression of AGL24 in developing flowers. For this BOP1 and BOP2 are recruited to the promoter of AP1 in part through direct interactions with the TGA bZIP factor PAN (Xu *et al.*, 2010). In contrast, the *Mtnoot1pan* and *Mtnoot2pan* double mutant just show *noot1* or *noot2* phenotypes, respectively (Magne et al, unpublished data). It may be worth to test the *Mtnoot Mtpan Mtap1* tripe mutants.

NBCL1 genes regulate shoot branching and control strigolactones production

Shoot branching patterns result from the spatio-temporal regulation of axillary bud outgrowth. Numerous endogenous, developmental and environmental factors are integrated at the bud and plant levels to determine the number of growing shoots. In legume, the mutants show increased branches in *M. trunctula* and *P. sativum*. This is more evident in the *coch1* mutant producing cotyledonary branches and also small branches at upper nodes. In contrast, WT plants and the *nbcl2* mutant never produce cotyledonal branches and just a few small branches can be observed at upper nodes. This shoot branching phenotype was to our knowledge, never reported in previous studies for mutants of the *NBCL* genes in eudicot. In monocot plant, recent findings unveiled a BOP orthologue, HvCUL4, with a role in branching in barley. *Hvcul4* mutants show a reduced tilling and deregulated number of axillary buds in an axil (Tavakol *et al.*, 2015). TRU1, the orthologue in maize, also plays a role in regulating branching. *Zmtru1* mutants displayed an increased axillary branching, an opposite phenotype of *Hvcul4* mutant. Moreover, the *NBCLs*, *BdCUL4* and *BdLAXA*, in *Brachypodium* have a role in regulating axillary branching and act antagonistically (Magne *et al.*, 2020). Similar to the phenotype observed in the *Hvcul4* mutants, *Bdcul4* also reduced the tillers while the *Bdlaxa* greatly increased the axillary branching. In the maize axillary meristem, the expression of *ZmTRU1* was directly activated by ZmTB1(Dong *et al.*, 2017). Despite the different functions in axillary

branching, the orthologue of *AtBOP1/2* in barley, maize, and *Brachypodium* are regulating the axillary branch development. The connection between BOP and key branching regulator BRC1/TB1 makes BOP an important branching regulator.

Legumes are useful for shoot-branching researches because of several features that facilitate studies of axillary buds and long-distance signaling. They have long internodes separating axillary buds and the shoot tip, are easy to graft, are amenable to root xylem-sap extraction, and their axillary buds are accessible for hormone applications, growth measurements, and other related analyses. Additionally, for many pea varieties, most axillary buds are dormant but have the potential for release throughout development (Beveridge *et al.*, 2009). The orthologues of *AtBOP1/2* were also expressed in the axillary bud in several *Populus* species (Sjödin *et al.*, 2009; Howe *et al.*, 2015; Wang *et al.*, 2019b).

In pea, the *COCH1* expression in axillary buds suggests that NBCL1 may represent new actors regulating branching. Indeed, our results suggest that PsCOCH1 acts as a negative regulator of shoot branching and as an integrator of multiple pathways. Our grafting experiments indicate that PsCOCH1 is required for the production of a long-distance signal repressing bud outgrowth. In addition, because only *coch1* grafted on *coch1* rootstock show an increased branching, it also shows that COCH1 participates in the perception of the branching signal. In addition, the fact that the *Pscoch1* mutant responds to SL application suggests that PsCOCH1 act upstream of the SL signaling. In support of this, we showed that *PsCOCH1* expression in axillary buds and roots was rapidly reduced by SL treatment, especially in root. These data indicate that *PsCOCH1* was negatively regulated by SL and correlate with the repression of bud growth with the same treatment. As described previously (Foo et al., 2005), SL biosynthesis *RMS1* and *RMS5* genes are also downregulated by the SL treatment. Because the expression of these genes is repressed by SL treatment in *coch1* background, the highest expression observed in the mutant might reflect a reduced SL content in the *coch1* background. Similar to previous *RMS1* expression data, *RMS5* has the characteristic acropetally expression profile, with higher expression in the roots (Johnson *et al.*, 2006).

***NBCL* genes are involved in flowering-time regulation**

Flowering time is a major adaptive trait in the life strategy of flowering plants, which have to synchronize their reproduction with favorable environmental conditions. The transition from vegetative growth to flowering, termed floral induction, is controlled by physiological signals and genetic networks that integrate environmental (photoperiod and temperature) and endogenous (stage of the plant) conditions (Levy & Dean, 1998; Colasanti & Sundaresan, 2000; Srikanth & Schmid, 2011; Ietswaart *et al.*, 2012; Romera-branchat *et al.*, 2014). BOP1 and BOP2 are expressed in lateral organs close to boundaries of the SAM during vegetative development (Ha *et al.*, 2004, 2007; Norberg *et al.*, 2005; Hepworth *et al.*, 2005; Karim *et al.*, 2009; Xu *et al.*, 2010; Couzigou *et al.*, 2012). Floral induction in Arabidopsis by FT requires direct repression of BOP genes by the homeodomain protein PENNYWISE (PNY), which binds to the promoters of *BOP1* and *BOP2* (Andrés *et al.*, 2015). Ectopic *BOP* gene expression in the *pny* mutant or the gain-of-function *bop1-6d* mutation strongly reduced *FD* transcription and confers the late flowering of *pny* and *bop1-6d* mutants (Andrés *et al.*, 2015).

Our work also shows that the legume *NBCLs* are also involved in flowering-time regulation. Mutations in *PsCOCH1* and *MtNOOT2* result in late flowering although the *Pscoch2* and *Mtnoot1* mutants are not delayed. The *nbcl1nbcl2* double mutants are also delayed for flowering in both species. Consequently, the *PsFTa1* (former as *FTLa*) expression level was extremely downregulated in *Pscoch1* and *Pscoch1coch2* mutant. In contrast, the *PsLF* (*PsTFL1c*) expression was greatly upregulated in *Pscoch1* and *Pscoch1coch2* mutants. While in *coch2* mutant, either *PsFTa1* or *PsLF* show a wild type level of expression. In addition, the *PsCOCH1* expression was increased in the *coch2* mutant and also the *PsCOCH2* expression was elevated in the *coch2* mutant. This indicates that the *NBCL* genes repress each other and that *PsCOCH1* activate *FTa1* and repress the *PsLF* expression. However, the *FT* gene regulation model for *PsCOCH1* gene in pea was opposite to the *BOPs* in Arabidopsis, where *BOPs* repress the *FT* expression through reduced *FD* transcription (Andrés *et al.*, 2015). Indeed, there are several differences between Arabidopsis and legumes relating to flowering time control, with evolutionary and genetic data indicating the likely involvement of legume-specific genes and mechanisms. For example, legumes lack a clear ortholog of the key Arabidopsis vernalization-responsive gene, *FLC* (Hecht *et al.*, 2005) and the ability to respond to vernalization

has likely evolved independently in legumes and other plant families (Bouché *et al.*, 2017). A mode of action was recently proposed in Arabidopsis, where FT and TSF proteins interact with BRC1 in axillary buds to inhibit floral induction. The *brc1-2* mutant is highly branched, and its lateral branches flower earlier (Niwa *et al.*, 2013). To confirm that the FT module is different in Arabidopsis and pea and to better understand the results we got, the expression of *PsBRC1* in *Pscoch1* has to be tested.

NBCL functions in aerial vegetative and reproductive organs patterning are conserved in grasses

Our *Brachypodium NBCL* study supported well the previous findings and fit with the roles attributed to the barley *NCBLs*. *BdCUL4* is involved in the control of tillering and in the promotion of the proximal/distal leaf differentiation and especially for the correct formation of the ligular region. BdCUL4 is required for the formation of the ligule and auricles as described for its barley ortholog *HvUniculme4* (Tavakol *et al.*, 2015; Magne *et al.*, 2020). This work involving several plant models and their corresponding *nbcl1* mutants revealed also a common ontology of the organ located at the leaf axil in dicots and grasses. *Mtnoot1*, *Pscoch1*, show modified stipules (asymmetry, simplification or complete homeosis in leaves), *Ljnbcl1* lack nectaries that are supposed to be modified stipules (Irmisch, 1861; Heyn, 1976), *Atbop1bop2* lack stipules and the grasses barley and *Brachypodium* lack the ligule. These organs, dicots stipules and nectaries, and monocot ligules are all located at the leaf axil a region of the leaf that corresponds to a boundary zone whose functioning is regulated by these *NBCL* boundary genes. The *nbcl* mutant phenotypes reported for all these organs suggests that dicots stipules and nectaries, and monocot ligules have a common origin and should have a common ancestral organ at the leaf axil which has diversified during plant evolution. Interestingly, *nbcl1* mutants increased the branching in legumes, while *Hvcul4* and *Bdcul4* reduced the tillering in monocot. In contrast, the legume *nbcl2* mutant has no phenotype alone while *Bdlaxa* and *Hvlaxa* displayed strong defects alone (Jost *et al.*, 2016; Magne *et al.*, 2020). Furthermore, both *BdCUL4* and *BdLAXA* are regulating the inflorescence determinacy (Magne *et al.*, 2020). In legume, the NBCLs were redundantly regulating plant development and the *nbcl1nbc2* increased the defects observed in single mutant stipule, leaf, and flower organs. Consistent with this, in *Brachypodium* the *BdCUL4* and *BdLAXA* also have

redundant functions in plant development. The *Bdcul4laxa* double mutants indeed show a dwarf phenotype and strongly modified spikelet development resulting in sterility. This phenotype is also observed in the *Mtnoot1noot2* double mutant. In addition, *Bdcul4laxa* double mutants show an extreme modification of the leaf architecture resulting in curling leaves. Thus our study is in agreement with other ones and shows that the *NBCL* genes have been conserved in dicots and grasses and are redundantly regulating the inflorescence architecture patterning and the control of floral organ identity.

NBCL1-dependent abscission process are not conserved in grass

NBCL1 genes in legumes and in other dicots are involved in aerial organs abscission (Couzigou *et al.*, 2015). To investigate the role of the *NBCL* genes in the abscission process in grasses, *B. distachyon* was used as a model plant since it has not been selected for a non-abscission character or for spikelet architecture modification that impacts the seed shedding. Unfortunately, *Bdcul4* and *Bdlaxa* single mutants alone were not altered in the abscission process (Magne *et al.*, 2020). A strong overlap between the two gene expressions was observed in almost all the organs of the plant. Thus, because of their potential redundancies, the double mutant *Bdcul4laxa* was constructed and characterized to clearly determine if the abscission process is NBCL-dependent in grasses. Our work shows that abscission was not modified in the *Bdcul4laxa* double mutant. Thus, we can conclude that the NBCL1-dependent abscission process is not conserved in the grass.

Investigation of potential interacting partners and downstream targets of NOOT proteins

NBCL genes encode BTB/POZ and ankyrin repeats domains, do not have DNA binding elements or nuclear localization signals, and do not encode transcription factors *sensu stricto*. The NOOT proteins are co-transcriptional factors and their interacting partners directly interact with downstream target genes promotor sequences to control their activation or repression. In *M. truncatula*, Magne et al., (unpublished data) show that the MtNOOT1 and MtNOOT2 are able to form homo and heterodimers together and identified the nodule specific TGA type bZIP TF, MtPAN, as a direct interacting partner of the two MtNOOT proteins. Unfortunately,

the *Mtpan* mutation alone or in combination with noot mutations did not alter the nodule identity. For this reason, we thought it could be interesting to test other potential interacting transcription factors. A recent publication mentioned that NBCL proteins are also able to interact with members of the Arabidopsis ALOG proteins (Xu *et al.*, 2016). In *Medicago*, there are at least 10 genes encoding ALOG proteins, all of them displaying DNA-binding sequence and nuclear localization signals. Among them, *MtTALOG1* is particularly interesting because of its high expression in nodule and aerial organs. Our preliminary results show that the mutation *Mtalog1* increased the nodule number and the nodules were multi-lobed suggesting that MtALOG1 could have a role in nodulation and nodule organ identity. Indeed, preliminary results from *Mtnoot1alog1* double mutant show that the nodules are also multi-lobed and changed the ratio of the nodule to root conversion in *noot1*. Therefore, it could worth analyzing in detail the nodule identity of these double mutants and to test if these MtALOG transcription factors are also able to interact with the MtNOOT proteins. ALOG proteins represent thus candidates of interest that are susceptible to interact specifically with NBCL proteins in nodules. The identification of the NOOT interacting partner among TGA bZIP and ALOG protein families will significantly improve our understanding of the gene network involved in nodule development and identity. In addition, the identification of the MtALOG1 as a potential interacting partner of the NOOT proteins provides the opportunity to identify the downstream targets of this transcription factor.

Moreover, in Arabidopsis, class II *MtKNOX* genes are involved in symbiosis (Azarakhsh *et al.*, 2015; Elisabetta *et al.*, 2016). Magne *et al.*, (2018a) highlighted that class II *MtKNOX* genes expression levels and expression patterns were modified in *Mtnoot* mutants and observed a switch of the proMtKNOX9::GUS expression pattern from the NCM region to the peripheral vasculature. Based on this work, we constructed a proMtKNOX3::GUS transgenic line and introduced the transgene in the *noot* mutants by crossing. Similarly to the proMtKNOX9::GUS expression pattern, proMtKNOX3::GUS is expressed in the entire nodule primordia at an early stage in wild type and in the *noot1* and *noot1noot2* mutant. In contrast, proMtKNOX3::GUS expressed pattern was detected in the apical meristem at later stages of nodule development. The fusion was also expressed on the root cylinder but was absent from the nodule peripheral vasculature. In contrast, in the *noot1* and *noot1noot2* mutants,

the proMtKNOX3::GUS fusion expression was lost from the apical misterm region and switch to the vasculature and the base of the nodule. This confirms previous results and indicates that some elements of the root developmental program have been reused for the development of the nodule vascular bundle. In addition, it appears that some regulatory elements like the class II *MtKNOX* genes have also been recruited for the NCM development. It is known that class I *KNOX* genes are the indirect target of *NBCL* and are involved in the stem cell niche division, proliferation and maintenance throughout complex phytohormone regulations (Žádníková & Simon, 2014). Thus, a regulatory loop involving NBCL, class I KNOX and class II KNOX may be involved in the identity and the maintenance of the different meristematic zones in the apical part of the nodule.

CONCLUSIONS

This PhD work shows that an ancestral function of the *NBCL* genes is conserved for the stipules/nectaries/ligules, leaves, and flowers patterning across dicots and grasses. The *NBCLs* function redundantly regulates aerial and underground plant development. Surprisingly, NBCLs are also controlling the phytohormone pathway to shape plant architecture. This work also shows that the role of the *NBCL* genes in symbiotic organ identity is conserved in different legumes whatever the nodule meristem nature. It finally indicates that not only the *NBCL* genes, but complete functional modules involving may be ALOG was recruited several times in evolution for plant shaping and inception of new specialized organs.

REFERENCES

Abe M, Kobayashi Y, Yamamoto S, Ichinoki H, Notaguchi M, Goto K. **2005**. FD , a bZIP Protein Mediating Signals from the Floral Pathway Integrator FT at the Shoot Apex. *Science* **309**: 1052–1057.

Aguilar-Martínez JA, Poza-Carrión C, Cubas P. **2007**. Arabidopsis Branched1 acts as an integrator of branching signals within axillary buds. *Plant Cell* **19**: 458–472.

Aichinger E, Kornet N, Friedrich T, Laux T. **2012**. Plant Stem Cell Niches. *Annual Review of Plant Biology* **63**: 615–636.

Aida M, Ishida T, Fukaki H, Fujisawa H, Tasaka M. **1997**. Genes involved in organ separation in Arabidopsis: An analysis of the cup-shaped cotyledon mutant. *Plant Cell* **9**: 841–857.

Aida M, Ishida T, Tasaka M. **1999**. Shoot apical meristem and cotyledon formation during Arabidopsis embryogenesis: Interaction among the CUP-SHAPED COTYLEDON and SHOOT MERISTEMLESS genes. *Development* **126**: 1563–1570.

Aida M, Tasaka M. **2006a**. Genetic control of shoot organ boundaries. *Current Opinion in Plant Biology* **9**: 72–77.

Aida M, Tasaka M. **2006b**. Morphogenesis and patterning at the organ boundaries in the higher plant shoot apex. *Plant Molecular Biology* **60**: 915–928.

Aida M, Vernoux X, Furutani M, Traas J, Tsaka M. **2002**. Erratum: Roles of PIN-FORMED1 and MONOPTEROS in pattern formation of the apical region of the Arabidopsis embryo (Development (2002) vol. 129 (3965-3974)). *Development* **129**: 4877.

Akiyama K, Matsuzaki KI, Hayashi H. **2005**. Plant sesquiterpenes induce hyphal branching in arbuscular mycorrhizal fungi. *Nature* **435**: 824–827.

Alonso-Cantabrana H, Ripoll JJ, Ochando I, Vera A, Ferrándiz C, Martínez-Laborda A. **2007**. Common regulatory networks in leaf and fruit patterning revealed by mutations in the Arabidopsis ASYMMETRIC LEAVES1 gene. *Development* **134**: 2663–2671.

Alunni B, Gourion B. **2016**. Terminal bacteroid differentiation in the legume-rhizobium symbiosis: nodule-specific cysteine-rich peptides and beyond. *The New phytologist* **211**: 411–417.

Alvarez-Buylla ER, Benítez M, Adriana C-P, Cador ÁC, Folter S de, Buen AG de, Garay-Arroyo A, García-Ponce B, Jaimes-Miranda F, V. R, *et al.* 2010. Flower Development. *The Arabidopsis Book* **1**: 1–57.

Andrés F, Coupland G. **2012**. The genetic basis of flowering responses to seasonal cues. *Nature Reviews Genetics* **13**: 627–639.

Andrés F, Romera-Branchat M, Martínez-Gallegos R, Patel V, Schneeberger K, Jang S, Altmüller J, Nürnberg P, Coupland G. **2015**. Floral induction in Arabidopsis by flowering locus t requires direct repression of blade-on-petiole genes by the homeodomain protein pennywise. *Plant Physiology* **169**: 2187–2199.

Andrews M, Andrews ME. **2017**. Specificity in legume-rhizobia symbioses. *International Journal of Molecular Sciences* **18**.

Andriankaja A, Boisson-Dernier A, Frances L, Sauviac L, Jauneau A, Barker DG, de Carvalho-Niebel F. **2007**. AP2-ERF transcription factors mediate Nod factor dependent Mt ENOD11 activation in root hairs via a novel cis-regulatory motif. *The Plant cell* **19**: 2866–85.

Ardley JK, Reeve WG, O'Hara GW, Yates RJ, Dilworth MJ, Howieson JG. **2013**. Nodule morphology, symbiotic specificity and association with unusual rhizobia are distinguishing features of the genus Listia within the southern African crotalarioid clade Lotononis s.l. *Annals of Botany* **112**: 1–15.

Arite T, Iwata H, Ohshima K, Maekawa M, Nakajima M, Kojima M, Sakakibara H, Kyozuka J. **2007**. DWARF10, an RMS1/MAX4/DAD1 ortholog, controls lateral bud outgrowth in rice. *Plant Journal* **51**: 1019–1029.

Arite T, Umehara M, Ishikawa S, Hanada A, Maekawa M, Yamaguchi S, Kyozuka J. **2009**. D14, a strigolactone-Insensitive mutant of rice, shows an accelerated outgrowth of tillers. *Plant and Cell Physiology* **50**: 1416–1424.

Arnaud N, Pautot V. **2014**. Ring the BELL and tie the KNOX: Roles for TALEs in gynoecium development. *Frontiers in Plant Science* **5**: 1–7.

Arrighi J-F, Barre A, Ben Amor B, Bersoult A, Soriano LC, Mirabella R, de Carvalho-Niebel F, Journet E-P, Ghérardi M, Huguet T, *et al.* 2006. The Medicago truncatula lysin motif-receptor-like kinase gene family includes NFP and new nodule-expressed genes. *Plant physiology* **142**: 265–79.

Azarakhsh M, Kirienko a. N, Zhukov V a., Lebedeva M a., Dolgikh E a., Lutova L a. 2015. KNOTTED1-LIKE HOMEOBOX 3: A new regulator of symbiotic nodule development. *Journal of Experimental Botany* **66**: 7181–7195.

Babb S, Muehlbauer GJ. **2003**. Genetic and morphological characterization of the barley uniculm2 (cul2) mutant. *Theoretical and Applied Genetics* **106**: 846–857.

Barbier FF, Dun EA, Beveridge CA. **2017**. Apical dominance. *Current Biology* **27**: R864–R865.

Barton MK. **2010**. Twenty years on: The inner workings of the shoot apical meristem, a developmental dynamo. *Developmental Biology* **341**: 95–113.

Battaglia M, Ripodas C, Clua J, Baudin M, Aguilar OM, Niebel A, Zanetti ME, Blanco FA. **2014**.

A Nuclear Factor Y Interacting Protein of the GRAS Family Is Required for Nodule Organogenesis, Infection Thread Progression, and Lateral Root Growth. *Plant Physiology* **164**: 1430–1442.

Becking JH. **1984**. Identification of the endophypte ofDryas andRubus (Rosaceae). *Plant and Soil* **78**: 105–128.

Becraft PW, Bongard-Pierce DK, Sylvester AW, Scott Poethig R, Freeling M, Poethig RS, Freeling M, Scott Poethig R, Freeling M. **1990**. The liguleless-1 gene acts tissue specifically in maize leaf development. *Developmental Biology* **141**: 220–232.

Behm JE, Geurts R, Kiers ET. **2014**. Parasponia: a novel system for studying mutualism stability. *Trends in Plant Science* **19**: 757–763.

Bell EM, Lin WC, Husbands AY, Yu L, Jaganatha V, Jablonska B, Mangeon A, Neff MM, Girke T, Springer PS. **2012**. Arabidopsis lateral organ boundaries negatively regulates brassinosteroid accumulation to limit growth in organ boundaries. *Proceedings of the National Academy of Sciences of the United States of America* **109**: 21146–21151.

Bencivenga S, Serrano-Mislata A, Bush M, Fox S, Sablowski R. **2016**. Control of Oriented Tissue Growth through Repression of Organ Boundary Genes Promotes Stem Morphogenesis. *Developmental Cell* **39**: 198–208.

Benedito VA, Torres-Jerez I, Murray JD, Andriankaja A, Allen S, Kakar K, Wandrey M, Verdier J, Zuber H, Ott T, *et al.* 2008. A gene expression atlas of the model legume Medicago truncatula. *Plant Journal* **55**: 504–513.

Benlloch R, Berbel A, Ali L, Gohari G, Millán T, Madueño F. **2015**. Genetic control of inflorescence architecture in legumes. *Frontiers in Plant Science* **6**: 1–14.

Benlloch R, Navarro C, Beltrán JP, Cañas LA. **2003**. Floral development of the model legume Medicago truncatula: Ontogeny studies as a tool to better characterize homeotic mutations. *Sexual Plant Reproduction* **15**: 231–241.

Berbel A, Ferrándiz C, Hecht V, Dalmais M, Lund OS, Sussmilch FC, Taylor S a., Bendahmane A, Ellis THN, Beltrán JP, *et al.* 2012. VEGETATIVE1 is essential for development of the compound inflorescence in pea. *Nature Communications* **3**.

Berbel A, Navarro C, Ferŕndiz C, Cañas LA, Madueño F, Beltrán JP. **2001**. Analysis of PEAM4, the pea AP1 functional homologue, supports a model for AP1-like genes controlling both floral meristem and floral organ identity in different plant species. *Plant Journal* **25**: 441–451.

Berg RH, Langenstein B, Silvester WB. **1999**. Development in the Datisca-Coriaria nodule type. *Canadian Journal of Botany* **77**: 1334–1350.

Berger Y, Harpaz-Saad S, Brand A, Melnik H, Sirding N, Alvarez JP, Zinder M, Samach A,

Eshed Y, Ori N. **2009**. The NAC-domain transcription factor GOBLET specifies leaflet boundaries in compound tomato leaves. *Development* **136**: 823–832.

Berry AM, Sunell LA. **1990**. The Infection Process and Nodule Development. *The Biology of Frankia and Actinorhizal Plants*: 61–81.

Besnard F, Vernoux T, Hamant O. **2011**. Organogenesis from stem cells in planta: Multiple feedback loops integrating molecular and mechanical signals. *Cellular and Molecular Life Sciences* **68**: 2885–2906.

Beveridge CA, Dun EA, Rameau C. **2009**. Pea Has Its Tendrils in Branching Discoveries Spanning a Century from Auxin to Strigolactones. *Plant Physiology* **151**: 985–990.

Beveridge CA, Kyozuka J. **2010**. New genes in the strigolactone-related shoot branching pathway. *Current Opinion in Plant Biology* **13**: 34–39.

Beveridge CA, Murfet IC. **1996**. The gigas mutant in pea is deficient in the floral stimulus. *Physiologia Plantarum* **96**: 637–645.

Beveridge CA, Ross JJ, Murfet IC. **1996**. Branching in Pea (Action of Genes Rms3 and Rms4). *Plant Physiology* **110**: 859–865.

Beveridge CA, Symons GM, Murfet IC, Ross JJ, Rameau C. **1997**. The rms1 mutant of pea has elevated indole-3-acetic acid levels and reduced root-sap zeatin riboside content but increased branching controlled by graft-transmissible signal(s). *Plant Physiology* **115**: 1251–1258.

Beveridge CA, Symons GM, Turnbull CGN. **2000**. Auxin Inhibition of Decapitation-Induced Branching Is Dependent on Graft-Transmissible Signals Regulated by Genes Rms1 and Rms2. *Plant Physiology* **123**: 689–698.

Beveridge CA, Weller JL, Singer SR, Hofer JMI. **2003**. Axillary meristem development. Budding relationships between networks controlling flowering, branching, and photoperiod responsiveness. *Plant Physiology* **131**: 927–934.

Blázquez MA, Ferrándiz C, Madueño F, Parcy F. **2006**. How floral meristems are built. *Plant Molecular Biology* **60**: 855–870.

Blixt S. **1967**. Linkage studies in Pisum.VII. the manifestation of the genes CRI and COCH and the bouble recessive in Pisum.

Boatwright JS, Wink M, van Wyk B-E. **2011**. The generic concept of Lotononis (Crotalarieae, Fabaceae): Reinstatement of the genera Euchlora, Leobordea and Listia and the new genus Ezoloba. *Taxon* **60**: 161–177.

Bolduc N, O'connor D, Moon J, Lewis M, Hake S. **2012**. How to pattern a leaf. *Cold Spring Harbor Symposia on Quantitative Biology* **77**: 47–51.

Bomblies K, Doebley JF. **2006**. Pleiotropic effects of the duplicate maize FLORICAULA/LEAFY genes zfl1 and zfl2 on traits under selection during maize domestication. *Genetics* **172**: 519–531.

Bommert P, Whipple C. **2018**. Grass inflorescence architecture and meristem determinacy. *Seminars in Cell and Developmental Biology* **79**: 37–47.

Bonnett o. t. 1935. The development of the barley spike. *Journal of Biological Education* **51**: 451–457.

Bonnett OT. **1936**. The development of the wheat spike. *Journal of Agricultural Research* **53**: 445–451.

Booker J, Auldridge M, Wills S, McCarty D, Klee H, Leyser O. **2004**. MAX3/CCD7 is a carotenoid cleavage dioxygenase required for the synthesis of a novel plant signaling molecule. *Current Biology* **14**: 1232–1238.

Booker J, Sieberer T, Wright W, Williamson L, Willett B, Stirnberg P, Turnbull C, Srinivasan M, Goddard P, Leyser O. **2005**. MAX1 encodes a cytochrome P450 family member that acts downstream of MAX3/4 to produce a carotenoid-derived branch-inhibiting hormone. *Developmental Cell* **8**: 443–449.

Borghi L, Bureau M, Simon R. **2007**. Arabidopsis JAGGED LATERAL ORGANS is expressed in boundaries and coordinates KNOX and PIN activity. *Plant Cell* **19**: 1795–1808.

Bouché F, Woods DP, Amasino RM. **2017**. Winter memory throughout the plant kingdom: Different paths to flowering. *Plant Physiology* **173**: 27–35.

Bowman JL, Alvarez J, Weigel D, Meyerowitz EM, Smyth DR. **1993**. Control of flower development in Arabidopsis thaliana by APETALA1 and interacting genes. *Development* **743**: 721–743.

Bowman JL, Eshed Y. **2000**. Formation and maintenance of the shoot apical meristem. *Trends in Plant Science* **5**: 110–115.

Bradley D, Ratcliffe O, Vincent C, Carpenter R, Coen E. **1997**. Inflorescence commitment and architecture in Arabidopsis. *Science* **275**: 80–83.

Brand A, Shirding N, Shleizer S, Ori N. **2007**. Meristem maintenance and compound-leaf patterning utilize common genetic mechanisms in tomato. *Planta* **226**: 941–951.

Braun N, de Saint Germain A, Pillot J-P, Boutet-Mercey S, Dalmais M, Antoniadi I, Li X, Maia-Grondard A, Le Signor C, Bouteiller N, *et al.* 2012. The Pea TCP Transcription Factor PsBRC1 Acts Downstream of Strigolactones to Control Shoot Branching. *Plant Physiology* **158**: 225–238.

Breakspear A, Liu C, Roy S, Stacey N, Rogers C, Trick M, Morieri G, Mysore KS, Wen J, Oldroyd GED, *et al.* 2014. The Root Hair "Infectome" of Medicago truncatula Uncovers Changes in

Cell Cycle Genes and Reveals a Requirement for Auxin Signaling in Rhizobial Infection. *The Plant Cell Online* **26**: 4680–4701.

Brkljacic J, Grotewold E, Scholl R, Mockler T, Garvin DF, Vain P, Brutnell T, Sibout R, Bevan M, Budak H, *et al.* 2011. Brachypodium as a Model for the Grasses: Today and the Future. *Plant Physiology* **157**: 3–13.

Bureau M, Rast MI, Illmer J, Simon R. 2010. JAGGED LATERAL ORGAN (JLO) controls auxin dependent patterning during development of the Arabidopsis embryo and root. *Plant Molecular Biology* **74**: 479–491.

Busch BL, Schmitz G, Rossmann S, Piron F, Ding J, Bendahmane A, Theres K. 2011. Shoot branching and leaf dissection in tomato are regulated by homologous gene modules. *Plant Cell* **23**: 3595–3609.

Camp RO den, Streng A, Mita S De, Cao Q, Polone E, Liu W, Ammiraju JSS, Kudrna D, Wing R, Untergasser A, *et al.* 2011. LysM-Type Mycorrhizal Receptor Recruited for Rhizobium Symbiosis in Nonlegume Parasponia. *Science* **331**: 909–912.

Canet JV, Dobón A, Fajmonová J, Tornero P. 2012. The BLADE-ON-PETIOLE genes of Arabidopsis are essential for resistance induced by methyl jasmonate. *BMC Plant Biology* **12**: 1–13.

Canet JV, Dobón A, Roig A, Tornero P. 2010. Structure-function analysis of npr1 alleles in Arabidopsis reveals a role for its paralogs in the perception of salicylic acid. *Plant, Cell and Environment* **33**: 1911–1922.

Carmona MJ, Calonje M, Martínez-Zapater JM. 2007. The FT/TFL1 gene family in grapevine. *Plant Molecular Biology* **63**: 637–650.

Causier B, Schwarz-Sommer Z, Davies B. 2010. Floral organ identity: 20 years of ABCs. *Seminars in Cell and Developmental Biology* **21**: 73–79.

Cerri MR, Frances L, Kelner A, Fournier J, Middleton PH, Auriac M-C, Mysore KS, Wen J, Erard M, Barker DG, *et al.* 2016. The Symbiosis-Related ERN Transcription Factors Act in Concert to Coordinate Rhizobial Host Root Infection. *Plant physiology* **171**: 1037–54.

Cerri MR, Wang Q, Stolz P, Folgmann J, Frances L, Katzer K, Li X, Heckmann AB, Wang TL, Downie JA, *et al.* 2017. The ERN1 transcription factor gene is a target of the CCaMK/CYCLOPS complex and controls rhizobial infection in Lotus japonicus. *New Phytologist* **215**: 323–337.

Chahtane H, Vachon G, Le Masson M, Thévenon E, Périgon S, Mihajlovic N, Kalinina A, Michard R, Moyroud E, Monniaux M, *et al.* 2013. A variant of LEAFY reveals its capacity to stimulate meristem development by inducing RAX1. *Plant Journal* **74**: 678–689.

Chakrabarti M, Zhang N, Sauvage C, Muños S, Blanca J, Cañizares J, Diez MJ, Schneider R,

Mazourek M, McClead J, *et al.* 2013. A cytochrome P450 regulates a domestication trait in cultivated tomato. *Proceedings of the National Academy of Sciences of the United States of America* **110**: 17125–17130.

Champagne C, Sinha N. **2004**. Compound leaves: Equal to the sum of their parts? *Development* **131**: 4401–4412.

Chen H, Chou M, Wang X, Liu S, Zhang F, Wei G. **2013**. Profiling of differentially expressed genes in roots of Robinia pseudoacacia during nodule development using suppressive subtractive hybridization. (S Lin, Ed.). *PloS one* **8**: e63930.

Cheng Y, Dai X, Zhao Y. **2006**. Auxin biosynthesis by the YUCCA flavin monooxygenases controls the formation of floral organs and vascular tissues in Arabidopsis. *Genes and Development* **20**: 1790–1799.

Cho E, Zambryski PC. **2011**. ORGAN BOUNDARY1 defines a gene expressed at the junction between the shoot apical meristem and lateral organs. *Proceedings of the National Academy of Sciences of the United States of America* **108**: 2154–2159.

Chuck G, Meeley R, Hake S. **2008**. Floral meristem initiation and meristem cell fate are regulated by the maize AP2 genes ids1 and sid1. *Development* **135**: 3013–3019.

Chuck G, Muszynski M, Kellogg E, Hake S, Schmidt RJ. **2002**. The control of spikelet meristem identity by the branched silkless1 gene in maize. *Science* **298**: 1238–1241.

Chung Y, Maharjan PM, Lee O, Fujioka S, Jang S, Kim B, Takatsuto S, Tsujimoto M, Kim H, Cho S, *et al.* 2011. Auxin stimulates DWARF4 expression and brassinosteroid biosynthesis in Arabidopsis. *Plant Journal* **66**: 564–578.

Clarke VC, Loughlin PC, Day D a., Smith PMC. **2014**. Transport processes of the legume symbiosome membrane. *Frontiers in Plant Science* **5**: 1–9.

Cline MG. **1991**. Apical dominance. *The Botanical Review* **57**: 318–358.

Coba de la Peña T, Fedorova E, Pueyo JJ, Lucas MM. **2018**. The Symbiosome: Legume and Rhizobia Co-evolution toward a Nitrogen-Fixing Organelle? *Frontiers in Plant Science* **8**: 1–26.

Colasanti J, Sundaresan V. **2000**. 'Florigen' enters the molecular age: Long-distance signals that cause plants to flower. *Trends in Biochemical Sciences* **25**: 236–240.

Combier J-P, Frugier F, de Billy F, Boualem A, El-Yahyaoui F, Moreau S, Vernie T, Ott T, Gamas P, Crespi M, *et al.* 2006. MtHAP2-1 is a key transcriptional regulator of symbiotic nodule development regulated by microRNA169 in Medicago truncatula. *Genes & Development* **20**: 3084–3088.

Cook CE, Whichard LP, Turner B, Wall ME, Egley GH. **1966**. Germination of Witchweed (Striga

lutea Lour.): Isolation and Properties of a Potent Stimulant. *Science* **154**: 1189–1190.

Corbesier L, Vincent C, Jang S, Fornara F, Fan Q, Searle I, Giakountis A, Farrona S, Gissot L, Turnbull C, *et al.* 2007. FT Protein Movement Contributes to Long-Distance Signaling in Floral Induction of Arabidopsis. *SCIENCE* **316**: 1030–1034.

Corby HDL. **1988**. TYPES OF RHIZOBIAL NODULES AND THEIR DISTRIBUTION AMONG THE LEGUMINOSAE. *National Herbarium & Botanic* **13**: 53–123.

Cosson V, Durand P, D'Erfurth I, Kondorosi A, Ratet P. **2015**. Medicago truncatula Transformation Using Leaf Explants. In: Wang K.(eds) Agrobacterium Protocols. Methods in Molecular Biology, vol 1223. Springer, New Youk, NY. 115–127.

Costa J-L, Lindblad P. **2002**. Cyanobacteria in Symbiosis with Cycads. In: Cyanobacteria in Symbiosis. Dordrecht: Kluwer Academic Publishers, 195–205.

Costes E, Crespel L, Denoyes B, Morel P, Demene MN, Lauri PE, Wenden B. **2014**. Bud structure, position and fate generate various branching patterns along shoots of closely related Rosaceae species: A review. *Frontiers in Plant Science* **5**: 1–11.

Couzigou JM, Magne K, Mondy S, Cosson V, Clements J, Ratet P. **2015**. The legume NOOT-BOP-COCH-LIKE genes are conserved regulators of abscission, a major agronomical trait in cultivated crops. *New Phytologist* **209**: 228–240.

Couzigou JM, Mondy S, Sahl L, Gourion B, Ratet P. **2013**. To be or noot to be: Evolutionary tinkering for symbiotic organ identity. *Plant Signaling and Behavior* **8**: 8–10.

Couzigou J-M, Zhukov V, Mondy S, Abu el Heba G, Cosson V, Ellis THN, Ambrose M, Wen J, Tadege M, Tikhonovich I, *et al.* 2012. NODULE ROOT and COCHLEATA Maintain Nodule Development and Are Legume Orthologs of Arabidopsis BLADE-ON-PETIOLE Genes. *The Plant Cell* **24**: 4498–4510.

Dahleen L, Franckowiak JD, Lundqvist U. **2007**. Descriptions of barley genetic stocks for 2007. *Barley Genetics Newsletter*: 154–187.

Dai Y, Ogilvie HA, Liu Y, Huang M, Markillie LM, Mitchell HD, Borrego EJ, Kolomiets M V., Gaffrey MJ, Orr G, *et al.* 2019. Rosette core fungal resistance in Arabidopsis thaliana. *Planta* **250**: 1941–1953.

Dalmais M, Antelme S, Ho-Yue-Kuang S, Wang Y, Darracq O, d'Yvoire MB, Cézard L, Légée F, Blondet E, Oria N, *et al.* 2013. A TILLING Platform for Functional Genomics in Brachypodium distachyon. *PLoS ONE* **8**.

Dart .P.J. **1977**. Infection and development of leguminous nodules. in: A treatise on dinitrogen fixation. Section III, Biology.Edited by R.W.F. Hardy and W.S. Silver. John Wiley & Sons. *A*

treatise on dinitrogen fixation. Section III, Biology.: 367–472.

Dawson JO. **2008**. Ecology Of Actinorhizal Plants. In: Nitrogen-fixing Actinorhizal Symbioses. Dordrecht: Springer Netherlands, 199–234.

Dénarié Jean and Debellé Frédéric. **1996**. Rhizobium Lipo-Chitooligosaccharide Nodulation Factors: Signaling Molecules Mediating Recognition and Morphogenesis. *Annual Review of Biochemistry* **65**: 503–535.

Derbyshire P, Byrne ME. **2013**. MORE SPIKELETS1 Is Required for Spikelet Fate in the Inflorescence of Brachypodium. *Plant Physiology* **161**: 1291–1302.

Devi B. **2014**. Investigating a conserved role for BLADE-ON-PETIOLE and class I TGA bZIP transcription factors in regulation of inflorescence architecture and lignin biosynthesis in Arabidopsis thaliana and Populus trichocarpa By Bhaswati Devi A thesis submitted to the F.

Diédhiou I, Diouf D. **2018**. Transcription factors network in root endosymbiosis establishment and development. *World Journal of Microbiology and Biotechnology* **34**: 37.

Dobrovolskaya O, Pont C, Sibout R, Martinek P, Badaeva E, Murat F, Chosson A, Watanabe N, Prat E, Gautier N, *et al.* 2015. Frizzy panicle drives supernumerary spikelets in bread wheat. *Plant Physiology* **167**: 189–199.

Doebley J, Stec A, Gustus C. **1995**. teosinte branched1 and the origin of maize: Evidence for epistasis and the evolution of dominance. *Genetics* **141**: 333–346.

Doebley J, Stec A, Hubbard L. **1997**. The evolution of apical dominance in maize. *Nature* **386**: 485–488.

Domagalska MA, Leyser O. **2011**. Signal integration in the control of shoot branching. *Nature Reviews Molecular Cell Biology* **12**: 211–221.

Dong X, Lee J, Nou I-S, Hur Y. **2014**. Expression Characteristics of LSH Genes in Brassica Suggest their Applicability for Modification of Leaf Morphology and the Use of their Promoter for Transgenesis . *Plant Breeding and Biotechnology* **2**: 126–138.

Dong Z, Li W, Unger-Wallace E, Yang J, Vollbrecht E, Chuck G. **2017**. Ideal crop plant architecture is mediated by tassels replace upper ears1, a BTB/POZ ankyrin repeat gene directly targeted by TEOSINTE BRANCHED1. *Proceedings of the National Academy of Sciences of the United States of America* **114**: E8656–E8664.

Doyle JJ. **1998**. Phylogenetic perspectives on nodulation: Evolving views of plants and symbiotic bacteria. *Trends in Plant Science* **3**: 473–478.

Doyle JJ. **2011**. Phylogenetic Perspectives on the Origins of Nodulation. *Molecular Plant-Microbe Interactions* **24**: 1289–1295.

Draper J, Mur LAJ, Jenkins G, Ghosh-Biswas GC, Bablak P, Hasterok R, Routledge APM. **2001**. Brachypodium distachyon. A New Model System for Functional Genomics in Grasses. *Plant Physiology* **127**: 1539–1555.

Dun EA, Germain A de Saint, Rameau C, Beveridge CA. **2012**. Antagonistic action of strigolactone and cytokinin in bud outgrowth control. *Plant Physiology* **158**: 487–498.

Eaglesham ARJ, Szalay AA. **1983**. Aerial stem nodules on Aeschynomene spp. *Plant Science Letters* **29**: 265–272.

Ehrhardt DW, Morrey Atkinson E, Long SR. **1992**. Depolarization of alfalfa root hair membrane potential by Rhizobium meliloti nod factors. *Science* **256**: 998–1000.

Eklöf S, Åstot C, Sitbon F, Moritz T, Olsson O, Sandberg G. **2000**. Transgenic tobacco plants co-expressing Agrobacterium iaa and ipt genes have wild-type hormone levels but display both auxin- and cytokinin-overproducing phenotypes. *Plant Journal* **23**: 279–284.

Elisabetta A, Giacomo D, Laffont C, Sciarra F, Iannelli MA, Frugier F, Frugis G, Di Giacomo E, Laffont C, Sciarra F, *et al.* 2016. KNAT3/4/5-like class 2 KNOX transcription factors are involved in Medicago truncatula symbiotic nodule organ development. *New Phytologist* **213**: 822–837.

Engstrom EM, Izhaki A, Bowman JL. **2004**. Promoter bashing, microRNAs, and Knox genes. New insights, regulators, and targets-of-regulation in the establishment of lateral organ polarity in Arabidopsis. *Plant Physiology* **135**: 685–694.

Estornell LH, Agustí J, Merelo P, Talón M, Tadeo FR. **2013**. Elucidating mechanisms underlying organ abscission. *Plant Science* **199**–**200**: 48–60.

Etchells JP, Moore L, Jiang WZ, Prescott H, Capper R, Saunders NJ, Bhatt AM, Dickinson HG. **2012**. A role for BELLRINGER in cell wall development is supported by loss-of-function phenotypes. *BMC Plant Biology* **12**: 1–12.

de Faria SM, Sutherland JM, Sprent JI. **1986**. A new type of infected cell in root nodules of Andira spp. (leguminosae). *Plant Science* **45**: 143–147.

Ferguson BJ, Reid JB. **2005**. Cochleata: Getting to the root of legume nodules. *Plant and Cell Physiology* **46**: 1583–1589.

Fernandez-Lopez M, Goormachtig S, Gao M, D'Haeze W, Van Montagu M M Van, Holsters M. **1998**. Ethylene-mediated phenotypic plasticity in root nodule development on Sesbania rostrata. *Proceedings of the National Academy of Sciences of the United States of America* **95**: 12724–8.

Ferraioli S, Tatè R, Rogato A, Chiurazzi M, Patriarca EJ. **2004**. Development of Ectopic Roots from Abortive Nodule Primordia. *Molecular Plant-Microbe Interactions* **17**: 1043–1050.

Ferrándiz C, Fourquin C, Prunet N, Scutt CP, Sundberg EVA, Trehin C, M. aurélie C, Vialette-

Guiraud. **2010**. Carpel Development. In: Kader J-C, Delseny M, eds. Advances in Botanical Research. Burlington: Elsevier, 1–73.

Ferrándiz C, Gu Q, Martienssen R, Yanofsky MF. **2000**. Redundant regulation of meristem identity and plant architecture by FRUITFULL, APETALA1 and CAULIFLOWER. *Development (Cambridge, England)* **127**: 725–34.

Floyd SK, Bowman JL. **2010**. Gene expression patterns in seed plant shoot meristems and leaves: Homoplasy or homology? *Journal of Plant Research* **123**: 43–55.

Fonouni-Farde C, Kisiala A, Brault M, Emery RJN, Diet A, Frugier F. **2017**. DELLA1-Mediated Gibberellin Signaling Regulates Cytokinin-Dependent Symbiotic Nodulation. *Plant physiology* **175**: 1795–1806.

Fonouni-Farde C, Tan S, Baudin M, Brault M, Wen J, Mysore KS, Niebel A, Frugier F, Diet A. **2016**. DELLA-mediated gibberellin signalling regulates Nod factor signalling and rhizobial infection. *Nature Communications* **7**: 12636.

Foo E, Bullier E, Goussot M, Foucher F, Rameau C, Beveridge CA. **2005**. The branching gene RAMOSUS1 mediates interactions among two novel signals and auxin in pea. *Plant Cell* **17**: 464–474.

Foo E, Davies NW. **2011**. Strigolactones promote nodulation in pea. *Planta* **234**: 1073–1081.

Foucher F, Morin J, Courtiade J, Cadioux S, Ellis N, Banfield MJ, Rameau C, Génétique D, National I, Recherche D, *et al.* 2003. DETERMINATE and LATE FLOWERING Are Two TERMINAL FLOWER1 / CENTRORADIALIS Homologs That Control Two Distinct Phases of Flowering Initiation and Development in Pea. *The Plant Cell* **15**: 2742–2754.

Foyer CH, Nguyen H, Lam HM. **2019**. Legumes—The art and science of environmentally sustainable agriculture. *Plant Cell and Environment* **42**: 1–5.

Franche C, Laplaze L, Duhoux E, Bogusz D. **1998**. Actinorhizal symbioses: Recent advances in plant molecular and genetic transformation studies. *Critical Reviews in Plant Sciences* **17**: 1–28.

Franckowiak JD, Lundqvist U. **2010**. *Descriptions of barley genetic stocks for 2010*.

Frankowski K, Wilmowicz E, Kućko A, Zienkiewicz A, Zienkiewicz K, Kopcewicz J. **2015**. Profiling the BLADE-ON-PETIOLE gene expression in the abscission zone of generative organs in Lupinus luteus. *Acta Physiologiae Plantarum* **37**: 1–7.

Franssen HJ, Xiao TT, Kulikova O, Wan X, Bisseling T, Scheres B, Heidstra R. **2015**. Root developmental programs shape the Medicago truncatula nodule meristem. *Development* **142**: 2941–2950.

Frendo P, Matamoros M a., Alloing G, Becana M. **2013**. Thiol-based redox signaling in the nitrogen-fixing symbiosis. *Frontiers in Plant Science* **4**: 1–10.

Froussart E, Bonneau J, Franche C, Bogusz D. **2016**. Recent advances in actinorhizal symbiosis signaling. *Plant Molecular Biology* **90**: 613–622.

Fu ZQ, Dong X. **2013**. Systemic Acquired Resistance: Turning Local Infection into Global Defense. *Annual Review of Plant Biology* **64**: 839–863.

Furumizu C, Alvarez JP, Sakakibara K, Bowman JL. **2015**. Antagonistic Roles for KNOX1 and KNOX2 Genes in Patterning the Land Plant Body Plan Following an Ancient Gene Duplication. *PLoS Genetics* **11**: 1–24.

Gallavotti A, Barazesh S, Malcomber S, Hall D, Jackson D, Schmidt RJ, McSteen P. **2008**. sparse inflorescence1 encodes a monocot-specific YUCCA-like gene required for vegetative and reproductive development in maize. *Proceedings of the National Academy of Sciences of the United States of America* **105**: 15196–15201.

Gallavotti A, Zhao Q, Kyozuka J, Meeley RB, Ritter MK, Doebley JF, Pè ME, Schmidt RJ. **2004**. The role of barren stalk1 in the architecture of maize. *Nature* **432**: 630–635.

Gamas P, Brault M, Jardinaud M-F, Frugier F. **2017**. Cytokinins in Symbiotic Nodulation: When, Where, What For? *Trends in Plant Science* **22**: 792–802.

Gauthier-Coles C, White RG, Mathesius U. **2019**. Nodulating Legumes Are Distinguished by a Sensitivity to Cytokinin in the Root Cortex Leading to Pseudonodule Development. *Frontiers in Plant Science* **9**: 1901.

Ge L, Yu J, Wang H, Luth D, Bai G, Wang K, Chen R. **2016**. Increasing seed size and quality by manipulating BIG SEEDS1 in legume species. *PNAS* **113**: 12414–12419.

Gehlot HS, Panwar D, Tak N, Tak A, Sankhla IS, Poonar N, Parihar R, Shekhawat NS, Kumar M, Tiwari R, *et al.* 2012. Nodulation of legumes from the Thar desert of India and molecular characterization of their rhizobia. *Plant and Soil* **357**: 227–243.

Gendron JM, Liu JS, Fan M, Bai MY, Wenkel S, Springer PS, Barton MK, Wang ZY. **2012**. Brassinosteroids regulate organ boundary formation in the shoot apical meristem of Arabidopsis. *Proceedings of the National Academy of Sciences of the United States of America* **109**: 21152–21157.

Di Giacomo E, Laffont C, Sciarra F, Iannelli MA, Frugier F, Frugis G. **2016**. KNAT3/4/5-like class 2 KNOX transcription factors are involved in Medicago truncatula symbiotic nodule organ development. *New Phytologist* **213**: 822–837.

Di Giacomo E, Sestili F, Iannelli MA, Testone G, Mariotti D, Frugis G. **2008**. Characterization of KNOX genes in Medicago truncatula. *Plant Mol Biol* **67**: 135–150.

Gingerich DJ, Hanada K, Shiu SH, Vierstra RD. **2007**. Large-scale, lineage-specific expansion of a bric-a-brac/tramtrack/broad complex ubiquitin-ligase gene family in rice. *Plant Cell* **19**: 2329–2348.

Girin T, Sorefan K, Østergaard L. **2009**. Meristematic sculpting in fruit development. *Journal of Experimental Botany* **60**: 1493–1502.

Gómez-Mena C, Sablowski R. **2008**. Arabidopsis thaliana Homeobox Gene1 establishes the basal boundaries of shoot organs and controls stem growth. *Plant Cell* **20**: 2059–2072.

Gomez-Roldan V, Fermas S, Brewer PB, Puech-Pagès V, Dun EA, Pillot JP, Letisse F, Matusova R, Danoun S, Portais JC, *et al.* 2008. Strigolactone inhibition of shoot branching. *Nature* **455**: 189–194.

González-Sama A, Lucas MM, De Felipe MR, Pueyo JJ. **2004**. An unusual infection mechanism and nodule morphogenesis in white lupin (Lupinus albus). *New Phytologist* **163**: 371–380.

Goodstein DM, Shu S, Howson R, Neupane R, Hayes RD, Fazo J, Mitros T, Dirks W, Hellsten U, Putnam N, *et al.* 2012. Phytozome: A comparative platform for green plant genomics. *Nucleic Acids Research* **40**: 1178–1186.

Gourion B, Sulser S, Frunzke J, Francez-Charlot A, Stiefel P, Pessi G, Vorholt JA, Fischer HM. **2009**. The PhyR-σEcfG signalling cascade is involved in stress response and symbiotic efficiency in Bradyrhizobium japonicum. *Molecular Microbiology* **73**: 291–305.

Gourlay CW, Hofer JM, Ellis TH. **2000**. Pea compound leaf architecture is regulated by interactions among the genes UNIFOLIATA, cochleata, afila, and tendril-lessn. *The Plant cell* **12**: 1279–94.

Greb T, Clarenz O, Schafer E, Herrero R, Schmitz G, Theres K. **2003**. Molecular analysis of the LATERAL SUPPRESSOR gene in Arabidopsis. *Genes & Development* **17**: 1175–1187.

Gresshoff PM, Mens C, Ferguson BJ, Li D, Haaima LE. **2018**. Local and Systemic Effect of Cytokinins on Soybean Nodulation and Regulation of Their Isopentenyl Transferase (IPT) Biosynthesis Genes Following Rhizobia Inoculation. *Frontiers in Plant Science* **9**: 1–14.

Guan D, Stacey N, Liu C, Wen J, Mysore KS, Torres-Jerez I, Vernie T, Tadege M, Zhou C, Wang Z -y., *et al.* 2013. Rhizobial Infection Is Associated with the Development of Peripheral Vasculature in Nodules of Medicago truncatula. *Plant Physiology* **162**: 107–115.

Guinel FC. **2009**. Getting around the legume nodule: II. Molecular biology of its peripheral zone and approaches to study its vasculature. *Botany* **87**: 1139–1166.

Guo M, Thomas J, Collins G, Timmermans MCP. **2008**. Direct repression of KNOX loci by the ASYMMETRIC LEAVES1 complex of Arabidopsis. *Plant Cell* **20**: 48–58.

Guo S, Xu Y, Liu H, Mao Z, Zhang C, Ma Y, Zhang Q, Meng Z, Chong K. **2013**. The interaction between OsMADS57 and OsTB1 modulates rice tillering via DWARF14. *Nature Communications* **4**: 1–12.

Ha CM, Jun JH, Nam HG, Fletcher JC. **2004**. BLADE-ON-PETIOLE1 Encodes a BTB/POZ

Domain Protein Required for Leaf Morphogenesis in Arabidopsis thaliana. *Plant and Cell Physiology* **45**: 1361–1370.

Ha CM, Jun JH, Nam HG, Fletcher JC. **2007**. BLADE-ON-PETIOLE1 and 2 Control Arabidopsis Lateral Organ Fate through Regulation of LOB Domain and Adaxial-Abaxial Polarity Genes . *The Plant Cell* **19**: 1809–1825.

Ha CM, Kim GT, Kim BC, Jun JH, Soh MS, Ueno Y, Machida Y, Tsukaya H, Nam HG. **2003**. The BLADE-ON-PETIOLE 1 gene controls leaf pattern formation through the modulation of meristematic activity in Arabidopsis. *Development* **130**: 161–172.

Hadri A-E, Spaink HP, Bisseling T, Brewin NJ. **1998**. Diversity of Root Nodulation and Rhizobial Infection Processes. In: The Rhizobiaceae. Dordrecht: Springer Netherlands, 347–360.

Hafeez F, Akkermans ADL, Chaudhary AH. **1984**. Observations on the ultrastructure of Frankia sp. in root nodules of Datisca cannabina L. *Plant and Soil* **79**: 383–402.

Hagemann W, Gleissberg S. **1996**. Organogenetic capacity of leaves: The significance of marginal blastozones in angiosperms. *Plant Systematics and Evolution* **199**: 121–152.

Hake S, Smith HMS, Holtan H, Magnani E, Mele G, Ramirez J. **2004**. the Role of Knox Genes in Plant Development . *Annual Review of Cell and Developmental Biology* **20**: 125–151.

Hamant O, Pautot V. **2010**. Plant development: A TALE story. *Comptes Rendus - Biologies* **333**: 371–381.

Han Y, Zhang C, Yang H, Jiao Y. **2014**. Cytokinin pathway mediates APETALA1 function in the establishment of determinate floral meristems in Arabidopsis. *Proceedings of the National Academy of Sciences of the United States of America* **111**: 6840–6845.

Hay A, Tsiantis M. **2010**. KNOX genes: Versatile regulators of plant development and diversity. *Development* **137**: 3153–3165.

Hayward A, Stirnberg P, Beveridge C, Leyser O. **2009**. Interactions between auxin and strigolactone in shoot branching control. *Plant Physiology* **151**: 400–412.

Hecht V, Foucher F, Ferrándiz C, Macknight R, Navarro C, Morin J, Vardy ME, Ellis N, Beltrán JP, Rameau C, *et al.* 2005. Conservation of Arabidopsis flowering genes in model legumes. *Plant physiology* **137**: 1420–34.

Heckmann AB, Lombardo F, Miwa H, Perry JA, Bunnewell S, Parniske M, Wang TL, Downie JA. **2006**. Lotus japonicus nodulation requires two GRAS domain regulators, one of which is functionally conserved in a non-legume. *Plant physiology* **142**: 1739–50.

Heisler MG, Hamant O, Krupinski P, Uyttewaal M, Ohno C, Jönsson H, Traas J, Meyerowitz EM. **2010**. Alignment between PIN1 polarity and microtubule orientation in the shoot apical meristem

reveals a tight coupling between morphogenesis and auxin transport. *PLoS Biology* **8**.

Hempel FD, Weigel D, Mandel MA, Ditta G, Zambryski PC, Feldman LJ, Yanofsky MF. **1997**. Floral determination and expression of floral regulatory genes in Arabidopsis. *Development* **124**: 3845–3853.

Hepworth SR, Pautot VA. **2015**. Beyond the Divide: Boundaries for Patterning and Stem Cell Regulation in Plants. *Frontiers in Plant Science* **6**: 1–19.

Hepworth SR, Zhang Y, McKim S, Li X, Haughn GW. **2005**. BLADE-ON-PETIOLE-Dependent Signaling Controls Leaf and Floral Patterning in Arabidopsis. *THE PLANT CELL ONLINE* **17**: 1434–1448.

Van Den Heuvel S. **2004**. Protein Degradation: CUL-3 and BTB - Partners in Proteolysis. *Current Biology* **14**: 59–61.

Heyn C. **1976**. *An old wuestin revived: "What are the stipules of Lotus?"*

Hirsch AM. **1992**. Developmental biology of legume nodulation. *New Phytologist* **122**: 211–237.

Hirsch S, Kim J, Munoz A, Heckmann AB, Downie JA, Oldroyd GED. **2009**. GRAS Proteins Form a DNA Binding Complex to Induce Gene Expression during Nodulation Signaling in Medicago truncatula. *THE PLANT CELL ONLINE* **21**: 545–557.

Hocher V, Auguy F, Argout X, Laplaze L, Franche C, Bogusz D. **2006**. Expressed sequence-tag analysis in Casuarina glauca actinorhizal nodule and root. *New Phytologist* **169**: 681–688.

Hoffmann B, Trinh TH, Leung J, Kondorosi A, Kondorosi E. **1997**. A new Medicago truncatula line with superior in vitro regeneration, transformation, and symbiotic properties isolated through cell culture selection. *Molecular Plant-Microbe Interactions* **10**: 307–315.

Hong L, Qian Q, Zhu K, Tang D, Huang Z, Gao L, Li M, Gu M, Cheng Z. **2010**. ELE restrains empty glumes from developing into lemmas. *Journal of Genetics and Genomics* **37**: 101–115.

Horváth B, Yeun LH, Domonkos Á, Halász G, Gobbato E, Ayaydin F, Miró K, Hirsch S, Sun J, Tadege M, *et al.* 2011. Medicago truncatula IPD3 Is a Member of the Common Symbiotic Signaling Pathway Required for Rhizobial and Mycorrhizal Symbioses. *Molecular Plant-Microbe Interactions* **24**: 1345–1358.

Hossain MS, Hoang NT, Yan Z, Tóth K, Meyers BC, Stacey G. **2019**. Characterization of the Spatial and Temporal Expression of Two Soybean miRNAs Identifies SCL6 as a Novel Regulator of Soybean Nodulation. *Frontiers in Plant Science* **10**: 475.

Howe GT, Horvath DP, Dharmawardhana P, Priest HD, Mockler TC, Strauss SH. **2015**. Extensive transcriptome changes during natural onset and release of vegetative bud dormancy in Populus. *Frontiers in Plant Science* **6**: 1–28.

Huang X, Ding J, Effgen S, Turck F, Koornneef M. **2013**. Multiple loci and genetic interactions involving flowering time genes regulate stem branching among natural variants of Arabidopsis. *New Phytologist* **199**: 843–857.

Hubbard L, Mcsteen P, Doebley J, Hake S. **2002**. Expression Patterns and Mutant Phenotype of teosinte branched1 Correlate With Growth Suppression in Maize and Teosinte. *Genetics* **162**: 1927–1935.

Hussey G. **1971**. In vitro growth of vegetative tomato shoot apices. *Journal of Experimental Botany* **22**: 688–701.

Ibáñez F, Wall L, Fabra A. **2017**. Starting points in plant-bacteria nitrogen-fixing symbioses: intercellular invasion of the roots. *Journal of Experimental Botany* **68**: erw387.

Ichihashi Y, Aguilar-Martínez JA, Farhi M, Chitwood DH, Kumar R, Millon L V., Peng J, Maloof JN, Sinha NR. **2014**. Evolutionary developmental transcriptomics reveals a gene network module regulating interspecific diversity in plant leaf shape. *Proceedings of the National Academy of Sciences of the United States of America* **111**.

Ietswaart R, Wu Z, Dean C. **2012**. Flowering time control: Another window to the connection between antisense RNA and chromatin. *Trends in Genetics* **28**: 445–453.

Imanishi L, Perrine-Walker FM, Ndour A, VayssiÃ¨res A, Conejero G, Lucas M, Champion A, Laplaze L, Wall L, Svistoonoff S. **2014**. Role of auxin during intercellular infection of Discaria trinervis by Frankia. *Frontiers in Plant Science* **5**: 1–9.

Iyer LM, Aravind L. **2012**. ALOG domains: Provenance of plant homeotic and developmental regulators from the DNA-binding domain of a novel class of DIRS1-type retroposons. *Biology Direct* **7**: 1–8.

Izhaki A, Alvarez JP, Cinnamon Y, Genin O, Liberman-Aloni R, Eyal Y. **2018**. The Tomato BLADE ON PETIOLE and TERMINATING FLOWER Regulate Leaf Axil Patterning Along the Proximal-Distal Axes. *Frontiers in Plant Science* **9**: 1–10.

Jaeger KE, Wigge PA, Lane C. **2007**. FT Protein Acts as a Long-Range Signal in Arabidopsis. *Current Biology* **2**: 1050–1054.

Jakoby M, Weisshaar B, Dröge-Laser W, Vicente-Carbajosa J, Tiedemann J, Kroj T, Parcy F. **2002**. bZIP transcription factors in Arabidopsis. *Trends in Plant Science* **7**: 106–111.

Ji HS, Chu SH, Jiang W, Cho Y Il, Hahn JH, Eun MY, McCouch SR, Koh HJ. **2006**. Characterization and mapping of a shattering mutant in rice that corresponds to a block of domestication genes. *Genetics* **173**: 995–1005.

Jiao YS, Liu YH, Yan H, Wang ET, Tian CF, Chen WX, Guo BL, Chen WF. **2015**. Rhizobial

Diversity and Nodulation Characteristics of the Extremely Promiscuous Legume Sophora flavescens. *Molecular Plant-Microbe Interactions* **28**: 1338–1352.

Jin Y, Liu H, Luo D, Yu N, Dong W, Wang C, Zhang X, Dai H, Yang J, Wang E. **2016**. DELLA proteins are common components of symbiotic rhizobial and mycorrhizal signalling pathways. *Nature Communications* **7**: 12433.

Johnson X, Brcich T, Dun EA, Goussot M, Haurogne K, Beveridge CA, Rameau C. **2006**. Branching Genes Are Conserved across Species. Genes Controlling a Novel Signal in Pea Are Coregulated by Other Long-Distance Signals. *Plant Physiology* **142**: 1014–1026.

Johnston R, Wang M, Sun Q, Sylvester AW, Hake S, Scanlon MJ. **2014**. Transcriptomic analyses indicate that maize ligule development recapitulates gene expression patterns that occur during lateral organ initiationw open. *Plant Cell* **26**: 4718–4732.

Jost M, Taketa S, Mascher M, Himmelbach A, Yuo T, Shahinnia F, Rutten T, Druka A, Schmutzer T, Steuernagel B, *et al.* 2016. A homolog of Blade-On-Petiole 1 and 2 (BOP1/2) controls internode length and homeotic changes of the barley inflorescence. *Plant Physiology* **171**: pp.00124.2016.

Jun JH, Ha CM, Fletcher JC. **2010**. BLADE-ON-PETIOLE1 Coordinates Organ Determinacy and Axial Polarity in Arabidopsis by Directly Activating ASYMMETRIC LEAVES2. *The Plant Cell* **22**: 62–76.

Kaló P, Gleason C, Edwards A, Marsh J, Mitra RM, Hirsch S, Jakab J, Sims S, Long SR, Rogers J, *et al.* 2005. Nodulation signaling in legumes requires NSP2, a member of the GRAS family of transcriptional regulators. *Science (New York, N.Y.)* **308**: 1786–9.

Kanehara K, Liu Y, Do P, Coupland G, Nakamura Y, Andre F. **2014**. Arabidopsis florigen FT binds to diurnally oscillating phospholipids that accelerate flowering. *NATURE COMMUNICATIONS* |: 1–7.

Kanrar S, Bhattacharya M, Arthur B, Courtier J, Smith HMS. **2008**. Regulatory networks that function to specify flower meristems require the function of homeobox genes PENNYWISE and POUND-FOOLISH in Arabidopsis. *Plant Journal* **54**: 924–937.

Kanu SA, Dakora FD. **2017**. Symbiotic functioning, structural adaptation, and subcellular organization of root nodules from Psoralea pinnata (L.) plants grown naturally under wetland and upland conditions in the Cape Fynbos of South Africa. *Protoplasma* **254**: 137–145.

Kardailsky I, Shukla VK, Ahn JH, Dagenais N, Christensen SK, Nguyen JT, Chory J, Harrison MJ, Weigel D. **1999**. Activation Tagging of the Floral Inducer FT. *Science* **286**: 1962–1966.

Karim MR, Hirota a., Kwiatkowska D, Tasaka M, Aida M. **2009**. A Role for Arabidopsis PUCHI in Floral Meristem Identity and Bract Suppression. *the Plant Cell Online* **21**: 1360–1372.

Kebrom TH, Spielmeyer W, Finnegan EJ. **2013**. Grasses provide new insights into regulation of shoot branching. *Trends in Plant Science* **18**: 41–48.

Kellogg EA, Camara PEAS, Rudall PJ, Ladd P, Malcomber ST, Whipple CJ, Doust AN. **2013**. Early inflorescence development in the grasses (Poaceae). *Frontiers in Plant Science* **4**: 1–16.

Kemmeren P, Van Berkum NL, Vilo J, Bijma T, Donders R, Brazma A, Holstege FCP. **2002**. Protein interaction verification and functional annotation by integrated analysis of genome-scale data. *Molecular Cell* **9**: 1133–1143.

Khan M. **2013**. *Interactions of BLADE-ON-PETIOLE1 and 2 with TALE Homeobox Genes in the Regulation of Flowering and Inflorescence Architecture in Arabidopsis Thaliana*.

Khan M, Ragni L, Tabb P, Salasini BC, Chatfield S, Datla R, Lock J, Kuai X, Després C, Proveniers M, *et al.* 2015. Repression of lateral organ boundary genes by pennywise and pound-foolish is essential for meristem maintenance and flowering in Arabidopsis. *Plant Physiology* **169**: 2166–2186.

Khan M, Tabb P, Hepworth SR. **2012a**. BLADE-ON-PETIOLE1 and 2 regulate Arabidopsis inflorescence architecture in conjunction with homeobox genes KNAT6 and ATH1. *Plant Signaling and Behavior* **7**: 788–792.

Khan M, Xu H, Hepworth SR. **2014**. BLADE-ON-PETIOLE genes: Setting boundaries in development and defense. *Plant Science* **215**–**216**: 157–171.

Khan M, Xu M, Murmu J, Tabb P, Liu Y, Storey K, McKim SM, Douglas CJ, Hepworth SR. **2012b**. Antagonistic Interaction of BLADE-ON-PETIOLE1 and 2 with BREVIPEDICELLUS and PENNYWISE Regulates Arabidopsis Inflorescence Architecture. *Plant Physiology* **158**: 946–960.

Kimura S, Koenig D, Kang J, Yoong FY, Sinha N. **2008**. Natural Variation in Leaf Morphology Results from Mutation of a Novel KNOX Gene. *Current Biology* **18**: 672–677.

Kobayashi Y, Kaya H, Goto K, Iwabuchi M. **1999**. A Pair of Related Genes with Antagonistic Roles in Mediating Flowering Signals. *Science* **286**: 1960–1963.

Kobayashi K, Maekawa M, Miyao A, Hirochika H, Kyozuka J. **2010**. PANICLE PHYTOMER2 (PAP2), encoding a SEPALLATA subfamily MADS-box protein, positively controls spikelet meristem identity in rice. *Plant and Cell Physiology* **51**: 47–57.

Kobayashi Y, Weigel D. **2007**. Move on up, it's time for change - Mobile signals controlling photoperiod-dependent flowering. *Genes and Development* **21**: 2371–2384.

Kohlen W, Ng JLP, Deinum EE, Mathesius U. **2018**. Auxin transport, metabolism, and signalling during nodule initiation: Indeterminate and determinate nodules. *Journal of Experimental Botany* **69**: 229–244.

Komatsu M, Chujo A, Nagato Y, Shimamoto K, Kyozuka J. **2003a**. Frizzy panicle is required to prevent the formation of axillary meristems and to establish floral meristem identity in rice spikelets. *Development* **130**: 3841–3850.

Komatsu K, Maekawa M, Ujiie S, Satake Y, Furutani I, Okamoto H, Shimamoto K, Kyozuka J. **2003b**. LAX and SPA: Major regulators of shoot branching in rice. *Proceedings of the National Academy of Sciences of the United States of America* **100**: 11765–11770.

Kong F, Zhang T, Liu J, Heng S, Shi Q, Zhang H, Wang Z, Ge L, Li P, Lu X, *et al.* 2017. Regulation of Leaf Angle by Auricle Development in Maize. *Molecular Plant* **10**: 516–519.

Koppolu R, Anwar N, Sakuma S, Tagiri A, Lundqvist U, Pourkheirandish M, Rutten T, Seiler C, Himmelbach A, Ariyadasa R, *et al.* 2013. Six-rowed spike4 (Vrs4) controls spikelet determinacy and row-type in barley. *Proceedings of the National Academy of Sciences of the United States of America* **110**: 13198–13203.

Koppolu R, Schnurbusch T. **2019**. Developmental pathways for shaping spike inflorescence architecture in barley and wheat. *Journal of Integrative Plant Biology* **61**: 278–295.

Kumar S, Mishra RK, Kumar A, Srivastava S, Chaudhary S. **2009**. Regulation of stipule development by COCHLEATA and STIPULE-REDUCED genes in pea Pisum sativum. *Planta* **230**: 449–458.

Kumar S, Sharma V, Chaudhary S, Kumari R, Kumari N, Mishra P. **2011**. Interaction between COCHLEATA and UNIFOLIATA genes enables normal flower morphogenesis in the garden pea, Pisum sativum. *Journal of Genetics* **90**: 309–314.

Kumar S, Stecher G, Tamura K. **2016**. MEGA7: Molecular Evolutionary Genetics Analysis Version 7.0 for Bigger Datasets. *Molecular biology and evolution* **33**: 1870–1874.

Kuppusamy KT, Ivashuta S, Bucciarelli B, Vance CP, Gantt JS, Vandenbosch KA. **2009**. Knockdown of CELL DIVISION CYCLE16 Reveals an Inverse Relationship between Lateral Root and Nodule Numbers and a Link to Auxin in Medicago truncatula 1[W][OA]. *Plant Physiology* **151**: 1155–1166.

Kyozuka J, Konishi S, Nemoto K, Izawa T, Shimamoto K. **1998**. Down-regulation of RFL, the FLO/LFY homolog of rice, accompanied with panicle branch initiation. *Proceedings of the National Academy of Sciences of the United States of America* **95**: 1979–1982.

Kyozuka J, Shimamoto K. **2002**. Ectopic expression of OsMADS3, a rice ortholog of AGAMOUS, caused a homeotic transformation of lodicules to stamens in transgenic rice plants. *Plant and Cell Physiology* **43**: 130–135.

Kyozuka J, Tokunaga H, Yoshida A. **2014**. Control of grass inflorescence form by the fine-tuning of meristem phase change. *Current Opinion in Plant Biology* **17**: 110–115.

Lal S, Pacis LB, Smith HMS. **2011**. Regulation of the SQUAMOSA PROMOTER-BINDING PROTEIN-LIKE genes/microRNA156 Module by the homeodomain proteins PENNYWISE and POUND-FOOLISH in arabidopsis. *Molecular Plant* **4**: 1123–1132.

Lalani Wijesundara TI, Van Holm LHJ, Kulasooriya SA. **2000**. Rhizobiology and nitrogen fixation of some tree legumes native to Sri Lanka. *Biology and Fertility of Soils* **30**: 535–543.

Laplaze L, Duhoux E, Franche C, Frutz T, Svistoonoff S, Bisseling T, Bogusz D, Pawlowski K. **2000**. Casuarina glauca Prenodule Cells Display the Same Differentiation as the Corresponding Nodule Cells. *Molecular Plant-Microbe Interactions* **13**: 107–112.

Laporte P, Lepage A, Fournier J, Catrice O, Moreau S, Jardinaud M-F, Mun J-H, Larrainzar E, Cook DR, Gamas P, *et al.* 2014. The CCAAT box-binding transcription factor NF-YA1 controls rhizobial infection. *Journal of Experimental Botany* **65**: 481–494.

Larrainzar E, Wienkoop S. **2017**. A Proteomic View on the Role of Legume Symbiotic Interactions. *Frontiers in Plant Science* **8**: 1–13.

Laufs P, Peaucelle A, Morin H, Traas J. **2004**. MicroRNA regulation of the CUC genes is required for boundary size control in Arabidopsis meristems. *Development* **131**: 4311–4322.

Lavin M, Doyle JJ, Palmer JD. **1990**. Evolutionary Significance of the Loss of the Chloroplast-DNA Inverted Repeat in the Leguminosae Subfamily Papilionoideae. *Evolution* **44**: 390.

Lawrie AC. **1983**. Infection and Nodule Development in Aotus ericoides (Vent.) G. Don, A Woody Native Australian Legume. *Journal of Experimental Botany* **34**: 1168–1180.

Lee DK, Geisler M, Springer PS. **2009**. LATERAL ORGAN FUSION1 and LATERAL ORGAN FUSION2 function in lateral organ separation and axillary meristem formation in Arabidopsis. *Development* **136**: 2423–2432.

Lei Y, Su S, He L, Hu X, Luo D. **2019**. A member of the ALOG gene family has a novel role in regulating nodulation in Lotus japonicus. *Journal of Integrative Plant Biology* **61**: 463–477.

Lejeune-Hénaut I, Hanocq E, Béthencourt L, Fontaine V, Delbreil B, Morin J, Petit A, Devaux R, Boilleau M, Stempniak JJ, *et al.* 2008. The flowering locus Hr colocalizes with a major QTL affecting winter frost tolerance in Pisum sativum L. *Theoretical and Applied Genetics* **116**: 1105–1116.

Lelandais-Brière C, Moreau J, Hartmann C, Crespi M. **2016**. Noncoding RNAs, Emerging Regulators in Root Endosymbioses. *Molecular Plant-Microbe Interactions* **29**: 170–180.

Levin JZ, Meyerowitz EM. **1995**. UFO: An Arabidopsis gene involved in both floral meristem and floral organ development. *Plant Cell* **7**: 529–548.

Levy J, Bres C, Geurts R, Chalhoub B, Kulikova O, Journet E, Ane J-M, Lauber E, Bisseling T, Denarie J, *et al.* 2004. A Putative Ca 2 and Calmodulin- Dependent Protein Kinase Required. *Science*

303: 1361–1364.

Levy YY, Dean C. **1998**. The transition to flowering. *Plant Cell* **10**: 1973–1989.

Lewis MW, Leslie ME, Liljegren SJ. **2006**. Plant separation: 50 Ways to leave your mother. *Current Opinion in Plant Biology* **9**: 59–65.

Li C, Bangerth F. **2003**. Stimulatory effect of cytokinins and interaction with IAA on the release of lateral buds of pea plants from apical dominance. *Journal of Plant Physiology* **160**: 1059–1063.

Li X, Fu Z, Wang Y, Xiong G, Wang X, Liu X, Li J, Qian Q, Zeng D, Teng S, *et al.* 2003. Control of tillering in rice. *Nature* **422**: 618–621.

Li N, Li Y. **2014**. Ubiquitin-mediated control of seed size in plants. *Frontiers in Plant Science* **5**: 1–6.

Li N, Li Y. **2016**. Signaling pathways of seed size control in plants. *Current Opinion in Plant Biology* **33**: 23–32.

Li X, Sun L, Tan L, Liu F, Zhu Z, Fu Y, Sun X, Sun X, Xie D, Sun C. **2012**. TH1, a DUF640 domain-like gene controls lemma and palea development in rice. *Plant Molecular Biology* **78**: 351–359.

Li N, Wang Y, Lu J, Liu C. **2019**. Genome-wide identification and characterization of the ALOG gene family in Petunia. *International Journal of Genomics* **2019**.

Liebsch D, Sunaryo W, Holmlund M, Norberg M, Zhang J, Hall HC, Helizon H, Jin X. **2014**. Class I KNOX transcription factors promote differentiation of cambial derivatives into xylem fibers in the Arabidopsis hypocotyl. *Development* **141**: 4311–4319.

Lifschitz E. **2008**. Multiple regulatory roles for Self-Pruning in the shoot system of tomato. *Plant Physiology* **148**: 1737–1738.

Liljegren SJ. **2012**. Organ abscission: Exit strategies require signals and moving traffic. *Current Opinion in Plant Biology* **15**: 670–676.

Liljegren SJ, Ditta GS, Eshed Y, Savidge B, Bowmant JL, Yanofsky MF. **2000**. SHATTERPROOF MADS-box genes control dispersal in Arabidopsis. *Nature* **404**: 766–770.

Liljegren SJ, Gustafson-Brown C, Pinyopich A, Ditta GS, Yanofsky MF. **1999**. Interactions among APETALA1, LEAFY, and TERMINAL FLOWER1 specify meristem fate. *Plant Cell* **11**: 1007–1018.

Limpens E, Franken C, Smit P, Willemse J. **2003**. LysM Domain Receptor Kinases Regulating Rhizobial Nod Factor. **302**: 630–633.

Lindstrom K, Martinez-Romero E. **2007**. International Committee on Systematics of Prokaryotes; Subcommittee on the taxonomy of Agrobacterium and Rhizobium: Minutes of the meeting, 23-24 July 2006, Arhus, Denmark. *INTERNATIONAL JOURNAL OF SYSTEMATIC AND EVOLUTIONARY*

MICROBIOLOGY **57**: 1365–1366.

Linkies A, Graeber K, Knight C, Leubner-Metzger G. **2010**. The evolution of seeds. *New Phytologist* **186**: 817–831.

Liu K, Cao J, Yu K, Liu X, Gao Y, Chen Q, Zhang W, Peng H, Du J, Xin M, *et al.* 2019. Wheat TaSPL8 Modulates Leaf Angle Through Auxin and Brassinosteroid Signaling . *Plant Physiology* **181**: 179–194.

Liu YC, Lei YW, Liu W, Weng L, Lei MJ, Hu XH, Dong Z, Luo D, Yang J. **2018a**. LjCOCH interplays with LjAPP1 to maintain the nodule development in Lotus japonicus. *Plant Growth Regulation* **85**: 267–279.

Liu M, Li H, Su Y, Li W, Shi C. **2016**. G1/ELE functions in the development of rice lemmas in addition to determining identities of empty glumes. *Frontiers in Plant Science* **7**: 1–12.

Liu S, Ratet P, Magne K. **2020**. Nodule diversity, evolution, organogenesis and identity. In: FRENDO P, FRUGIER F, MASSON-BOIVIN C, eds. Advances in Botanical Research Regulation of Nitrogen-Fixing Symbioses in Legumes. Elsevier, 119–180.

Liu WYY, Ridgway HJ, James TK, James EK, Chen W-M, Sprent JI, Young JPW, Andrews M. **2014**. Burkholderia sp. Induces Functional Nodules on the South African Invasive Legume Dipogon lignosus (Phaseoleae) in New Zealand Soils. *Microbial Ecology* **68**: 542–555.

Liu C, Teo ZWN, Bi Y, Song S, Xi W, Yang X, Yin Z, Yu H. **2013**. A Conserved Genetic Pathway Determines Inflorescence Architecture in Arabidopsis and Rice. *Developmental Cell* **24**: 612–622.

Liu C, Thong Z, Yu H. **2009**. Coming into bloom: The specification of floral meristems. *Development* **136**: 3379–3391.

Liu H, Zhang C, Yang J, Yu N, Wang E. **2018b**. Hormone modulation of legume-rhizobial symbiosis. *Journal of Integrative Plant Biology* **60**: 632–648.

Lo SF, Yang SY, Chen KT, Hsing YI, Zeevaart JAD, Chen LJ, Yu SM. **2008**. A novel class of gibberellin 2-oxidases control semidwarfism, tillering, and root development in rice. *Plant Cell* **20**: 2603–2618.

Long JA, Barton MK. **1998**. The development of apical embryonic pattern in Arabidopsis. *Development* **125**: 3027–3035.

Long J, Barton MK. **2000**. Initiation of axillary and floral meristems in Arabidopsis. *Developmental Biology* **218**: 341–353.

Lotocka B, Kopcińska J, Skalniak M. **2012**. Review article: The meristem in indeterminate root nodules of Faboideae. *Symbiosis (Philadelphia, Pa.)* **58**: 63–72.

LPWG. **2013a**. Towards a new classification system for legumes: Progress report from the 6th International Legume Conference. *South African Journal of Botany* **89**: 3–9.

LPWG. **2013b**. Legume phylogeny and classification in the 21st century: Progress, prospects and lessons for other species-rich clades. *Taxon* **62**: 217–248.

LPWG. **2017**. A new subfamily classification of the leguminosae based on a taxonomically comprehensive phylogeny. *Taxon* **66**: 44–77.

Ma X, Cheng Z, Wu F, Jin M, Zhang L, Zhou F, Wang J, Zhou K, Ma J, Lin Q, *et al.* 2013. BEAK LIKE SPIKELET1 is Required for Lateral Development of Lemma and Palea in Rice. *Plant Molecular Biology Reporter* **31**: 98–108.

MacAlister CA, Park SJ, Jiang K, Marcel F, Bendahmane A, Izkovich Y, Eshed Y, Lippman ZB. **2012**. Synchronization of the flowering transition by the tomato terminating flower gene. *Nature Genetics* **44**: 1393–1398.

Madsen LH, Tirichine L, Jurkiewicz A, Sullivan JT, Heckmann AB, Bek AS, Ronson CW, James EK, Stougaard J. **2010**. The molecular network governing nodule organogenesis and infection in the model legume Lotus japonicus. *Nature Communications* **1**.

Magne K, Couzigou J-M, Schiessl K, Liu S, George J, Zhukov V, Sahl L, Boyer F, Iantcheva A, Mysore KS, *et al.* 2018a. MtNODULE ROOT1 and MtNODULE ROOT2 are essential for indeterminate nodule identity. *Plant Physiology* **178**: 297–316.

Magne K, George J, Berbel Tornero A, Broquet B, Madueño F, Andersen SU, Ratet P. **2018b**. Lotus japonicus NOOT-BOP-COCH-LIKE1 is essential for nodule, nectary, leaf and flower development. *Plant Journal* **94**: 880–894.

Magne K, Liu S, Massot S, Dalmais M, Morin H, Sibout R, Bendahmane A, Ratet P. **2020**. Roles of BdUNICULME4 and BdLAXATUM-A in the non- domesticated grass Brachypodium distachyon. *The Plant Journal*: 1–15.

Malcomber ST, Preston JC, Reinheimer R, Kossuth J, Kellogg EA. **2006**. Developmental Gene Evolution and the Origin of Grass Inflorescence Diversity. *Advances in Botanical Research* **44**: 425–481.

Mandel MA, Yanofsky MF. **1995**. The Arabidopsis AGL8 MADS Box Gene 1 s Expressed in lnflorescence Meristems and 1 s Negatively Regulated by APETALAI. *The Plant Cell* **7**: 1763–1771.

Mantilla-Perez MB, Salas Fernandez MG. **2017**. Differential manipulation of leaf angle throughout the canopy: Current status and prospects. *Journal of Experimental Botany* **68**: 5699–5717.

Marchler-Bauer A, Zheng C, Chitsaz F, Derbyshire MK, Geer LY, Geer RC, Gonzales NR, Gwadz M, Hurwitz DI, Lanczycki CJ, *et al.* 2013. CDD: Conserved domains and protein three-

dimensional structure. *Nucleic Acids Research* **41**: 348–352.

Marsh JF, Rakocevic A, Mitra RM, Brocard L, Sun J, Eschstruth A, Long SR, Schultze M, Ratet P, Oldroyd GED. **2007**. Medicago truncatula NIN Is Essential for Rhizobial-Independent Nodule Organogenesis Induced by Autoactive Calcium/Calmodulin-Dependent Protein Kinase. *PLANT PHYSIOLOGY* **144**: 324–335.

Mathieu J, Warthmann N, Schmid M, Ku F. **2007**. Report Export of FT Protein from Phloem Companion Cells Is Sufficient for Floral Induction in Arabidopsis. *Current Biology* **19**: 1055–1060.

Maugarny A, Gonçalves B, Arnaud N, Laufs P. **2015**. *CUC Transcription Factors: To the Meristem and Beyond*. Elsevier Inc.

McAdam EL, Reid JB, Foo E. **2018**. Gibberellins promote nodule organogenesis but inhibit the infection stages of nodulation. *Journal of Experimental Botany* **69**: 2117–2130.

McGarry RC, Ayre BG. **2012**. Manipulating plant architecture with members of the CETS gene family. *Plant Science* **188**–**189**: 71–81.

McKim SM, Stenvik G-E, Butenko M a., Kristiansen W, Cho SK, Hepworth SR, Aalen RB, Haughn GW. **2008**. The BLADE-ON-PETIOLE genes are essential for abscission zone formation in Arabidopsis. *Development* **135**: 1537–1546.

McSteen P. **2009**. Hormonal regulation of branching in grasses. *Plant Physiology* **149**: 46–55.

Mele G, Ori N, Sato Y, Hake S. **2003**. The knotted1-like homeobox gene BREVIPEDICELLUS regulates cell differentiation by modulating metabolic pathways. *Genes and Development* **17**: 2088–2093.

Michael J. Dilworth, Euan K. James, William E. Newton. **2008**. Nitrogen-fixing Leguminous Symbioses:Nitrogen Fixation: Origins, Applications, and Research Progress volume7. In: Michael J. Dilworth, Euan K. James, William E. Newton, eds. Nitrogen-fixing Leguminous Symbioses. Springer.

Middleton PH, Jakab J, Penmetsa R V., Starker CG, Doll J, Kalo P, Prabhu R, Marsh JF, Mitra RM, Kereszt A, *et al.* 2007. An ERF Transcription Factor in Medicago truncatula That Is Essential for Nod Factor Signal Transduction. *THE PLANT CELL ONLINE* **19**: 1221–1234.

Minakuchi K, Kameoka H, Yasuno N, Umehara M, Luo L, Kobayashi K, Hanada A, Ueno K, Asami T, Yamaguchi S, *et al.* 2010. FINE CULM1 (FC1) Works Downstream of Strigolactones to Inhibit the Outgrowth of Axillary Buds in Rice. *Plant & cell physiology* **51**.

Mitra RM, Gleason CA, Edwards A, Hadfield J, Downie JA, Oldroyd GED, Long SR. **2004**. A Ca2+/calmodulin-dependent protein kinase required for symbiotic nodule development: Gene identification by transcript-based cloning. *Proceedings of the National Academy of Sciences* **101**: 4701–4705.

Moon J, Candela H, Hake S. **2013**. The Liguleless narrow mutation affects proximal-distal signaling and leaf growth. *Development (Cambridge)* **140**: 405–412.

Moreno MA, Harper LC, Krueger RW, Dellaporta SL, Freeling M. **1997**. Liguleless1 Encodes a Nuclear-Localized Protein Required for Induction of Ligules and Auricles During Maize Leaf Organogenesis. *Genes and Development* **11**: 616–628.

Muehlbauer GJ, Fowler JE, Freeling M. **1997**. Sectors expressing the homeobox gene liguleless3 implicate a time-dependent mechanism for cell fate acquisition along the proximal-distal axis of the maize leaf. *Development* **124**: 5097–5106.

Mukherjee K, Brocchieri L, Bürglin TR. **2009**. A comprehensive classification and evolutionary analysis of plant homeobox genes. *Molecular Biology and Evolution* **26**: 2775–2794.

Müller D, Waldie T, Miyawaki K, To JPC, Melnyk CW, Kieber JJ, Kakimoto T, Leyser O. **2015**. Cytokinin is required for escape but not release from auxin mediated apical dominance. *Plant Journal* **82**: 874–886.

Murakami Y, Miwa H, Imaizumi-Anraku H, Kouchi H, Downie JA, Kawaguchi M, Kawasaki S. **2006**. Positional cloning identifies Lotus japonicus NSP2, a putative transcription factor of the GRAS family, required for NIN and ENOD40 gene expression in nodule initiation. *DNA Research* **13**: 255–265.

Murfet I, Symons G. **2000**. Double mutant rms2 rms5 expresses a transgressive, profuse branching phenotype. *Pisum Genetics* **32**: 33–38.

Murray JD, Karas BJ, Sato S, Tabata S, Amyot L, Szczyglowski K. **2007**. A Cytokinin Perception Mutant Colonized by Rhizobium in the Absence of Nodule Organogenesis. *Science* **315**: 101–104.

Nan W, Shi S, Jeewani DC, Quan L, Shi X, Wang Z. **2018**. Genome-wide identification and characterization of wALOG family genes involved in branch meristem development of branching head wheat. *Genes* **9**.

Napoli C. **1996**. Highly branched phenotype of the petunia dad1-1 mutant is reversed by grafting. *Plant Physiology* **111**: 27–37.

Naramoto S, Hata Y, Kyozuka J. **2020**. The origin and evolution of the ALOG proteins, members of a plant-specific transcription factor family, in land plants. *Journal of Plant Research* **4**.

Ndoye I, de Billy F, Vasse J, Dreyfus B, Truchet G. **1994**. Root nodulation of Sesbania rostrata. *Journal of bacteriology* **176**: 1060–8.

Newcomb W, Pankhurst CE. **1982**. Fine structure of actinorhizal root nodules of Coriaria arborea (Coriariaceae). *New Zealand Journal of Botany* **20**: 93–103.

Ng JLP, Hassan S, Truong TT, Hocart CH, Laffont C, Frugier F, Mathesius U. **2015**. Flavonoids

and Auxin Transport Inhibitors Rescue Symbiotic Nodulation in the Medicago truncatula Cytokinin Perception Mutant cre1. *The Plant Cell* **27**: 2210–2226.

Niwa M, Daimon Y, Kurotani KI, Higo A, Pruneda-Paz JL, Breton G, Mitsuda N, Kay SA, Ohme-Takagi M, Endo M, *et al.* 2013. BRANCHED1 interacts with FLOWERING LOCUS T to repress the floral transition of the axillary meristems in Arabidopsis. *Plant Cell* **25**: 1228–1242.

Norberg M, Holmlund M, Nilsson O. **2005**. The BLADE ON PETIOLE genes act redundantly to control the growth and development of lateral organs. *Development* **132**: 2203–2213.

Nordström A, Tarkowski P, Tarkowska D, Norbaek R, Åstot C, Dolezal K, Sandberg G. **2004**. Auxin regulation of cytokinin biosynthesis in Arabidopsis thaliana: A factor of potential importance for auxin-cytokinin-regulated development. *Proceedings of the National Academy of Sciences of the United States of America* **101**: 8039–8044.

Okagaki RJ, Haaning A, Bilgic H, Heinen S, Druka A, Bayer M, Waugh R, Muehlbauer GJ. **2018**. ELIGULUM-A regulates lateral branch and leaf development in barley. *Plant Physiology* **176**: pp.01459.2017.

Oldroyd GED. **2013**. Speak, friend, and enter: Signalling systems that promote beneficial symbiotic associations in plants. *Nature Reviews Microbiology* **11**: 252–263.

Oldroyd GED, Murray JD, Poole PS, Downie JA. **2011**. The Rules of Engagement in the Legume-Rhizobial Symbiosis. *Annual Review of Genetics* **45**: 119–144.

Op den Camp RHM, Polone E, Fedorova E, Roelofsen W, Squartini A, Op den Camp HJM, Bisseling T, Geurts R. **2012**. Nonlegume Parasponia andersonii Deploys a Broad Rhizobium Host Range Strategy Resulting in Largely Variable Symbiotic Effectiveness . *Molecular Plant-Microbe Interactions* **25**: 954–963.

Op den Camp R, Streng A, De Mita S, Cao Q, Polone E, Liu W, Ammiraju JSS, Kudrna D, Wing R, Untergasser A, *et al.* 2011. LysM-type mycorrhizal receptor recruited for rhizobium symbiosis in nonlegume Parasponia. *Science (New York, N.Y.)* **331**: 909–12.

Opanowicz M, Vain P, Draper J, Parker D, Doonan JH. **2008**. Brachypodium distachyon: making hay with a wild grass. *Trends in Plant Science* **13**: 172–177.

Ori N, Eshed Y, Chuck G, Bowman JL, Hake S. **2000**. Mechanisms that control knox gene expression in the Arabidopsis shoot. *Development* **127**: 5523–5532.

Osipova MA, Mortier V, Demchenko KN, Tsyganov VE, Tikhonovich IA, Lutova LA, Dolgikh EA, Goormachtig S. **2012**. WUSCHEL-RELATED HOMEOBOX5 Gene Expression and Interaction of CLE Peptides with Components of the Systemic Control Add Two Pieces to the Puzzle of Autoregulation of Nodulation. *PLANT PHYSIOLOGY* **158**: 1329–1341.

Parcy F. **2005**. Flowering : a time for integration. *Int. J. Dev. Biol* **49**: 585–593.

Parcy F, Bomblies K, Weigel D. **2002**. Interaction of LEAFY, AGAMOUS and TERMINAL FLOWER1 in maintaining floral meristem identity in Arabidopsis. *Development* **129**: 2519–2527.

Patterson SE. **2001**. Cutting loose. Abscission and dehiscence in Arabidopsis. *Plant Physiology* **126**: 494–500.

Patterson SE, Bolivar-Medina JL, Falbel TG, Hedtcke JL, Nevarez-McBride D, Maule AF, Zalapa JE. **2016**. Are We on the Right Track: Can Our Understanding of Abscission in Model Systems Promote or Derail Making Improvements in Less Studied Crops? *Frontiers in Plant Science* **6**.

Pawlowski K, Bisseling T. **1996**. Rhizobial and Actinorhizal Symbioses: What Are the Shared Features? *The Plant Cell* **8**: 1899–1913.

Pawlowski K, Demchenko KN. **2012**. The diversity of actinorhizal symbiosis. *Protoplasma* **249**: 967–979.

Peng P, Liu L, Fang J, Zhao J, Yuan S, Li X. **2017**. The rice TRIANGULAR HULL1 protein acts as a transcriptional repressor in regulating lateral development of spikelet. *Scientific Reports* **7**: 1–15.

Pichon M, Journet E, Dedieu A, Billy F De, Truchet G, Barker DG, Biologie L De, Plantes R. **1992**. Rhizobium meliloti Elicits Transient Expression of the Early Nodulin Gene ENOD12 in the Differentiating Root Epidermis of Transgenic Alfalfa. *October* **4**: 1199–1211.

Pidkowich MS, Klenz JE, Haughn GW. **1999**. The making of a flower: Control of floral meristem identity in Arabidopsis. *Trends in Plant Science* **4**: 64–70.

Pin PA, Nilsson O. **2012**. The multifaceted roles of FLOWERING LOCUS T in plant development. *Plant, Cell and Environment* **35**: 1742–1755.

Pintard L, Willems A, Peter M. **2004**. Cullin-based ubiquitin ligases: Cul3-BTB complexes join the family. *EMBO Journal* **23**: 1681–1687.

Plet J, Wasson A, Ariel F, Le Signor C, Baker D, Mathesius U, Crespi M, Frugier F. **2011**. MtCRE1-dependent cytokinin signaling integrates bacterial and plant cues to coordinate symbiotic nodule organogenesis in Medicago truncatula. *Plant Journal* **65**: 622–633.

Pnueli L, Gutfinger T, Hareven D, Ben-naim O, Ron N, Adir N, Lifschitz E. **2001**. Tomato SP-Interacting Proteins Define a Conserved Signaling System That Regulates Shoot Architecture and Flowering. *The Plant Cel* **13**: 2687–2702.

Poulter RTM, Goodwin TJD. **2005**. DIRS-1 and the other tyrosine recombinase retrotransposons. *Cytogenetic and Genome Research* **110**: 575–588.

Poursarebani N, Seidensticker T, Koppolu R, Trautewig C, Gawroński P, Bini F, Govind G,

Rutten T, Sakuma S, Tagiri A, *et al.* 2015. The genetic basis of composite spike form in barley and 'miracle-wheat'. *Genetics* **201**: 155–165.

Radutoiu S, Madsen LH, Madsen EB, Felle HH, Umehara Y, Grønlund M, Sato S. **2003**. Plant recognition of symbiotic bacteria. : 585–592.

Radutoiu S, Madsen LH, Madsen EB, Jurkiewicz A, Fukai E, Quistgaard EMH, Albrektsen AS, James EK, Thirup S, Stougaard J. **2007**. LysM domains mediate lipochitin-oligosaccharide recognition and Nfr genes extend the symbiotic host range. *EMBO Journal* **26**: 3923–3935.

Ragni L, Belles-Boix E, Günl M, Pautot V. **2008**. Interaction of KNAT6 and KNAT2 with Brevipedicellus and Pennywise in Arabidopsis inflorescences. *Plant Cell* **20**: 888–900.

Raman S, Greb T, Peaucelle A, Blein T, Laufs P, Theres K. **2008**. Interplay of miR164, CUP-SHAPED COTYLEDON genes and LATERAL SUPPRESSOR controls axillary meristem formation in Arabidopsis thaliana. *Plant Journal* **55**: 65–76.

Rameau C, Murfet IC, Laucou V, Floyd RS, Morris SE, Beveridge CA. **2002**. Pea rms6 mutants exhibit increased basal branching. *Physiologia Plantarum* **115**: 458–467.

Randoux M, Davière JM, Jeauffre J, Thouroude T, Pierre S, Toualbia Y, Perrotte J, Reynoird JP, Jammes MJ, Hibrand-Saint Oyant L, *et al.* 2014. RoKSN, a floral repressor, forms protein complexes with RoFD and RoFT to regulate vegetative and reproductive development in rose. *New Phytologist* **202**: 161–173.

Rast MI, Diger Simon R, Leyser O, Pourquié O. **2008**. The meristem-to-organ boundary: more than an extremity of anything This review comes from a themed issue on Pattern formation and developmental mechanisms Edited by. *Current Opinion in Genetics & Development* **18**: 287–294.

Rast MI, Simon R. **2008**. The meristem-to-organ boundary: more than an extremity of anything. *Current Opinion in Genetics and Development* **18**: 287–294.

Rast MI, Simon R. **2012**. Arabidopsis JAGGED LATERAL ORGANS Acts With ASYMMETRIC LEAVES2 to Coordinate KNOX and PIN Expression in Shoot and Root Meristems. *Plant Cell* **24**: 2917–2933.

Ratcliffe OJ, Bradley DJ, Coen ES. **1999**. Separation of shoot and floral identity in Arabidopsis. *Development* **126**: 1109–1120.

Reddy GV, Heisler MG, Ehrhardt DW, Meyerowitz EM. **2004**. Real-time lineage analysis reveals oriented cell divisions associated with morphogenesis at the shoot apex of Arabidopsis thaliana. *Development* **131**: 4225–4237.

Ren G. **2018**. The evolution of determinate and indeterminate nodules within the Papilionoideae subfamily.

Ren D, Li Y, Zhao F, Sang X, Shi J, Wang N, Guo S, Ling Y, Zhang C, Yang Z, *et al.* 2013. MULTI-FLORET SPIKELET1, which encodes an AP2/ERF protein, determines spikelet meristem fate and sterile lemma identity in rice. *Plant Physiology* **162**: 872–884.

Ren D, Rao Y, Wu L, Xu Q, Li Z, Yu H, Zhang Y, Leng Y, Hu J, Zhu L, *et al.* 2016. The pleiotropic ABNORMAL FLOWER AND DWARF1 affects plant height, floral development and grain yield in rice. *Journal of Integrative Plant Biology* **58**: 529–539.

Renier A, De Faria SM, Jourand P, Giraud E, Dreyfus B, Rapior S, Prin Y. **2011**. Nodulation of Crotalaria podocarpa DC. by Methylobacterium nodulans displays very unusual features. *Journal of Experimental Botany* **62**: 3693–3697.

Reyes-Olalde JI, Zuñiga-Mayo VM, Chávez Montes RA, Marsch-Martínez N, de Folter S. **2013**. Inside the gynoecium: At the carpel margin. *Trends in Plant Science* **18**: 644–655.

Roberts JA, Elliott KA, Gonzalez-Carranza ZH. **2002**. Abscission, dehiscence, and other cell separation processes. *Annual Review of Plant Biology* **53**: 131–158.

Roeder AHK, Ferra´ndiz C, Yanofsky MF. **2003**. The Role of the REPLUMLESS Homeodomain Protein in Patterning the Arabidopsis Fruit. *Current Biology* **13**: 1630–1635.

Rogers LA, Campbell MM. **2004**. The genetic control of lignin deposition during plant growth and development. *New Phytologist* **164**: 17–30.

Romera-branchat M, Andre F, Coupland G. **2014**. Flowering responses to seasonal cues : what ' s new ? *Current Opinion in Plant Biology* **21**: 120–127.

Roux B, Rodde N, Jardinaud MF, Timmers T, Sauviac L, Cottret L, Carrère S, Sallet E, Courcelle E, Moreau S, *et al.* 2014. An integrated analysis of plant and bacterial gene expression in symbiotic root nodules using laser-capture microdissection coupled to RNA sequencing. *Plant Journal* **77**: 817–837.

Sachs JL, Ehinger MO, Simms EL. **2010**. Origins of cheating and loss of symbiosis in wild Bradyrhizobium. *Journal of Evolutionary Biology* **23**: 1075–1089.

Sachs T, Thimann K V. 1964. Release of Lateral Buds from Apical Dominance. *Nature* **201**: 939–940.

Sachs T, Thimann K V. 1967. the Role of Auxins and Cytokinins in the Release of Buds From Dominance. *American Journal of Botany* **54**: 136–144.

Sakamoto T, Morinaka Y, Ohnishi T, Sunohara H, Fujioka S, Ueguchi-Tanaka M, Mizutani M, Sakata K, Takatsuto S, Yoshida S, *et al.* 2006. Erect leaves caused by brassinosteroid deficiency increase biomass production and grain yield in rice. *Nature Biotechnology* **24**: 105–109.

Santi C, Bogusz D, Franche C. **2013**. Biological nitrogen fixation in non-legume plants. *Annals of Botany* **111**: 743–767.

Schiessl K, Muiño JM, Sablowski R. **2014**. Arabidopsis JAGGED links floral organ patterning to tissue growth by repressing Kip-related cell cycle inhibitors. *Proceedings of the National Academy of Sciences of the United States of America* **111**: 2830–2835.

Schmitz G, Theres K. **2005**. Shoot and inflorescence branching. *Current Opinion in Plant Biology* **8**: 506–511.

Scholthof K-BG, Irigoyen S, Catalan P, Mandadi K. **2018**. Brachypodium: A monocot grass model system for plant biology. *The Plant Cell* **30**: tpc.00083.2018.

Schumacher K, Schmitt T, Rossberg M, Schmitz G, Theres K. **1999**. The Lateral suppressor (Ls) gene of tomato encodes a new member of the VHIID protein family. *Proceedings of the National Academy of Sciences of the United States of America* **96**: 290–295.

Sharma V, Chaudhary S, Kumar A, Kumar S. **2012**. COCHLEATA controls leaf size and secondary inflorescence architecture via negative regulation of UNIFOLIATA (LEAFY ortholog) gene in garden pea Pisum sativum. *Journal of Biosciences* **37**: 1041–1059.

Shimizu-Sato S, Mori H. **2001**. Control of outgrowth and dormancy in axillary buds. *Plant Physiology* **127**: 1405–1413.

Shuai B, Reynaga-pen CG, Springer PS. **2002**. The LATERAL ORGAN BOUNDARIES Gene Defines a Novel, Plant-Specific Gene Family. *Society* **129**: 747–761.

Silverstone AL, Mak PYA, Martínez EC, Sun TP. **1997**. The new RGA locus encodes a negative regulator of gibberellin response in Arabidopsis thaliana. *Genetics* **146**: 1087–1099.

Singh S, Katzer K, Lambert J, Cerri M, Parniske M. **2014**. CYCLOPS, A DNA-binding transcriptional activator, orchestrates symbiotic root nodule development. *Cell Host and Microbe* **15**: 139–152.

Sinharoy S, Saha S, Chaudhury SR, DasGupta M. **2009**. Transformed Hairy Roots of Arachis hypogea: A Tool for Studying Root Nodule Symbiosis in a Non–Infection Thread Legume of the Aeschynomeneae Tribe. *Molecular Plant-Microbe Interactions* **22**: 132–142.

Sjödin A, Street NR, Sandberg G, Gustafsson P, Jansson S. **2009**. The Populus Genome Integrative Explorer (PopGenIE): A new resource for exploring the Populus genome. *New Phytologist* **182**: 1013–1025.

Smit P, Limpens E, Geurts R, Fedorova E, Dolgikh E, Gough C, Bisseling T. **2007**. Medicago LYK3, an entry receptor in rhizobial nodulation factor signaling. *Plant physiology* **145**: 183–91.

Smit P, Raedts J, Portyanko V. **2005**. NSP1 of the GRAS Protein Family Is Essential for Rhizobial Nod Factor. **08250**: 1789–1792.

Smith HM, Hake S. **2003**. The Interaction of Two Homeobox Genes, BREVIPEDICELLUS and

PENNYWISE , Regulates Internode Patterning in the Arabidopsis Inflorescence. *The Plant Cell* **15**: 1717–1727.

Smyth DR. **2005**. Morphogenesis of flowers - Our evolving view. *Plant Cell* **17**: 330–341.

Snowden KC, Simkin AJ, Janssen BJ, Templeton KR, Loucas HM, Simons JL, Karunairetnam S, Gleave AP, Clark DG, Klee HJ. **2005**. The Decreased apical dominance1/Petunia hybrida Carotenoid Cleavage Dioxygenase8 gene affects branch production and plays a role in leaf senescence, root growth, and flower development. *Plant Cell* **17**: 746–759.

Soltis DE, Smith SA, Cellinese N, Wurdack KJ, Tank DC, Brockington SF, Refulio-Rodriguez NF, Walker JB, Moore MJ, Carlsward BS, *et al.* 2011. Angiosperm phylogeny: 17 genes, 640 taxa. *American Journal of Botany* **98**: 704–730.

Soltis DE, Soltis PS, Morgan DR, Swensen SM, Mullin BC, Dowd JM, Martin PG. **1995**. Chloroplast gene sequence data suggest a single origin of the predisposition for symbiotic nitrogen fixation in angiosperms. *Proceedings of the National Academy of Sciences of the United States of America* **92**: 2647–2651.

Sorefan K, Booker J, Haurogne K, Goussot M, Bainbridge K, Foo E, Chatfield S, Ward S, Beveridge C, Rameau C, *et al.* 2003. MAX4 and RMS1are orthologous dioxygenase-like genes that regulate shoot branching in Arabidopsis and pea. *Genes and Development*: 1469–1474.

Souer E, Van Houwelingen A, Kloos D, Mol J, Koes R. **1996**. The no apical Meristem gene of petunia is required for pattern formation in embryos and flowers and is expressed at meristem and primordia boundaries. *Cell* **85**: 159–170.

Souza F, Freitas M, Miana S, De souza Moreira FM, Da Silva MF, De Faria SM. **1992**. *Occurrence of nodulation in legume species in the Amazon region of Brazil*. John Wiley & Sons, Ltd (10.1111).

Soyano T, Hayashi M. **2014**. Transcriptional networks leading to symbiotic nodule organogenesis. *Current Opinion in Plant Biology* **20**: 146–154.

Soyano T, Kouchi H, Hirota A, Hayashi M. **2013**. NODULE INCEPTION Directly Targets NF-Y Subunit Genes to Regulate Essential Processes of Root Nodule Development in Lotus japonicus (JM McDowell, Ed.). *PLoS Genetics* **9**: e1003352.

Sprent JI. **1988**. Which steps are essential for the formation of functional legume nodules? *New Phytologist* **111**: 129–153.

Sprent JI. **2007**. Evolving ideas of legume evolution and diversity: A taxonomic perspective on the occurrence of nodulation: Tansley review. *New Phytologist* **174**: 11–25.

Sprent JI. **2008a**. evoluttion and diversity of legume symbiosis. In: M.J. Dilworth et al. (eds.),

Nitrogen-fixing Leguminous Symbioses , 1–21. Springer Science+Business Media B.V. 2008, 1–2.

Sprent JI. **2008b**. Evolution and Diversity of Legume Symbiosis. In: Nitrogen-fixing Leguminous Symbioses. Dordrecht: Springer Netherlands, 1–21.

Sprent JI. **2008c**. 60Ma of legume nodulation. What's new? What's changing? *Journal of Experimental Botany* **59**: 1081–1084.

Sprent JI. **2009**. *Legume nodulation : a global perspective*. Wiley-Blackwell.

Sprent JI, Ardley JK, James EK. **2013**. From North to South: A latitudinal look at legume nodulation processes. *South African Journal of Botany* **89**: 31–41.

Sprent JI, Ardley J, James EK. **2017**. Biogeography of nodulated legumes and their nitrogen-fixing symbionts. *New Phytologist* **215**: 40–56.

Sprent JI, James EK. **2007**. Legume Evolution: Where Do Nodules and Mycorrhizas Fit In? *Plant Physiology* **144**: 575–581.

Sprent JI, Sutherland JM, Faria SM de, Dilworth MJ, Corby HDL, Becking JH, Materon LA, Drozd JW. **1987**. A Century of Nitrogen Fixation Research: Present Status and Future Prospects. *Philosophical Transactions of the Royal Society Society of London. Series B: Biological Sciences* **317**: 67–67.

Srikanth A, Schmid M. **2011**. Regulation of flowering time : all roads lead to Rome. *Cell. Mol. Life Sci* **68**: 2013–2037.

Stirnberg P, van de Sande K, Leyser HMO. **2002**. MAX1 and MAX2 control shoot lateral branching in Arabidopsis. *Development* **129**: 1131–1141.

Stougaard J, Schauser L, Roussis A, Stiller J. **1999**. A plant regulator controlling development of symbiotic root nodules. *Nature* **402**: 191–195.

Sussex IM. **1989**. *Developmental Programming of the Shoot kleristem*.

Suzaki T, Kawaguchi M. **2014**. Root nodulation: A developmental program involving cell fate conversion triggered by symbiotic bacterial infection. *Current Opinion in Plant Biology* **21**: 16–22.

Svistoonoff S, Hocher V, Gherbi H. **2014**. Actinorhizal root nodule symbioses: What is signalling telling on the origins of nodulation? *Current Opinion in Plant Biology* **20**: 11–18.

Sy A, Giraud E, Jourand P, Garcia N, Willems A, Lajudie P de, Prin Y, Neyra M, Gillis M, Boivin-Masson C, *et al.* 2001. Methylotrophic MethylobacteriumBacteria Nodulate and Fix Nitrogen in Symbiosis with Legumes. *Journal of Bacteriology* **183**: 214–220.

Sylvester AW, Cande WZ, Freeling M. **1990**. *Division and differentiation during normal and*

liguleless-1 maize leaf development.

Tajima R, Abe J, Lee ON, Morita S, Lux A. **2008**. Developmental Changes in Peanut Root Structure during Root Growth and Root-structure Modification by Nodulation. *Annals of Botany* **101**: 491–499.

Takada S, Hibara KI, Ishida T, Tasaka M. **2001**. The CUP-SHAPED COTYLEDON1 gene of Arabidopsis regulates shoot apical meristem formation. *Development* **128**: 1127–1135.

Takeda S, Aida M. **2011**. Establishment of the embryonic shoot apical meristem in Arabidopsis thaliana. *J Plant Res* **124**: 211–219.

Takeda S, Hanano K, Kariya A, Shimizu S, Zhao L, Matsui M, Tasaka M, Aida M. **2011**. CUP-SHAPED COTYLEDON1 transcription factor activates the expression of LSH4 and LSH3, two members of the ALOG gene family, in shoot organ boundary cells. *Plant Journal* **66**: 1066–1077.

Tamaki S, Matsuo S, Wong HL, Yokoi S, Shimamoto K. **2007**. Hd3a protein is a mobile flowering signal in rice. *Science* **316**: 1033–1036.

Tanaka M, Takei K, Kojima M, Sakakibara H, Mori H. **2006**. Auxin controls local cytokinin biosynthesis in the nodal stem in apical dominance. *Plant Journal* **45**: 1028–1036.

Tavakol E, Okagaki R, Verderio G, Shariati J. V, Hussien A, Bilgic H, Scanlon MJ, Todt NR, Close TJ, Druka A, *et al.* 2015. The Barley Uniculme4 Gene Encodes a BLADE-ON-PETIOLE-Like Protein That Controls Tillering and Leaf Patterning. *Plant Physiology* **168**: 164–174.

Taylor S a, Hofer JMI, Murfet IC, Sollinger JD, Singer SR, Knox MR, Ellis THN. **2002**. Proliferating inflorescence meristem,a MADS-Box Gene That Regulates Floral Meristem Identity in Pea1. *Society* **129**: 1150–1159.

Teo ZWN, Song S, Wang YQ, Liu J, Yu H. **2014**. New insights into the regulation of inflorescence architecture. *Trends in Plant Science* **19**: 158–165.

Teper-bamnolker P, Samach A. **2005**. The Flowering Integrator FT Regulates SEPALLATA3 and FRUITFULL Accumulation in Arabidopsis Leaves. *The Plant Cell* **17**: 2661–2675.

Theologis A, Huynh T V., Davis RW. **1985**. Rapid induction of specific mRNAs by auxin in pea epicotyl tissue. *Journal of Molecular Biology* **183**: 53–68.

Thompson JD, Higgins DG, Gibson TJ. **1994**. CLUSTAL W: improving the sensitivity of progressive multiple sequence alignment through sequence weighting, position-specific gap penalties and weight matrix choice. *Nucleic Acids Research* **22**: 4673–4680.

Tian C, Zhang X, He J, Yu H, Wang Y, Shi B, Han Y, Wang G, Feng X, Zhang C, *et al.* 2014. An organ boundary-enriched gene regulatory network uncovers regulatory hierarchies underlying axillary meristem initiation. *Molecular Systems Biology* **10**: 755.

Tirichine L, Imaizumi-Anraku H, Yoshida S, Murakami Y, Madsen LH, Miwa H, Nakagawa T, Sandal N, Albrektsen AS, Kawaguchi M, *et al.* 2006a. Deregulation of a Ca 2+ /calmodulin-dependent kinase leads to spontaneous nodule development. *Nature* **441**: 1153–1156.

Tirichine L, James EK, Sandal N, Stougaard J. **2006b**. Spontaneous root-nodule formation in the model legume Lotus japonicus: A novel class of mutants nodulates in the absence of rhizobia. *Molecular Plant-Microbe Interactions* **19**: 373–382.

Tirichine L, Sandal N, Madsen LH, Radutoiu S, Albrektsen AS, Sato S, Asamizu E, Tabata S, Stougaard J. **2007**. A Gain-of-Function Mutation in a Root Nodule Organogenesis. *Science (New York, N.Y.)* **2680**: 104–107.

Toriba T, Tokunaga H, Shiga T, Nie F, Naramoto S, Honda E, Tanaka K, Taji T, Itoh JI, Kyozuka J. **2019**. BLADE-ON-PETIOLE genes temporally and developmentally regulate the sheath to blade ratio of rice leaves. *Nature Communications* **10**: 1–13.

Townsley BT, Sinha NR, Kang J. **2013**. KNOX1 genes regulate lignin deposition and composition in monocots and dicots. *Frontiers in Plant Science* **4**: 121.

Truchet G, Camut S, Billy F de, Odorico R, Vasse J. **1989**. The Rhizobium-legume symbiosis Two methods to discriminate between nodules and other root-derived structures. *Protoplasma* **149**: 82–88.

Tsuda K, Kurata N, Ohyanagi H, Hake S. **2014**. Genome-wide study of KNOX regulatory network reveals brassinosteroid catabolic genes important for shoot meristem function in rice. *Plant Cell* **26**: 3488–3500.

Turck F, Fornara F, Coupland G. **2008**. Regulation and Identity of Florigen: FLOWERING LOCUS T Moves Center Stage. *Annual Review of Plant Biology* **59**: 573–594.

Turnbull CGN, Booker JP, Leyser HMO. **2002**. Micrografting techniques for testing long-distance signalling in Arabidopsis. *Plant Journal* **32**: 255–262.

Udvardi MK, Tabata S, Parniske M, Stougaard J. **2005**. Lotus japonicus: Legume research in the fast lane. *Trends in Plant Science* **10**: 222–228.

Umehara M, Hanada A, Yoshida S, Akiyama K, Arite T, Takeda-Kamiya N, Magome H, Kamiya Y, Shirasu K, Yoneyama K, *et al.* 2008. Inhibition of shoot branching by new terpenoid plant hormones. *Nature* **455**: 195–200.

Valverde C, Wall LG. **1999**. Regulation of nodulation in Discaria trinervis (Rhamnaceae)-Frankia symbiosis. *Canadian Journal of Botany* **77**: 1302–1310.

Vasse J, de Billy F, Camut S, Truchet G. **1990**. Correlation between ultrastructural differentiation of bacteroids and nitrogen fixation in alfalfa nodules. *Journal of Bacteriology* **172**: 4295–4306.

Veerappan V, Kadel K, Alexis N, Scott A, Kryvoruchko I, Sinharoy S, Taylor M, Udvardi M,

Dickstein R. **2014**. Keel petal incision a simple and efficient method for genetic crossing in Medicago truncatula. *PLANT METHODS* **10**: 1–10.

Van De Velde W, Guerra JCP, De Keyser A, De Rycke R, Rombauts S, Maunoury N, Mergaert P, Kondorosi E, Holsters M, Goormachtig S. **2006**. Aging in legume symbiosis. A molecular view on nodule senescence in Medicago truncatula. *Plant Physiology* **141**: 711–720.

van Velzen R, Doyle JJ, Geurts R. **2019**. A Resurrected Scenario: Single Gain and Massive Loss of Nitrogen-Fixing Nodulation. *Trends in Plant Science* **24**: 49–57.

Vernié T, Kim J, Frances L, Ding Y, Sun J, Guan D, Niebel A, Gifford ML, de Carvalho-Niebel F, Oldroyd GED. **2015**. The NIN Transcription Factor Coordinates Diverse Nodulation Programs in Different Tissues of the *Medicago truncatula* Root. *The Plant Cell* **27**: 3410–3424.

Vogel JP, Garvin DF, Leong OM, Hayden DM. **2006**. Agrobacterium-mediated transformation and inbred line development in the model grass Brachypodium distachyon. *Plant Cell, Tissue and Organ Culture* **84**: 199–211.

Vroemen CW, Mordhorst AP, Albrecht C, Kwaaitaal MACJ, Vries SC de. **2003**. Program Jaminan Kesehatan Nasional. *The Plant Cel* **15**: 1563–1578.

Wagner D, Sablowski RWM, Meyerowitz EM. **1999**. Transcriptional activation of APETALA1 by LEAFY. *Science* **285**: 582–584.

Waites R, Hudson A. **1995**. phantastica: A gene required for dorsoventrality of leaves in Antirrhinum majus. *Development* **121**: 2143–2154.

Walsh J, Waters CA, Freeling M. **1998**. The maize gene liguleless2 encodes a basic leucine zipper protein involved in the establishment of the leaf blade-sheath boundary. *Genes and Development* **12**: 208–218.

Wang J. **2014**. Regulation of flowering time by the miR156-mediated age pathway. *Journal of Experimental Botany* **65**: 4723–4730.

Wang H, Chen J, Wen J, Tadege M, Li G, Liu Y, Mysore KS, Ratet P, Chen R. **2008**. Control of compound leaf development by Floricaula/Leafy Ortholog Single Leaflet1 in Medicago truncatula. *Plant Physiology* **146**: 1759–1772.

Wang Q, Hasson A, Rossmann S, Theres K. **2016**. Divide et impera: Boundaries shape the plant body and initiate new meristems. *New Phytologist* **209**: 485–498.

Wang Y, Li J. **2011**. Branching in rice. *Current Opinion in Plant Biology* **14**: 94–99.

Wang Q, Liu J, Zhu H. **2018**. Genetic and Molecular Mechanisms Underlying Symbiotic Specificity in Legume-Rhizobium Interactions. *Frontiers in Plant Science* **9**: 1–8.

Wang Y, Salasini BC, Khan M, Devi B, Bush M, Subramaniam R, Hepworth SR. **2019a**. Clade I TGACG-Motif Binding Basic Leucine Zipper Transcription Factors Mediate BLADE-ON-PETIOLE-Dependent Regulation of Development. *Plant Physiology* **180**: 937–951.

Wang J, Tian Y, Li J, Yang K, Xing S, Han X, Xu D, Wang Y. **2019b**. Transcriptome sequencing of active buds from Populus deltoides CL. and Populus × zhaiguanheibaiyang reveals phytohormones involved in branching. *Genomics* **111**: 700–709.

Weir I, Lu J, Cook H, Causier B, Schwarz-Sommer Z, Davies B. **2004**. Cupuliformis establishes lateral organ boundaries in Antirrhinum. *Development* **131**: 915–922.

Wellensiek SJ. **1959**. Neutronic mutations in peas. *Euphytica* **8**: 209–215.

Weller JL, Liew LC, Hecht VFG, Rajandran V, Laurie RE, Ridge S, Wenden B, Schoor JKV, Jaminon O, Blassiau C, *et al.* 2012. A conserved molecular basis for photoperiod adaptation in two temperate legumes. *Proceedings of the National Academy of Sciences of the United States of America* **109**: 21158–21163.

Werner GD a., Cornwell WK, Sprent JI, Kattge J, Kiers ET. **2014**. A single evolutionary innovation drives the deep evolution of symbiotic N2-fixation in angiosperms. *Nature Communications* **5**: 1–9.

Whipple CJ. **2017**. Grass inflorescence architecture and evolution: the origin of novel signaling centers. *New Phytologist* **216**: 367–372.

Wigge PA, Kim MC, Jaeger KE, Busch W, Schmid M, Lohmann JU. **2005**. Integration of Spatial and Temporal Information During Floral Induction in Arabidopsis. *Science* **309**: 1056–1059.

William DA, Su Y, Smith MR, Lu M, Baldwin DA, Wagner D. **2004**. Genomic identification of direct target genes of LEAFY. *Proceedings of the National Academy of Sciences of the United States of America* **101**: 1775–1780.

Winter CM, Austin RS, Blanvillain-Baufumé S, Reback MA, Monniaux M, Wu MF, Sang Y, Yamaguchi A, Yamaguchi N, Parker JE, *et al.* 2011. LEAFY Target Genes Reveal Floral Regulatory Logic, cis Motifs, and a Link to Biotic Stimulus Response. *Developmental Cell* **20**: 430–443.

Woerlen N, Allam G, Popescu A, Corrigan L, Pautot V, Hepworth SR. **2017**. Repression of BLADE-ON-PETIOLE genes by KNOX homeodomain protein BREVIPEDICELLUS is essential for differentiation of secondary xylem in Arabidopsis root. *Planta* **245**: 1079–1090.

Wojciechowski MF, Sanderson MJ, Steele KP, Liston A. **2000**. Molecular phylogeny of the "Temperate Herbaceous Tribes" of Papilionoid legumes: a supertree approach. In: Bruneau PSH and A, ed. Royal Botanic Gardens, Kew., 277–298.

Woodburn T, Zhang J, Li L, Liu K, Gan Y, Huang L, Coulter J a., Li J. **2018**. Soil–Plant Indices Help Explain Legume Response to Crop Rotation in a Semiarid Environment. *Frontiers in Plant Science* **9**: 1–13.

Wu X-M, Yu Y, Han L-B, Li C-L, Wang H-Y, Zhong N-Q, Yao Y, Xia G-X. **2012**. The Tobacco BLADE-ON-PETIOLE2 Gene Mediates Differentiation of the Corolla Abscission Zone by Controlling Longitudinal Cell Expansion. *Plant Physiology* **159**: 835–850.

Xiao TT, Schilderink S, Moling S, Deinum EE, Kondorosi E, Franssen H, Kulikova O, Niebel A, Bisseling T. **2014**. Fate map of Medicago truncatula root nodules. *Development* **141**: 3517–3528.

Xu M, Hu T, McKim SM, Murmu J, Haughn GW, Hepworth SR. **2010**. Arabidopsis BLADE-ON-PETIOLE1 and 2 promote floral meristem fate and determinacy in a previously undefined pathway targeting APETALA1 and AGAMOUS-LIKE24. *Plant Journal* **63**: 974–989.

Xu C, Park SJ, Van Eck J, Lippman ZB. **2016**. Control of inflorescence architecture in tomato by BTB/POZ transcriptional regulators. *Genes and Development* **30**: 2048–2061.

Xue Z, Liu L, Zhang C. **2020**. Regulation of Shoot Apical Meristem and Axillary Meristem Development in Plants. *International Journal of Molecular Sciences* **21**: 2917.

Yamaguchi N, Wu MF, Winter CM, Berns MC, Nole-Wilson S, Yamaguchi A, Coupland G, Krizek BA, Wagner D. **2013**. A Molecular Framework for Auxin-Mediated Initiation of Flower Primordia. *Developmental Cell* **24**: 271–282.

Yan DW, Zhou Y, Ye SH, Zeng LJ, Zhang XM, He ZH. **2013**. BEAK-SHAPED GRAIN 1/TRIANGULAR HULL 1, a DUF640 gene, is associated with grain shape, size and weight in rice. *Science China Life Sciences* **56**: 275–283.

YAN D, ZHOU Y, YE S, ZENG L, ZHANG X, HE Z. **2013**. BEAK-SHAPED GRAIN 1/TRIANGULAR HULL 1, a DUF640 gene, is associated with grain shape, size and weight in rice. **56**: 275–283.

Yang F, Wang Q, Schmitz G, Müller D, Theres K. **2012**. The bHLH protein ROX acts in concert with RAX1 and LAS to modulate axillary meristem formation in Arabidopsis. *Plant Journal* **71**: 61–70.

Yano K, Yoshida S, Muller J, Singh S, Banba M, Vickers K, Markmann K, White C, Schuller B, Sato S, *et al.* 2008. CYCLOPS, a mediator of symbiotic intracellular accommodation. *Proceedings of the National Academy of Sciences* **105**: 20540–20545.

Yaxley JL, Jablonski W, Reid JB. **2001**. Leaf and flower development in pea (Pisum sativum L.): Mutants cochleata and unifoliata. *Annals of Botany* **88**: 225–234.

Yoshida H, Nagato Y. **2011**. Flower development in rice. *Journal of Experimental Botany* **62**: 4719–4730.

Yoshida A, Sasao M, Yasuno N, Takagi K, Daimon Y, Chen R, Yamazaki R, Tokunaga H, Kitaguchi Y, Sato Y, *et al.* 2013. TAWAWA1, a regulator of rice inflorescence architecture, functions through the suppression of meristem phase transition. *Proceedings of the National Academy of Sciences of the United States of America* **110**: 767–772.

Yoshida A, Suzaki T, Tanaka W, Hirano HY. **2009**. The homeotic gene long sterile lemma (G1) specifies sterile lemma identity in the rice spikelet. *Proceedings of the National Academy of Sciences of the United States of America* **106**: 20103–20108.

Young ND, Debellé F, Oldroyd GED, Geurts R, Cannon SB, Udvardi MK, Benedito VA, Mayer KFX, Gouzy J, Schoof H, *et al.* 2011. The Medicago genome provides insight into the evolution of rhizobial symbioses. *Nature* **480**: 520–4.

Yu Y. **2019a**. New Interacting Partners of BLADE-ON-PETIOLE in Regulation of Plant Development. *Plant Physiology* **180**: 697–698.

Yu Y. **2019b**. Liguleless1, a Conserved Gene Regulating Leaf Angle and a Target for Yield Improvement in Wheat. *Plant physiology* **181**: 4–5.

Yu H, Xu Y, Tan EL, Kumar PP, Ft LT, Of S, Of O. **2002**. AGAMOUS-LIKE24,a dosage-dependent mediator of the flowering signals. *PNAS* **99**: 16336–16341.

Žádníková P, Simon R. **2014**. How boundaries control plant development. *Current Opinion in Plant Biology* **17**: 116–125.

Zhang B, Holmlund M, Lorrain S, Norberg M, Bakó L, Fankhauser C, Nilsson O. **2017**. BLADE-ON-PETIOLE proteins act in an E3 ubiquitin ligase complex to regulate PHYTOCHROME INTERACTING FACTOR 4 abundance. *eLife* **6**: 1–19.

Zhang Z, Hu Q, Liu Y, Cheng P, Cheng H, Liu W, Xing X, Guan Z, Fang W, Chen S, *et al.* 2019. Strigolactone represses the synthesis of melatonin, thereby inducing floral transition in Arabidopsis thaliana in an FLC-dependent manner. *Journal of Pineal Research* **67**: 1–11.

Zhang Y, Zhang Y, Tessaro MJ, Tessaro MJ, Lassner M, Lassner M, Li X, Li X. **2003**. Knockout analysis of Arabidopsis transcription factors TGA2, TGA5, and TGA6 reveals their redundant and essential roles in systemic acquired resistance. *Plant Cell* **15**: 2647–2653.

Zhao S, Fernald RD. **2005**. Comprehensive algorithm for quantitative real-time polymerase chain reaction. *Journal of Computational Biology* **12**: 1047–1064.

Zhao L, Nakazawa M, Takase T, Manabe K, Kobayashi M, Seki M, Shinozaki K, Matsui M. **2004**. Overexpression of LSH1, a member of an uncharacterised gene family, causes enhanced light regulation of seedling development. *Plant Journal* **37**: 694–706.

Zhou C, Han L, Li G, Chai M, Fu C, Cheng X, Wen J, Tang Y, Wang ZY. **2014**. STM/BP-like

KNOXI is uncoupled from ARP in the regulation of compound leaf development in Medicago truncatula. *Plant Cell* **26**: 1464–1479.

Zhukov VA, Kuznetsova EV, Ovchinnikova E., Rychagova T., Titov VS, Pinaev AG, Borisov AY, Moffet M, Domoney C, Ellis THN, *et al.* 2007. Gene-based markers of pea linkage group V for mapping genes related to symbioses. *Pisum Genetics* **39**: 19–25.

Zou J, Chen Z, Zhang S, Zhang W, Jiang G, Zhao X, Zhai W, Pan X, Zhu L. 2005. Characterizations and fine mapping of a mutant gene for high tillering and dwarf in rice (Oryza sativa L.). *Planta* **222**: 604–612.

Zou J, Zhang S, Zhang W, Li G, Chen Z, Zhai W, Zhao X, Pan X, Xie Q, Zhu L. 2006. The rice HIGH-TILLERING DWARF1 encoding an ortholog of Arabidopsis MAX3 is required for negative regulation of the outgrowth of axillary buds. *Plant Journal* **48**: 687–698.

université PARIS-SACLAY | ÉCOLE DOCTORALE Sciences du végétal : du gène à l'écosystème

Titre : Rôles des gènes *NOOT-BOP-COCH-LIKE* dans le développement des plantes et dans l'identité des organes symbiotiques.

Mots clés : Légumineuse, *Brachypodium*, Développement, Symbiose fixatrice d'azote, Gènes *NOOT-BOP-COCH-LIKE*, *ALOG*

Résumé : Les gènes NODULE-ROOT de *Medicago truncatula*, *BLADE-ON-PETIOLE* d'*Arabidopsis thaliana* et *COCHLEATA* de *Pisum sativum* font partie d'un clade spécifique *NOOT-BOP-COCH-LIKE1* (*NBCL1*) hautement conservé et qui appartient à la famille de gènes *NON-EXPRESSOR OF PATHOGENESIS RELATED PROTEIN1 LIKE*. Chez les légumineuses, les membres du clade *NBCL1* sont connus comme les principaux régulateurs de l'identité des organes symbiotiques (nodules). Les membres du clade NBCL2 (*MtNOOT2*) jouent également un rôle clé dans l'établissement et le maintien de l'identité de l'organe symbiotique, en redondance avec les gènes NBCL1. Il a également été démontré que ces gènes végétaux NBCL sont impliqués dans l'abscission. Les gènes NBCL sont également conservés chez les plantes monocotylédones chez lesquelles ils contrôlent différents aspects du développement.

Ce travail de thèse vise à mieux comprendre les rôles des gènes *NBCL1* et *NBCL2* dans le développement des plantes légumineuses et chez *Brachypodium* et à découvrir de nouveaux acteurs moléculaires impliqués dans la régulation de l'identité des nodules dépendante de NBCL1, en utilisant de nouveaux mutants d'insertion TILLING et Tnt1 chez deux espèces de légumineuses (*Medicago* et *Pisum*). En outre, nous avons utilisé les mutations KO CRISPR chez *Brachypodium* pour mieux comprendre leur rôle chez les plantes monocotylédones

Ce travail de thèse a permis d'élucider les nouvelles fonctions des gènes *NBCL1* dans le développement des tiges et l'architecture des plantes. Nous avons également révélé que les membres du clade NBCL2, spécifique aux légumineuses, fonctionnent de manière redondante avec le clade NBCL1 et jouent des rôles importants dans le développement des feuilles, des stipules, des inflorescences et des fleurs. De plus, nous avons montré un rôle dans le développement, l'établissement et le maintien de l'identité des nodosités, et par conséquent dans le succès et l'efficacité de l'association symbiotique.

Dans cette thèse, nous avons également exploré les rôles des gènes NBCL *BdUNICULME4* et *BdLAXATUM-A*, dans le développement de *B. distachyon* à l'aide de doubles mutants. Nous avons confirmé les résultats précédents et révélé une nouvelle fonction pour ces deux gènes dans l'architecture des plantes, la formation des ligules et des inflorescences, ainsi que dans la teneur en lignine.

Ce travail de thèse a finalement permis l'identification et la caractérisation de nouveaux mutants pour les gènes de *M. truncatula* ALOG (*Arabidopsis LSH1* et *Oryza G1*). Les protéines ALOG sont des partenaires d'interaction potentiels pour les *NBCLs*. Nous avons montré que certains membres ALOG jouent un rôle important dans le développement des nodules et des organes aériens.

Dans l'ensemble, ce travail de thèse suggère qu'au cours de l'évolution, le programme de développement des nodules a été recruté à partir de programmes de régulation préexistants pour le développement et l'identité des nodosités.

Title: Roles of the *NOOT-BOP-COCH-LIKE* genes in plant development and in the symbiotic organ identity.

Keywords: Legume, *Brachypodium*, Development, Nitrogen fixing symbiosis, *NOOT-BOP-COCH-LIKE* genes, *ALOG*

Abstract: The *Medicago truncatula NODULE-ROOT*, the *Arabidopsis thaliana BLADE-ON-PETIOLE*, and the *Pisum sativum COCHLEATA* genes are members of a highly conserved *NOOT-BOP-COCH-LIKE1* (*NBCL1*) specific clade that belongs to the *NON-EXPRESSOR OF PATHOGENESIS RELATED PROTEIN1 LIKE* gene family. In legumes, the members of this *NBCL1* clade are known as key regulators of the symbiotic organ identity. The members of the NBCL2 clade (*MtNOOT2*) also play a key role in the establishment and maintenance of the symbiotic nodule identity, redundantly with *NBCL1* while without significant phenotype alone. These NBCL plant genes were also shown to be involved in abscission. In addition, NBCL genes are also conserved in monocotyledon plants in which they also control different aspects of development.

The present thesis work aims to better understand the roles of the *NBCL1* and *NBCL2* genes in development in both legume and *Brachypodium* plants and to discover new molecular actors involved in the NBCL1-dependent regulation of the nodule identity using novel TILLING and Tnt1 insertional mutants in two legume species, *Medicago*, and *Pisum*. In addition we used CRISPR knock-out mutations in *Brachypodium* to better understand their roles in monocotyledon plants.

This thesis work unraveled new functions of the *NBCL1* genes in plant shoot development and plant architecture. We also revealed that the members of the legume-specific *NBCL2* redundantly function with *NBCL1* sub-clade and play important roles in leaf, stipule, inflorescence and flower development. In addition we showed a role in nodule development, identity establishment and maintenance, and consequently in the success and efficiency of the symbiotic association.

In this thesis, we also explored the roles of the highly conserved NBCL genes, *BdUNICULME4* and *BdLAXATUM-A*, in the development of *B. distachyon* using double mutants. We confirmed previous results and reveal a new function for these two genes in plant architecture, ligule and inflorescence formation, and also lignin content.

This thesis work has finally allowed the identification and the characterization of new mutants for *M. truncatula* ALOG (*Arabidopsis LSH1* and *Oryza G1*) genes. ALOG proteins are potential interacting partners for NBCL. We showed that some ALOG members play important roles in nodule and aerial organ development.

Altogether, this thesis work suggests that during evolution, the nodule developmental program was recruited from pre-existing regulatory programs for nodule development and identity.

Université Paris-Saclay
Espace Technologique / Immeuble Discovery
Route de l'Orme aux Merisiers RD 128 / 91190 Saint-Aubin, France